

***Rhodococcus fascians*-plant interactions:
microbiological and molecular aspects**

A thesis submitted in fulfilment of the requirements for
the degree of

Doctor of Philosophy in Biotechnology

at the University of Canterbury

by

Pragatheswari Dhandapani

University of Canterbury

2014

Acknowledgements

I would like to express my sincere thanks to my supervisors, Professor Paula Jameson and Dr Jianchen Song for their valuable guidance, support and assistance throughout my PhD work. To Paula, thank you for giving me the opportunity and encouragement that helped me to achieve my goal of learning molecular biological techniques. I am also appreciative and indebted to you Paula, for helping me to settle in to a new environment and rendering your support and friendship in my time of grief. I am very grateful to you for your advice and critical appraisal of this thesis. To Jason, thanks so much for being there for me in the lab supporting, training and guiding me on techniques, especially in the skill of RT-qPCR. I would like to especially thank you Jason, for the advice, discussions and valuable suggestions you offered during my thesis writing.

I would like to express my sincere thanks to Neil Andrews for helping and assisting me in the preparation and operation of the SEM. I especially thank and am also grateful to Graeme Bull for his assistance, advice and teaching me the histological techniques for light microscopic observations. It is a great delight to express my thanks and gratitude to Jan McKenzie for her valuable assistance, suggestions and inspiring technical advice on light microscopy and SEM analysis. Thanks Jan for your stable support and assistance in my image analysis and interpretation, and for critical evaluation of my results. Sincere thanks to Matt Walters for his guidance and assistance in graphic presentation.

I would like to thank everyone all in our lab group, especially Thomas Evans, Dave O'Keefe, Davon and Anish, Annu Ninan and all my lab colleagues for their help, support and kindness. I thank Justin (Zhaoji Quiang) for his assistance, help and for teaching me the cloning techniques. Many thanks to Jackie Healy for her help and assistance in the lab and timely provision of resources for the research work.

I would like to thank my friends at the Biological Sciences, for their help, support and providing an encouraging atmosphere for the research work.

Very special thanks and gratitude to my family; my husband Sakthi, without whose support and constant encouragement I would not have done this, and to my kids, Prapthi and Sachin, for their love, adjustments and patience all through my project work.

Abstract

Rhodococcus fascians, a plant pathogenic actinomycete with a very broad host range, causes leafy galls and other malformations. The plant hormone, group, the cytokinins has been implicated in the alteration of host morphology. The aim of this project was to gain insight into the interaction of the cytokinin biosynthetic, isopentenyltransferase (*IPT*), cytokinin activating (*LOG* (The Lonely Guy)) and the cytokinin metabolic, cytokinin oxidase/dehydrogenase (*CKX*) gene families of both *Pisum sativum* and *R. fascians* during infection of the plant.

R. fascians colonisation and infection of pea were examined using scanning electron microscopy (SEM) and light microscopy. The expression of genes related to cytokinin biosynthesis, activation and metabolism were isolated and assessed with polymerase chain reaction (PCR) and real time-quantitative PCR (RT-qPCR) analysis. Primers were designed to discriminate between pea genes and *R. fascians* genes. In addition, the response of the pea cotyledons to *R. fascians* was measured through chlorophyll estimation and the expression of the transporter genes, sucrose transporter (*SUT*) and amino acid permease (*AAP*) which were assayed through RT-qPCR. The pea response regulators were monitored as an indirect measure of the level of endogenous cytokinins in pea.

Two *R. fascians* strains, the avirulent strain 589 and the virulent strain 602, were selected for this project based on their virulence and similar growth rate under identical conditions. The virulence of *R. fascians* virulent strain 602 was also confirmed through Koch's postulates. The phenotypic alterations in the pea infected with the virulent strain 602 included stunted growth, multiple shoots, small leaves, thickened primary roots and reduced secondary root growth. Delayed senescence of shoots and dark green, intact cotyledons were also observed. Microscopic analyses revealed epiphytic colonisation by both the avirulent strain 589 and the virulent strain 602 in pea cotyledons, roots, shoots and leaves and endophytic colonisation in the seed coat from the time of seed inoculation to 45 days post inoculation (dpi).

The expression of *R. fascians* genes was relatively high at 5 and 9 dpi in pea cotyledons and at 15 and 25 dpi in roots and shoots of pea infected with the virulent strain 602. The expression of *RfIPT*, *RfLOG* and *RfCKX* was not detected both in the control pea and the pea infected with the avirulent strain 589.

The cytokinin biosynthesis, metabolism and response regulator (*RR*) multi-gene families of *PsIPTs*, *PsLOGs*, *PsCKXs* and *PsRRs* revealed differential and tissue-specific expression patterns. The expression of *PsIPTs* and *PsLOGs* was induced immediately after inoculation with the *R. fascians* virulent strain 602 in the cotyledon but not in roots and shoots, and the expression level reduced at later growth stages. The *PsCKXs* and *PsRRs* expression level increased with the growth of the host infected with the virulent strain 602. In pea infected with the avirulent strain 589 the expression of *PsIPTs*, *PsLOGs* and *PsCKXs* gene family members generally increased after 25 dpi in cotyledons, roots and shoots, whereas *PsRRs* expression was low at all time points.

The up-regulation of *PsIPTs* and *PsLOGs* immediately after inoculation in cotyledons and at 15 dpi in roots and shoots by *R. fascians* virulent strain leads to elevated cytokinins which is reflected by the up-regulation of *PsRRs*. The plant responds to elevated cytokinin by producing phenotypic changes including shoot malformations. The plant activates its cytokinin homeostasis mechanism due to change in cytokinin level which is indicated by up-regulation of *PsCKXs*. Generally, the expression of the *PsRRs* was also up-regulated over time following infection by the *R. fascians* virulent strain. This indicates the presence of biologically active cytokinins in the host which maintain the symptoms. The outcome due to the avirulent strains indicates that, even though *PsIPTs* and *PsLOGs* are up-regulated at later growth stages (25 to 35 dpi), expression of *PsCKX* gene families were varied (either up-regulated or down regulated after 25 dpi). However, *PsRRs* expression was down-regulated suggesting low cytokinins levels in tissues which may be due to the activation of homeostatic mechanisms of the plant to reduce the level of biologically active cytokinins.

The chlorophyll content increased in cotyledons infected with the virulent strain 602 and *PsSUTs* and *PsAAPs* expression pattern in pea cotyledon and shoot infected with the virulent strain 602 indicates that *R. fascians* converts the infected tissue into a sink for their establishment and growth.

Table of Contents

	Page
Acknowledgements	i
Abstract	ii
List of Figures	ix
List of Tables	xv
Abbreviations	xvi
CHAPTER 1 INTRODUCTION	1
1.1 Background	1
1.2 Cytokinins	2
1.2.1 Cytokinin biosynthesis and metabolism	4
1.2.1.1 Biosynthesis of cytokinin in plants and microbes	6
1.2.1.2 Key enzymes involved in cytokinin biosynthesis	10
1.2.1.3 Cytokinin inactivation	15
1.2.2 Cytokinin translocation, perception and signalling	18
1.2.2.1 Cytokinin perception and signalling	19
1.2.2.2 The response regulators (<i>RRs</i>)	20
1.2.3 Cytokinins in plant- microbe interactions	23
1.3 <i>Rhodococcus fascians</i>	26
1.3.1 Phytopathogen	26
1.3.2 Symptoms	29
1.3.3 Molecular basis of virulence in <i>R. fascians</i>	31
1.3.3.1 Importance of the <i>fas</i> locus in virulence	34
1.3.4 <i>R. fascians</i> and plant hormones	38
1.3.4.1 Cytokinin	38
1.3.4.2 Auxins	44
1.5 Objectives	46

CHAPTER 2 GENERAL MATERIALS AND METHOD

2.1	<i>Pisum sativum</i> growth conditions	50
2.2	<i>Rhodococcus fascians</i> culture strains	52
2.3	Inoculation of <i>P. sativum</i> plants	52
2.4	Microscopy	53
	2.4.1 Scanning electron microscopy (SEM)	53
	2.4.2 Light microscopy	54
2.5	Microbial Count	56
2.6	Chlorophyll estimation	57
2.7	Gene identification in silico	57
	2.7.1 Phylogenetic analysis	58
2.8	RNA extraction and cDNA synthesis	58
	2.8.1 TRIzol®/Tri Reagent ®RNA Extraction	58
	2.8.2 cDNA synthesis	59
2.9	DNA/RNA quantification	59
	2.9.1 Agarose gel electrophoresis	59
	2.9.2 Nanodrop™ Spectrophotometry	60
2.10	Polymerase chain Reaction (PCR)	61
2.11	PCR Primer Design	61
2.12	DNA Purification	62
2.13	Gene Expression Analysis	62
	2.13.1 Experimental design	62
	2.13.2 Sample preparation	63
	2.13.3 Nucleic acid extraction	63
	2.13.4 Reverse transcription	63
	2.13.5 Primer design for RT-qPCR	64
	2.13.6 RT-qPCR validation	64
	2.13.7 RT-qPCR reactions	64
	2.13.8 Reference genes	65
	2.13.9 Gene expression data analysis	65

CHAPTER 3 *RHODOCOCCUS FASCIANS-PISUM SATIVUM* INTERACTIONS

3.1	Introduction	66
3.2	Materials and Methods	67
3.2.1	Confirmation of the integrity of the stored <i>R. fascians</i> strains	67
3.2.1.1	<i>Rhodococcus fascians</i> strains	67
3.2.1.2	PCR of <i>RfIPT</i> , <i>RfLOG</i> and <i>RfCKX</i> genes in <i>R. fascians</i> strains	70
3.3	Results	70
3.3.1	Confirmation of Koch's postulates	70
3.3.2	Polymerase chain reaction (PCR) and screening of <i>R. fascians</i> isolates for <i>RfIPT</i> , <i>RfLOG</i> and <i>RfCKX</i> genes	72
3.3.2.1	Phylogenetic analysis of <i>RfIPT</i> , <i>RfLOG</i> and <i>RfCKX</i>	77
3.3.3	Growth of <i>R. fascians</i> and <i>P. sativum</i> plants infected with <i>R. fascians</i>	82
3.3.3.1	<i>R. fascians</i> growth curves and strain selection	82
3.3.3.2	Growth responses of <i>P. sativum</i> inoculated with <i>R. fascians</i>	83
3.3.4	Microbiological traits	86
3.3.4.1	Detection of <i>R. fascians</i> in <i>P. sativum</i>	86
3.3.4.2	Study of <i>R. fascians</i> colonisation in <i>P. sativum</i> using scanning electron microscopy	88
3.3.4.3	Light microscopy study of <i>P. sativum</i> plants inoculated with <i>R. fascians</i>	102
3.4	Discussion	127

CHAPTER 4 IDENTIFICATION, ISOLATION AND EXPRESSION OF CYTOKININ GENES IN *P. SATIVUM* AND *R. FASCIANS*

4.1	Introduction	134
4.2	Materials and Methods	135

4.2.1	Identification and isolation of cytokinin biosynthesis and metabolism genes	135
4.2.2	Plant material and <i>R. fascians</i> strains	136
4.2.3	Polymerase chain reaction (PCR)	136
4.2.4	Cloning of PCR amplification of target gene	137
4.2.5	Expression analysis of cytokinin biosynthesis and metabolic genes	137
4.3	Results	137
4.3.1	Cytokinin biosynthesis, metabolism and response regulator genes identification and isolation	137
4.3.1.1	Isopentenyl transferase (<i>PsIPT</i>)	137
4.3.1.2	The Lonely Guy (<i>PsLOG</i>)	141
4.3.1.3	Cytokinin oxidase/ dehydrogenase (<i>PsCKX</i>)	143
4.3.1.4	Pea Response Regulators (<i>PsRR</i>)	144
4.3.2	Housekeeping/ reference genes identification and isolation	149
4.3.3	Optimisation of RT-qPCR	150
4.3.3.1	Reference genes normalisation	155
4.3.4	Relative expression of cytokinin biosynthesis, metabolic and response regulator genes in different tissues of <i>P. sativum</i> inoculated with <i>R. fascians</i> .	158
4.3.4.1	Relative expression of <i>R. fascians</i> cytokinin biosynthesis and metabolic genes in <i>P. sativum</i> and <i>R. fascians</i> cultures	159
4.3.4.2	Relative expression of cytokinin biosynthesis, metabolic and response regulator genes in tissues of <i>P. sativum</i> infected with <i>R. fascians</i>	161
4.3.4.2.1	Isopenteny transferase (<i>PsIPT</i>)	161
4.3.4.2.2	The Lonely Guy (<i>PsLOG</i>)	163
4.3.4.2.3	Cytokinin oxidases/ dehydrogenases (<i>PsCKX</i>)	170
4.3.4.2.4	Pea response regulators (<i>PsRR</i>)	175
4.4	Discussion	181

**CHAPTER 5 SOURCE-SINK TRANSITIONS IN *P. SATIVUM*
COTYLEDONS INFECTED WITH *R. FASCIANS***

5.1	Introduction	194
5.2	Materials and Methods	197
5.3	Results	197
	5.3.1 Chlorophyll content of <i>P. sativum</i> infected with <i>R. fascians</i>	197
	5.3.2 Identification and isolation of pea transporter genes (<i>PsSUT</i> and <i>PsAAP</i>)	203
	5.3.3 <i>In planta</i> quantitative expression of pea transporter genes in <i>P. sativum</i> infected with <i>R. fascians</i> strains	206
5.4	Discussion	214

CHAPTER 6 FINAL DISCUSSION AND FUTURE WORK 217

REFERENCES 227

APPENDICES 243

List of Figures

		Page
Figure 1.1	Structures of different naturally occurring cytokinin bases	3
Figure 1.2	Cytokinin conjugates with sugars, sugar phosphates and others	3
Figure 1.3	Current model of isoprenoid cytokinin biosynthetic pathways in higher plants and in the infected plant cells by <i>A. tumefaciens</i>	7
Figure 1.4	tZRMP biosynthesis by <i>A. tumefaciens</i>	9
Figure 1.5	Proposed mechanism of <i>A. tumefaciens</i> infection on plants	10
Figure 1.6	Reaction catalysed by the CKX enzyme	16
Figure 1.7	The two-component circuitry in cytokinin signalling in the past decade	21
Figure 1.8	Model of the cytokinin response pathway in <i>Arabidopsis</i>	23
Figure 1.9	Schematic representation and (putative function of the different regions of pFiD188	33
Figure 1.10	Schematic representation of the linear plasmid pFiD188 of the <i>R. fascians</i> strain D188 and the organisation of <i>att</i> and <i>fas</i> operons	37
Figure 1.11	Modulation of plant cytokinin signalling by <i>R. fascians</i> -originated cytokinins	44
Figure 2.1	Standardisation for medium for pea growth and inoculation of <i>R. fascians</i>	51
Figure 2.2	<i>P. sativum</i> experimental set up in a growth room	53
Figure 2.3	RNA integrity in a gel. RNA gel demonstrating intact and degraded RNA along with Millennium markers™	60
Figure 3.1	Confirmation of Koch's postulates by <i>R. fascians</i> virulent strain 602 infection on pea plants	71
Figure 3.2	PCR products for <i>fasD</i> and <i>fasE</i> genes in <i>R. fascians</i> isolates	72

Figure 3.3	PCR for sequencing of <i>RfIPT</i> , <i>RfLOG</i> and <i>RfCKX</i> genes in <i>R. fascians</i> virulent strain 602	74
Figure 3.4	PCR for detection of the <i>RfIPT</i> , <i>RfLOG</i> and <i>RfCKX</i> genes in <i>R. fascians</i> cultures	75
Figure 3.5	Phylogenetic tree of IPT	79
Figure 3.6	Phylogenetic tree of CKX	80
Figure 3.7	Phylogenetic tree of LOG	81
Figure 3.8	Growth curve of <i>R. fascians</i> avirulent (589) and virulent (602) strains	82
Figure 3.9	Growth stages of <i>P. sativum</i> infected with <i>R. fascians</i>	84
Figure 3.10	Morphology of <i>P. sativum</i> plants inoculated with <i>R. fascians</i> avirulent strain (589) and virulent strain (602)	85
Figure 3.11	Colonisation capacities of <i>R. fascians</i> strains 589 (Avirulent) and 602 (Virulent) in <i>P. sativum</i>	87
Figure 3.12	Scanning electron micrographs of <i>R. fascians</i> avirulent and virulent strain cultures	90
Figure 3.13	Surface colonisation of <i>R. fascians</i> on <i>P. sativum</i>	91
Figure 3.14	Surface colonisation of <i>R. fascians</i> on <i>P. sativum</i> at 5 dpi	92
Figure 3.15	Surface colonisation of <i>R. fascians</i> on <i>P. sativum</i> at 9 dpi	93
Figure 3.16	Surface colonisation of <i>R. fascians</i> on <i>P. sativum</i> at 11 dpi	95
Figure 3.17	Surface colonisation of <i>R. fascians</i> on <i>P. sativum</i> at 20 dpi	96
Figure 3.18	Surface colonisation of <i>R. fascians</i> on <i>P. sativum</i> at 25 dpi	97
Figure 3.19	Surface colonisation of <i>R. fascians</i> on <i>P. sativum</i> at 30 dpi	98
Figure 3.20	Surface colonisation of <i>R. fascians</i> on <i>P. sativum</i> at 35 dpi	99
Figure 3.21	Surface colonisation of <i>R. fascians</i> on <i>P. sativum</i> at 40 dpi	100
Figure 3.22	Surface colonisation of <i>R. fascians</i> on <i>P. sativum</i> at 45 dpi	101

Figure 3.23	Light micrographs showing the gram stained <i>R. fascians</i> avirulent isolates at 2 and 7 d growth in 523 media	103
Figure 3.24	Light micrographs showing the gram stained <i>R. fascians</i> virulent isolates at 2 and 7 d growth in 523 media	104
Figure 3.25	Light micrographs of transverse sections of <i>P. sativum</i> cotyledon with seed coat after 4 h imbibitions (4 hpi) in Klambt medium or <i>R. fascians</i> avirulent strain 589 and virulent strain 602	106
Figure 3.26	Light micrographs of transverse sections of <i>P. sativum</i> seed coat tissue without or with <i>R. fascians</i> avirulent strain 589 and virulent strain 602 at 2 d post inoculation (dpi)	107
Figure 3.27	Light micrographs of transverse sections of <i>P. sativum</i> cotyledon without or with <i>R. fascians</i> avirulent strain 589 and virulent strain 602 at 2 dpi	108
Figure 3.28	Light micrographs of longitudinal sections of <i>P. sativum</i> radicle without or with <i>R. fascians</i> avirulent strain 589 and virulent strain 602 at 2 dpi	109
Figure 3.29	Light micrographs of transverse section of <i>P. sativum</i> seed coat tissue with <i>R. fascians</i> avirulent strain 589 and virulent strain 602 at 5 dpi	110
Figure 3.30	Light micrographs of transverse section of <i>P. sativum</i> cotyledon tissue without or with <i>R. fascians</i> avirulent strain 589 and virulent strain 602 at 5 dpi	111
Figure 3.31	Light micrographs of longitudinal section of <i>P. sativum</i> root tissue without or with <i>R. fascians</i> avirulent strain 589 and virulent strain 602 at 5 dpi	112
Figure 3.32	Light micrographs of longitudinal section of <i>P. sativum</i> shoot tissue without or with <i>R. fascians</i> avirulent strain 589 and virulent strain 602 at 5 dpi	114
Figure 3.33	Light micrographs of transverse section of <i>P. sativum</i> cotyledon tissue without or with <i>R. fascians</i> avirulent strain 589 and virulent strain 602 at 9 dpi	115

Figure 3.34	Light micrographs of longitudinal section of <i>P. sativum</i> root without or with <i>R. fascians</i> avirulent strain 589 and virulent strain 602 at 9 dpi	116
Figure 3.35	Light micrographs of longitudinal section of <i>P. sativum</i> shoot without or with <i>R. fascians</i> avirulent strain 589 and virulent strain 602 at 9 dpi	117
Figure 3.36	Light micrographs of transverse section of <i>P. sativum</i> cotyledon tissue without or with <i>R. fascians</i> avirulent strain 589 and virulent strain 602 at 15 dpi	118
Figure 3.37	Light micrographs of longitudinal section of <i>P. sativum</i> root without or with <i>R. fascians</i> avirulent strain 589 and virulent strain 602 at 15 dpi	119
Figure 3.38	Light micrographs of longitudinal section of <i>P. sativum</i> shoot without or with <i>R. fascians</i> avirulent strain 589 and virulent strain 602 at 15 dpi	120
Figure 3.39	Light micrographs of transverse section of <i>P. sativum</i> cotyledon tissue without or with <i>R. fascians</i> avirulent strain 589 and virulent strain 602 at 25 dpi	121
Figure 3.40	Light micrographs of longitudinal section of <i>P. sativum</i> root without or with <i>R. fascians</i> avirulent strain 589 and virulent strain 602 at 25 dpi	122
Figure 3.41	Light micrographs of longitudinal section of <i>P. sativum</i> shoot without or with <i>R. fascians</i> avirulent 589 strain and virulent 602 strain at 25 dpi	123
Figure 3.42	Light micrographs of transverse section of <i>P. sativum</i> cotyledon tissue without or with <i>R. fascians</i> avirulent strain 589 and virulent strain 602 at 35 dpi	124
Figure 3.43	Light micrographs of longitudinal section of <i>P. sativum</i> root without or with <i>R. fascians</i> avirulent strain 589 and virulent strain 602 at 35 dpi	125
Figure 3.44	Light micrographs of longitudinal section of <i>P. sativum</i> shoot without or with <i>R. fascians</i> avirulent strain 589 and virulent strain 602 at 35 dpi	126
Figure 4.1	PCR products for <i>PsIPT1</i> and <i>PsIPT2</i>	138

Figure 4.2	Phylogenetic tree of <i>IPT</i>	142
Figure 4.3	Phylogenetic tree of <i>LOG</i>	145
Figure 4.4	Phylogenetic tree of <i>CKX</i>	146
Figure 4.5	Phylogenetic tree of <i>RR</i>	148
Figure 4.6	Total RNAs isolated using TRIzol reagent	150
Figure 4.7	Rotor-Gene Q quantification of cDNA from pea tissues assessment with two reference genes <i>UI8S</i> and <i>PsGAP</i> and one target gene <i>PsIPT1</i>	152
Figure 4.8	The RT-qPCR performed at 58°C annealing temperature	153
Figure 4.9	Gel analysis of PCR products	153
Figure 4.10	The RT-qPCR reaction of reference gene <i>PsEF</i> with PsEFF1R1 primer	156
Figure 4.11	The expression (Ct values) of four reference genes	157
Figure 4.12	Relative expressions of <i>RfIPT</i> , <i>RfLOG</i> and <i>RfCKX</i> in <i>P. sativum</i> cotyledon, root, shoot tissue and <i>R. fascians</i> cultures	160
Figure 4.13	Relative expression of <i>PsIPT1</i> , 2, 3 and <i>RfIPT</i> in <i>P. sativum</i> cotyledon tissue	164
Figure 4.14	Relative expression of <i>PsIPT1</i> , 2, 3 and <i>RfIPT</i> in <i>P. sativum</i> root tissue	165
Figure 4.15	Relative expression of <i>PsIPT1</i> , 2, 3 and <i>RfIPT</i> in <i>P. sativum</i> shoot tissue	166
Figure 4.16	Relative expression of <i>PsLOG1</i> , 6, 8 and <i>RfLOG</i> in <i>P. sativum</i> cotyledon tissue	168
Figure 4.17	Relative expression of <i>PsLOG1</i> , 6, 8 and <i>RfLOG</i> in <i>P. sativum</i> root tissue	169
Figure 4.18	Relative expression of <i>PsLOG1</i> , 6, 8 and <i>RfLOG</i> in <i>P. sativum</i> shoot tissue	171
Figure 4.19	Relative expression of <i>PsCKX1</i> , 2, 3, 4, 5 and <i>RfCKX</i> in <i>P. sativum</i> cotyledons tissues	173

Figure 4.20	Relative expression of <i>PsCKX1</i> , 2, 3, 4, 5 and <i>RfCKX</i> in <i>P. sativum</i> root tissues	174
Figure 4.21	Relative expression of <i>PsCKX1</i> , 2, 3, 4, 5 and <i>RfCKX</i> <i>P. sativum</i> shoot tissues	176
Figure 4.22	Relative expression of <i>PsRR3</i> , 5, 6 and 9 in <i>P. sativum</i> cotyledon tissues	178
Figure 4.23	Relative expression of <i>PsRR3</i> , 5, 6 and 9 in <i>P. sativum</i> root tissues	179
Figure 4.24	Relative expression of <i>PsRR3</i> , 5, 6 and 9 in <i>P. sativum</i> shoot tissues	180
Figure 5.1	Morphology of <i>P. sativum</i> plants and cotyledons infected with or without <i>R. fascians</i>	199
Figure 5.2	Total chlorophyll content in cotyledon tissues of <i>P. sativum</i> infected with <i>R. fascians</i>	200
Figure 5.3	Total chlorophyll content in root tissues of <i>P. sativum</i> infected with <i>R. fascians</i>	201
Figure 5.4	Total chlorophyll content in shoot tissues of <i>P. sativum</i> infected with <i>R. fascians</i>	202
Figure 5.5	Phylogenetic tree of <i>SUT</i>	204
Figure 5.6	Phylogenetic tree of <i>AAP</i>	205
Figure 5.7	Relative expression of <i>PsSUT1a</i> , 2 and <i>PsSUF1</i> in <i>P. sativum</i> cotyledon tissues	209
Figure 5.8	Relative expression of <i>PsAAP7b</i> , <i>PsAAP7a(1)</i> , <i>PsAAP7a(2)</i> and <i>PsAAP8a</i> in <i>P. sativum</i> cotyledon tissues	210
Figure 5.9	Relative expression of <i>PsAAP8a</i> , <i>PsAAP2a (1)</i> and <i>PsAAP2a (4)</i> in <i>P. sativum</i> cotyledon tissues	211
Figure 5.10	Relative expression of <i>PsSUF1</i> and <i>PsAAP2a(1)</i> in <i>P. sativum</i> shoot	213

List of Tables

Table 1.1	Some of the examples of host ranges of <i>Rhodococcus fascians</i>	27
Table 1.2	Key genes involved in cytokinin biosynthesis and metabolism	35
Table 1.3.	Cytokinins detected in the culture supernants of <i>Rhodococcus fascians</i>	39
Table 3.1	<i>Rhodococcus fascians</i> strains used in this study and their details	68
Table 3.2	<i>Rhodococcus fascians</i> primers	73
Table 3.3	Virulence / avirulence classifications of various <i>Rhodococcus fascians</i> isolates	76
Table 4.1	Specific PCR <i>PsIPT</i> primers	139
Table 4.2	Degenerate <i>PsIPT</i> PCR primers	140
Table 4.3	Degenerate <i>PsLOG</i> PCR primers	141
Table 4.4	Specific <i>PsCKX</i> primers	143
Table 4.5	Sequences of the selected RT-qPCR primers for expression analysis of <i>P. sativum</i> and <i>R. fascians</i> genes of interest and reference genes	154
Table 5.1	Sequences of the selected RT-qPCR primers used for expression analysis of <i>P. sativum</i> transporter genes of interest	206

Abbreviations

2MeS	2-methylthio
2MeScZ	2-methylthio- <i>cis</i> -zeatin
2MeScZR	2MeScZ riboside
2MeSiP	2-methylthio-isopentenyladenine
2MeSiPR	2-methylthioisopentenyladenosine
2MeStZ	2-methylthio- <i>trans</i> -zeatin
2MeStZR	2MeScZ riboside
ADP	adenosine diphosphate
AHK	<i>Arabidopsis</i> histidine kinase
AMP	adenosine monophosphate
ARR	<i>Arabidopsis</i> response regulator
avir-cot	<i>R. fascians</i> avirulent strain 589 inoculated cotyledon
avir-root	<i>R. fascians</i> avirulent strain 589 inoculated root
avir-shoot	<i>R. fascians</i> avirulent strain 589 inoculated shoot
BLAST	basic local alignment tool
bp	base pairs
cDNA	complementary DNA
CKX	cytokinin oxidase/dehydrogenase
con-cot	control cotyledon
con-root	control root
con-shoot	control shoot
cZ	<i>cis</i> -zeatin
DMAPP	dimethylallyl diphosphate
dpi	days post inoculation
DTT	dithiothreitol
DZ	dihydrozeatin
FAD	flavine adenine dinucleotide
Fas	fasciation
GUS	β -glucuronidase
HMBDP	hydroxymethylbutenyldiphosphate
hpi	hour post imbibition (inoculation)
IAA	indole-3-acetic acid

iP	isopentenyladenine
iP9G	isopentenyl-9-glucoside
iPA	isopentenyladenosine
iPRMP	isopentenyl adenosine monophosphate
IPT	isopentenyltransferase
LOG	The Lonely Guy
MBP	maltose binding protein
MEP	methylerythritol
mRNA	messenger RNA
ms-iPA	methylthio-isopentenyladenosine
MVA	mevalonate
ORF	open reading frame
PAI	pathogenicity island
PCR	polymerase chain reaction
RNA	ribonucleic acid
RR	response regulator
RT-qPCR	reverse transcriptase quantitative polymerase chain reaction
SD	standard deviation
SUF	sucrose facilitator
SUT	sucrose transporter
tRNA	transfer RNA
tZ	<i>trans</i> -zeatin
vir-cot	<i>R. fascians</i> virulent strain 602 inoculated cotyledon
vir-root	<i>R. fascians</i> virulent strain 602 inoculated root
vir-shoot	<i>R. fascians</i> virulent strain 602 inoculated shoot
Z	zeatin
ZR	zeatin riboside

CHAPTER 1 INTRODUCTION

1.1 Background

The study of plant-pathogen interactions is a major research field. While plant hormones play key roles in plant developmental processes and growth, they are also involved in responses to pathogens (Robert-Seilaniantz et al., 2007). Certain gall-forming pathogens manipulate the plant hormones, cytokinin and auxin, to facilitate the infection processes (Anderson et al., 2010). One such group includes *Agrobacterium tumefaciens*, *A. rhizogenes*, *Pseudomonas savastanoi* pv. *syringae*, *Pantoea agglomerans* and *Rhodococcus fascians* (Choi et al., 2011, Lee et al., 2009, Pertry et al., 2010, Robert-Seilaniantz et al., 2007).

Gall-forming pathogens interfere with plant homeostasis mechanisms either by producing the plant hormones themselves such as *P. savastanoi* pv. *syringae* and *P. agglomerans* or by modifying the host hormone metabolism through gene transfer as exemplified by *A. tumefaciens* and *A. rhizogenes* (Jameson, 2000, Robert-Seilaniantz et al., 2007). Galls incited by *A. tumefaciens* are a consequence of the integration into the plant genome of genes conferring overproduction of cytokinin and auxin in plant tissues. Deletion of the cytokinin biosynthesis gene (the isopentenyl transferase (*IPT*) gene) from the transferred DNA results in rooty galls, whereas, the deletion of the auxin genes (tryptophan -2- monooxygenase and indoleactamide hydrolase) results in the formation of shooty galls (Morris, 1987). Changes in the ratio of cytokinin: auxin leading to shooty or rooty galls follows the classic organogenesis model of (Skoog and Miller, 1957), whereby a higher ratio of cytokinin: auxin promotes shoot organogenesis and the opposite promotes root organogenesis.

The focus of this study is the plant pathogen *R. fascians*. Infection by *R. fascians* causes leafy deformation, fasciation, leafy galls and formation of witches' broom in a wide range of monocot and dicot plants (Vereecke et al., 2000, Vereecke et al., 2003). As infection of the plants by *R. fascians* causes shooty and leafy galls, the malformations could be expected to, but do not, contain elevated levels of cytokinin relative to auxin (Eason et al., 1996, Galis et al., 2005b, Manes et al., 2001).

The key to *Rhodococcus* "breaking the rule" may lie with the interaction between cytokinin synthase (FasD) and lysine decarboxylase/ phosphoribohydrolase (FasF) (the enzymes the bacterium uses to synthesise cytokinin) and cytokinin oxidase / dehydrogenase (CKX), the

enzyme that the plant uses to degrade active cytokinins (Galuszka et al., 2001, Houba-Herlin et al., 1999, Morris et al., 1999, Pertry et al., 2010).

In this thesis, an attempt has been made to study the expression of plant and bacterial genes coding for cytokinin synthesis and degradation through interaction of cytokinin synthase (*IPT*), cytokinin activating (*LOG*) and cytokinin degrading genes (*CKX*) present in both pea (*Pisum sativum*) and *R. fascians* during the infection process.

1.2 CYTOKININS

Cytokinins (CK) are a group of mobile plant hormones that are involved in a wide variety of plant growth and development processes. From the time kinetin was first isolated from autoclaved products of herring sperm DNA as a cell division promoting factor in 1955 (Armstrong and Firtel, 1989, Miller et al., 1955 a, Miller et al., 1955 b), a number of compounds with cytokinin activity have been identified, including trans-zeatin (tZ) as a naturally occurring cytokinin (Letham, 1963), diphenylurea as a synthetic compound (Mok and Mok, 2001, Shantz and Steward, 1955) and several natural CKs with aromatic side chains (Strnad, 1997).

The first natural cytokinin, zeatin, was isolated from maize (*Zea mays*) embryos (Letham, 1963). Since then many naturally occurring compounds of cytokinins have been identified. The naturally occurring cytokinins are adenine derivatives which are classified into two groups depending on the structure of side chain: isoprenoid-type cytokinins are N⁶-isopentyladenine (iP) derivatives and aromatic cytokinins carrying an aromatic side chain at the N⁶ terminus. (Mok and Mok, 2001, Sakakibara, 2006). The isoprenoid cytokinins are further distinguished by the absence or presence of hydroxyl groups and the stereo-isomeric position of the side chain leading to the basic four forms: N⁶-isopentenyl adenine (iP), trans-zeatin (tZ), cis-zeatin (cZ) and dihydrozeatin (DZ) (Figure 1.1). All natural cytokinin nucleobases have the corresponding nucleosides, nucleotides and glycosides (Figure 1.2).

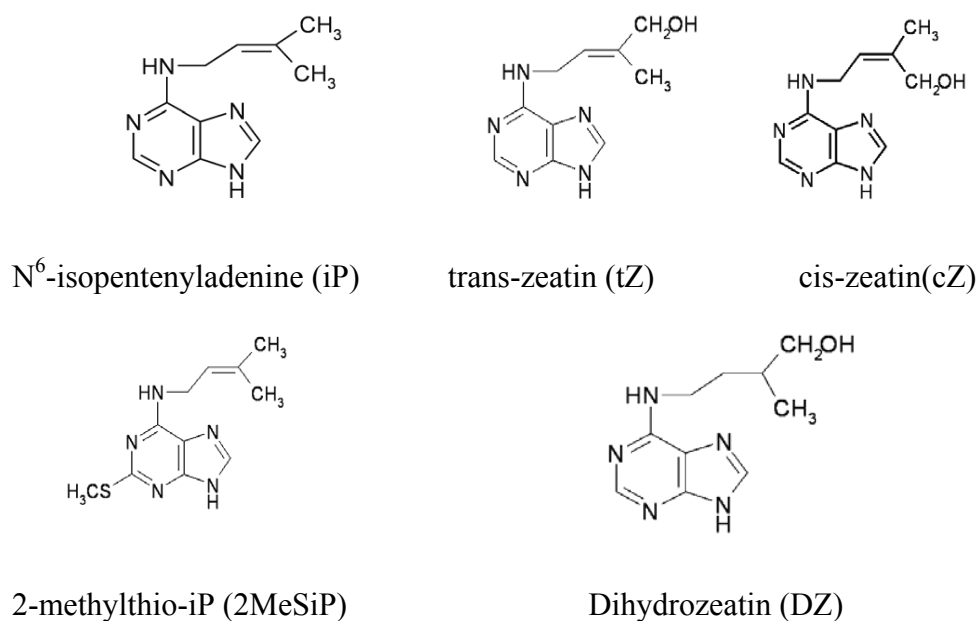


Figure 1.1: **Structures of different naturally occurring cytokinin bases** (Sakakibara, 2006). Reproduced with permission from Annual Reviews.

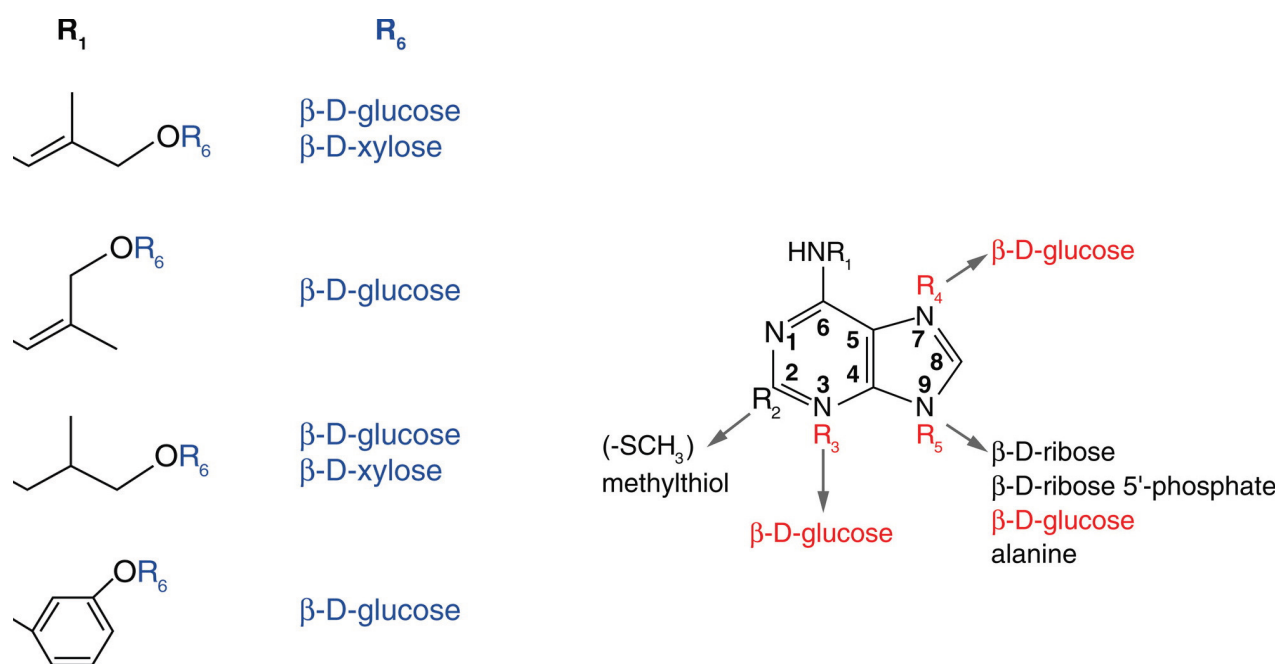


Figure 1.2. **Cytokinin conjugates with sugars, sugar phosphates and others.**

O-Glycosylation of side chain (Coloured in blue) is catalysed by zeatin O-glycosyltransferase or O-xylosyltransferase. N-glycosylation of adenine moiety (coloured in red) is catalysed by cytokinin N-glycosyltransferase (Sakakibara, 2006). Reproduced with permission from Annual Reviews.

Differences have been found in the activity and stability of the different cytokinin forms *in vivo*, even though there is no widely accepted mode of action of these structural variants (Kamada-Nobusada and Sakakibara, 2009). In cucumber and *Amaranthus caudatus* bioassay, it was seen that among the cytokinin nucleobases (tZ, iP and cZ), tZ was most active and cZ was least active form (Kamínek et al., 1979). By measuring the cytokinins-ligand affinity to cytokinin (CK) receptors the relative biological activities of cytokinins were estimated. The *Arabidopsis* cytokinin receptors (AHK3 and AHK4/ WOL/CRE) in *in vitro* and *in vivo* studies showed that iP and tZ have much higher affinities than cZ and DZ (Romanov et al., 2006, Spichal et al., 2004). However, a cytokinin receptor in maize (ZmHK1) responded to cZ and tZ with similar sensitivity (Yonekura-Sakakibara et al., 2004) which implies that the relative activities of cytokinins might vary among plant species.

Cytokinin causes *de novo* organ formation from cultured tissues (Skoog and Miller, 1957), it stimulates leaf expansion and seed germination (Miller, 1961), delays leaf senescence, enhances stress tolerance, vascular differentiation, chloroplast biosynthesis, nutrient balance, and root, shoot and inflorescence growth and branching (Muller and Sheen, 2007) and promotes the outgrowth of axillary buds (Chatfield et al., 2000). Cytokinin has been considered as a crucial regulator of meristem function, where cytokinin-deficient plants showed decreased size of the shoot apical meristem (SAM) and organ primordia formation (Werner et al., 2003, Werner et al., 2001). Over-expression of the cytokinin synthase gene in plants indicated that cytokinins stimulate leaf growth via cell division, control vascular development by stimulating cambial activity and influence reproductive development and embryo maturation (Werner et al., 2003). Cytokinin receptor mutants showed that cytokinins delay leaf senescence by retaining chlorophyll, regulate seed size and germination and control cytokinin metabolism (Riefler et al., 2006). The diverse and specific expression patterns of cytokinin biosynthesis (*IPT*, *LOG*) and metabolism (*CKX*) genes independently suggest a wide range of developmental functions from the ovule, embryo, primary and lateral root primordia, shoot meristem and veins to flowers (Hirose et al., 2008, Kuroha et al., 2009, Miyawaki et al., 2004, Werner et al., 2003).

1.2.1 Cytokinin biosynthesis and metabolism

Cytokinin biosynthesis was previously believed to be restricted only to plant roots, with the cytokinin and then distributed to other parts of plant, but now it is known that many parts of

the plant are capable of synthesising cytokinins (Miyawaki et al., 2004, Takei et al., 2004a). In plants, based on the origin of the side chain donor, there are two pathways for isoprenoid production, the mevalonate (MVA) pathway, which also operates in animals, fungi, Archaea and a few bacteria, and which is located in the cytosol and mitochondria (Rohmer et al., 1993); and the methylerythritol phosphate (MEP) pathway, which is localised in plastids (Hecht et al., 2001). In the MVA pathway condensation of three acetyl-CoA molecules leads to mevalonate, which on phosphorylation produces isopentenyl diphosphate which can be isomerised to dimethylallyldiphosphate (DMAPP). The MEP pathway yields 4-hydroxy-3-methyl-2-(E)-butenyldiphosphate (HMBDP) from reduction of methylerythritol phosphate (Frébert et al., 2011). Both HMBDP and DMAPP work as cytokinin precursors in cytokinin biosynthesis (Krall et al., 2002, Sakakibara, 2005).

It has been shown that there are two distinct cytokinin biosynthesis pathways: one is the direct pathway, also called the *de novo* biosynthetic pathway; and the second is referred to as the indirect tRNA pathway. The current model of *de novo* cytokinin biosynthesis as described by Hirose et al. (2008), involves the isopentenyltransferase (IPT) enzyme in the initial step. The plant IPTs uses ADP and ATP as the adenine moiety (Brugière et al., 2008, Kakimoto, 2003). The initial major product formed by IPT is an iP nucleotide such as iP riboside 5'-triphosphate (iPRTP) or iP riboside 5'-diphosphate (iPRDP) using dimethylallyl diphosphate (DMAPP) and ATP or ADP as precursors (Kakimoto, 2001, Sakakibara, 2005). The iP nucleotides are converted to tZ nucleotides by cytochrome P450 mono-oxygenases, *CYP735A1* and *CYP735A2* in *Arabidopsis* (Takei et al., 2004a). The iP- and tZ- nucleotides are converted to biologically active nucleobases by dephosphorylation and deribosylation, but the enzymes involved have not been identified. Recently, a novel pathway was identified which directly releases the active cytokinin from the nucleotide. The key enzyme is a cytokinin nucleoside 5'-monophosphate phosphoribohydrolase, and the gene responsible is known as the Lonely Guy (*LOG*) (Kurakawa et al., 2007).

The indirect pathway (Figure 1.3) involves binding of methylallyl diphosphate (DMAPP) to an adenine base of the anticodon region of tRNA. This step is catalysed by tRNA-isopentenyltransferase (tRNA-IPT). Specific tRNA species can undergo prenylation at the adenine adjacent to the 3'-end of the anticodon by tRNA-IPT (Murai, 1994). Prenylated – tRNA has a cis-hydroxyl group, thus degradation of prenylated tRNA generates cZ (Kamada-

Nobusada and Sakakibara, 2009). It has been suggested that due to slow turnover rates and lack of tissue specificity for tRNA breakdown suggests that this is not the predominant pathway of cytokinin biosynthesis in plants (Mok and Mok, 2001, Oka, 2003). The *MiaA* gene is thought to catalyse the transfer of a DMAPP side chain to tRNA in bacteria (Connolly and Winkler, 1991, Gray et al., 1992). Kakimoto et al. (2001) and (Takei et al. 2001a) showed that, based on phylogenetic analysis, *AtIPT2* and *AtIPT9* from *Arabidopsis* are similar to *MiaA*.

1.2.1.1 Biosynthesis of cytokinin in plants and microbes

Cytokinin biosynthesis in bacteria and plants differs in some aspects (Sugawara et al. 2008) (Figure 1.4). In bacteria, IPT enzymes utilise AMP as substrate, while purified *AtIPT4* from *Arabidopsis* uses ATP and ADP preferentially over AMP as a substrate. So, the product of the plant enzyme is likely to be isopentenyladenosine-5'-triphosphate (iPTP) and isopentenyladenosine-5'-diphosphate (iPDP) (Takei et al., 2001a).

Research on the substrate preference and subcellular localisation of the Tmr from *A. tumefaciens* showed that this enzyme is targeted to the plastids of the infected plant cells and uses 1-hydroxy-2-methyl-2-(E)-butenyl 4-diphosphate (HMBDP) from methylerythritol phosphate (MEP) pathway as the major substrate and trans-zeatin riboside 5' monophosphate (tZMP) can be directly converted to trans-zeatin riboside (tZR) without P450 monooxygenase-mediated hydroxylation (Sakakibara, 2005). Abe et al. (2007) found that the purified recombinant IPT from mulberry accepts dADP (deoxyadenosine diphosphate, dATP as prenyl acceptors and IPP (isopentenyl diphosphate), HMBDP and GPP (geranyl diphosphate) as prenyl donors, to produce a series of cytokinin analogues and this enzyme also produces trans-zeatin riboside phosphates from HMBDP.

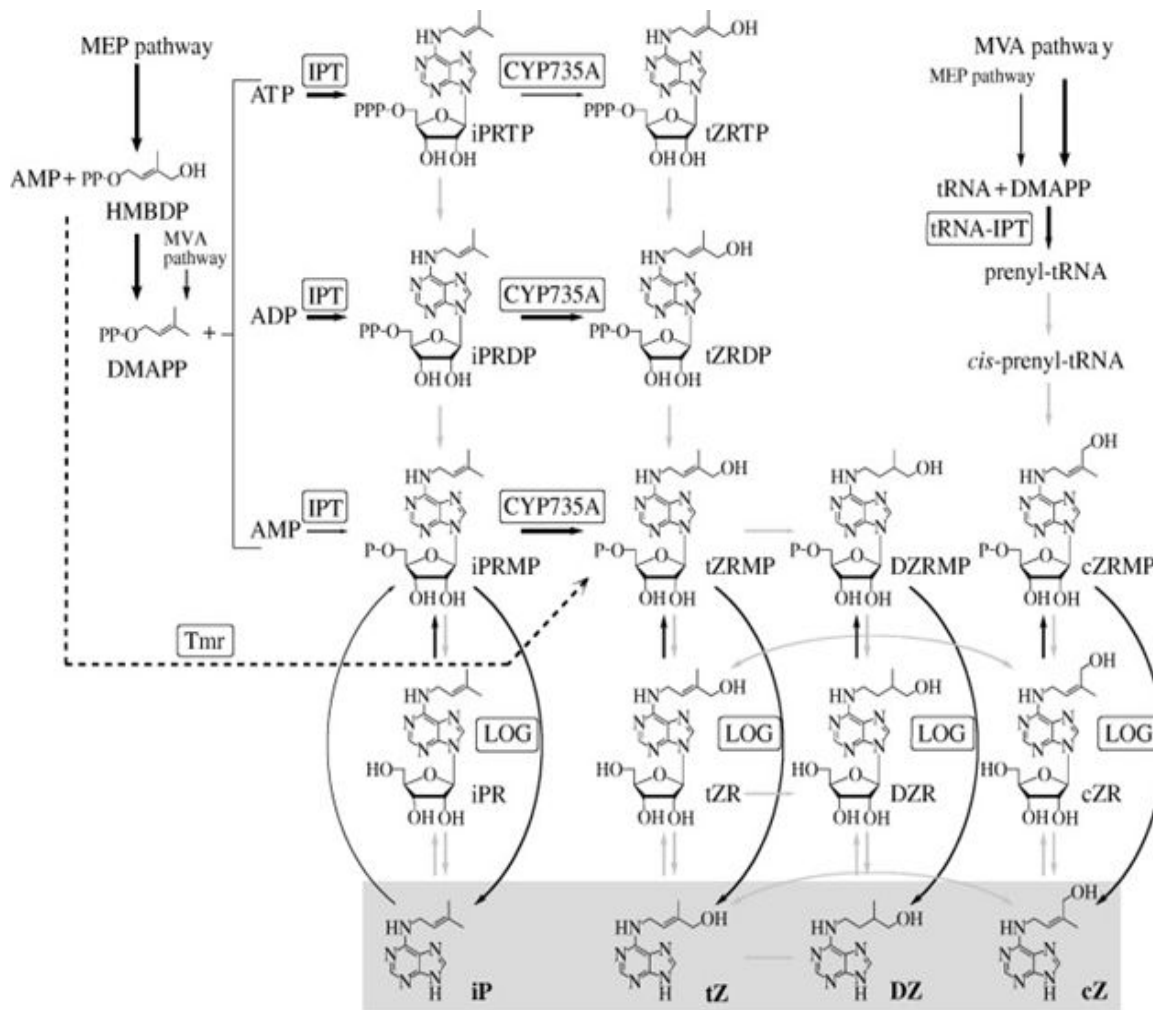


Figure 1.3 Current model of isoprenoid cytokinin biosynthetic pathways in higher plants and in infected plant cells by *A. tumefaciens*. (Kamada-Nobusada and Sakakibara 2009).

Reproduced with permission from Elsevier Limited.

In *Arabidopsis*, two pathways were suggested for the production of cytokinin: an iPRMP independent (Åstot et al., 2000) and an iPRMP-dependent pathway (Takei et al., 2004b). When zeatin is formed via iP, this occurs by hydroxylation of the prenyl side chain mediated by two cytochrome P450 monooxygenases, *CYP735A1* and *CYP735A2* (Figure 1.3). These enzymes were shown to preferentially hydroxylate iP nucleotides over iPR and iP. Thereby producing mainly tZ. The *cis*-isomer was produced at a negligible level (Takei et al., 2004b). tZ can be further converted to dihydrozeatin by a reductase, which was detected in *Phaseolus vulgaris* seeds (Mok and Mok, 2001). In the iPRMP-independent pathway, zeatin would be produced by directly transferring a hydroxylated side chain precursor to adenine nucleotides (Åstot et al., 2000) and indeed, *AtIPT7* was able to use HMBDP as well as DMAPP as a side

chain donor (Takei et al., 2003). *AtIPT1*, 3, 5 seemed to be correlated with iP as well as tZ production and are localised to plastids, where the MEP pathway, delivering HMBDP as well as DMAPP as a side chain donor, is active. This suggested that these proteins could directly produce tZ (Kasahara et al., 2004, Miyawaki et al., 2006). However, their over-expression resulted predominantly in iP accumulation and labelling experiments in wild type and *AtIPT1* over-expressing *Arabidopsis* plants indicated that DMAPP is the main side chain donor for tZ production *in planta* (Sakakibara et al., 2005, Sun et al., 2003). Mevastatin, an MVA pathway inhibitor, reduced iPRMP-independent tZ biosynthesis, suggesting that the side chain precursor is delivered via the MVA pathway (Åstot et al. 2000). Since an extensive fraction of the cZ side chain is delivered via the MVA pathway (Kasahara et al., 2004), another hypothesis proposed that iPRMP-independent tZ biosynthesis *in planta* could proceed via cZ derivatives (Sakakibara et al., 2005). The produced cZ could then subsequently be converted to tZ mediated by a *cis-trans* isomerase (Figure 1.3), although to date this enzyme has only been detected in *P. vulgaris* (Bassil et al., 1993).

Finally, the biologically active cytokinin forms are thought to be the free bases. There are two distinct pathways to convert cytokinin nucleotides to their free bases (Figure 1.3). The first one involves a two-step reaction in which the cytokinin nucleotides are subsequently dephosphorylated and deribosylated. Partially purified wheat germ extracts exhibited high 5'-ribonucleotide phosphohydrolase activity towards AMP and iPMP, while ADP and ATP were dephosphorylated at a lower rate (Chen and Kristopeit, 1981a) and also exhibited adenosine nucleosidase activity towards adenosine and iPR (Chen and Kristopeit, 1981b). However, to date, the corresponding genes have not been identified. More recently, a second free base releasing pathway was discovered in rice, where the *LONELY GUY (LOG)* gene encodes a protein with cytokinin-specific phosphoribohydrolase activity, which results in the direct liberation of free-base forms from cytokinin monophosphate nucleotides. A homologous *LOG* gene family has also been detected in the *Arabidopsis* genome (Kurakawa et al., 2007).

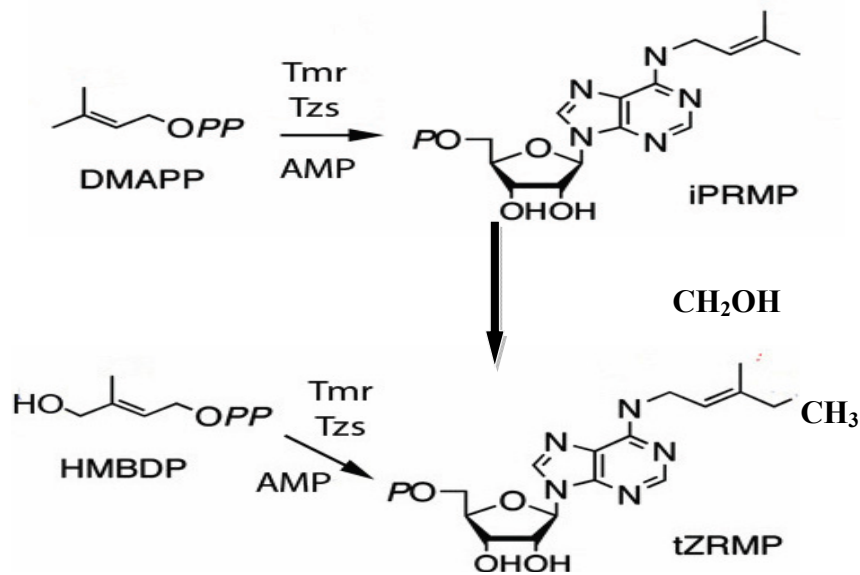


Figure 1.4 tZRMP biosynthesis by *A. tumefaciens* via an iPRMP-dependent pathway by hydroxylation of iPRMP or via an independent pathway by using HMBDP as a side chain donor. Cited from Pertry (2009). Reproduced with permission from <http://hdl.handle.net/1854/LU-529624>

Unlike *A. thaliana* IPTs, *Agrobacterium* IPTs, *Tmr* and *Tzs*, catalyse the N-prenylation of AMP using DMAPP or HMBDP as an isoprene donor in vitro (Blackwell and Horgan, 1994, Sakakibara et al., 2005, Sugawara et al., 2008). The bacterial enzyme does not utilise ATP or ADP (Figure 1.4). Isotope-tracer experiments by Sakakibara et al. (2005) verified that HMBDP and not DMAPP was the major substrate of *Tmr* in planta after infection by *A. tumefaciens*. They further showed that tZRMP is directly produced in *A. tumefaciens* infected plant cells by *Tmr* (Figure 1.4) and crown galls and *Tmr*-overexpressing transgenic plants exclusively contain tZ-type of cytokinins (Faiss et al., 1997, Morris, 1986).

Figure 1.5 clearly shows the mechanism of *A. tumefaciens* infection on plant which was proposed by Sakakibara et al. (2005). When *A. tumefaciens* infects plant the T-DNA region is transferred to the host cells and integrated into the nuclear genome. The cytokinin biosynthesis enzyme, *Tmr*, targets to and functions in the plastids of the infected host plant cell. It uses HMBDP, an intermediate of the MEP pathway, to produce high amounts of tZ without CYP735A-mediated hydroxylation (Sakakibara et al. 2005), to induce tumorigenesis. The auxin genes *Tms1* and *Tms2* are also expressed in the host and these may help in

repressing the host's CYP735-mediated cytokinin hydroxylation. The HMBDP pool available for Tmr may be larger than DMAPP in the plastids (Rohdich et al., 2002).

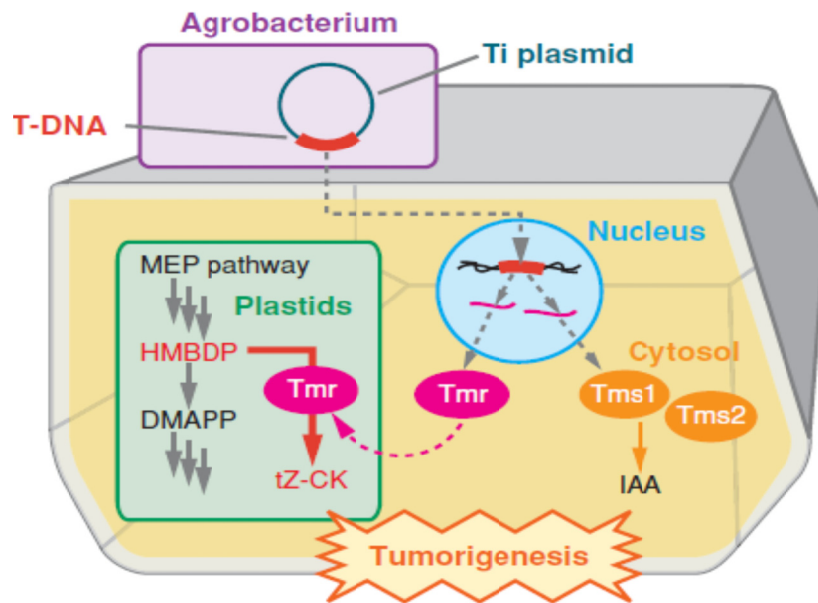


Figure 1.5 **Proposed mechanism of *A. tumefaciens* infection on plants** (Sakakibara 2006). Reproduced with permission from Annual Reviews.

1.2.1.2 Key enzymes involved in cytokinin biosynthesis

Isopentenyl Transferases (IPT): The enzyme considered to be the rate-limiting enzyme in isoprenoid cytokinin biosynthesis is adenosine phosphate- isopentenyl transferase (IPT; EC 2.5.1.27) (Kakimoto, 2001, Takei et al., 2001a) which catalyses N-prenylation of adenosine 5' phosphate (AMP, ADP or ATP) at the N⁶-terminus with dimethyl diphosphate (DMAPP) or 1-hydroxy-2-methyl-2-(E)-butenyl 4-diphosphate (HMBDP). This enzyme activity, leading to the formation of isopentenyladenine riboside monophosphate (iPRMP), was first demonstrated in a slime mold, *Dictyostelium discoideum* (Taya et al., 1978). The first cytokinin biosynthetic enzyme to be identified was from *A. tumefaciens* (Akiyoshi et al., 1984, Barry et al., 1984). The *tms* locus is composed of two genes responsible for production of auxin, and the *tmr* locus consists of a gene responsible for production of cytokinin. When the *tmr* (*IPT*) gene was cloned and expressed in *Escherichia coli*, the extract were shown to catalyse production of iPMP from DMAPP and AMP (Akiyoshi et al. 1984, Barry et al. 1984). The *tzs* gene is responsible for high level of cytokinin production in *A. tumefaciens*

strains (Morris et al., 1993). Other gall-forming bacteria, such as *P. syringae* pv. *savastanoi* (Powell and Morris, 1986), *P. agglomerans* (Lichter et al., 1995) and *R. fascians* (Crespi et al. 1992, Goethals et al. 2001) have genes resembling *tmr* and *tzs*, and these are considered responsible for cytokinin production in these bacteria (Akiyoshi et al., 1987).

IPTs have been identified in higher plants (Kakimoto, 2003, Sakamoto et al., 2006, Sakano et al., 2004, Takei et al., 2001a, Zubko et al., 2002). The *A. thaliana* genome encompasses a small gene family of seven adenosine phosphate *-IPT* members (*AtIPT1*, *AtIPT3-AtIPT8*) (Kakimoto 2001, Takei et al 2001a). These enzymes show diverse subcellular localisation (Kasahara et al. 2004): four *AtIPTs* (*AtIPT1*, *AtIPT3*, *AtIPT5* and *AtIPT8*) are localised in plastids (Kasahara et al., 2004) and *AtIPT3* and *AtIPT5* show relatively higher level of expression than the others (Miyawaki et al., 2004, Takei et al., 2001a). *AtIPT4* and *AtIPT7* were detected in the cytosol and mitochondria of both root and leaf cells (Kashara et al 2004). Some sequences of *AtIPT6* and *OsIPT6* appear to be pseudo-genes in some cultivars (Kamada-Nobusada and Sakakibara 2009). Rice has eight *IPTs* (*OsIPT1- OsIPT8*) (Sakamoto et al. 2006), involved in the N-prenylation step of cytokinin biosynthesis. *AtIPTs* and *OsIPTs* prefer ATP or ADP to AMP as prenyl acceptor, and utilise DMAPP as the prenyl-donor (Kakimoto 2001, Sakamoto et al. 2006) (Figure 1.3). In addition, *IPT* genes have been identified in petunia (Zubko et al., 2002), hop (Sakano et al. 2004), maize (Brugiere et al., 2008), pea (Tanaka et al., 2006), wheat (Song et al., 2012), Chinese cabbage (Liu et al., 2013) and other crops.

Each member of the *IPT* gene family has a specific expression pattern. For example, in *Arabidopsis*, the predominant expression of *AtIPT1* was seen in xylem, root tips, leaf axils, ovules and immature seeds, *AtIPT3* expression was seen in phloem tissues, *AtIPT4* and *AtIPT8* in immature seeds, *AtIPT5* in root primordia, upper part of young inflorescences and fruit abscission zones and *AtIPT7* in the endodermis of root elongation zones, trichomes and young leaves and some pollen tubes (Miyawaki et al. 2004). Tanaka et al. (2006) showed that the expression of *PsIPT1* and *PsIPT2* in *Pisum sativum* (pea) increased to a high level after decapitation of stems.

Besides the genes encoding *de novo IPTs*, the plant and bacterial genomes also include genes for tRNA isopentenyl transferases (tRNA-*IPTs*; EC2.5.1.8). These enzymes enable

N-prenylation of the adenosine bound to tRNA molecules and degradation of such a modified RNA mainly results in release of *cis*-zeatin [cZ, N6-(4-hydroxy-3-methyl-*cis*-2-butenyl) adenine] (Figure 1.3). tRNA-IPT is widely found in diverse organisms, from bacteria to animals and plants. *Arabidopsis* and rice have two genes for tRNA-IPT isozymes, *AtIPT2* and *AtIPT9* in *Arabidopsis* (Miyawaki et al. 2006) and *OsIPT9* and *OsIPT10* in rice (Sakamoto et al. 2006). Miyawaki et al. (2006) showed that a mutant deficient in both tRNA-IPTs resulted in low cZ content, whereas, levels of iP and tZ type cytokinins were unaffected. They also suggested that prenylated tRNA-degradation is the main pathway to supply cZ in *Arabidopsis*. As shown in Figure 1.3, the prenyl group of tZ and iP is mainly produced through the MEP pathway by *IPTs*, whereas a substantial part of cZ comes from the MVA pathway in *Arabidopsis*, where *AtIPT2*, is localised to the cytosol (Kasahara et al. 2004). Some enzymes have been identified are involved in regulation of this pathway: a zeatin *cis-trans*-isomerase, partly purified from bean seeds, was shown to play a critical role in conversion of *cis*-zeatin to physiologically active *trans*-zeatin (Bassil et al. 1993). In the case of bacteria, as discussed in Section 1.2.1, the *MiaA* gene is thought to catalyse the transfer of a DMAPP side chain to tRNA in bacteria to form *cis*-zeatin (Mathews et al., 1992). Recent structural studies on tRNA-IPTs from *Pseudomonas aeruginosa* (Xie et al., 2007) and *Saccharomyces cerevisiae* (Zhou and Huang, 2008) have revealed that *IPT* and tRNA-IPT share a conserved reaction mechanism and critical amino acid residues. The early calculations of the turnover rates of tRNA led to the suggestion that tRNA degradation was not a major pathway of cytokinin synthesis. However, tRNA-derived cytokinins cannot be neglected as some plant species such as maize and rice contain substantial amount of cZ- type cytokinins (Sakakibara 2006). The specific location of cytokinin moieties in the tRNAs at position 37 adjacent to the 3' end of the anticodon and their distribution in the tRNAs indicates the role of cytokinins in tRNA function (Prinsen et al., 1997).

Cytokinin biosynthesis via hydrolysis of tRNA to its constituents led to substantial contribution to the cytokinin pool in both plant pathogenic and symbiotic bacteria. Other cytokinin moieties attached to tRNA in bacteria include methylthio-derivatives. The plant-associated bacteria such as *Rhizobium leguminosarum*, *A. tumefaciens* and *R. fascians* were found to contain 2-methyl-thioribosylzeatin (ms^2io^6A) in their tRNAs (Cherayil and Lipsett, 1977). In the case of bacterial tRNAs, 2 methylthio-adenosine (2MeSiPR) might be a major cytokinin component (Prinsen et al., 1997). Anton et al. (2008) showed that RimO, a

MiaB-like enzyme, functions as a methylthiotransferases, and methylthiolates tRNA in *E. coli*.

Cytochrome P450 monooxygenases (*CYP735As*): The iP-nucleotides produced by isopentenyltransferase in plants undergo hydroxylation at the prenyl side-chain by cytochrome P450 monooxygenases to synthesise tZ-nucleotides. In *Arabidopsis*, two cytochrome P450 monooxygenases, *CYP735A1* and *CYP735A2*, catalyse the above reaction (Takei et al., 2004b). Takei et al. (2004b) showed that *CYP735As* utilises iP-nucleotides, but not iP-nucleosides (Figure 1.3), due to stereo-specificity of the reaction. cZ-nucleotides are not converted by *CYP735As* and also both *CYP735A1* and *CYP735A2* preferentially catalyse iPRMP and iPRDP rather than iPRTP.

‘The Lonely guy’ (LOG): The name *LOG* comes from its rice mutant phenotype in which maintenance of the shoot meristem is defective and flowers often contain only one stamen but no pistil, thus ‘lonely guy’ (Kurakawa et al., 2007). The idea that *LOG* functions in cytokinin metabolism during plant pathogens *A. rhizogenes* and *R. fascians* interaction with plants resulted in production of cytokinins and *LOG*-homologous genes (*riorf52* and *fasF* respectively) were located close to *IPT* genes in each bacterium (Crespi et al., 1994, Moriguchi et al., 2001). In the case of *R. fascians*, genes of the *LOG* homologues (*fasF*) and *IPT* (*fasD*) are co-transcribed as a single operon and releases cytokinin bases from their nucleotides (Crespi et al. 1994, Pertry et al. 2010).

LOG is annotated as a lysine decarboxylase, which catalyses the decarboxylation of L-lysine to generate cadaverine, a polyamine. The partially purified nucleosidases and nucleotidases from wheat germ, were found to not only react with cytokinin nucleotides and nucleobases but also to hydrolyse adenosine or AMP with higher specificity indicating a wide range of substrate specificity (Chen and Kristopeit, 1981a, Chen and Kristopeit, 1981b), whereas *LOG* specifically reacted with only cytokinin nucleoside 5'-monophosphate, but not with di- or triphosphates (Kurakawa et al., 2007).

Kurakawa et al. (2007) through *LOG* gene isolation and mapping of rice found four putative genes, *LOG2*, *LOG3*, *LOG4* and *LOG6* on chromosome 1. Through mutant studies, the *LOG* gene was isolated and subsequently it was found that there were ten genes that have high sequence similarity to *LOG* in the rice genome. *Arabidopsis* also has a similar number of

homologues (Kurakawa et al. 2007). These *LOG* gene families show a variety of expression patterns and, through *in situ* hybridisation analysis of *LOG* mRNA, it was found that *LOG* expression was restricted to a subset of cells in the meristem, and included the entire region of presumptive stem cells (Kurakawa et al. 2007). To examine the *in vivo* function of *LOG*, Kurakawa et al. (2007) examined the transcript levels of the cytokinin inducible response regulator genes (*OsRR1* and *OsRR5*) in the meristem and found that the *log6* mutant had lower active cytokinin levels in the shoot meristem. All these findings led to the conclusion that a *LOG*-dependent direct pathway could be dominant in the shoot meristem (Kurakawa et al. 2007) and that *LOG* is a cytokinin-activating enzyme that might regulate meristem activity.

To study the detailed mechanism of the direct activation pathway for active cytokinin synthesis, Kuroha et al. (2009) focused on *LOG*-like genes in *Arabidopsis*. *A. thaliana* *LOG* genes (*AtLOG1* to *AtLOG9*) were isolated with significant similarity to rice *LOG*. Through phylogenetic analysis with rice and moss it was shown that the *LOG*-like proteins diverged into two clades, where *AtLOG1* to *AtLOG8* belong to clade I, which includes the rice *LOG* gene family, and *AtLOG8* and *AtLOG9* belong to clade II along with moss *LOG*-like proteins. Through detailed analysis of seven *AtLOG* genes, Kuroha et al. (2009) demonstrated that *AtLOG1*, *AtLOG3*, *AtLOG4* and *AtLOG7* had similar substrate affinities (K_m) and catalytic efficiencies (k_{cat}/K_m) as rice *LOG*. *AtLOG*:GFP (green fluorescent protein) analysis showed that seven *AtLOGs* are localised in the cytosol and nuclei and through *AtLOG*_{pro}: GUS (β -glucuronidase) fusion genes differential expression of *LOGs* in *Arabidopsis* was seen during plant development: *AtLOG1* expressed in vascular tissues of root, cotyledon, shoot apical meristem, junction of stem and cauline leaf and in immature flowers; *AtLOG2* and *AtLOG3* had similar patterns of expression in root hairs, basal margins of immature leaves, root procambium, vascular tissues of immature leaves, axillary buds and ovular funiculus; *AtLOG4* expressed in immature vascular tissues of lateral roots, vascular tissues of cotyledon, shoots apical region and vascular tissues of stems; *AtLOG5* expressed in mature primary roots, immature leaves, axillary bud and ovule; *AtLOG7* expressed in root elongation region, cotyledon, immature leaves, pollen and immature trichomes; and *AtLOG8* expressed in mature roots and vascular tissue, cotyledons, flowers, stems and fruit abscission zones. These results indicate that expression of *AtLOGs* is spatially and quantitatively differentiated but overlaps in some tissues (Kuroha et al. 2009). Through these results it was seen that the

expression pattern of *AtLOGs* and *AtIPTs* (Miyawaki et al. 2004) overlap in lateral root primordia, fruit abscission zones, ovules and root and leaf vascular tissues, which suggests that the cytokinin nucleotides synthesised by *IPTs* in these sites and are activated locally by *LOGs* to act as autocrine or paracrine signals (Kuroha et al. 2009). The differential expression pattern of *AtIPTs* and *AtLOGs* also suggests that a portion of cytokinin precursors is translocated from cell to cell and/ or over a long range before becoming active forms. The *log3 log4 log7* mutant showed defects in shoot growth at the reproductive stage, whereas root growth was enhanced (Kuroha et al. 2009).

Recently, Tokunaga et al. (2012) analysed the metabolic flow of cytokinin activation in *Arabidopsis log* multiple mutants using a stable isotope-labeled tracer (iPR(+15) and iPR(+10)), quantified by liquid chromatography-mass spectrophotometry (LC-MS). In the case of young seedlings of the *Atlog1log2log3log4log7* mutant, the levels of tZRPs(+15) and tZR(+15) were significantly elevated, where tZR(+15) is the product of dephosphorylation of tZRPs(+15). The tZ(+10) and tZ7G(+10) were reduced. Tokunaga et al. (2012) showed that the conversion rate from the cytokinin nucleoside to the nucleobase in the two- step pathway was much slower than the *LOG*-catalysed conversion from nucleotide to nucleobase and also that *LOG*-dependent pathway is predominately mediated during the vegetative growth. Tokunaga et al. (2012) suggested that *AtLOG7* is the major contributor to the cytokinin activation in the whole plants because *log1log2log3log4log5log8* sextuple mutant showed a milder phenotype than *log3log4log7* triple mutant. It was seen that *AtLOG7* was required for maintenance of shoot apical meristem size and normal root growth along with *AtLOG3* and *AtLOG4* (Tokunaga et al., 2012). In this study, *AtLOG6* and *AtLOG9* were not considered because no functional *AtLOG6* and *AtLOG9* mRNAs have been detected in *Arabidopsis* (Kuroha et al. 2009).

1.2.1.3 Cytokinin inactivation

Cytokinin oxidase/ dehydrogenase (CKX): The first report of oxidative cleavage of cytokinins on conversion of labelled isopentenyladenine to adenine in crude tobacco cell culture extracts was reported in 1971 (Pačes et al., 1971). Whitty and Hall (1974) cited by Frébort et al. (2011) then described similar activity in *Zea mays* kernels and coined the name cytokinin oxidase. This enzyme leads to irreversible inactivation by cytokinin oxidase/ dehydrogenases (*CKX*; EC1.5.99.12), oxidative cleaves the N⁶- side chain of cytokinin bases

and ribosides to yield adenine and adenosine respectively (Figure 1.6). This enzyme is a flavin adenine dinucleotide- containing oxidoreductase that selectively cleaves the unsaturated N⁶ side chain from zeatin, iP and their corresponding ribosides (Ma, 2008). *CKX* is believed to be responsible for most of the metabolic cytokinin inactivation and plays an important role in maintaining cytokinin homeostasis in many plant species (Mok and Mok, 2001). The genes that encode *CKX* were first isolated from maize (Houba-Herlin et al., 1999, Morris et al., 1999). From then on putative or characterised *CKX* genes have been reported in several plants including *Arabidopsis* (seven *AtCKX* genes), rice (eleven *OsCKX* homologues), barley, wheat, maize (thirteen *ZmCKX*), orchid, cotton, *Medicago truncatula* and pea (two *PsCKX*) (Bilyeu et al., 2001, Galuszka et al., 2004, Wang et al., 2009, Werner et al., 2006). *CKX* activity was also detected in two non-plant species: the slime mold *Dictyostelium discoideum* (Armstrong and Firtel, 1989) and, albeit at extremely low levels, in *Saccharomyces cerevisiae* (Schmulling et al., 2003). Moreover, putative *CKX*s have also been found in *Nostoc*, a cyanobacterium (Werner et al., 2006) and two actinomycetes, *R. fascians* (Crespi et al. 1994) and *S. turgidiscabies* (Joshi and Loria 2007).

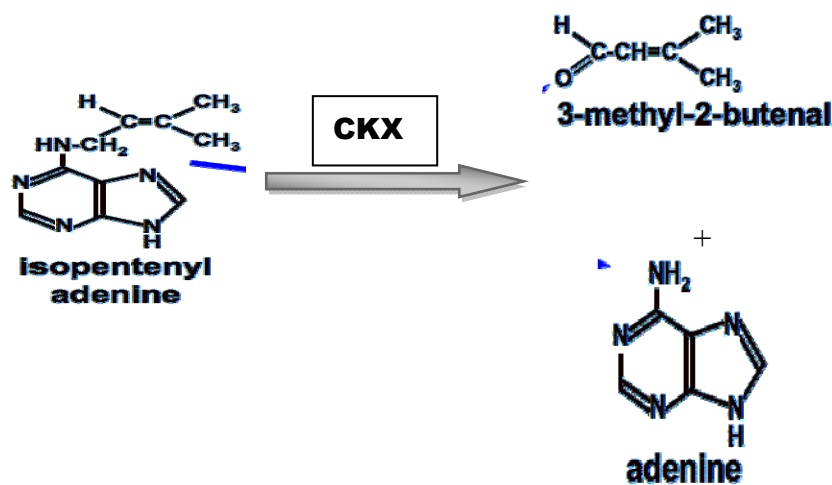


Figure 1.6 Reaction catalysed by the CKX enzyme

Of the five *CKX* gene family members in *Arabidopsis*, systematic evaluation in tobacco revealed that *CKX2*, *CKX4* and *CKX6* showed highest activity with the free bases iP and tZ, while other *CKX* gene families, unexpectedly, preferred glucosides or nucleotides as substrates (Galuszka et al., 2007). The *CKX* genes show relatively high level of sequence similarity and contain several conserved domains (Schmulling et al., 2003). The location of

these genes differed, for instance in the case of *Arabidopsis*, two (*AtCKX1* and *AtCKX3*) are in vacuoles, one (*AtCKX7*) in the cytosol, and the remaining four *AtCKX* are probably in the apoplast (Werner et al. 2003). Through promoter: GUS fusion studies, Miyawaki et al. (2003) and Werner et al. (2003 and 2006) have described the differential expression patterns of *AtCKX*: *AtCKX1* and *AtCKX2* express in the shoot apex, *AtCKX4* and *AtCKX5* in young leaves, *AtCKX5* also in the procambial region of the root meristem and *AtCKX4* in stomatal precursor cells.

Werner et al. (2003) provided insights into cytokinin function and *Arabidopsis* plants that over-express the members of *AtCKX* gene family. In the *CKX* over-expressing plants, the growth of the shoot was completely arrested after germination and root growth was enhanced indicating the role of cytokinin in promoting shoot meristem growth and inhibiting root growth. The transgenic plants had increased cytokinin breakdown of 30 to 45% compared to wild type plants and reduced expression of the *ARR5: GUS* constructs. Werner et al. (2006), through a survey of microarray data, revealed that the *AtCKX3* transcript was most abundant in callus and cell suspensions suggesting its function during the cell cycle. Miyawaki et al. (2004) showed that there were a number of *AtCKX* expression domains overlapping with *IPT* genes, including cell division zones of stomata formation, axillary buds, procambial region of root meristem and root primordial cells, and endo-reduplicating cells (trichomes, stipules).

The response of *Pisum sativum* *CKX* expression and specific activity was studied by Vaseva-Gemisheva et al. (2005). They identified two putative *CKX* genes in pea (*PsCKX1* and *PsCKX2*) from existing sequences in TIGR *Medicago trunculata* database and studied the relative expression in the tissues of stressed young pea plants. High levels of expression of *PsCKX1* and *PsCKX2* were noticed in control leaves and revealed tissue specific expression. A low nodulating mutant of pea R50 (*sym16*), which accumulates cytokinin, was studied by Held et al. (2008). During development, activity of *PsCKX* was significantly reduced compared to wild type in tissues, particularly in mature roots and nodules, where decreased activity correlated with elevated cytokinin content (Held et al., 2008).

The maize *CKX1* gene was up-regulated during different abiotic stress, as well as induced by cytokins and abscisic acid which led to increased cytokinin degradation (Brugiere et al., 2003). The study of *CKX* activity changes during vegetative growth of plants which are

stressed differently would provide the interplay between growth and stress acclimation and their dependence on cytokinin hormone changes (Vaseva-Gemisheva et al., 2005). Song et al. (2012) showed that among ten sets of *TaCKX* genes, at least three were specifically or preferentially expressed during seed development. The key genes, *TaIPT2* and *TaCKX1* were most highly expressed during early seed development.

Evans et al. (2012b) studied the role of cytokinins in regulating leaf senescence in *Trifolium repens* through chlorophyll assay and expression of *TrCKX2*. The consistent high expression of *TrCKX2* in senescing leaves with reduction in chlorophyll, led to the suggestion that *CKX* may play a prominent role in facilitating the progression of senescence (Evans et al., 2012b). Recently, Le et al. (2012) identified *GmIPT* and *GmCKX* (14 *GmIPT* and 17 *GmCKX*) genes in soybean and analysed their responses under normal and drought conditions. They revealed that tRNA- type *GmIPT2*, 3 and 14 expression was high in soybean (Le et al. 2012). Liu et al. (2013) identified 13 *BrIPTs* and 12 *BrCKXs* genes in Chinese cabbage, characterised their expression patterns in various tissues and organ under abiotic stresses and exogenous cytokinin. They found that the tRNA-IPT *BrIPT2*, *BrIPT9-1* and *BrIPT9-2* to be highly induced under growth-limiting conditions.

1.2.2 Cytokinin translocation, perception and signalling

As reviewed by Kudo et al. (2010) cytokinins are mobile phytohormones and in higher plants have systems to mobilize the cytokinin across the plasma membrane and transport in *Arabidopsis* may be through the proton-coupled multiphasic cytokinin transport systems. Through selective transport the plant cells are capable of absorbing cytokinin nucleobases by *AtPUP1* and *AtPUP2*, (*Arabidopsis* purine permease) (Burkle et al., 2003, Füsseder et al., 1989) and nucleosides (Singh et al., 1988) were tZ- type and iP-type cytokinins accumulate in xylem and phloem respectively (Corbesier et al., 2003, Takei et al., 2001b) It was demonstrated that xylem sap predominantly contains tZ-type cytokinins and phloem sap predominantly contains iP-type and cZ-type cytokinins (Hirose et al., 2008). This unequal distribution in vascular transporting systems together with the spatial expression patterns of cytokinins metabolic genes suggest that cytokinins act both as local and long-distance signals (Hirose et al. 2008).

The synthesised cytokinin must be translocated to target cells by diffusion and / or by selective transport system (Sakakibara, 2006). Translocation of cytokinins is apparently mediated by subsets of purine permeases and nucleoside transporters by sharing the purine and the sugar conjugate transport systems, respectively (Burkle et al., 2003, Gillissen et al., 2000). *Arabidopsis* cytokinins are perceived by three histidine kinases CRE1/AHK4, AHK3 and AHK2 (Inoue et al., 2001, Suzuki et al., 2001, Yamada et al., 2001) (Figure 1.7). Although it had been anticipated that the cytokinin signal would be perceived at the plasma membrane, recently the cytokinin receptors have been shown to be localized mainly to the endoplasmatic reticulum (Wulfetange et al., 2011). The receptor is autophosphorylated once cytokinin is bound and then the phosphoryl group is transferred via an Asp-residue to the receiver domain of the receptor. Eventually, histidine phosphotransfer proteins (AHPs) transmit the signal to the response regulators (ARRs) which then regulate the cellular responses (Werner and Schmülling, 2009).

1.2.2.1 Cytokinin perception and signalling

The cytokinins are perceived by histidine kinases and transduced by a two-component signaling system. The cytokinin signaling pathway is similar to bacteria and yeast two-component signal transduction pathways: specifically the His-Asp multistep phosphorelays, which are comprised of sensor kinases, histidine phosphotransfer proteins and response regulators (Hwang et al., 2012) (Figure 1.7).

The *Arabidopsis* cytokinin receptor kinases, *Arabidopsis* Histidine Kinase (AHK2, AHK3 and AKH4) / cytokinin response (CRE1)/ Woodenleg (WOL1), contain a conserved extra-cellular cytokinin- binding domain called CHASE (cyclises/ a histidine kinases associated sensory extracellular) domain, a histidine kinase domain and a receiver domain. AHK4 was identified as a cytokinin response gene due to its ability to complement both yeast and *E. coli* histidine kinase mutants in a cytokinin-dependent manner (Inoue et al., 2001, Suzuki et al., 2001). Two groups independently showed that AHK2, AHK3 in the shoot and AHK4 in the root, function as positive elements in cytokinin signaling through triple receptor knockout mutants (Higuchi et al., 2004, Nishimura et al., 2004). The three cytokinin receptors differ in their biological functions and biochemical properties (Heyl et al., 2012). For example AHK3 is predominantly expressed in shoot tissues, while CRE1/AHK4 expression and signalling is

more confined to the roots (Higuchi et al., 2004, Ueguchi et al., 2001). Although iP, tZ, and the synthetic CK thidiazuron (TDZ) proved to be the most potent cytokinins in the *E. coli*-based receptor bioassays, the activity of particular cytokinin derivatives differs among receptors as well as among plant species.

The five *Arabidopsis* histidine-phosphotransfer proteins (AHPs) mediate the phosphotransfer from the receptor kinases to the response regulators. AHPs are expressed ubiquitously and transcription is not affected by the presence of cytokinin (Tanaka et al., 2006). The sixth AHP, AHP6 lacks the conserved His residue and so is unable to accept a phosphoryl group and is called a pseudo-AHP. It negatively interferes with pathway activity, mainly competing with AHP1 to 5 for interaction with the activated receptors (Hwang et al., 2012) and its function may contribute to the generation of sharper signalling boundaries within a tissue (Mähönen et al., 2006). From the AHPs, the phosphoryl group is passed over to the nuclear ARRs (Figure 1.7).

1.2.2.2 The response regulators (RRs)

The *Arabidopsis* response regulators (ARR) fall into four classes based on phylogenetic analysis and domain structure: type-A ARRs, type-B ARRs, type-C ARRs and the *Arabidopsis* pseudo-response regulators (APRRs) (Schaller et al., 2007). The 10 type-A ARRs are primary transcriptional targets of cytokinin signalling and contain short C-terminal extensions beyond the conserved receiver domain (Brandstatter and Kieber, 1998, D'Agostino et al., 2000, Imamura et al., 1998). The 11 type-B ARRs contain C-terminal output domains that have DNA binding and transactivating activity (Sakai et al., 1998, Sakai et al., 2000). Type-B are protein regulators of cytokinin signaling that controls the transcription of a subset of cytokinin-regulated targets, including the type-A ARRs (Hwang and Sheen, 2001, Mason et al., 2005, Sakai et al., 2001, Taniguchi et al., 2007).

The type-C ARRs are more distantly related to type-A and type-B ARRs receiver domain sequences, do not contain the output domain of type-B ARRs and are not transcriptionally regulated by cytokinin, but their over-expression results in reduced sensitivity to cytokinin (Kiba et al., 2004).

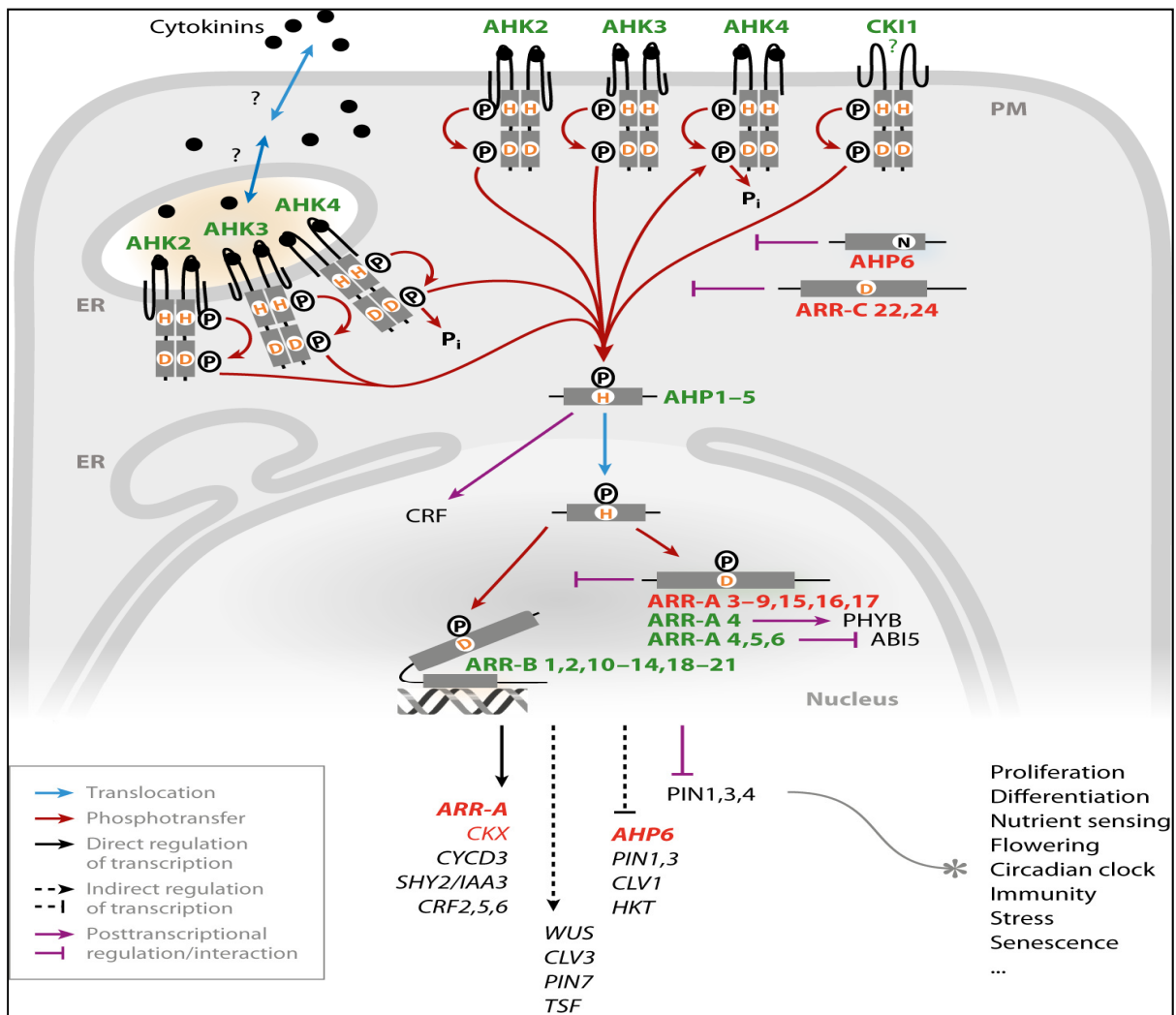


Figure 1.7 The two-component circuitry in cytokinin signalling in the past decade. The core cytokinin signaling circuitry, showing *Arabidopsis* His kinases (AHKs), *Arabidopsis* His phosphotransfer proteins (AHPs), and *Arabidopsis* response regulators (ARRs) in a model cell. Conserved His and Asp residues, which accept a phosphoryl group (P), are indicated by orange H and D letters, respectively. Boldface indicates core signalling components, green indicates positive regulators of cytokinin signaling, and red indicates negative regulators. Selected connections to other signals and genes are indicated. Additional abbreviations: ARR-A/B/C, type-A/B/C *Arabidopsis* response regulator; ER, endoplasmic reticulum; CRF, cytokinin response factor; PM, plasma membrane. (cited from Hwang et al. 2012). Reproduced with permission from Annual Reviews.

Jain et al. (2006) identified ten type-A response regulator genes in rice, the model monocot plant. They showed the overlapping/differential expression patterns in various organs in response to light and induction of *OsRR* genes by cytokinin even in the absence of *de novo* protein synthesis led to their suggestion that these type-A response regulators might be the primary cytokinin response genes.

The model for the cytokinin response in *Arabidopsis*, derived from the research conducted over the last decade was illustrated by Kieber and Schaller (2010) (Figure 1.8). In *Arabidopsis* the HPT proteins are called AHPs (*Arabidopsis* histidine-containing phosphotransfer proteins) which are in flux between cytosol and nucleus (Punwani et al., 2010) (Figure 1.8). Upon entering the nucleus, the phosphorylated AHP can pass its phosphate to members of a transcription factor family, the type-B ARRs (*Arabidopsis* response regulators), which regulates the transcriptional changes that characterise the cytokinin response including both induction and repression of cytokinin-regulated genes (Argyros et al., 2008).

There are three types of positive regulators in the primary response pathway, cytokinin receptors, AHP proteins and type-B response regulators that act within a signalling circuit. There is a need for negative feedback to dampen the response upon high or prolonged signal input, to turn off the pathway once the signal is removed. The type-A ARRs response regulators play a major role in such negative regulation in *Arabidopsis* (To et al., 2007). The genes for the type-A ARRs are direct targets of type-B ARRs and are strongly and rapidly induced in response to cytokinin (Hwang and Sheen, 2001, Sakai et al., 2001).

Use of response regulators as a surrogate measure of endogenous cytokinin has been reported in previous studies (Werner et al. 2003, Depyudt et al. 2009b). Werner et al. (2003) showed that the ectopic *AtCKX* expression in *Arabidopsis* decreased cytokinin content which was reflected by strong reduction in *ARR5: GUS* activity and was more severe in the shoots than in the roots.

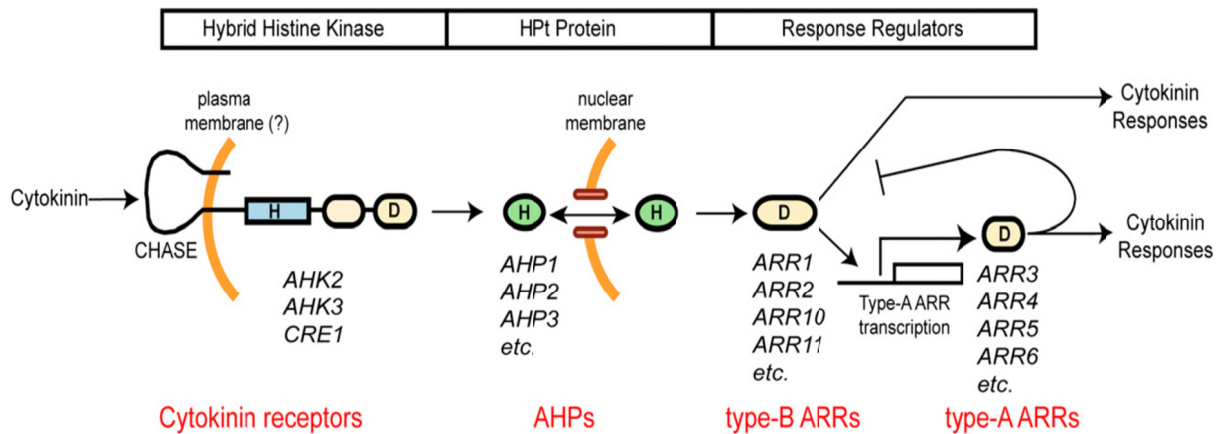


Figure 1.8 Model of the cytokinin response pathway in *Arabidopsis*. Cytokinin binds to the extracellular CHASE domain of a cytokinin receptor, initiating a phosphorelay that ultimately results in the phosphorylation of the ARR proteins. The His (H) and Asp (D) residues that become phosphorylated are indicated on each protein. Note that some type-A ARRs are also found in the cytoplasm, but for simplicity they are only shown in the nucleus (Kieber and Schaller 2010). Reproduced with permission from RightsLink.

1.2.3 Cytokinins in plant-microbe interactions

During their life span plants encounter a variety of microbes and cytokinin plays a significant role in pathogenicity or symbiotic interactions between many plant and microbes. As this study is mainly based on the gall-forming bacterium, *Rhodococcus fascians*, this section deals with all other gall-forming bacteria/ hyperplasia bacteria and *R. fascians* is covered in detail in Section 1.3.

The model gall-forming bacterium is *Agrobacterium tumefaciens* which is a pathogenic bacterium that causes crown gall disease, a plant tumor affecting a wide range of plant species. Crown galls develop upon transfer of a portion of the tumor-inducing (Ti) plasmid, the transfer-DNA (T-DNA), into the genome of the bacterium's plant hosts (Chilton et al., 1980). When phenolic molecules are released from plant wounded cells *Agrobacterium* detects it and T-DNA transfer is initiated along with the induction of *vir* genes expression (McCullen and Binns, 2006). The T-DNA encoded genes are expressed which alter plant hormone levels, leading to altered cell division and tumor formation. There are two classes of genes in T-DNA: oncogenes and opine-related genes. The tumour phenotype is generated by oncogenes which alter the phytohormone synthesis and sensitivity in the infected plant cells

(Escobar and Dandekar, 2003). The T-DNA from *A. tumefaciens* strains has five oncogenes: *iaaM*, *iaaH*, *IPT*, *6b* and *5* (Zhu et al., 2000). The *iaaM* converts tryptophan to indole-3-acetamide and *iaaH* catalyses it to indole acetic acid (Klee et al., 1984). The *IPT* gene catalyses the rate-limiting step in cytokinin biosynthesis from AMP to iPMP (Åstot et al., 2000). Jameson (2000) has reviewed in detail about *A. tumefaciens* its reaction to cytokinin production and *A. tumefaciens* strains lose their pathogenicity when cured of their Ti plasmid.

Pseudomonas syringae subsp. *savastanoi* (= *P. savastanoi* pv. *savastanoi*) (Young et al., 1996) causes hyperplasia symptoms on olive, oleander and ash. Symptom development on host plants depends on the bacterial production of indole 3-acetic acid (IAA) and cytokinin that alters the hormonal balance of the infected tissue (Iacobellis et al., 1994, Surico et al., 1985) causing proliferation of plant cells and producing tumorous outgrowths (knots) on trunks and branches of olive trees (*Olea europaea*) (Wilson, 1935). In *P. savastanoi* the *hrp* genes seem to be required for bacterial multiplication within host tissues and together with phytohormone production play a fundamental role in its pathogenesis (Sisto et al., 2004). The cytokinin (*ipt*) and auxin (*iaaM/H*) genes of *P. syringae* pv. *savastanoi* are borne on different plasmids, as reviewed by Jameson (2000), where the strain PB213 isolated from oleander had *iaaM/H* genes on a 73kb plasmid (pIAA2) (Comai et al. 1982) while the cytokinin biosynthetic gene (*ipt*) was located on a 42-kb plasmid (pCK1) (Macdonald et al., 1986).

Pantoea agglomerans is widespread in nature and has been associated with plants as a common epiphyte or endophyte. However, some isolates have evolved as plant pathogens. *P. agglomerans* pv. *gypsophylae* induces gall formation in gypsophila, and causes problems in gypsophila nurseries by inhibiting root development in cuttings. *P. agglomerans* pv. *betae* elicits tumorous outgrowths on both beet and gypsophila, resulting in economic losses especially in the table beet industry (Barash and Manulis-Sasson, 2007, Weinthal et al., 2007). Galls are mainly induced at the crown region and have a brownish, rough and necrotic appearance (Chalupowicz et al., 2006). Virulence is dependent on the presence of a non-conjugative pPATH plasmid containing a pathogenicity island, which carries an *hrp/hrc* gene cluster, virulence genes encoding effector proteins, and phytohormone biosynthetic genes (Weinthal et al., 2007). Both *P. agglomerans* pv. *gypsophylae* and *P. agglomerans* pv. *betae* produce auxin via plasmid-located indole-3-acetamide (IAM) pathway and via chromosome-located indole-3-pyruvate (IPyA) pathway (Barash and Manulis-Sasson, 2007).

The role of phytohormones in *Plasmodiophora brassicae* infection causing clubroot disease mainly in *Brassica rapa* spp. *pekinensis* (Chinese cabbage) is well recognised. The secondary phase of the life cycle of *P. brassicae* occurs in the cortex and the stele of hypocotyls and roots of the infected plants, forming galls through cell division and elongation of newly formed cells (Ingram and Tommerup 1972; cf Devos et al. (2005). The morphological changes such as hyperplasia and hypertrophy in the infected host root are mainly due to plant hormone imbalance. Ando et al. (2005) investigated the involvement of five putative *IPT* genes expression in *B. rapa* roots using Northern blot analysis. *BrIPT1*, 3, 5 and 7 expression in *P. brassicae* infected roots were induced before the clubroot formation, but the expression was repressed in clubs at 20 dpi. Devos and Prinsen (2006) compared the plant hormone concentration between control and infected *Arabidopsis* using the *CYCB1; 1::GUS*, *DR5::GUS* and *ARR5::GUS* constructs. They found *ARR5::GUS* and *DR5::GUS* up-regulated upon infection suggesting increased accumulation of active cytokinins and auxin respectively. Through hormone and proteome studies it was postulated that at the first stage of infection *Plasmodiophora* plasmodial-produced cytokinins trigger a local re-initiation of cell division in the root cortex and a *de novo* meristematic area is established which acts as a sink for host-derived indole-3-acetic acid, carbohydrates, nitrogen and energy to maintain the pathogen and to trigger gall development (Devos et al., 2006).

Streptomyces turgidiscabies, like *R. fascians*, is a Gram-positive pathogenic species, which causes potato scab. It produces the phytotoxin thaxtomin (Bukhalid et al., 1998) which inhibits cellulose biosynthesis in expanding plant tissues, stimulates Ca^{2+} spiking and leads to cell death (Loria et al., 2006). Kers et al. (2005) discovered the genes homologous to the six genes in the *fas* operon similar to *R. fascians*. The *S. turgidiscabies* *fas* operon is colinear with the *fas* operon of *R. fascians*, where *fas6* appears to have undergone a rearrangement on the *S. turgidiscabies* chromosome. A common origin in both the pathogens for this operon is suggested by Loria et al. (2006). The presence of the *fas* operon on the *S. turgidiscabies* PAI (pathogenicity island) was unexpected as this pathogen is not known to cause plant galls. However, Loria et al. (2006) demonstrated that *A. thaliana* produced leafy galls when inoculated with *S. turgidiscabies* Δnos mutant, in which thaxtomin production has almost been eliminated, suggesting that *S. turgidiscabies* produces cytokinins through an *IPT* gene that has activities similar to those produced by *R. fascians*. Since gall formation has not been

reported, so far, in nature, the role of this cytokinin biosynthesis pathway in potato scab disease is still speculative, although it could be responsible for the formation of the bigger, excessive lesions (Joshi and Loria, 2007).

1.3 *Rhodococcus fascians*

1.3.1 Phytopathogen

Rhodococcus fascians (Tilford, 1936) (Goodfellow, 1984), known as *Corynebacterium fascians* until 1984, is a Gram-positive, rod-shaped, aerobic, non-spore forming, nonmotile bacterium with cell walls containing mycolic acids (Holt, 1994). The *Rhodococcus* genus has been placed in the order Actinomycetales, suborder Corynebacterineae, and family Norcardiaceae (Gürtler, 2004).

The genus *Rhodococcus* is genetically diverse and contains at least one human pathogen (*R. equi*) (Finnerty, 1992) as well the phytopathogen *Rhodococcus fascians*. *Rhodococcus* is closely related to the genus *Corynebacterium*, which contains both plant and animal pathogens, and to *Mycobacterium*, a genus containing human and animal pathogens. Both *Rhodococcus* and *Nocardia* have many features similar to those of soil borne actinomycetes such as *Streptomyces* (Larkin et al., 1998) including cell wall composition (presence of long chain mycolic acids) and 16S rRNA sequences (Rainey et al., 1995).

For many years the taxonomic position of the bacterium was debated. Tilford (1936) first isolated the bacterium from fasciated growths on geranium and chrysanthemum and named it *Phytomonas fascians*, then later (Lacey, 1936) named it *Bacterium fascians* based on the characteristic post-division grouping and the occurrence of round intracellular bodies. The organism was subsequently isolated from fasciated sweet peas and garden peas by Tilford (1936), who named it *Corynebacterium fascians*. Finally, supported by phenotypic, biochemical, and genetic data, the phytopathogen was repositioned within the Actinomycetales, in the genus *Rhodococcus* and re-named *Rhodococcus fascians* (Goodfellow, 1984).

Rhodococcus fascians is pleiomorphic, exhibiting mycelia growth with fragmentation into rod-shaped or coccoid elements. It produces moist, cream to orange colonies which are either

smooth or rough, but this is not correlated with pathogenicity (Bradbury, 1986). It causes growth abnormalities on plants that are similar to those of plant hormone imbalances (Pertry et al., 2010).

R. fascians is widely distributed and has been reported from at least 19 states of the United States of America, Mexico, Canada, Northern Europe, the Middle East, Asia, Australia, and New Zealand; it has been reported on the African continent in Egypt, and in South America in Columbia (Anonymous, 2006). *R. fascians* has a reported host range of 87 plant genera spanning 40 families (Vereecke et al., 2003). The range of susceptible plants is exceptionally broad, encompassing both monocots, dicots and woody as well as herbaceous plants (Table 1.1). In its broad host range it resembles *A. tumefaciens* and both differ from other well studied gall forming bacteria, *P. savastanoni* and *P. agglomerans* pv *gypsophilae* (*E. herbicola* pv. *gypsophilae*) which have very restricted host ranges (Burr et al., 1991, Gardan et al., 1992).

Table 1.1 Some of the examples of host ranges of *Rhodococcus fascians*

Family	Name of the host	Reference
Fabaceae	<i>Acacia mearnsii</i>	Quoirin et al. (2004)
	<i>Cicer arietinum</i>	Jacobs et al. (1965)
	<i>Lathyrus odoratus</i>	Tilford (1936)
	<i>Melilotus officianlis</i>	Hoof et al. (1979)
	<i>Pisum sativum</i>	Tilford (1936)
Solanaceae	<i>Nicotiana tabacum</i>	Tilford (1936)
	<i>Nicotiana plumbaginifolia</i>	Vereecke et al. (2000)
	<i>Petunia sp.</i>	Lacey (1939)
	<i>Solanum tuberosum</i>	Lacey (1955)
Brassicaceae	<i>Arabidopsis thaliana</i>	Vereecke et al. (2000)

	<i>Brassica oleraceae</i> var. <i>botrytis</i>	Moore (1943)
Chenopodiaceae	<i>Beta vulgaris</i>	Lacey (1955)
Scrophulariaceae	<i>Buddleja davidii</i>	Pape (1938)
Campulanaeae	Campanula x ‘Sarastro’	Putnam and Miller (2007)
Caricaceae	<i>Carica x heilbornii</i>	Pennycock et al. (1989)
Apocynaceae	<i>Catharanthus roseus</i>	Vereecke et al. (2000)
Asteraceae	<i>Chrysanthemum indicum</i>	Lacey (1936)
Scrophulariaceae	<i>Hebe elliptica</i>	Cooksey and Keim (1983)
Saxifragaceae	<i>Heuchera sanguine</i>	Lacey (1936)
Liliaceae	<i>Hosta</i> sp.	Putnam and Miller (2006)
Convolvulaceae	<i>Ipomoea purpurea</i>	Faivre-Amiot (1967)
Crassulaceae	<i>Kalanchoë blossfeldiana</i>	Miller et al. (1980)
Rosaceae	<i>Rubus idaeus</i>	Jones et al. (1977)

Source: (Putnam and Miller 2007)

R. fascians is a well-adapted epiphyte and the bacterium mainly colonises aerial plant parts. The bacteria occur on both sides of the leaves, located mainly on leaf edges. The stem and crown are colonised to a lesser extent (Cornelis et al., 2001, Vereecke et al., 2003). The presence of *R. fascians* on a host plant does not necessarily lead to the development of symptoms, indicating a strict regulation of the bacterial virulence signals. Triggered by unknown environmental conditions the bacterium will invade plant tissues. Although stomata were colonised, they were not used as preferred entryways (Cornelis et al., 2001). Vereecke et al. (2003) stated that the bacteria penetrated directly through the cuticle and epidermis via the formation of ingressions sites, but which were not accompanied by extensive cell necrosis. Cornelis et al. (2001) stated that from one week post inoculation bacteria can be observed inside the *Nicotiana tabacum* and *Arabidopsis thaliana* plant tissue. They were mainly

located in intercellular spaces and occurred throughout the tissues, although fewer bacteria resided in the deeper cell layers (Cornelis et al., 2001). In contrast to other phytopathogens, such as *A. tumefaciens*, *P. syringae* pv. *savastanoi* and *P. agglomerans*, *R. fascians* has not been detected in vascular tissues (Goethals et al., 2001b).

The interaction of *R. fascians* with its hosts starts with the colonisation on aerial plant surface, where the microbe behaves as a saprophytic epiphyte and does not provoke any visible symptoms (Cornelis et al. 2001). It forms large epiphytic colonies embedded in a protective slime layer of bacterial origin (Francis et al. 2007). When the plant responds to the presence of the pathogen by modulating its primary metabolism (Depuydt et al. 2009), the bacteria senses this and incites a switch in their behaviour from harmless epiphyte into pathogenic endophyte (Stes et al. 2013). *R. fascians* then colonises the interior of its hosts and the induced hyperplasia represent a specific niche which is exploited by the bacteria (Cornelis et al. 2001, Vereecke et al. 2003). During the endophytic colonisation, the bacteria undergo a series of adaptations to the new environment (Cornelis et al., 2001, Forizs et al., 2009, Stes et al., 2011, Vereecke et al., 2002).

1.3.2 Symptoms

Rhodococcus fascians was first isolated and identified in 1930 as the casual agent of sweet pea fasciations (Tilford, 1936). Since then, the symptoms caused by *R. fascians* in diverse plants have been described (Goethals et al., 2001b). The disease symptoms caused by *R. fascians* vary, on occasion appearing to be similar to those caused by *A. tumefaciens* (Brown, 1927, Williams, 1934) or to the leafy galls caused by viral infection and viroids (Zutra et al., 1994), to insect injury (Dowson, 1957), or to chemical substances produced by mixed bacterial populations (Lacey, 1936) as cited in Putnam and Miller (2007) .

Infection of dicot plants can result in the local proliferation of meristematic tissue, leading to galls that are covered with leaflets, known as leafy galls (Vereecke et al., 2000). On monocot plants, such as lilies, *R. fascians* provokes severe malformation of long side shoots (Miller et al., 1980, Vantomme et al., 1982).

Symptoms in infected plants include proliferation of partially expanded buds known as leafy galls, misshapen, thickened leaves or shoots termed fasciations, and proliferation of buds in

leaf axils described as witches' broom. The level and types of induced malformations depend on plant species, or cultivar, plant age, bacterial strain, inoculation method, and growth conditions of both interacting partners (Lacey 1939, Eason et al. 1995). The complexity of symptom development is illustrated by the necessary and continuous presence of the bacterium for symptom persistence (Vereecke et al., 2000).

Leaf deformation is characterised by the wrinkling of the lamina and swelling of petioles and veins which results in enlarged parenchyma cells and growth of the vascular tissues. Vereecke et al. (2000) observed patches of "green islands" on the lamina in tobacco, possibly representing sites with increased chlorophyll content.

A witches' broom is characterised by a bunch of fleshy stems with misshapen and aborted leaves that develop on the crown of the host plant. This leads to dwarfism and production of fewer blossoms (Baker, 1950). As shown by Roussaux (1975) in peas, this was accompanied by initial stimulation of epicotyl growth, but soon the growth of the terminal bud was blocked and plants become dwarfed and had fewer blossoms (Brown 1927, Tilford 1936 as cited by Goethals et al. 2001).

Rhodococcus fascians most severe symptom is leafy galls which originate from a local amplification of multiple buds that are inhibited for outgrowth. The leafy gall symptom caused by *R. fascians* was described in detail by Lacey (1936) in sweet peas as "a number of very short, hypertrophied shoots [which] develop at the base of the plant or cutting, sometimes only just appearing above the soil-level, but spreading horizontally till a large gall-like mass is produced". Roussaux (1975) and Vereecke et al. (2000) have pointed out that the presence of bacteria is essential for the multiplication of the shoots and for gall persistence. The formation of leafy galls is also characterised by an alteration of apical dominance, resulting in the development of multiple lateral embryonic buds situated in the axils of the leaf primordia by the elimination of the bacteria. If the bacterial activity in isolated leafy galls is inhibited, then the shoot outgrowth is activated and these shoots can develop roots and grow into normal fertile plants. So, in contrast to crown galls caused by *A. tumefaciens* that rely on transgenic production of phytohormones, leafy galls are non-autonomous structures, and gall maintenance depends on the presence of *R. fascians* (Goethals et al., 2001b).

Root growth is affected in some hosts by *R. fascians*. Under conditions of artificial inoculation and severe infection thickening of main roots and inhibition of secondary roots occurs resulting in a reduced root system overall (Eason et al., 1995, Vereecke et al., 2003). In the case of tomato, pea and cucumber, atrophy of secondary roots was seen (Faivre-Amiot, 1967). Galls comprised of tightly compressed masses of buds were reported on naturally infected raspberry in Scotland by Jones et al. (1977). Miller et al. (1980) observed that deformed bulbs produced reduced root growth in naturally infected lilies, but plants that only showed symptoms above ground generally had well developed root systems.

1.3.3 Molecular basis of virulence in *R. fascians*

The pathogenicity of *A. tumefaciens*, *P. syringae* pv. *savastanoi*, *P. agglomerans* and *R. fascians* was found to be determined by factors borne on specific plasmids, where these plasmids harbour genes for cytokinin and / or auxin biosynthesis (Jameson, 2000).

Earlier studies were done to understand the association between plasmids, virulence and cytokinin production in *R. fascians*. Murai et al. (1980) found that the most virulent strains of *C. fascians* had a large circular plasmid and also produced 8-13 times more cis-zeatin than avirulent strains, whereas Lawson et al. (1982) reported that all of 10 virulent and avirulent isolates contained a single 78 MDa circular plasmid only, which led to the conclusion that there was no association between virulence and circular plasmids (Lawson et al., 1982). Crespi et al. (1992) showed that virulence in *R. fascians* wild-type strain D188 was controlled by the genes on a conjugative fasciation-inducing large linear plasmid, pFiD188 of about 200 kb. They also observed that strains cured of pFiD188 were avirulent (D188-5), and re-introduction of the plasmid led to virulence of the strain. This avirulent strain could penetrate plants but the endophytic population was lower than the virulent strain (D188) (Cornelis et al., 2001). The pFiD188 is similar to the linear plasmids of other actinomycetes including *Streptomyces* and *Mycobacterium* (Hinnebusch and Tilly, 1993, Picardeau and Vincent, 1997).

Crespi et al. (1992) also reported that a gene encoding an isopentenyl transferase (*IPT*) was located on the 200 kb linear plasmid and within the *fas* operon of the plasmid. This gene was originally known as *fasI* (Crespi et al., 1994) but now it is designated as *FasD*. This was confirmed by Stange et al. (1996), who showed that out of 36 strains of *R. fascians*, only

those strains scoring as virulent on *P. sativum* contained the *fasD* gene which was determined by both Southern blotting and RFLP analysis. They also proposed that *fasD* could be used as a marker for virulence in *R. fascians*, where the presence of the gene correlated perfectly with pathogenicity. Conversely, absence of the gene was associated with avirulence. Through PCR it was determined that for most of the virulent strains the *fasD* gene was localized to a 200 kb \pm 10 kb linear plasmid. Notably, three virulent isolates lacked this plasmid, but contained *fasD* either on a linear plasmid of 130kb or on a large circular plasmid (Stange et al., 1996). Until the use of pulsed-field gel electrophoresis to mobilise large linear plasmids into gels, the location of the *fasI* gene on linear plasmids remained undetected (Jameson 2000). *R. fascians* is the only plant pathogen with virulence genes on a linear plasmid (Francis et al. 2007).

The *R. fascians* linear plasmid has four conserved regions, R1, R2, R3 and R6 that are implicated in plasmid maintenance (Francis et al., 2007) (Figure 1.9). The conserved R1 region encompasses the left border of pFiD188 and harbours mainly genes putatively involved in plasmid replication, natural transformation and partitioning. In the case of region R3, a locus with homology to the tight adherence locus (*tad*) of different organisms was identified (Tomich et al., 2007). The region R2 mostly consists of conserved hypothetical proteins, thought to play a role in conjugation by forming a membrane associated conjugation complex and region R6 also encodes hypothetical proteins, but its role in the biology of the linear plasmid is currently unknown (Francis et al. 2007). Other than the above regions, the linear plasmid pFiD188 harbours three unique regions U1, U2 and U3 that encode specific features of *R. fascians* (Figure 1.9). Recently, Francis et al. (2012) analysed the sequence of the linear plasmid of strain D188 and pFiD188.

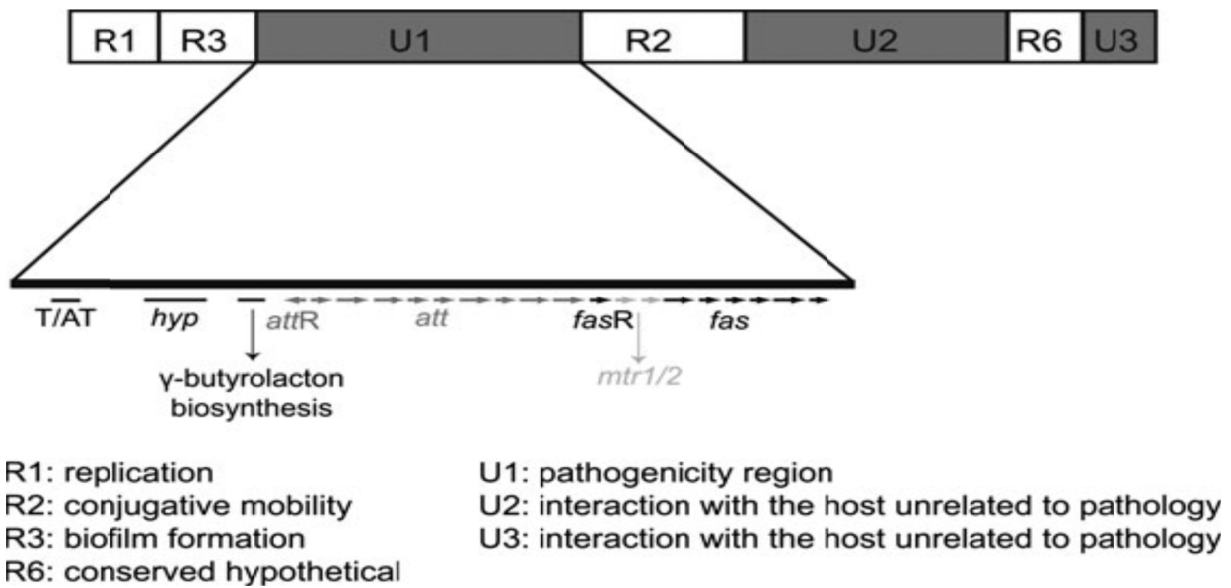


Figure 1.9 Schematic representation and (putative) function of the different regions of pFiD188. Source: Stes et al. (2010). Reproduced with permission from Springer.

Francis (2009), through functional analysis of some of the genes in the U2 and U3 regions, has revealed that they are not involved in the pathology of the organism, but may play a role in the ecology of the interaction with the host, where U2 carries the *nrp* locus and U3 harbours *stk* locus (Francis et al. 2007, 2012). The unique region U1, on the other hand, encodes the main pathogenicity region of *R. fascians*.

The U1 region is the largest unique region on pFiD188 and contains at least three pathogenicity loci: *hyp*, *att* and *fas* (Crespi et al. 1992). The observations made by Crespi et al. (1992) showed that mutants in the hypervirulent (*hyp*) locus induce enhanced symptoms on plants and suggested that the Hyp proteins negatively control the virulence signals or virulence gene expression. The locus has three open reading frames (ORFs), of which two are hypothetical (ORF 1 and ORF 2) and the other, ORF 3, is homologous to RNA helicases and possibly controls virulence gene transcription, mRNA stability, or translation initiation (Goethals et al., 2001b, Pertry et al., 2009).

The other two loci, *fas* and *att*, in the U1 region are fundamental for pathogenicity and have been extensively studied (Goethals et al. 2001). Maes et al. (2001) studied the *att* locus

identified by Crespi et al. (1992) via an insertion mutant strain D188-att1 with reduced virulence, where tobacco plants infected with D188- att1 at an apical wounding site developed smaller leafy galls compared with the wild type. Maes et al. (2001) elaborated on the importance of the *att* locus in the pathogenesis of *R. fascians* in tobacco plants by showing that the *att* locus contains nine open reading frames homologous to arginine and β -lactam biosynthetic genes (eight genes *attA* to *attH*) and a ninth gene, *attX*, has a translocator domain and a membrane location which suggests that the product synthesised by *att*-encoded protein is actively exported, which is corroborated by the detection of inducing factors (IFs) and a tenth regulatory gene (*attR*) that belongs to the LysR family of transcriptional regulators. Meas et al. (2001) showed that the *att* locus plays an important regulatory role in the virulence of *R. fascians* on tobacco through the biosynthesis of inducing factors (IFs) which are also required for *fas* locus induction for activating virulence gene expression.

Positioned between the *att* and *hyp* loci is another locus (Figure 1.9) which is putatively involved in the biosynthesis of a γ -butyrolacton-like autoregulatory factor, which are known as quorum sensing molecules of diverse Gram-positive bacteria (Nishida et al., 2007). This locus might trigger virulence gene expression in a cell density dependent manner (Stes et al., 2010). There is also a putative toxin-antitoxin system located in the U1 region (Fig. 1.13) where, in the case of *Mycobacterium tuberculosis* such systems induce a metabolic dormancy during disadvantageous growth conditions in the host (Zhu et al., 2006). In *R. fascians* this locus might provide a mechanism for survival of the bacteria inside the host plant tissues (Francis 2009).

Francis et al. (2012) found additional to U1 region, U2 and U2 regions in pFiD188 linear plasmid which is unique for *R. fascians*. The functional analysis of *stk* and *nrp* loci in U2 and U3 regions respectively, indicated that their role in symptom development was limited compared to *fas*, *att* and *hyp* loci in U1 region and is the main pathogenicity region and pFiD188 as a typical rhodoccal plasmid involved in virulence and interaction with host along with plasmid maintenance (Francis et al., 2012).

1.3.3.1 Importance of the *fas* locus in virulence

The *fas* locus codes for the most important virulence factors of *R. fascians* and mutations in this locus leads to a complete loss of, or strongly reduced, virulence (Crespi et al. 1992; 1994;

Temmerman et al. 2000). The locus carries nine genes in three transcriptional units (Figure 1.10): the first unit consists of the *fasR* gene that codes for a transcriptional regulator of the AraC family; the second unit contains two genes that are homologous to S-adenosyl-methionine (SAM)- dependent methyltransferases (*mtr1* and *mtr2*); the third unit comprises the six genes of the *fas* operon (*fasA*, *fasB*, *fasC*, *fasD*, *fasE* and *fasF*) that encodes the cytokinin biosynthetic machinery and is essential for virulence (Crespi et al. 1992; 1994; Temmerman et al. 2000; Pertry et al. 2010). Over the years, various designations have been used for the main genes involved in cytokinin biosynthesis and metabolisms, the genes with their synonyms are given in Table 1.2.

Table 1.2 Key genes involved in cytokinin biosynthesis and metabolism used in this project

Name	Gene abbreviations/synonyms	Remarks
Isopentenyl transferase	<i>orf4</i> , <i>fas1</i> , <i>fasD</i> , <i>RfIPT</i> *	Cytokinin biosynthesis gene
The Lonely Guy/ glutathione transferase/lysine decarboxylase	<i>orf6</i> , <i>fas2</i> , <i>fasF</i> , <i>RfLOG</i> *	Cytokinin activating gene
Cytokinin oxidase/ dehydrogenase	<i>orf5</i> , <i>fas5</i> , <i>fasE</i> , <i>RfCKX</i> *	Cytokinin degradation gene

[Note: *The *R. fascians* cytokinin genes isolated in this project are designated as *RfIPT*, *RfLOG* and *RfCKX*].

Pertry et al. (2009) showed that the G+C content of all genes of the *fas* locus is much lower than that of the genome and suggested that this implied that the *fas* locus might have been acquired via horizontal gene transfer as a pathogenicity island, which specifies a region in the chromosome that contains one, or commonly many, virulence genes present in pathogenic bacteria but absent in non-pathogenic bacteria of the same or related species (Francis et al., 2007, Hacker et al., 1990). The same situation was described in a *fas*-like operon of

Streptomyces turgidiscabies, a recently evolved scab-causing Gram-positive pathogen that can also induce leafy galls on tobacco (Joshi and Loria, 2007).

The central gene, *fasD*, encodes for an isopentenyl transferase is involved in the first committed step of cytokinin biosynthesis (Crespi et al., 1992, Sakakibara, 2005). The *fasE* and *fasF* gene products show similarity to cytokinin oxidase/ dehydrogenases, and glutathione-(S)-transferases/ lysine decarboxylases, respectively (Figure 1.10). Francis et al.(2007) reported that although *fas* transcription is constitutive, translation of the *fas* messenger RNAs is highly responsive to several environmental signals. In the early steps of the interaction, virulence is absolutely dependent on the activity of the Att proteins that produce an autoregulatory compound (Temmerman et al. 2000; Maes et al. 2001; Cornelis et al. 2002) (Figure 1.10).

The *fasR* lies to the upstream of the *fas* genes that encodes a key transcriptional regulator, a member of the AraC family (Martin and Rosner, 2001, Temmerman et al., 2000) that is essential for the *fas* gene expression because the *fasR* mutant is nonvirulent. Temmerman et al. (2000) proposed a working model suggesting that *fasR*, in combination with the autoregulatory compounds, controls the expression of a translational activator that will mediate translation of the constitutively produced messenger RNAs.

Pertry et al. (2010) showed that equally important for pathogenicity is the *fasA* gene that is homologous to P450 cytochrome monooxygenase, hydroxylates iP to form tZ and cZ, implying that the hydroxylated cytokinins are essential for the induction of disease. Goethals et al. (2001) reviewed that *fasB* gene product shows homology to two different proteins: the amino-terminus is similar to ferredoxins and the carboxy-terminus to the α -subunit of pyruvate dehydrogenase and *fasC* is homologous to the β -subunit of pyruvate dehydrogenase. It was suggested by Crespi et al. (1994) that maybe the *fasB-fasC* system generates the reducing power and electron transport system necessary for the functioning of the FasA protein.

Pertry et al. (2010) reported that the mutations in *fasE*, that encodes a cytokinin dehydrogenase/oxidase (*CKX*) involved in cytokinin breakdown, lead to reduced symptoms, suggesting that an optimal balance in the produced cytokinins is determinative for induction

and maintenance of the disease. Also, they showed that the strains defective in *fasF*, which codes for a lysine decarboxylase /phosphoribohydrolase (*LOG*), are not impaired in symptom initiation, but are unable to maintain the deformations. Pertry et al. (2010) implied that this protein is probably involved in the production of an additional level of cytokinins. They also showed reduced levels of Z-type cytokinins in D188-*fasF* and implied that the phosphoribohydrolase activity of FasF is mainly involved in release of cZ and tZ from their respective nucleotides (Pertry et al. 2010).

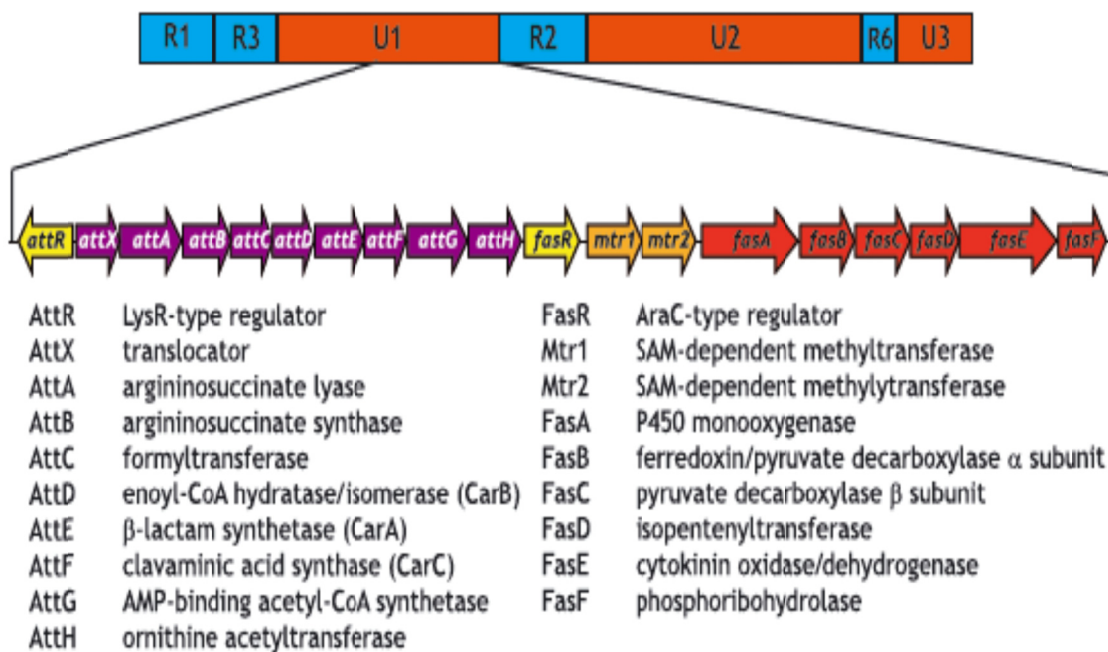


Figure. 1.10 Schematic representation of the linear virulence plasmid pFiD 188 of the *R. fascians* strain D 188 and the organisation of *att* and *fas* operons. The different conserved R and unique U regions and corresponding homologies of the *att* and *fas* genes are indicated. Source: Stes et al. (2013). Reproduced with permission from John Wiley and Sons.

A fourth locus *vic* has been identified on the *R. fascians* chromosome (Vereecke et al., 2002). The gene *vicA*, which encodes a malate synthase enzyme, is functional in the glyoxalate shunt of the Kerbs cycle. VicA is required in the interaction of *R. fascians* with its host. Cornelis et al., (2001) suggested that when *R. fascians* colonises the plant surface then penetrates the plant tissue and colonises the intercellular spaces, the virulence genes become active and form symptomatic tissues with strong meristematic activity. They suggested that this process alters the metabolic state of the host plant (tobacco) and the spectrum of compounds that serve as nutritional factors for *R. fascians*. During the catabolism of these nutrients

glyoxylate is formed. Vereecke et al., (2002) implied that the functional VicA protein is essential to remove this toxic metabolite or this leads to accumulation of glyoxylate which leads to suppression of growth or death of the bacteria.

1.3.4 *Rhodococcus fascians* and plant hormones

Many plant-associated bacteria can influence their hosts either by modulating the production of plant hormones of the host or by producing the hormones themselves. Hyperplasia inducing bacteria, such as *A. tumefaciens* genetically transforms plant cells to produce cytokinin and auxin (and opines) (Zhu et al., 2000), whereas *P. agglomerans* and *P. syringae* pv. *savastanoi*, secrete high amounts of cytokinins and auxins to facilitate or initiate gall development (Barash and Manulis-Sasson, 2007, Jameson, 2000, Sisto et al., 2004). In contrast to the above mentioned bacteria, Manes et al. (2001) reported elevated levels of auxin in *R. fascians* – induced leafy galls on tobacco, but they did not detect cytokinins in infected tobacco tissue. Eason et al. (1996) and Galis et al. (2005b) showed that *P. sativum* infected with *R. fascians* virulent strain had lower levels of cytokinin than the avirulent strain but still caused shoot malformations.

From the range of symptoms induced by *R. fascians* on host plants, it is clear that infection by the bacterium causes an imbalance in plant hormones. The symptoms provoked by *R. fascians* on plants were initially explained by the ability of the bacteria to destroy auxins (Kemp, 1978, Roussaux, 1965). Some symptoms could be displayed by the addition of gibberellin (Roussaux, 1975), or by addition of cytokinin (Oduro and Munnecke, 1975b, Thimann and Sachs, 1966). Beside cytokinin and auxin, *R. fascians* is reported to act on other hormones. Simon-Mateo et al. (2006) suggested that it can block abscisic acid and gibberellin synthesis in infected plants.

1.3.4.1 Cytokinin

The disease symptoms caused by *R. fascians* in plants such as wrinkling of leaves, formation of green islands, delayed senescence, and root inhibition, are indicative of cytokinin effects. Some of these symptoms can be mimicked by the addition of cytokinin (Depuydt et al., 2008, Oduro and Munnecke, 1975b).

In 1966, Thimann and Sachs were the first to propose a role for cytokinin in the symptoms associated with *R. fascians* infection in host plants. They reported that *Corynebacterium tumefaciens* produced a chloroform-soluble cytokinin- active substance in infected pea tissue. Since then 12 cytokinins or cytokinin- like compounds have been isolated and well characterised from the culture supernatant of the bacteria. Klämbt et al. (1966) isolated three cytokinin- active fractions from the cultures of *R. fascians* and later Helgeson and Leonard (1966) identified the compounds through ultraviolet absorption and mass spectrometry as isopentenyladenine (iP), nicotinamide and 6-methylaminopurine although the latter two are not considered to be active cytokinins. Later, zeatin (Z), zeatin riboside (ZR), cis-zeatin riboside (cZR), isopentenyladenosine (iPA), methylthioisopentenyladenine (ms-iP), methylthioisopentenyladenosine (ms-iPA) were identified as compounds secreted by *R. fascians* into culture medium (Table 1.3).

Table 1.3. Cytokinins detected in the culture supernants of *Rhodococcus fascians*

Cytokinin	Chemical Name	Abbreviations		Reference
Isopentenyladenine	6-(-3methyl-2-butenylamino)purine	iP	i ⁶ Ade	Helgeson and Leonard (1966) Pertry et al. (2009)
Isopentenyladenosine	6-(-3methyl-2-butenylamino)-9-β-D-ribofuranosyl purine	iPA	i ⁶ A	Rathbone and Hall (1972)
Zeatin or <i>trans</i> -Zeatin	6-(-4-hydroxy-3-methyl-2- <i>trans</i> -butenylamino)purine	Z or tZ	t-io ⁶ Ade	Scarborough et al. (1973) Eason et al. (1996) Pertry et al. (2009)
Dihydrozeatin	-	DZ	-	Eason et al. (1996)

Zeatin riboside	6-(-4-hydroxy-3-methyl-2- <i>trans</i> -butenylamino)-9-β-D-ribofuranosylpurine	ZR	t-io ⁶ A	Murai et al. (1980) Eason et al. (1996)
<i>cis</i> -Zeatin	6-(-4-hydroxy-3-methyl-2- <i>cis</i> -butenylamino)purine	cZ	c-io ⁶ Ade	Scarborough et al. (1973) Eason et al. (1996) Pertry et al. (2009)
<i>cis</i> -Zeatin riboside	6-(-4-hydroxy-3-methyl-2- <i>cis</i> -butenylamino)-9-β-D-ribofuranosylpurine	cZR	c-io ⁶ A	Jameson et al. (1991) Eason et al. (1996)
Methylthio-isopentenyladenine	6-(-3methyl-2-butenylamino)-2-methylthio-purine	ms-iP	ms ² io ⁶ Ad e	Murai et al. (1980)
Methylthio-isopentenyladenosine	6-(-3methyl-2-butenylamino)-2-methylthio-9-β-D-ribofuranosylpurine	ms-iPA	ms ² i ⁶ A	Murai et al. (1980) Jameson et al. (1991)
Methylthio- <i>trans</i> -zeatin	6-(-4-hydroxy-3-methyl-2- <i>trans</i> -butenylamino)-2-methylthiopurine	ms-t-Z/ 2MeStZ	-	Armstrong et al. (1976) Pertry et al. (2009)
Methylthio- <i>cis</i> -zeatin	6-(-4-hydroxy-3-methyl-2- <i>cis</i> -butenylamino)-2-methylthiopurine	2MeScZ	-	Pertry et al. (2009)
6-Methylaminopurine	-	-	m ⁶ Ade	Helgeson and Leonard (1966)

The cytokinin ribosides from tRNA degradation and cytokinin-active bases were recovered from the culture medium of *R. fascians* strains through bioassay and gas/liquid chromatography-mass spectrometry by Murai et al. (1980) and the presence of both free cytokinin- active bases and ribonucleosides in the culture medium suggested that tRNA may serve as one of the primary sources of cytokinin released by *R. fascians*, which was also reported by Scarbrough et al. (1973) and Armstrong et al. (1976). The increased production of isopentenyladenine and *cis*-zeatin by virulent strains compared with avirulent strains correlated with the degree of pathogenicity. Murai et al. (1980) inferred that the increase of iP in culture of virulent strains was indicative of an alternate biosynthetic pathway.

Eason et al. (1996) studied the role of cytokinin in pathogenicity of *R. fascians*, where the cytokinins secreted from *R. fascians* strains were purified, separated and quantified by a combination of high pressure liquid chromatography (HPLC) and radioimmunoassay (RIA). They found non-hydroxylated cytokinins were present 1000-fold higher than hydroxylated cytokinins in liquid culture, and contrary to Murai et al. (1980), virulent strains secreted only slightly higher levels of iP, iPA and ms-iPA than avirulent strains. The cytokinins detected in the culture supernatant of the avirulent strain were suggested to arise from tRNA which may account for high levels of *cis*-isomer of zeatin, whereas the elevated levels of cytokinin by virulent strains were thought to be due to *de novo* biosynthesis via a cytokinin synthase homologous to the cytokinin biosynthetic genes isolated from *Agrobacterium* and *Pseudomonas*. Eason et al. (1996) also showed that *Pisum sativum* inoculated with virulent strains of *R. fascians* had slight increase of iP and ms-iP but had lower levels of cytokinin nucleotides than plants inoculated with the avirulent strains.

Jameson (2000) noted that *R. fascians* secreted little hydroxylated (*Z*-types) cytokinin into culture medium when compared to other gall-forming bacteria, *P. syringae* pv. *savastoni*, *P. agglomerans* or acetosyringone-induced *A. tumefaciens* C58, whereas all four bacteria secreted similar quantities of non- hydroxylated (iP-types) cytokinins into culture. She suggested that the non-hydroxylated forms originated from tRNA.

Galis et al. (2005b) confirmed the results of Eason et al. (1996): an elevated level of cytokinin was not observed in pea inoculated with a virulent strain whereas the nonvirulent strain caused a transient increase in several cytokinins. They postulated that any elevation in

plant cytokinin might be so localised and transient that it was not detected, but also suggested the possibility of a novel cytokinin being produced that was causing the disease symptoms, which they were not able to detect by the radioimmunoassay. Galis et al. (2005a) using transgenic tobacco harbouring an *AtCKX3*: GUS promoter construct showed the up-regulation of *AtCKX3* by a virulent strain of *R. fascians* but the expression was not induced with avirulent strain and an active role for this enzyme at some stage of the infection process was inferred.

Depuydt et al. (2008) through transcript profiling demonstrated that class-I *KNOX* genes were transcribed in symptomatic leaves of *A. thaliana* and the expression of *AtIPT5* and *AtIPT7* was switched off at 7 dpi. Furthermore, *AtCKX3* was up-regulated along with *ARR5* indicating increased cytokinin signalling in *R. fascians* infected plants. They also showed that several types of cytokinins: tZMP, tZMP and iPMP decreased overtime with the down regulation of *AtIPT* genes. With the increase in CKX activity the substrates N-glucosides and iP decreased in accordance with up-regulation of *AtCKX3*.

Even though the disease symptoms due to *R. fascians* infection of host plants is similar to the ones produced by addition of exogenous cytokinins and the symptoms of abundant shoot proliferation, inhibition of root growth and delayed senescence are all typical cytokinin effects, the cytokinin analysis of pea seedlings infected with different *R. fascians* strains did not show marked differences in the levels of cytokinin (Eason et al. 1996, Galis et al. 2005b). These studies indicated that a more complex process was occurring and Vereecke et al. (2000) postulated that novel compounds produced by *R. fascians* were involved in disrupting plant hormone balances, ultimately leading to disease. They also found that auxin levels in plants carrying leafy galls were higher than those of control plants and suggested that auxins and molecules of bacterial origin were also involved in leafy gall formation.

Pertry et al. (2009) have shown that in *A. thaliana*, the cytokinin receptors AHK3 and AHK4 are essential for symptom development and that the cytokinin perception machinery is induced upon infection. They suggested that the pathology is induced by the secretion of a mix of six synergistically acting cytokinins: iP, tZ, cZ and their 2-methylthio (2MeS) derivatives and that these cytokinins are perceived by the cytokinin receptors AHK3 and AHK4. These cytokinins levels were higher in virulent D188 supernatant than D188-5

avirulent strain and suggested that this may be due to the linear plasmid which is responsible for virulence-associated production. Based on their study they proposed the model for the modus operandi of the *R. fascians* cytokinins in *Arabidopsis*. They suggested that, initially, the bacterial cytokinins are perceived by AHK3 and, in parallel, strongly activate AHK4 expression in shoots, increasing the plant tissue sensitivity to cytokinin and the synergistic action of cytokinin leads to developmental alterations in the plant. They suggested that the cytokinins are degraded by the feedback and homeostatic mechanisms of the plant which results in the degradation of the bacterial cytokinins. cZ and the less toxic 2MeSZ accumulate in infected tissues due to inadequate degradation by CKX which might lead to continuous tissue proliferation and symptom maintenance (Pertry et al. 2009). However, the data on the cytokinins levels in avirulent strain D188-5 infected *Arabidopsis* was not published and the comparison was made only with mock control.

Depuydt et al. (2009b) examined the expression of all the genes involved in cytokinin metabolism, perception and signal transduction during the infection of *R. fascians* virulent strain D188 in *Arabidopsis*. The microarray analysis revealed down regulation of *AtIPT3*, with up-regulation of two *AtCKXs*, six type-A *ARRs* and sugar transport genes, confirming the onset of cytokinin homeostasis mechanism in plants. Depuydt et al. (2009b) showed the differential expression of cytokinin-associated genes during *R. fascians* infection at 7, 14 and 24 dpi, where *R. fascians* D188 (virulent strain) had strong expression of *ARR6* and 7 with other *ARRs* induced at 24 dpi. This indicates the presence of cytokinin in *Arabidopsis* infected with virulent strain D188 compared to avirulent D188-5.

Upon infection of plants by *R. fascians*, plant-and pathogen derived cytokinins inversely affect the plant defense mechanism as illustrated by Choi et al. (2011) in Figure 1.11. The cascade of events due to hyperactive cytokinin responses downstream of AHK3 and AHK4 (Figure 1.11), leads to induction of *KNOX* genes including *KNAT1* ectopic expression which results in aberrant cell divisions in leaves due to cytokinin-inducing cyclins such as *CYCD3* which causes leaf serrations in *A. thaliana* (Depuydt et al. 2008). In normal conditions, *KNOX* proteins induce cytokinin biosynthetic *IPT* genes (Yanai et al., 2005), but *R. fascians* induced *KNOX* proteins in infected plant does not increase cytokinin production in plants which can be seen by the down regulation of *IPT* genes during *R. fascians* infection (Depuydt et al., 2009b). Choi et al. (2011) indicated that *R. fascians* secretes effectors or auxin to

specifically suppress AHK2, AHK3 and *ARR2*-mediated defence mechanism (Figure 1.11) suggesting that pathogen-derived auxin specifically suppresses the cytokinin-induced defense response during *R. fascians* infection.

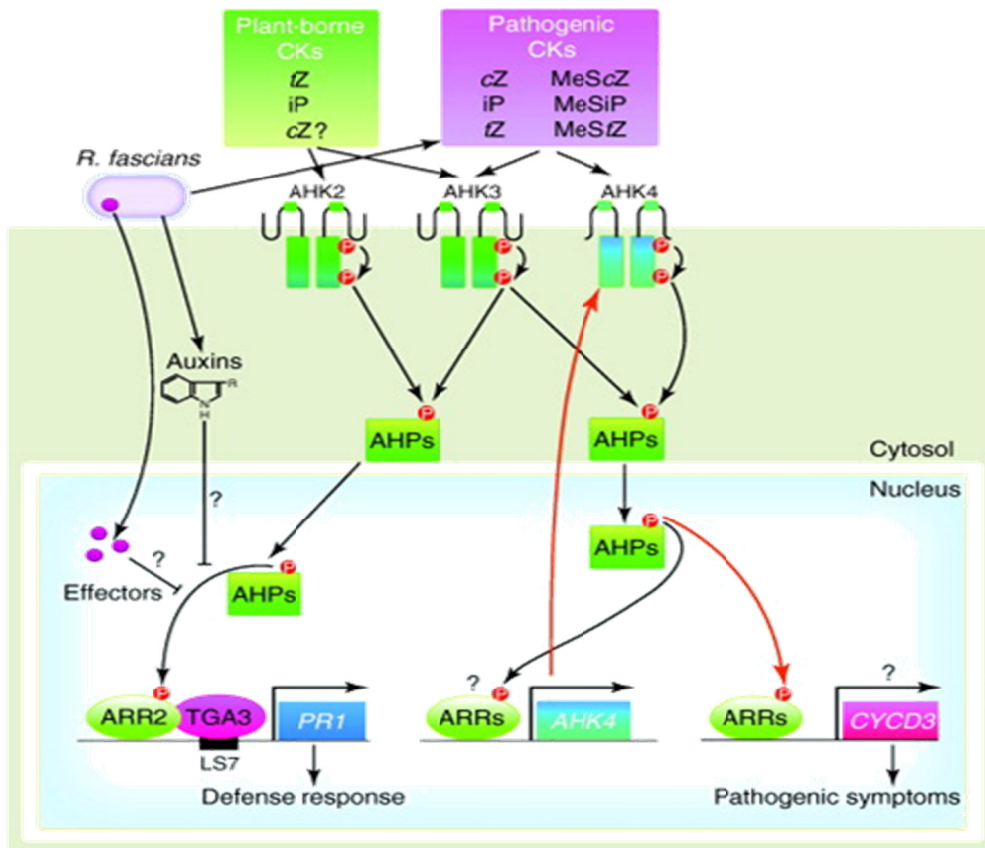


Figure 1.11 **Modulation of plant cytokinin signalling by *R. fascians*-originated cytokinins.** Source: Choi et al. (2011). Reproduced with permission from Elsevier Limited.

1.3.4.2. Auxins

The disease symptoms of *R. fascians*, such as vascular tissue differentiation, cell enlargement, and inhibition of bud outgrowth are not solely attributed to cytokinin but they are also typical auxin effects.

The ability to produce the plant hormone indole-3-acetic acid (IAA) is widespread among soil, epiphytic and tissue colonising bacteria (Patten and Glick, 1996) where, in the case of

A. tumefaciens, and *P. syringae* pv. *savastanoi*, IAA is involved in pathogenesis (Clark et al., 1993, Mazzola and White, 1994, Morris, 1986), while in others like *Rhizobium*, *Azospirillum*, and other *Pseudomonas* spp. IAA stimulates plant growth and increases the release of plant metabolites that the bacteria can utilise (Bar and Okon, 1993, Patten and Glick, 1996).

Patten and Glick (1996) have indicated that it is the extent to which bacterial sources of auxin modify endogenous levels of free IAA in the plant that ultimately decides whether the relationship is beneficial or pathogenic, where an optimal level of IAA enhances growth, while supraoptimal levels elicit the disease response. In the case of *P. agglomerans*, the IPyA (Indole-3-pyruvic acid) pathway is used for IAA production and is associated with epiphytic fitness of the bacteria on host plants, whereas the IAM (Indole-3-acetamide) pathway has been linked to the development of galls induced by the bacterium (Gafni et al., 1991, Manulis et al., 1998).

Vereecke et al. (2000) observed that auxin levels in plants showing leafy galls were much higher than those in control plants and suggested that the cell swelling, lateral root initiation and the effects on vascular tissues which are all associated with *R. fascians* infection can also be attributed to increased auxin production in infected *Atropa belladonna* plants. Manes et al. (2001) also confirmed the above report that the level of IAA production was enhanced in infected tobacco plants with the virulent strain of *R. fascians* compared to control plants within 1 to 2 weeks post inoculation.

Vandeputte et al. (2005) observed that *R. fascians* has the ability to produce and secrete significant amounts of IAA through the IPyA (Indole-3-pyruvic acid) pathway. The amount of IAA secreted by *R. fascians* was higher than or comparable to that secreted by the plant pathogens *A. rhizogenes* and *Xanthomonas campestris*, respectively. They also noticed that the amount of IAA secreted by *R. fascians* in the culture medium increased with the addition of infected-plant extracts and tryptophan but not with tryptophan alone. However, a global transcriptomics study using microarrays combined with profiling of primary metabolites on *R. fascians* virulent strain D188 infected *Arabidopsis thaliana* by Depuydt et al. (2009b) revealed active suppression of an oxidative burst which implies that auxin secreted by *R. fascians* might be involved in plant defence suppression. It has been suggested that auxin

could play a role in the initiation of symptoms by suppressing plant defence (Depuydt et al., 2009b, Robert-Seilaniantz et al., 2007), and could also function in the epiphytic survival of the bacteria (Goethals et al. 2001).

Stes et al. (2012) recently demonstrated that the bacterial cytokinins stimulates auxin biosynthesis through indole-3-pyruvic acid (IPA) pathway in infected *Arabidopsis* with virulent *R. fascians* strain D188 which results in high auxin signaling and they also implied that auxin was used to reinforce symptom formation.

1.4 Objectives

The plant pathogenic actinomycete *Rhodococcus fascians* interacts with a wide range of hosts resulting mainly in the induction of shoot and leaf malformations. That the cytokinins have a role in *R. fascians*-induced symptoms is strongly supported by the presence of the *fas* operon of the linear virulence plasmid which consists of six genes involved in cytokinin biosynthesis and which is essential for virulence (Crespi et al. 1992). Further, Depuydt et al. (2009b) suggested that the over-representation of genes involved in cytokinin perception, signal transduction and homeostasis in microarray data supported the central role of cytokinin as a virulence determinant. Central to this project are isopentenyltransferase (IPT) which is encoded by the *fasD* gene (Crespi et al. 1992), *fasE* which is homologous to plant CKX and acts as a dehydrogenase and degrades cytokinins and *fasF* which is homologous to plant LOG and contributes to the bioactive cytokinin bases produced by *R. fascians* (Pertry et al. 2010).

Although extensive studies on the molecular aspects of *R. fascians*-plant interactions have revealed the virulence determinants the underlying molecular mechanism of shooty gall formation in hosts due to *R. fascians* infection seemingly without significantly elevated levels of cytokinin has been obscure. Previous workers have shown that the expression of plant genes involved in cytokinin homeostasis, *IPT* and *CKX*, was strongly affected upon infection (Galis et al. 2005a, Depuydt et al. 2008, Depuydt et al. 2009b, Pertry et al. 2010). The most rigorous work published to date has been on *Arabidopsis*. The present study was undertaken to illustrate the infection pattern of *R. fascians* on pea and to elucidate the outcome of the plant-pathogen interaction through the study of cytokinin biosynthetic and metabolic genes. The cytokinin activating enzyme, 'The Lonely Guy' (LOG) has so far only been studied in

rice and *Arabidopsis*. In this study, LOG was evaluated to understand its role in cytokinin biosynthesis and in *R. fascians*-pea interaction along with its homologue *fasF* (*R. fascians*).

As noted above, previous reports are mainly on the interaction between *R. fascians* with *A. thaliana* a non-natural host. In our lab, *A. thaliana* was found to have low infection rate and poor reproducibility when infected with *R. fascians* (Jason Song, personal communication). The nature of fasciation and the severity of the symptom induced by *R. fascians* depended on the host plant (Lacey 1939, Eason et al. 1995). It has been previously reported by Eason et al. (1995) that the severity of disease symptom depended on the host, origin of *R. fascians* strains and the virulence of the strains. The onset of *R. fascians* disease was first described by Brown (1927) on sweet pea (*Lathyrus odoratus*) and Tilford (1936) showed its pathogenic effect on sweet peas and garden pea. As the Jameson lab had previously used peas as the model plant, garden pea (*Pisum sativum*) was selected for this project as it is a natural host and also due to its ease of infection and speed of symptom development (5 to 7 days) when infected by *R. fascians* (Putnam and Miller 2007).

The number of tissues examined following *R. fascians* infection has also been limited. Depuydt et al. (2008) reported the response of *Arabidopsis* to *R. fascians* by analysing morphological, molecular and biochemical alteration that occurred in symptomatic leaves upon infection. They did not consider other parts of the plant such as the cotyledon, root and shoot which Eason et al. (1995, 1996) and Galis et al. (2005b) have shown to change morphologically and biochemically following inoculation by both virulent and avirulent strains of *R. fascians*.

Recently, Pertry et al. (2009) proposed a model for the "modus operandi of *R. fascians* cytokinins" in *Arabidopsis*, suggesting that due to the inability of *CKX* genes to eliminate all bacterial cytokinins, especially cZ and 2MeScZ, accumulation of these cytokinins caused shooty growth. In that report cytokinin production during infection was compared with *Arabidopsis* infected with *R. fascians* virulent strain and mock-inoculation, but data on the plants infected with avirulent strain was not included. So, it is not clear what happens to the accumulated cytokinins in the plants inoculated with the avirulent strain which do not show the disease symptoms. Eason et al. (1996) showed that pea inoculated with *R. fascians* virulent strains had only slightly increased levels of non-hydroxylated cytokinins iP, iPA and

ms-iPA and lower levels of cytokinin nucleotides than plants inoculated with avirulent strains. Further, Galis et al. (2005b) revealed a decrease in the levels of cytokinin free bases, ribosides, O-glucosides and nucleotides in the pea shoots inoculated with virulent strain compared to the shoots inoculated with avirulent strain. It is possible that the *fasF* strongly reduced the levels of nucleotides through the phosphoribohydrolase activity by *R. fascians* virulent strain and also 2MeSiP which is chromosomally produced might be used as precursor by Fas to form other cytokinins (Pertry et al. 2010). Pertry et al. (2009) reported that, in tobacco leafy galls, iP increased instead of cZ and 2MeScZ. This indicates that accumulation of specific cytokinin depends on the host. So, the inefficiency of *AtCKX* degradation on cZ and 2MeScZ model does not explain clearly the role of cytokinins in shoot malformation in different hosts.

In this study, pea was used as the model plant to investigate the response of the pea *IPT*, *LOG* and *CKX* genes following inoculation by both the virulent and avirulent strains of *R. fascians*. Response regulator (*RR*) genes were used as surrogate measures of the levels of bioactive cytokinins during infection. To gain insight into the possible morphological, microbiological and molecular alterations that occur in the interaction of *R. fascians* and pea, various plant organs including cotyledons, roots and shoots were analysed at different growth periods.

This research is based on the hypothesis that the key homeostatic mechanism for cytokinin is disrupted during infection of *R. fascians*. Therefore the expression pattern of family members of *IPT*, *LOG* and *CKX* might be expected to change either by down regulation of the plant *IPT* and *LOG* expression and or up-regulation of *CKX* and potentially the opposite for the *R. fascians* genes. The main objectives were:

1. To test the presence of cytokinin synthase (*IPT*), cytokinin activation (*LOG*) genes and cytokinin oxidase/ dehydrogenase (*CKX*) genes in *R. fascians* strains previously classified as virulent and avirulent, in order to assess the integrity of the virulent strains.
2. To illustrate the influence of an avirulent and a virulent strain of *R. fascians* in inoculated pea plants through microbiological and physiological studies.
3. To isolate members of the *IPT*, *LOG* and *CKX* gene family members in pea and in *R. fascians* in order to study the expression of *PsIPT*, *PsLOG* and *PsCKX* genes, and

simultaneously the expression of *R. fascians* *fas* genes (*RfIPT*, *RfLOG* and *RfCKX*) in pea inoculated with virulent and avirulent strains of *R. fascians* in different organs and at different stages of plant growth,

4. To isolate members of response regulator (*PsRR*) gene families from pea and monitor their expression as an indirect measure of the levels of bioactive cytokinins during infection.
5. To study the source-sink transitions that occur in cotyledons and shoot upon infection of pea by *R. fascians* by monitoring the expression of transporter gene (*PsSUT*, *PsSUF* and *PsAAP*) family members at different stages of growth.

Chapter 2 GENERAL MATERIALS AND METHODS

2.1 *Pisum sativum* growth conditions

The Bohatyr variety of *Pisum sativum* was selected for the study. The seeds were procured from Plant and Food Research Institute, Christchurch.

Initial work involved standardisation of the methodology for the surface sterilisation of seeds, seed germination, inoculation of *Rhodococcus fascians* and media for growth of inoculated peas plants (Figure 2.1).

Surface sterilisation of seeds: Three methods were used to select the best method:

- a. Seeds were soaked in 75% (v/v) ethanol for 30 s, rinsed three times with water, 3% (v/v) commercial bleach (containing 31.5 g L⁻¹ sodium hypochloride) was added for 3 min and then seeds were rinsed ten times with sterile water (Vedam et al., 2006).
- b. Seeds were washed in warm water with soap, soaked in 3% (v/v) hydrogen peroxide for 15 min and thoroughly washed with distilled water (Vasil'eva et al., 2007)
- c. Pea seeds were rinsed three times in tap water. Swirled for 2 min in 75% (v/v) ethanol and serially washed in sterile water two times and then soaked for 6 min in 10% (v/v) bleach (containing 31.5 g L⁻¹ sodium hypochloride). Seeds were then washed thoroughly four times in sterile water (Eason et al., 1996). This method was selected for further experiments as the seeds did not have any surface contamination during their growth.

Seed germination:

- a. The germination of seeds was initially done by placing the surface sterilised seeds in a sterile petri-dish with two pieces of damp sterile Whatman No.1 filter paper, germinated in the dark for 72 h (Eason et al. 1996), but this method was not used as the filter paper had to be wetted frequently and percentage of seed germination was only 45%.
- b. A modified method from Eason et al. (1996) was used to germinate the surface sterilised seeds on sterile soft agar (0.8% w/v) at room temperature for 72 h. Seed germination was 89%.

Seed inoculation with *Rhodococcus fascians*:

- a. Eason et al. (1996) method of using pre-germinated seeds immersed in mid log phase culture broth of *R. fascians* in Klambt broth, incubated at 26°C with shaking (ca.100 rpm) for one hour.
- b. A modified method of above, where whole pea seeds were added to *R. fascians* mid log phase culture broth in Kado and Heskett '523' incubated at 26°C with shaking at 121 rpm for 4 h. This method was selected for inoculation as the whole seed inoculation led to better growth and symptom development, whereas, in the pre-germinated seed inoculation some of the young seedlings were damaged due to handling.

Growth media for plants:

The inoculated seeds were placed in pots containing either sterile sand or vermiculite with Hoagland's mineral salt solution or sterile 500 ml containers with agar (0.6% w/v) and Hoagland's mineral salt solution (10% w/v). Agar was selected as the optimal medium for growth compared with sand or vermiculite as contamination was minimised.

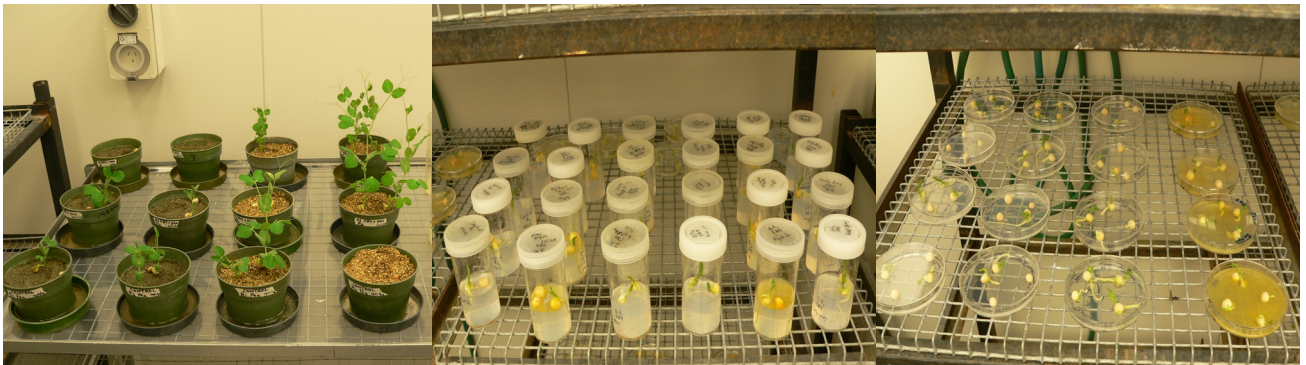


Figure 2.1. Standardisation for medium for pea growth and inoculation of *R. fascians*: sand, vermiculite (left) and agar (middle) and different methods of inoculation by *R. fascians* (right).

2.2 *Rhodococcus fascians* culture strains

The *R. fascians* strains, 589 (avirulent) and 602 (virulent) were used in this study based on previous studies (Eason et al., 1995, Eason et al., 1996). The cultures of *R. fascians* 589 and 602 (stored in 50% glycerol at -80°C), were re-streaked and sub-cultured in Kado and Heskett '523' medium (Appendix A.2.1), grown at 27°C for 2-3 days. The strains were then cultured into '523' broth and incubated at 26°C with shaking at ca. 150 rpm, until they reached mid log phase, estimated by BIO-RAD Smart Spec™ Plus spectrophotometer.

2.3 Inoculation of *P. sativum* seeds

The optimised method used to inoculate pea seeds with *R. fascians* was similar to that described by Eason et al. (1996). Seeds of Bohatyr peas were surface sterilised by rinsing with tap water and removing any debris by decanting the water, 75% (v/v) ethanol was added and the seeds were swirled for 2 min. The seeds were then serially washed with sterile water and then soaked for 6 min in 10% (v/v) bleach (commercial grade laundry bleach, containing 31.5 g L⁻¹ sodium hypochloride) with occasional swirling. The seeds were washed four times with sterile water and transferred to the mid log phase cultured broth of either strain 589 (avirulent) or 602 (virulent). The flasks with seeds for a mock control were incubated in Klambt broth (Appendix A.2.2). All flasks were placed in a shaker at 121 rpm at 26°C for 4 h.

Five to six seeds were placed in sterilised 500 ml containers with 0.6% (w/v) agar and 10% (w/v) Hoagland's mineral salts solution (Appendix A.2.3). The containers were placed in a growth room (Figure 2.2) in a randomised block design, with three treatments (control, avirulent and virulent) and 10 sampling times (2, 5, 9, 11, 15, 20, 25, 30, 35, 40 dpi), each with five replications. The plants were grown at 22°C with a 16 h photoperiod.

Samples of whole plants or separated cotyledons, roots and shoots were taken for a variety of purposes. The samples were stored in liquid nitrogen for gene expression studies, fixed in FAA (10% formaldehyde: 5% acetic acid: 50% alcohol) for light microscopy, cryopreserved for scanning electron microscopy. Fresh samples were used for chlorophyll estimation and microbial counts. For each sampling, 5 biological samples were collected from each treatment (control, avirulent and virulent).

The same experiment was repeated twice, with the same procedures and sampling



Figure 2.2 *P. sativum* experimental set up in a growth room.

2.4 Microscopy

2.4.1 Scanning electron microscopy (SEM)

The SEM was done using a freeze-drying methodology. The fresh plant samples (cotyledon, shoot, root, etc.) from each sampling time were freeze-dried in a vessel which was pre-cooled to -180°C using liquid N_2 . Samples from each of the specimens were placed altogether in one aluminium container which was coded for identification. The samples were kept as small as possible to ensure uniform freezing. The container was plunged into liquid N_2 to ensure rapid freezing. A fine wire mesh was placed over the top of the container to avoid the samples moving during the drying process. The containers were then placed in a modified Edwards freeze-drier, under a high vacuum with reduced temperature of -210°C overnight (16 h approximately).

The samples were removed, placed on double-sided carbon tabs and mounted on aluminium SEM stubs. The specimens were coated with gold in an Emtech K550X sputter-coater for 4 min at 1.2 amps, resulting in a coating thickness of about 200 \AA . The specimens were examined with a Leica S440 Scanning Electron Microscope. Microphotographs were taken.

The same procedure was followed to study some of the avirulent and virulent culture strains.

2.4.2 Light microscopy

2.4.2.1 *Rhodococcus fascians* cultures

Selected avirulent strains (589, 593, and 576) and virulent strains (602, 603, and 596) were grown on Kado and Heskett '523' media, inoculated into '523' broth and incubated in a shaker for 2 d. These cultures were processed for Gram staining (Beveridge and Davies, 1983).

2.4.2.2 Fixation, dehydration and embedding

Whole pea plants were sampled for light microscopy. A modified procedure of Carletom and Druvy (1957) for fixation, dehydration, embedding and microtoming was followed. Three replicates were collected and fixed in FAA (10% formaldehyde, 5% acetic acid and 50% alcohol/ethanol), under continuous vacuum for 48 h to expel all air from the samples. The samples were transferred to 70% (v/v) ethanol for 1 h minimum, again under vacuum to ensure there was no imbibed air. The tissue was stored in 70% (v/v) ethanol for dehydration. The dehydration was done with a TBA (tertiary butyl alcohol)/ethanol/water series:

10 TBA: 40 95% (v/v) ethanol: 50 water for 1 h

20 TBA: 50 95% (v/v) ethanol: 30 water for 1 h

35 TBA: 50 95% (v/v) ethanol: 15 water for 1 h

55 TBA: 40 95% (v/v) ethanol: 5 water for 1 h

75 TBA: 25 95% (v/v) ethanol for 1 h

100 TBA at 37°C for 1 h

100 TBA at 37°C for 1 h

100 TBA at 37°C, overnight

For infiltration with Ralwax, tissues were transferred to equal parts TBA: Ralwax and placed in an open bottle in a 60°C oven overnight so that the TBA could evaporate and allow the Ralwax to infiltrate the tissue (cellulose walls are slow to allow diffusion). Next day, the remaining mixture was poured and replaced with fresh Ralwax for 1 h. To ensure full infiltration, another change of Ralwax was done. The samples were then blocked on an embedding machine (Tissue-tek cryo console). In later samples, Ralwax wax was replaced by plain Paraplast wax (mp 56°C) due to the unavailability of Ralwax. The embedded blocks were hardened on the chill tray of the embedder, and kept at 4°C until sectioning.

Serial sections of the embedded tissue blocks were cut to a thickness of 10 – 13 μm thickness on a Lecia RM2165 microtome. The ribbon pieces were floated on a clean ethanol-wiped microscope slide flooded with distilled water, kept at 42°C on a hot plate for 1 min to remove the compression out of the tissue and relax the wax, and then the excess water was drained off the slides. The slides were incubated in a slanted position for 24-48 h on the hot plate. The slides were then kept in a 40°C oven until staining.

2.4.2.3 Staining

Sass's Safranin and fast green staining: The sections were de-waxed in 100% xylene at 50-55°C in a fumehood for 3 min and rinsed in 1:1 (v/v) xylene: absolute ethanol, then serially rinsed with 90%, 70% and 50% (v/v) ethanol, each for 2 min, and finally with distilled water for 2 min. The sections were treated with 1% aqueous safranin for 1 h, and then washed with distilled water, followed by serial dehydration with 50%, 70%, 90% and 95% (v/v) ethanol, each for 2 min. Counter stain 0.1% fast green FCF in 95% (v/v) ethanol was used for 5 to 30 s, and then treated with 100% ethanol for 2 min. The sections were then rinsed in 1:1 xylene: absolute ethanol and then 100% xylene at room temperature for a minimum of 3 min. The slides were mounted in Eukitt, dried in a 37°C oven for a minimum of 2 d (Johansen, 1940).

Ruthenium red staining: Following de-waxing of the sections, 0.05% (v/v) aqueous Ruthenium red was added to the slides for 10 min, followed by a rinse in distilled water. Dehydration was done using an alcohol - xylene series mentioned as above. The sections were cleared with 100% xylene at room temperature for a minimum of 3 min. The slides were mounted in Eukitt, dried in a 37°C oven for 2 d (Manes et al., 2001).

Haematoxylin-eosin staining: The section de-waxing and hydration were done as described above and stained with Mayer's Haemalum (double strength) for 5 min. The slides were held in running tap water for 10 min. The dehydration step until 100% ethanol was done. The counter stain 0.5% (v/v) Eosin Y (Sigma) in 100% ethanol was used to stain the sections for 1 min. Then sections were treated with 1:1 xylene–absolute ethanol and then 100% xylene at room temperature for 3 min, mounted in Eukitt and dried in a 37°C oven for a minimum of 2 d (Kitin et al., 2005)

Gram staining: The embedded sections were treated with 100% xylene to remove the wax and hydrated through absolute alcohol to water. The sections were stained with 2% (w/v) crystal violet for 2-3 min. The stain was washed off with Gram's iodine and then the slide was flooded with Gram's iodine for 2-3 min. The sections were then decolorized in absolute alcohol. Directly from absolute alcohol, the sections were stained with 1% (w/v) aqueous neutral red for 2-3 min and rinsed with water. The slides were blot dried and complete dehydration was done with 2:1 (v/v) aniline- xylene and then 100% xylene. The slides were then mounted in Eukitt and dried in a 37°C oven for a minimum of 2 d (Carletom and Druvy, 1957).

The stained sections were viewed using a Zeiss Axio Imager M1 compound microscope with brightfield (BF) and differential interference contrast (DIC) optics/lighting capabilities. Tissues were examined with 10x, 20x, 40x and 100x EC PLAN objectives. Micrographs were captured using a Zeiss AxioCam HRc cooled CCD camera at 1300x1030 pixel resolution for all magnification except the 100x objective where images were taken at 3900x3090 pixel resolution to facilitate later digital enlargement of specific areas to allow better visualisation of the fine details of *R. fascians*.

2.5 Microbial Counts

The microbial count was determined to estimate the *R. fascians* strain populations in or on infected pea plants where the number of Colony Forming Units (CFU) per ml of plant extract was calculated.

A protocol similar to that of Vereecke et al. (2002) was followed to determine the total bacterial population. The bacterial populations were determined in two ways: either complete plants were crushed to determine the total bacterial population (whole) or complete plants were treated with 6% bleach (containing 31.5 g L⁻¹ sodium hypochloride) for 1 min followed by two washings in sterile water prior to crushing the plants in a sterile pestle and mortar to evaluate the internal bacterial population. The pea plants were sampled from 4 h after inoculation (hpi) until 40 days post inoculation (dpi) at regular intervals of growth (i.e. 4 hpi, 2, 5, 7, 9, 11, 15, 20, 25, 30, 35 and 40 dpi). The control, avirulent and virulent pea plant samples were used to determine the bacterial populations.

Whole plant samples were crushed either with or without bleach treatment and a serial dilution plating technique with pour plate method was done. Crushed plant extracts were diluted to 10^{-1} and 10^{-2} dilutions and 1 ml was added to a sterile petri dish, then 15- 20 ml warm molten Hado and Heskett '523' media was added, mixed carefully with the extract and the plates were incubated at 26°C for 2 d. The colonies were counted and CFU per ml of plant extract was calculated and the values transformed logarithmically. Values resulting from two independent experiments were pooled.

CFU/ml = Number of colonies X dilution / amount of extract added

2.6 Chlorophyll Estimation

Samples of cotyledon, shoot and root treated with and without avirulent and virulent strains of *R. fascians* was used to estimate chlorophyll content at various growth stages from 4 hpi to 40 dpi. The total chlorophyll content was determined as described in Evans et al. (2012a). Fresh 0.1 g of cotyledons or shoot or root was weighed into 2 ml Eppendorf tubes and 1ml of dimethylformamide (DMF) was added. Samples were wrapped in aluminium foil and incubated at 4°C overnight, followed by centrifugation at 2.3×10^5 g for 5 min to settle the plant tissues. The absorbance of the supernatant (2 μ l) was used to read at 664 and 667 nm with a Nanodrop™ spectrophotometer (Thermo Fisher Scientific Inc.). The total chlorophyll was calculated using the equation of Wellburn (1994):

$$\text{Chl}_{\text{total}} = 7.12A_{664} + 18.12A_{667}$$

2.7. Gene identification in silico

To identify putative cytokinin biosynthesis and degradation genes, isopentenyl transferase (*IPT*), Lonely Guy (*LOG*), cytokinin oxidase/ dehydrogenase (*CKX*) and response regulator (*RR*) sequences in pea, all the family members of these multigene families from *Arabidopsis thaliana*, and the available legume homologues of *Medicago truncatula*, *Lotus japonicus*, *Glycine max*, were used as query sequences to BLAST search the GenBank database (<http://blast.ncbi.nlm.nih.gov>). The *R. fascians* and other microbial sequences of relevant *IPT*, *LOG* and *CKX* were also identified. Sequenced data were aligned using the ClustalX program (Thompson et al., 1997).

Gene identification was also done by Dr Jianchen Song based on a pea transcriptome sequence analysis.

2.7.1 Phylogenetic analysis

For phylogenetic analysis, orthologues from *Arabidopsis*, legumes, maize, rice and *R. fascians* of each gene of interest were used to construct a Neighbor-Joining (NJ) phylogenetic tree using ClustalX software (Thompson et al., 1997) and also through Maximum Parsimony method in MEGA4 (Tamura et al., 2007). Each tree was rooted with an out group orthologue.

2.8 RNA extraction and cDNA synthesis

For RNA extraction, cotyledons, roots, shoots and whole plants as well as avirulent (589) and virulent (602) strains of *R. fascians* were used. The plant tissues were immersed in liquid nitrogen immediately on harvest and stored at -80°C.

As RNA is very susceptible to degradation, care was taken to keep the environment free of RNA degrading enzymes (RNase) which are prevalent in the environment. The tissues were ground and mixed well in the presence of liquid nitrogen to prevent thawing of the samples. RNA zap was used on work surfaces, pipettes and other surfaces to eliminate RNase contamination. Hydrogen peroxide (3%) v/v was used on plastic and metal equipment. Aluminium foil which was baked at 300°C in an oven for a minimum of 4 h to free it from RNase contamination was used as a working surface on the bench during extraction. Commercially supplied RNase free filter tips and Eppendorf tubes were used for all RNA work. The whole process of RNA extraction was done in an RNase-free chamber.

2.8.1 TRIzol[®] / Tri Reagent[®] RNA Extraction

TRIzol[®] RNA extraction is a phenol-chloroform based extraction procedure. Phase separation of the aqueous phenol and organic chloroform containing fraction separates RNA into the aqueous fraction, leaving DNA on the interface and proteins in the organic fraction (Chomczynski and Sacchi, 1987).

The ground frozen plant tissue (50 -100 mg) was added to 1 ml of TRIzol[®] (Invitrogen) or Tri reagent (Ambion) in a 1.7 ml Eppendorf tube, vortexed for 20-30 s and allowed to stand for 3 min at room temperature. The tubes were centrifuged at 12,000 rpm for 2 min at 4°C. The supernatant was transferred to a new tube, 200 µl of chloroform was added and the mixture was shaken vigorously for 15 s and allowed to stand for 5 min at room temperature. Then the tube was centrifuged at 12,000 rpm for 15 min at 4°C. The top aqueous phase was

transferred to a new tube and stored for 2 min at room temperature. Isopropanol (500 μ l) was added, mixed gently and incubated for 10 min at room temperature, then centrifuged at 12,000 rpm for 5 min at 4 °C. The supernatant was discarded and the RNA pellet was washed with 1 ml 75% (v/v) ethanol, vortexed to suspend the pellet and centrifuged at 12,000 rpm for 1 min at 4°C and the supernatant discarded. The pellet was again rewashed in 1 ml of 75% (v/v) ethanol and centrifuged for 2 min at 12,000rpm at 4°C. Ethanol was removed and the pellet air-dried for 10 min to completely remove the ethanol. The RNA pellet was dissolved in 30 μ l RNase free water or 1x RNA secure (Invitrogen) and heated to 60°C for 10 min in a dry bath by tapping the bottom of the tube gently every 3-5 mins to dissolve the RNA pellet. The RNA was stored at -20°C prior to cDNA synthesis.

2.8.2 cDNA synthesis

The extracted RNA was converted to cDNA by reverse transcription. Based on the quality of RNA, 0.5 – 1 μ g of RNA was mixed with 1 μ l (100 pmoles) of random primer (pDN6), 1 μ l (50 pmoles) of oligo dT primer, 0.5 μ l of 25x RNA secure and made up to 10 μ l with DEPC water (Appendix A.2.8). The solution was incubated at 65°C for 10 min and then placed on ice for 5 min. The RT master mix (10 μ l) containing 4 μ l of 5x RT buffer, 2 μ l of 100 mM DTT, 1 μ l of 20 mM dNTPs mix, 1 μ l of Expand Reverse Transcriptase (50U/ μ L) (Roche) and 2 μ l of DEPC water was added. The reaction mixture was incubated at room temperature for 10 min, and then increased to 42°C for 60 min. The reaction was inactivated at 70°C for 15 min. The synthesised cDNA was diluted 5- fold with TE buffer and stored at -20°C.

2.9 DNA/RNA quantification

The integrity and purity of RNA/ DNA was checked using both a Nanodrop™ spectrophotometer and agarose gel electrophoresis. Spectrophotometry provided an estimate of the concentration and purity of the DNA and RNA. To determine the integrity and size of both DNA/RNA, gel electrophoresis was used.

2.9.1 Agarose gel electrophoresis

Throughout the research, to determine the quantity and to assess the quality of extracted RNA, PCR products, and for DNA purification, 1% to 2% (w/v) agarose gel electrophoresis was used. The gels were made by mixing an appropriate quantity of agarose in 1 xTAE buffer made from 25 x TAE buffer (Appendix A. 2.4), heated in a microven until all the agarose had

completely dissolved and a clear solution is obtained. Then the solution was allowed to cool to around 60°C and 2 µl of SYBR Safe™ DNA gel stain was added, mixed well and poured into the gel cradle with appropriate comb and allowed to set for minimum of 30 min. The gel well after solidification was kept in a gel tank containing 1 xTAE buffer and electrodes. Samples were loaded after mixing 1µl 6x loading buffer (Appendix A. 2.8), 2 µl sample and 3 µl of tank buffer (1x TAE). To quantify the size of the bands, 2 µl of Bioline HyperLadder 1 (Appendix A. 2.10) was used. The gel tank was closed and run at 70V or 100V for RNA/DNA to run 2/3 rd of the way down the gel. Gels were visualised using a Safe Imager™ blue-light transilluminator and/or a Chemi Genius 2 BioImaging System (Syngene). Images were visualised, recorded and analysed using GeneSnap image acquisition software (Synoptics Ltd).

The RNA integrity was assessed based on 28S and 18S rRNA bands (Figure 2.3). As the 28S rRNA should be approximately twice as intense as the 18S rRNA band, the ratio of 2:1 (28S:18S) is good indication of intact RNA (www.ambion.com). The DNA integrity was assessed based on the structure of the band and comparison with the size ladder.

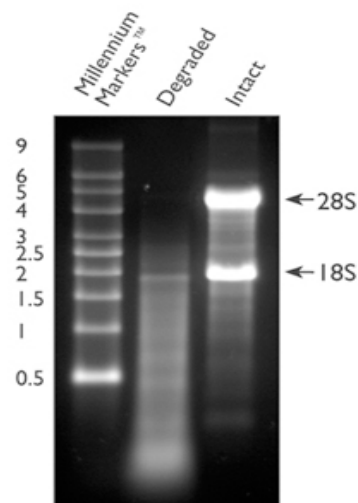


Figure 2.3 RNA integrity in a gel. RNA gel demonstrating intact and degraded RNA along with Millennium markers™. Image reproduced from Ambions TechNotes 8(3), (www.ambion.com).

2.9.2 Nanodrop™ Spectrophotometry

To measure the quantity and integrity of RNA/DNA in a sample a NanoDrop™ spectrophotometer (Thermo Fisher Scientific Inc.) was used. The NanoDrop utilises the absorbance peak of RNA/DNA (260 nm) to calculate the concentrations (ng/µl) and provides

an estimate of purity by assessing the 260/280 and 260/230 nm ratios. Samples with a 260/280 ratio of 1.8 -2.0 and 260/ 230 ratio of 1.8 – 2.2 was accepted as 'pure' RNA/DNA (www.ambion.com).

2.10 Polymerase Chain Reaction (PCR)

The Polymerase Chain Reaction (PCR) was used to amplify DNA fragments. The PCR reactions were carried out based on manufacturer instructions. Taq PCR reagent from Roche was used. A PCR mix was prepared with the following composition for a 20 µl PCR reaction:

10X Taq buffer	2 µl
dNTPs(2 mM)	2.5 µl
25 mM MgCl ₂	1 µl
Primers (10 pmol/ µl)	1 µl each
cDNA (95-fold diluted)	2 µl
Taq DNA polymerase (5U/ l)	0.2 µl
Water	10.3 µl

When multiple samples were done, a master mix with/ without template or and primers were prepared based on PCR reaction.

The standard PCR program consisted of 35 cycles of 94°C for 40 s, 50-60°C for 40 s, 72°C for 40 s followed by one cycle of 72°C for 5 min then held at 4 °C. When cDNA was being used, an initial cycle of 94°C for 5 min, 40°C for 5 min, 72°C for 5 min was performed to complete synthesis of the second DNA strand. Thermo-cycling was performed on either a BIORad DNA Engine Peltier Thermal Cycler or a MJ Research PTC-200 Peltier Thermal Cycler.

2.11 PCR primer design

Primers for PCR were designed using Primer Premier™ 5.00. Care was taken designing primers to minimise potential primer dimers, false priming and hairpin structures. Primers were designed with lengths between 18 and 25 nucleotides and melting temperatures (T_m) between 55°C and 65°C. For the purpose of a PCR reaction, long product length primers of 300 – 800 bp primers were designed.

Primers were also designed based on the pea plant transcriptome analysis for genes of interest.

2.12 DNA purification

To acquire pure DNA template for sequencing and nested PCR, DNA gel purification was done.

The PCR product was run in agarose gel electrophoresis to separate bands. A Safe Imager™ blue-light transilluminator was used to visualise the DNA, the bands were cut and stored at -20°C freezer prior to purification. To purify DNA from agarose gel and PCR products an UltraClean™ 15 DNA Purification Kit and Roche Agarose Gel DNA Extraction Kit were used. These kits use economical silica binding particles to extract DNA from agarose gels and enzymatic reactions. The desired DNA band is cut from the agarose gel and melted irreversibly in a chaotropic salt solution. Then the DNA is bound to UltraBIND silica particles in the presence of UltraSALT. The complex is micro centrifuged to discard the melted gel, the pellet was washed once in UltraWASH and concentrated, purified DNA was eluted in TE buffer.

DNA sequencing was performed at MACROGEN Inc, Korea.

2.13 Gene Expression Analysis

Relative gene expression was measured using reverse transcriptome quantitative polymerase chain reaction (RT-qPCR). The expression of each gene of interest and selected reference genes were quantified using a Rotor-Gene Q, Qiagen with the home-made SYBR Green master mix (Song et al., 2012) or the KAPA SYBR® FAST qPCR Kits (Kapa Biosystems, Boston, USA). This reaction utilises SYBR green which binds to double stranded DNA and fluoresces allowing the quantification of double stranded DNA. The accumulation of the PCR product is measured in terms of Relative Florescence Units (RFU).

The expression studies were done based on the RT-qPCR (MIQE) guidelines (Bustin et al., 2009).

2.13.1 Experimental Design

The RT-qPCR was done to study the relative expression of particular genes of interest between different tissues at different growth stages in pea plants with three treatments (control, avirulent and virulent). The sample maximisation method was used, where as many samples as possible were analysed in the same run, so that, run-to-run variation could be minimised between samples. As all samples could not be analysed in the same run, an inter-run calibrator (IRC) was used. These are identical samples that are tested with three

replicates in every run. A calibration factor was calculated by finding the average Ct (threshold cycle) value of three replicates in a run and selecting the highest mean Ct minus other replicate Ct values and correcting it with the sample Ct values, to remove the run-to-run differences, such that all samples were analysed in the same run (Derveaux et al., 2010). The experimental design was done in a 72 -well plate, where each run contained four genes with five samples (tissues: cotyledon/shoot/ root/ whole plant) from each treatment group (control, avirulent, virulent) and three replicates of calibrator samples. Three technical replicates (runs) were carried out for each biological replicate.

2.13.2 Sample preparation

The pea samples such as, seeds, cotyledons, roots, shoots and whole plants at various stages of growth from 4 h post inoculation (hpi), 2, 5, 9, 11, 15, 20, 25, 30, and 35 days post inoculation (dpi) were collected and immediately transferred to labelled and sterilised 1.5 ml Eppendorf or 15 to 50 ml centrifuge tubes, frozen in liquid N₂ and stored at -80°C.

2.13.3 Nucleic acid extraction

The tissue samples were ground in sterilized pre-frozen pestle and mortar, under liquid N₂ conditions to avoid degradation of samples. Each biological replicate was ground, mixed well with a pre-chilled spatula and stored in labelled and pre-frozen 1.5 ml Eppendorf tubes at -80°C for further RNA extraction. Care was taken throughout to avoid thawing of the sample. RNA was extracted from pea tissues by using TRIzol® extraction method (Section 2.9.1). The integrity and quality of isolated RNA was assessed by 1% agarose gel electrophoresis (Section 2.9.1). The concentration and purity of RNA was assessed by Nano Drop™ Spectrophotometer (Section 2.9.2). The RNA was stored in 1x RNA secure in -25°C freezer.

2.13.4 Reverse transcription

The RNA extracted was converted to cDNA by reverse transcription (Section 2.9.2). The cDNA was diluted 5-fold with TE buffer and stored at -20°C. The cDNA quality was assessed by RT-qPCR assay, where two reference genes and a target gene were used to assess the amplification curve and melting point curve of each cDNA sample.

2.13.5 Primer Design for RT-qPCR

Primers were designed which were unique and specific for the gene of interest based on *Pisum sativum* transcriptome analysis results and *R. fascians* BLAST search results using Primer Premier™ 5.00. (Section 2.11). All target gene primers used were between 18 – 25 nucleotides with 100-300 bp product length, and GC content between 45-60% with a melting temperature of 55-65°C. The PCR products were sequenced by running the PCR product on a 1.5% (w/v) agarose gel and visualising in a Safe Imager™ blue-light transilluminator. All bands of approximately expected size were excised from the agarose gel and purified using the Ultra Clean™15 DNA purification kit or Roche Agarose Gel DNA extraction kit (Section 2.12) and quantified using Hyper Ladder1. The purified DNA was sequenced by MACROGEN Inc. Korea (Section 2.12). From the sequenced data, the raw sequences of at least two forward and two reverse directions were aligned using ClustalX software to correct sequencing errors and a consensus sequence for each gene of interest (GOI) was generated (Song et al., 2012). The sequence verification after sequencing was done for each specific target gene with BLAST (<http://www.ncbi.nlm.gov/BLAST>) searching the GenBank database and each confirmed target gene was selected and designated to gene family level based on available annotated sequence or putative sequence of the target genes.

2.13.6 RT-qPCR validation

The RT-qPCR assay was validated with optimisation of primers by determining the optimal annealing temperature of all the target primers and reference genes, at 52°C, 55°C, 58°C and 60°C annealing temperature. A duplicate, no template control (NTC) was included in every run to test for DNA contamination and to assess for primer-dimers.

2.13.7 RT-qPCR reactions

The relative gene expression was studied using Rotor-Gene Q, Qiagen with the home-made SYBR Green master mix (Appendix A. 2.11) or the KAPA SYBR® FAST qPCR Kits (Kapa Biosystems, Boston, USA).

A reaction volume of 10 µl was used, consisting of 5 µl of Kapa qPCR buffer (Kapa Biosystems, Boston, USA), 2 µl of millipore water, 1 µl of cDNA, 1 µl of each forward and reverse primer. The thermal-cycle consisted of initial hold at 95°C for 10 mins, followed by 40 cycles of 95°C for 10 s, 58°C for 15 s and 72°C for 20 s and melt of 72°C to 95°C, raising

1 degree each step and 5 s wait for each step afterwards after 90 s of pre-melt conditioning on first step.

2.13.8 Reference genes

Reference genes/ housekeeping genes were used as internal controls to normalise the data by correcting for differences in quantities of cDNA used as template (Gutierrez et al., 2008, Vandesompele et al., 2002). To achieve accurate normalisation four reference genes *UI8S*, *PsEF*, *PsGAP* and *PsACT* were used for gene expression studies.

The reference genes were first compared for their expression stability over different cDNA samples of tissues at different growth stages, with three replicates. To minimise the possible errors by using one reference gene for normalisation, the geometric mean of four reference genes was calculated according to the method described by Song et al. (2012), and its correlation to the target gene was compared to each single gene of interest.

2.13.9 Gene expression data analysis

The relative gene expression was calculated based on the method of Pfaffl (2001) and Song et al. (2012). Gene expression was determined by comparing the expression of the gene of interest/ target gene to the average expression of four reference genes, *PsEF*, *PsGAP*, *PsACT* and *UI8S*.

Due to the fact that all samples could not be run in a single PCR run, an inter-run calibrator (IRC) was used (Section 2.15.1). The data analysis was done as described by Song et al. (2012): for each reference gene, a correction factor (CF) for each of the cDNA samples was calculated using the Ct value of this cDNA sample divided by the average Ct value of all cDNA samples of the same experiment. The values of three technical replicates were averaged to form the CF for each biological replicate of each reference gene. The final CF value for each biological replicate was created by averaging the CF value of four reference genes. For each cDNA sample, the Ct value of each target gene was corrected before analysis of its expression level.

CHAPTER 3 *RHODOCOCCUS FASCIANS-PISUM SATIVUM* INTERACTIONS

3.1 Introduction

The actinomycete *Rhodococcus fascians*, a biotrophic gram-positive plant pathogen, induces severe malformations including as leaf deformation, multiple shoot formation and overall stunted growth (Depuydt et al., 2008). The disease severity is dependent on the host species, cultivar, plant age, site of infection, bacterial strain and environmental or growth conditions (Vereecke et al., 2000).

R. fascians-plant interaction molecular studies revealed that virulence determinants are located on a linear plasmid pFi (Crespi et al., 1992, Crespi et al., 1994, Stange et al., 1996) and by sequence analysis the *fas* operon was identified consisting of six putative genes involved in cytokinin biosynthesis and which are essential for virulence (Crespi et al. 1992). The *FasD* codes for an isopentenyl transferase (IPT) protein involved in the first step in cytokinin biosynthesis, *FasE* is homologous to cytokinin oxidase/ dehydrogenase (*CKX*) genes (Schmülling et al., 2003) involved in cytokinin degradation and *FasF* is homologous to lysine decarboxylases, THE LONELY GUY (*LOG*), which encodes a phosphoribohydrolase representing a complementary pathway to produce zeatin bases directly from their nucleotides (Pertry et al., 2010). The presence of both *FasD* (*IPT*) and *FasE* (*CKX*) genes within the *fas* locus was correlated with pathogenicity and the absence of these genes (*fasD* and *fasE*) associated with avirulence (Crespi et al. 1994, Stange et al. 1996, Galis et al. 2005b). Crespi et al. (1992) showed that strains cured of the linear plasmid pFi 188 were avirulent and re-introduction of this plasmid restored virulence to the strain. As the *R. fascians* culture strains at University of Canterbury had been stored in glycerol for some years, it was important to determine both strain integrity and Koch's Postulates.

Although the original test plants for *R. fascians* were sweet peas and pea (Brown, 1927, Lacey, 1936, Tilford, 1936) cited from Putnam and Miller (2007), the main model plants used to study the morphological and cytological aspects of *R. fascians* infection by the Van Montagu and Vereecke groups have been mostly *Arabidopsis thaliana* (L.), a non-natural host of *R. fascians*, and occasionally *Nicotiana tabacum* (L.) (Manes et al., 2001). This thesis is based on the suggestion that the infection process of *R. fascians* would be better elucidated

if the bacterium were to be studied in association with a natural host. That the response of *R. fascians* and disease severity depends on host species has been clearly shown by previous studies (Goethals et al., 2001b, Vereecke et al., 2000).

The colonisation behaviour of *R. fascians* on *A. thaliana* and *N. tabacum* plants was studied by Cornelis et al. (2001) and they found that independent of the infection methods, *R. fascians* was found on the lamina of the leaves, older leaves, upper and lower sides of leaf and crown of *Arabidopsis* and on tobacco stems. The formation of a slime layer covering *R. fascians* colonies on the plant surface was associated with the collapse of epidermal cells and *R. fascians* subsequently penetrated into the plant tissues intercellularly (Cornelis et al., 2001). Mostly so far, the *R. fascians* colonisation and infection process has been observed in shoots, leaves and aerial parts to study leafy galls but not in other plant parts such as cotyledons and roots which can exhibit changes due to *R. fascians* infection. To infect plants, Van Montagu and Vereecke groups either dipped one or two week old *A. thaliana* and tobacco seedlings in to the culture or vacuum infiltrated the *R. fascians* culture in to the plant. Microscopic observations were usually made at only one or two time points (Cornelis et al., 2001, Manes et al., 2001). Vereecke et al. (2000) showed that the inoculation procedure was of great importance for the evaluation of symptom development on tobacco plants.

Little research has been carried out to elucidate the colonisation behaviour of *R. fascians* in other host tissues. In this thesis, *P. sativum*, a natural host of *R. fascians* infected simultaneously with seed imbibition was used to study the colonisation pattern of the bacteria in host tissues including cotyledons, roots and shoots from four hours post inoculation until 35 dpi at periodic intervals. In this chapter, the morphological traits of host and microbial traits of *R. fascians* during its interaction with *P. sativum* as the model plant for *R. fascians* infection is described.

3.2 Materials and Methods

3.2.1 Confirmation of the integrity of the stored *R. fascians* strains

3.2.1.1 *Rhodococcus fascians* strains

The thirty six strains of *Rhodococcus fascians* used in this study were obtained by Professor Paula Jameson from Professor R. O. Morris (Biochemistry Department, University of

Missouri, Columbia, MO, USA) in 1989 and used by Eason et al. (1996), Stange et al. (1996) and Galis et al. (2005b) in her lab. The *R. fascians* house numbers, strain designations, plant host from which they were isolated along with other details are given in Table 3.1. The house number in this Table will be referred to hereafter as strain number.

Table 3.1 *Rhodococcus fascians* strains used in this study and their details

House	Strain	Origin	Remarks
589	2602	PDDCC 260	From ICPB ^b CF1 Hilderbrand USA.
590	2603	PDDCC 2603	From ICPB CFI5 Davey Canada.
591	2604	PDDCC 2604	From ICPB CFI9 Tilford USA. ATCC ^d 12975.
592	2605	PDDCC 2605	From ICPB CF21 Tilford USA.
593	2606	PDDCC 2606	From ICPB CFI01 Domdroff USA.
594	5340	PDDCC 5340	Origin sweet pea shoot, Taylor UK.
595	5833	PDDCC 5833	Burkholder CF17 Tilford ATCC 12974 NCPB 3067-1
596	7108	PDDCC 7108	Origin <i>Verbascum nigrum</i> Miller 1978, causes leafy gall on bulblet.
597	7109	PDDCC 7109	Origin <i>Gladiolus</i> Miller 1978, causes leafy gall on bulblet.
598	7112	PDDCC 7112	Origin <i>Brodiea laxa</i> Miller 1978, causes leafy gall on bulblet.
599	7113	PDDCC 7113	Origin <i>Begonia</i> Van Hoof 1977, causes organoid tumours on roots.
600	7114	PDDCC 7114	Origin Dahlia stem base Van Hoof 1978.
601	6788	PDDCC 6788	Origin <i>Carica pubescens</i> Watson 1980, Bud proliferation.
602	6789	PDDCC 6789	Origin <i>Carica pubescens</i> Watson 1980, Bud proliferation.
603	6790	PDDCC 6790	Origin <i>Carica pubescens</i> Watson 1980, Bud proliferation.

604	6791	PDDCC 6791	Origin <i>Carica pubescens</i> Watson 1980, Bud proliferation.
605	6792	PDDCC 6792	Origin <i>Carica babaco</i> Watson 1980, Subterranean proliferation of buds on cuttings.
606	6793	PDDCC 6793	Origin <i>Carica babaco</i> Watson 1980, Subterranean proliferation of buds on cuttings.
607	7340	PDDCC 7340	Origin <i>Phytolacca octandra</i> Watson 1980, Bud proliferation.
608	7364	PDDCC 7364	Origin <i>Dahlia</i> Watson 1980, Bud proliferation on tubers.
609	6D-21	-	Kado 85 Dr. Anne Vidaver U of Nebraska Lincoln.
610	79-1	-	Kado 85 Dr. Anne Vidaver U of Nebraska Lincoln.
664	156	NCPPB 156	Origin <i>Chrysanthemum morifolium</i> Jacobs 1945 UK.
665	188	NCPPB ^c 188	Origin <i>Chrysanthemum morifolium</i> Dowson 1946 UK. Reisolate of NCPPB 156
666	469	NCPPB 469	Origin <i>Fragaria chiloensis</i> Lelliott 1975 UK.
667	764	NCPPB764	Origin <i>Fragaria chiloensis</i> (symptomless) .Crosse 1951 UK.
668	765	NCPPB765	Origin <i>Fragaria chiloensis</i> (symptomless) .Crosse 1951 UK.
669	766	NCPPB 766	Origin <i>Fragaria chiloensis</i> (symptomless) .Crosse 1951 UK.
670	1488	NCPPB 1488	Origin sweet pea Lelliot 1963 UK. ICPB CF115S.
671	1675	NCPPB 1675	Origin <i>Chrysanthemum morifolium</i> Jones 1964 UK.
672	1733	NCPPB 1733	Origin <i>Beloperone guttata</i> Oxtoby 1965 UK.
673	2210	NCPPB 2210	Origin <i>Tulipa gesneriana</i> Catton 1969 UK.
674	2554	NCPPB 2554	Origin <i>Phlox</i> sp. Baker 1973 UK.
675	2555	NCPPB 2555	Origin <i>Mesembryanthum</i> sp. Baker 1973 UK.

676	2556	NCPPB 2556	Origin <i>Petunia sp.</i> Baker 1973 UK.
677	2557	NCPPB 2557	Origin <i>Verbena sp.</i> Baker 1973 UK.

- a PDDCC Plant Disease Division Culture Collection, NZ.
b ICPB International Collection of Phytopathogenic Bacteria, USA.
c NCPPB National Collection of Plant Pathogenic Bacteria, UK.
- no culture collection number.

Source: (Eason, 1993).

3.2.1.2 PCR detection of *RfIPT*, *RfLOG* and *RfCKX* genes in *R. fascians* strains

The stock cultures of the bacterial strains were stored at -80 °C in 50% (v/v) glycerol. Prior to use the stock cultures were streaked on Kado and Heskett '523' medium (Kado and Heskett 1970) (Appendix B. 2.1) and grown at 26°C for two days. The modified method from Galis et al. (2005b) was used to transfer *R. fascians* cultures to PCR tubes. A toothpick was dipped into the culture and a small portion of bacteria was subsequently transferred to the tube containing 20 µl of sterile water. The culture was mixed well and 1 µl of suspension was transferred to a PCR tube.

The *R. fascians IPT*, *LOG* and *CKX* genes were identified through BLAST search of the GenBank database and specific primers were designed, which were unique to *R. fascians* and not *P. sativum*. The putative genes isolated and sequenced (Chapter 2). The PCR conditions for amplification of the genes were as outlined in Section 2.10. The annealing temperature used for all the genes was 55°C.

The rest of the materials and methods used in this chapter are outlined in Chapter 2.

3.3 Results

3.3.1 Confirmation of Koch's Postulates:

To establish the etiology of *R. fascians* virulent strain 602 in pea shoot malformation, the four criteria of Koch's postulates were established:

1. *R. fascians* was isolated from the symptomatic shoot (multiple shoot) of *P. sativum* infected with the virulent strain 602.
2. The isolated *R. fascians* virulent strain 602 was grown on a Kado and Heskett '523' medium plate using the dilution plating technique and incubated at 26°C for 2 d.

3. Kado and Heskett broth was inoculated with *R. fascians* virulent strain 602 and incubated at 26°C with shaking at 121 rpm until mid log phase. Whole seeds of *P. sativum* var. Bohatyr were added and incubated at 26°C with shaking at 121 rpm for 4 h.
4. The inoculated seeds were sown in sterile agar containers along with control (uninoculated) seeds and grown for disease symptom manifestation. The symptomatic shoot of infected pea plants was used to re-isolate the organism.

This confirmed Koch's postulates of *R. fascians* virulent strain 602 in pea plants (Figure 3.1).



Figure 3.1 **Confirmation of Koch's postulates by *R. fascians* virulent strain 602 infection on pea plants.** Control: uninoculated; Virulent: infected with *R. fascians* strain 602 strain

3.3.2 Polymerase chain reaction (PCR) and screening of *R. fascians* isolates for *RfIPT*, *RfLOG* and *RfCKX* genes

To confirm the presence of plasmids in the stored 36 strains of *R. fascians* used by Eason et al. (1996), Stange et al. (1996) and Galis et al. (2005b), all the 36 isolates of *R. fascians* were initially screened for the presence/ absence of *IPT* and *CKX* genes using the primers designed by Galis et al. (2005b).

The primers designed for *fasD* gene (*RfIPT*) and *fasE* (*RfCKX*) gene were:

- *fasE* f: 5' atcaatgggtggccggtatg
- *fasE* r: 5' gccttcgtggtggggtgaa
- *fasD* f: 5' agacgcaagcaaggtgat
- *fasD* r: 5' ttttatcagccggtcaaagg

An 850 bp product *fasD* and a 281 bp product of *fasE* were detected (Figure 3.2). The PCR products of *fasD* and *fasF* gene were present in 18 isolates of *R. fascians* and both the gene products were absent in the 18 other isolates, confirming the integrity the stored strains.

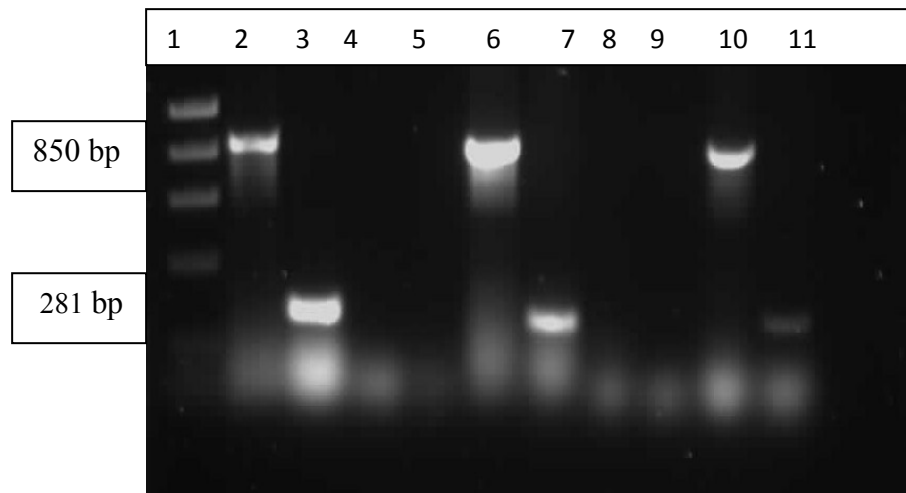


Figure 3.2 PCR products for *fasD* and *fasE* genes in *R. fascians* isolates.

Lane1: 1 kb ladder; lane2: strain 596 for *fasE* gene; lane3: strain 596 for *fasD* gene; lane 4: strain 593 for *fasE* gene; lane5: strain 593 for *fasD* gene; lane 6: strain 602 for *fasE* gene; lane7: strain 602 for *fasD* gene; lane8: strain 589 for *fasE* gene; lane 9: strain 589 for *fasD* gene; lane10: strain 601 for *fasE* gene; lane11: strain 601 for *fasD* gene. The expected product length of *fasE* is 850 bp and *fasD* gene is 281 bp.

The *R. fascians IPT*, *LOG* and *CKX* primers were re-designed to differentiate the expression of *R. fascians* cytokinin genes from *P. sativum IPT*, *CKX* and simultaneously *LOG* genes. The 36 isolates of *R. fascians* were again screened for the presence / absence of cytokinin genes, *IPT*, *LOG* and *CKX*. The genes were identified through BLAST searching GenBank database and primers were designed. The primers designed and used for the PCR reactions are shown in Table 3.2.

Table 3.2 *Rhodococcus fascians* primers

Gene	Primer	Sequence
<i>RfIPT</i>	RfIPT F1	5' CTTGTCGGAGTTCGCCTTCT
	RfIPT R1	5' GGAGTAACACTGGATACGGTTCG
	RfIPT F2	5' GACGGGTCTACCTACGGCTGT
	RfIPT R2	5' CGAAGTTGCCCTGATGTATGG
	RfIPT F3	5' ATTGTTGTTGCCGACCGTATC
	RfIPT R3	5' CGAAGTTGCCCTGATGTATGG
	RfIPT F4	5' GAGTTCGCCTTCTCCATTTC
	RfIPT R4	5' ACAGCACCGCATCTAACAGG
	RfIPT R5	5' CGACAGCACCGCATCTAAC
<i>RfCKX</i>	RfCKX F1	5' GAGTCACGGCTTTGGCTTG
	RfCKX R1	5' GGACAGCATTGACTGCGTAGG
	RfCKX F2	5' ACAATCCGTCTGACCGCTG
	RfCKX R2	5' CCGAAGTGCGTACACCAATC
	RfCKX F3	5' GAGTCACGGCTTTGGCTTGC
	RfCKX R3	5' GCAGCGGTCAGACGGATTGT
	RfCKX F4	5' TATGGTGACTTTATCAACCGTATG
	RfCKX R4	5' ATGAAGAATGTGTCGCAGTGAG
<i>RfLOG</i>	RfLOG F1	5 GAACCGTCGTTGGCGTGAT
	RfLOG R1	5 GAGAGCAAGGGGCGGTAATA
	RfLOG F2	5' ACACCTGGGGCTTCACAATA
	RfLOG R2	5' GCGGGGGTGATAAATCCTTC
	RfLOG F3	5' CGGGACCAAATATGGACAGC
	RfLOG R3	5' GCGGGGGTGATAAATCCTTC
	RfLOG R4	5' GCGGGTAATACTCGTTGTCGT
<i>U18S</i>	U18S F1	5' CGATCAGATACCGTCCTAGTCTCAAC
	U18S R1	5' CAGAACATCTAAGGGCATCACAGAC

Of the primers in Table 3.2 when tested for amplification, only the *RfIPTF1R1*, *RfIPTF2R2*, *RfIPTF4R5*, *RfCKXF1R1*, *RfCKXF2R2*, *RfLOGF1R1*, *RfLOGF3R3* and *U18S* products were isolated and sent for sequencing (Figure 3.3).

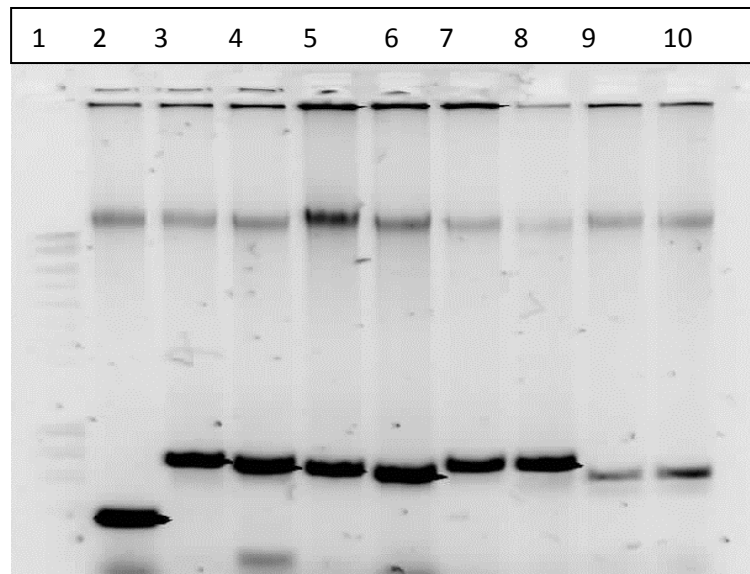


Figure 3.3 PCR for sequencing of *RfIPT*, *RfLOG* and *RfCKX* genes in *R. fascians* virulent strain 602 . Lane1: 1 kb ladder; lane 2 PCR for *RfLOG* gene; lanes 3-8 PCR for *RfCKX* gene; and lanes 9-10 PCR for *RfIPT* gene.

Among the sequenced PCR products which were identified as *R. fascians IPT*, *LOG* and *CKX* genes, the primers *RfIPTF1R1* with product length of 784 bp, *RfCKXF1R1* with product length of 793 bp and *RfLOGF3R3* with product length of 435 bp were used for PCR reactions with the 36 cultures to screen them for the presence of *IPT*, *LOG* and *CKX* genes. The *RfIPT*, *RfCKX* and *RfLOG* primers which were designed with product length of 200-400 bp were used later for gene expression studies in RT-qPCR (Chapter 4).

The PCR was performed with the 36 isolates, with the *RfIPT*, *RfLOG* and *RfCKX* gene primers at 55°C annealing temperature. Of these, 18 isolates showed the expected size single product for each of the genes studied and 18 isolates yielded no PCR products (Figure 3.4).

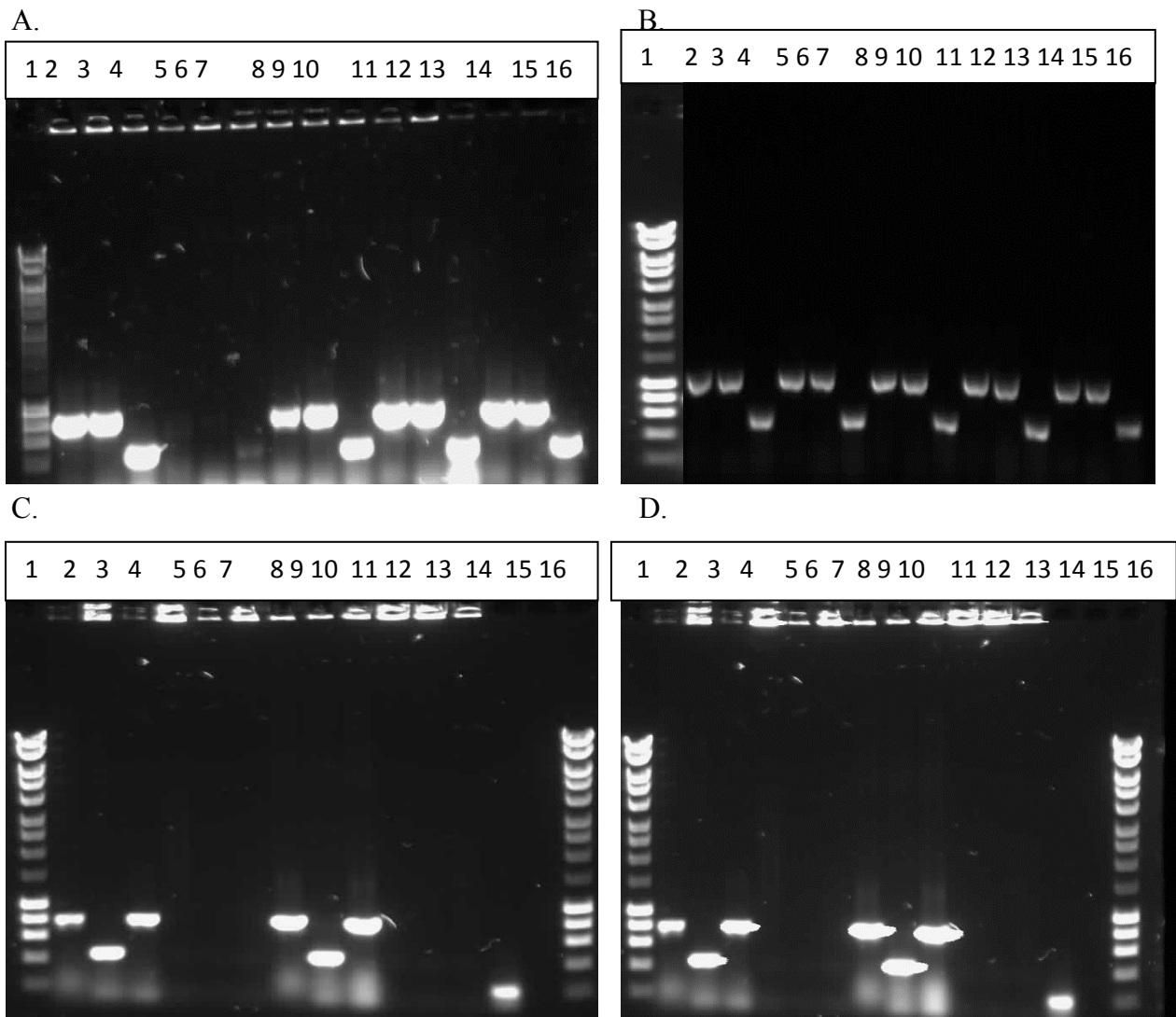


Figure 3.4 PCR for detection of the *RfIPT*, *RfLOG* and *RfCKX* genes in *R. fascians* cultures. **A.** Lane1: 1 kb DNA ladder; Lane2: strain 591*Rfipt* gene (784 bp); Lane3: strain 591*Rfckx* gene (793 bp); Lane4: strain 591 *Rflog* gene (435 bp); Lane5: strain 589 *Rfipt* gene; Lane6: strain 589 *Rfckx* gene; Lane7: strain 589 *Rflog* gene; Lane8: strain 592 *Rfipt* gene; Lane9: strain 592 *Rfckx* gene; Lane10: strain 592 *Rflog* gene; Lane11: strain 594*Rfipt* gene; Lane12: strain 594 *Rfckx* gene; Lane13: strain 594 *Rflog* gene; Lane14: strain 595 *Rfipt* gene; Lane15: strain 595 *Rfckx* gene and Lane16: strain 595*Rflog* gene. **B.** Lane1: 1 kb DNA ladder; Lane2: strain 596 *Rfipt* gene (784 bp); Lane3: strain 596 *Rfckx* gene (793 bp); Lane4: strain 596 *Rflog* gene (435 bp); Lane5: strain 598 *Rfipt* gene; Lane6: strain 598 *Rfckx* gene; Lane7: strain 598 *Rflog* gene; Lane8: strain 600 *Rfipt* gene; Lane9: strain 600 *Rfckx* gene; Lane10: strain 600 *log* gene; Lane11: strain 601 *ipt* gene; Lane12: strain 601 *ckx* gene; Lane13: strain 601 *Rflog* gene; Lane14: strain 602 *Rfipt* gene; Lane15: strain 602 *Rfckx* gene and Lane16: strain 602 *Rflog* gene. **C.** Lane1: 1 kb DNA ladder; Lane2: strain 591*Rfipt* gene (784 bp); Lane3: strain 591 *Rfckx* gene (793 bp); Lane4: strain 591 *Rflog* gene (435 bp); Lane5: strain 677 *Rfipt* gene; Lane6: strain 677 *Rfckx* gene; Lane7: strain 677*Rflog* gene; Lane8: strain 604 *Rf ipt* gene; Lane9: strain 604 *Rfckx* gene; Lane10: strain 604 *Rflog* gene; Lane11: strain 671 *Rfipt* gene; Lane12: strain 671 *Rfckx* gene; Lane13: strain 671*Rflog* gene; Lane14: strain 602 *UI8S* gene; Lane15: water and *Rfipt* gene and Lane16: 1 kb ladder. **D.** Lane1: 1 kb DNA ladder; Lane2: strain 602 *Rfipt* gene (784 bp); Lane3: strain 602 *Rfckx* gene (793 bp); Lane4: strain 602 *Rflog* gene (435 bp); Lane5: strain 589 *Rfipt* gene; Lane6: strain 589 *Rfckx* gene; Lane7: strain 589 *Rflog* gene; Lane8: strain 670 *Rf ipt* gene; Lane9: strain 670 *Rfckx* gene; Lane10: strain 670 *Rflog* gene; Lane11: strain 674 *Rfipt* gene; Lane12: strain 674 *Rfckx* gene; Lane13: strain 674 *Rflog* gene; Lane14: strain 602 *UI8S* gene; Lane15: water and *Rfipt* gene and Lane16: 1 kb ladder.

Based on the virulence tests by Stange et al. (1996) and the PCR analysis, the 36 isolates were confirmed as avirulent (A) and virulent (V) rating (Table 3.3).

Table 3.3 Virulence / avirulence classifications of various *Rhodococcus fascians* isolates

Sl.No.	Strain	<i>RfIPT</i>	<i>RfLOG</i>	<i>RfCKX</i>	Virulence classification ^c
1	589	-	-	-	A
2	590	-	-	-	A
3	591	+	+	+	V
4	592	+	+	+	V
5	593	-	-	-	A
6	594	+	+	+	V
7	595	+	+	+	V
8	596	+	+	+	V
9	597	-	-	-	A
10	598	+	+	+	V
11	599	+	+	+	V
12	600	+	+	+	V
13	601	+	+	+	V
14	602	+	+	+	V
15	603	+	+	+	V
16	604	+	+	+	V
17	605	+	+	+	V
18	606	+	+	+	V
19	607	-	-	-	A
20	608	-	-	-	A
21	609	-	-	-	A

22	610	+	+	+	V
23	664	-	-	-	A
24	665	+	+	+	V
25	666	+	+	+	V
26	667	-	-	-	A
27	668	-	-	-	A
28	669	-	-	-	A
29	670	+	+	+	V
30	671	-	-	-	A
31	672	-	-	-	A
32	673	-	-	-	A
33	674	-	-	-	A
34	675	-	-	-	A
35	676	-	-	-	A
36	677	-	-	-	A

^cRatings of Stange et al. (1996); V – virulent strain ; A – avirulent strain

3.3.2.1 Phylogenetic analysis of *RfIPT*, *RfLOG* and *RfCKX*

The sequenced *RfIPT*, *RfLOG* and *RfCKX* genes were phylogenetically analysed through the MEGA 4 program by Maximum Parsimony phylogenetic tree analysis with 10,000 bootstrap replications (Figure 3.5, 3.6 and 3.7). For phylogenetic analysis, the isolated IPT sequences of *R. fascians*, other microbes, *A. thaliana*, legumes (*G.max*, *L. japonicus*, *P. sativus*) and monocots *Z. mays*, *O. sativa* and *T. aestivum* from the BLAST GenBank database were aligned (Figure 3.5). The isolated *R. fascians* IPT grouped into a single clade along with other microbes such as *Streptomyces turgidiscabies* (G+ve) FasD, *R. fascians* (G+ve) FasD, *Pantoea agglomerans* pv. *gypsophila* (G-ve) FasD, *Pseudomonas savastanoi* (G-ve) FasD, *Agrobacterium vitis* (G-ve) FasD and *A. tumefaciens* (G-ve) FasD. The isolated *R. fascians* IPT grouped with the *R. fascians* D188 FasD with a bootstrap value of 100 and

S. turgidiscabies FasD with a bootstrap value of 99. The actinomycetes *S. turgidiscabies* FasD (G+ve), *R. fascians* D (188) (G+ve) FasD and the isolated *R. fascians* (G+ve) IPT cluster separately from the other gram negative bacteria. The plant IPT bifurcated to three clades. One clade had most of the legumes including *L. japonicus* (LjIPT1 to 4), *P. sativum* (PsIPT1 and 2) and *G.max* (GmIPT) along with *A. thaliana* (AtIPT1, 3 to 8). The monocot *Z. mays* IPT, *O. sativa* IPT and *T. aestivum* IPT formed a clade (bootstrap value 99). The AtIPT2 and LjIPT5 grouped together with bootstrap value 99. AtIPT9 grouped out as an out group. The tree was rooted with *Ralstonia solanacearum* (G-ve) FasD as an out group. (Figure 3.5).

In the case of *R. fascians* CKX, the phylogenetic tree analysis (Figure 3.6) revealed two main clades, one with microbial group and the other with plant group. The microbes, *R. fascians* (G+ve) CKX, *S. turgidiscabies* (G+ve) FasE, *Saccharopolyspora erythraea* (G+ve) FasE, *Streptoalloteichus hindustanus* (G+ve) FasE and *Legionella pneumophila* (G-ve) FasE as a subgroup. The isolated *R. fascians* CKX and *R. fascians* D188 FasE grouped together with bootstrap value of 100 and with *S. turgidiscabies* FasE the bootstrap value was 83. The separation of gram positive actinomycetes from gram negative bacteria was noticed in this grouping. The second clade consisted of PsCKX1, PsCKX2, *Medicago truncatula* CKX (MtCKX) and all *A. thaliana* CKXs (AtCKX1 to 7). *Stigmatella aurantiaca* (G-ve) FasE grouped as an out group which was rooted for analysis (Figure 3.6).

There was clear grouping of separate clades for *A. thaliana* LOGs (AtLOG1 to 9) and microbes FasF. All the microbial FasF analysed grouped together even though they sub grouped into different groups. The *R. fascians* LOG protein sequences grouped along with *A. rhizogenes* (G-ve) FasF and *Verrucomicrobium spinosum* (G-ve) FasF (bootstrap value 81) along with *Stenotrophomonas maltophilia* (G-ve) FasF. The isolated *R. fascians* (G+ve) LOG grouped with *R. fascians* (D188) FasF with boot strap value of 50. But the gram positive microbes and gram negative bacteria had similar FasF protein sequences. *Pseudomonas aeruginosa* (G-ve) FasF was used to root the tree as an out group (Figure 3.7).

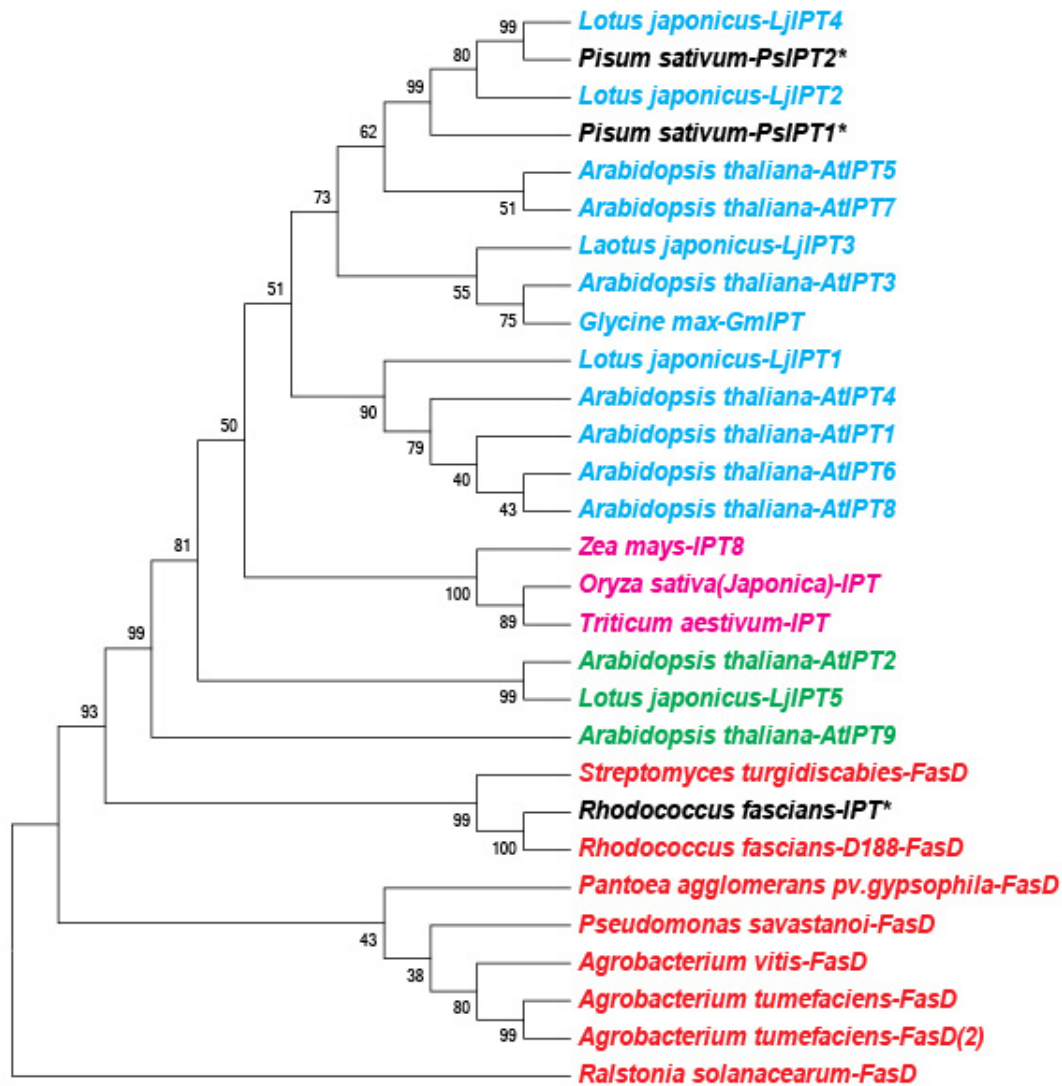


Figure 3.5 Phylogenetic tree of IPT. The Maximum Parsimony phylogenetic tree showing the relationship between the protein sequences of sequenced *R. fascians* IPT, *P. sativum* IPT (PsIPT): PsIPT1; PsIPT2, *Arabidopsis thaliana* IPT (AtIPT): AtIPT1(AB062607.1); AtIPT2(NM_128335); AtIPT3(BT001075.1); AtIPT4(AB062611.1); AtIPT5(AB062608.1); AtIPT6(AB062612.1); AtIPT7(AB062613.1); AtIPT8(AB062614.1); *AtIPT9*(NM122011), *Lotus japonicus* IPT (LjIPT): LjIPT1(DQ436462); LjIPT2(DQ436463); LjIPT3(DQ436464); LjIPT4(DQ436465); LjIPT5 (EU195535), *Glycine max* IPT (GmIPT) (AY550884), *Zea mays* IPT (ZmIPT): ZmIPT8(EU263131), *Oryza sativa* IPT (OsIPT): OsIPT (BAE47451.1), *Triticum aestivum* IPT (TaIPT): TaIPT (AEV76967.1). The microbial FasD: *Rhodococcus fascians* D188 FasD (YP007878707), *Streptomyces turgidiscabies* FasD (AAW49305.1), *Agrobacterium vitis* FasD (YP002540151.1), *Agrobacterium tumefaciens* FasD (YP001967412), *Pseudomonas savastanoi* FasD (AGC31315), *Pantoea agglomerans* pv. *gypsophila* FasD (Q47851), *Agrobacterium tumefaciens* FasD (2) (CAB44641.1). The tree was rooted by using *Ralstonia solanacearum* FasD (WP003277306.1). The node values are bootstrap values generated with 10,000 bootstrap replicates. * The sequences of *R. fascians* IPT and *P. sativum* IPTs isolated in this project.

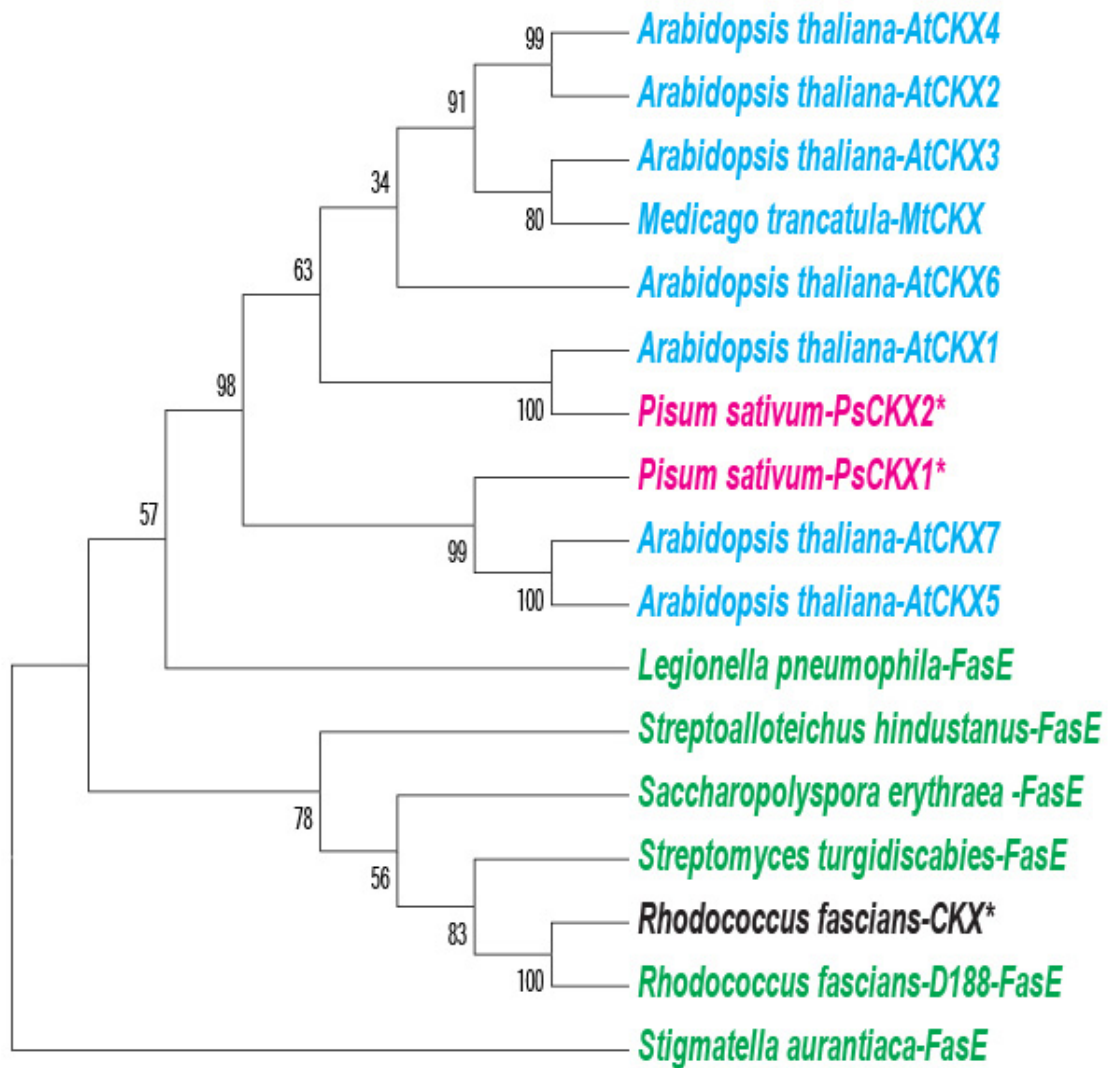


Figure 3.6 Phylogenetic tree of CKX. The Maximum Parsimony phylogenetic tree showing the relationship between the protein sequences of sequenced *R. fascians*, *P. sativum* CKX (PsCKX): PsCKX1; PsCKX2; *Arabidopsis thaliana* CKX (AtCKX): AtCKX1 (NM129714.2); AtCKX2 (NM127508.2); AtCKX3 (NM125079.2); AtCKX4 (NM179139.1); AtCKX5 (NM106199.5); AtCKX6 (NM116209.3); AtCKX7 (NM180532.2), *Medicago truncatula* CKX (MtCKX); MtCKX (XM003595136.1). The related microbial CKX protein sequences of *R. fascians* D188 FasE (YP007878704), (*Streptomyces turgidiscabies* FasE (AAW49304.1), *Streptoalloteichus hindustanus* FasE (ABL74933.1), *Legionella pneumophila* FasE (YP001251667.1), *Saccharopolyspora erythraea* FasE (YP001108723.1). The tree was rooted by using *Stigmatella aurantiaca* FasE (WP002616014.1). The node values are the bootstrap values generated with 10,000 bootstrap replicates. * The sequences of *R. fascians* CKX and *P. sativum* CKXs isolated in this project.

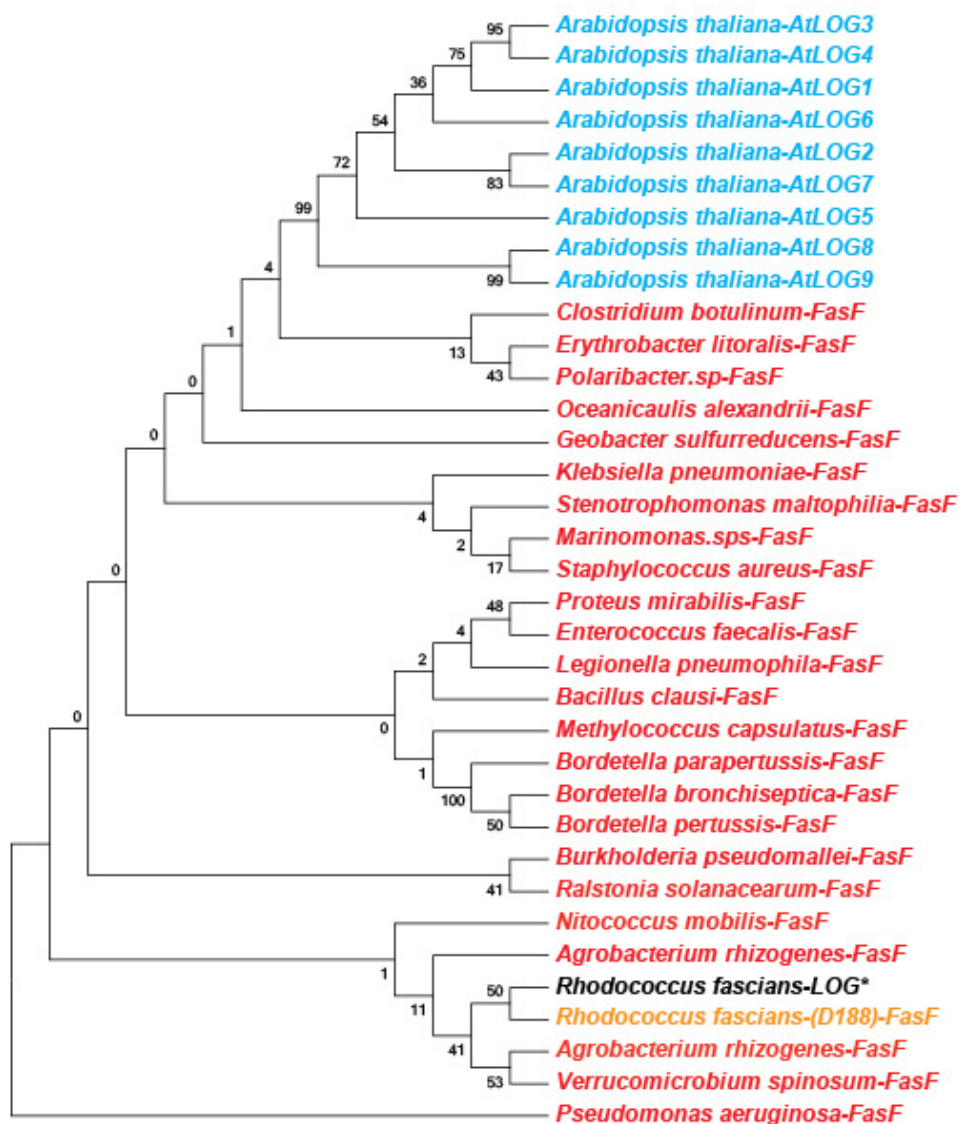


Figure 3.7 Phylogenetic tree of LOG. The Maximum Parsimony phylogenetic tree showing the relationship between, *Rhodococcus fascians* LOG (RfLOG), *Arabidopsis thaliana* LOG (AtLOG): At LOG1 (At2g28305); At LOG2 (At2g35990); At LOG3 (At2g37210); At LOG4 (At3g53450); At LOG5 (At4g35190); At LOG6 (At5g03270); At LOG7 (At5g06300); At LOG8 (At5g11950); At LOG9 (At5g26140), microbial LOGs: *R. fascians* (D188) FasF (YP007878704), *Agrobacterium rhizogenes*- FasF (NP066633.1), *Proteus mirabilis*- FasF (YP002150402.1), *Klebsiella pneumoniae*- FasF (YP002238174.1), *Burkholderia pseudomallei* FasF (YP107809), *Agrobacterium rhizogenes*- FasF (YP001961000.1), *Bordetella parapertussis*-FasF (NP882607.1), *Bordetella bronchiseptica*-FasF (NP886801.1), *Bordetella pertussis*-FasF (NP879395.1), *Verrucomicrobium spinosum*-FasF (WP009963116.1), *Nitococcus mobilis*-FasF (WP005001534.1), *Erythrobacter litoralis*-FasF (YP458867.1), *Marinomonas.sps*-FasF (WP009835866.1), *Methylococcus capsulatus*-FasF (YP114604.1), *Geobacter sulfurreducens*-FasF (NP953810.1), *Bacillus clausi*-FasF (YP175433.1), *Ralstonia solanacearum*-FasF (YP002259101.1), *Stenotrophomonas maltophilia*-FasF (YP001971820.1), *Legionella pneumophila*-FasF (YP001251246.1), *Staphylococcus aureus*-FasF (NP371204.1), *Oceanicaulis alexandrii*-FasF (WP009801747.1), *Enterococcus faecalis*-FasF (NP81404.1), *Polaribacter.sp*-FasF (YP007672300.1), *Clostridium botulinum*-FasF (WP003356945.1). The tree was rooted by using *Pseudomonas aeruginosa*-FasF (YP002442887.1). The node values are the bootstrap values generated with 10,000 bootstrap replicates. * The sequence of *R. fascians* LOG isolated in this project

3.3.3 Growth of *Rhodococcus fascians* and *Pisum sativum* plants infected with *R. fascians*

3.3.3.1 *R. fascians* growth curves and strain selection

Based on the previous studies (Eason et al., 1995, Eason et al., 1996) two *R. fascians* cultures, one avirulent strain 589 and virulent strain 602 were selected for this study. Flasks containing 523 media were inoculated with *R. fascians* cultures 589 and 602. These flasks were incubated at 26°C with shaking at ca. 150 rpm and at periodic intervals the growth of the bacteria was estimated using BIO-RAD Smart Spec™ Plus spectrophotometer.

The growth curves of both cultures 589 and 602 shows that the strains 589 and 602 have similar growth patterns in the culture medium (Figure 3.8). At 4 h both 589 and 602 strains are in the exponential phase of growth (Figure 3.8), at which time the seeds were inoculated.

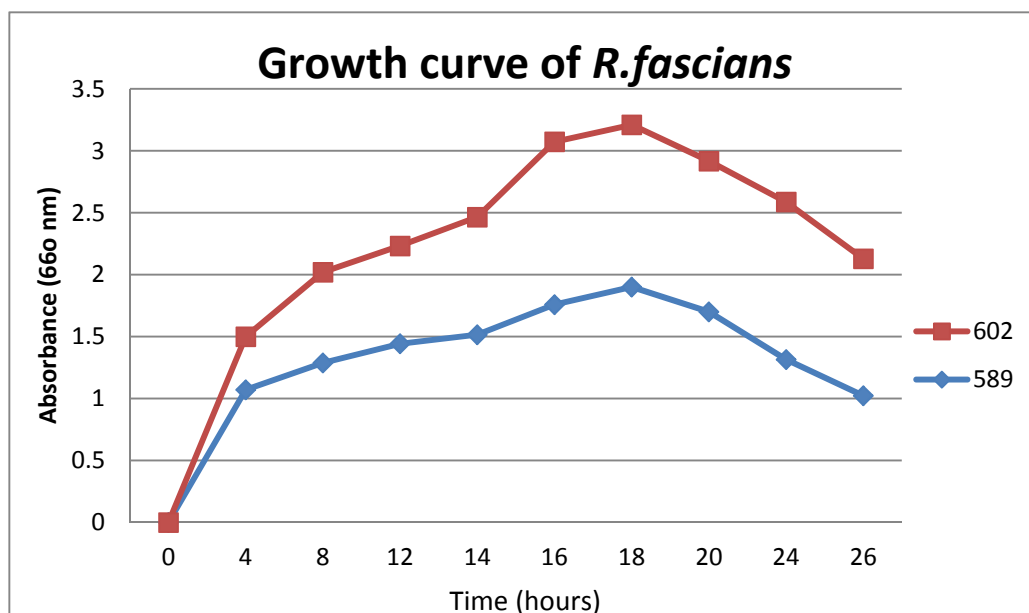




Figure 3.8 Growth curve of *R. fascians* avirulent (589) and virulent (602) strains. The red square  indicates virulent strain 602 growth curve and blue triangle  indicates avirulent strain 589 growth curve.

3.3.3.2 Growth responses of *P. sativum* inoculated with *R. fascians*.

Over 45 days the morphological differences between the mock inoculated seeds (con-plant), seeds inoculated with avirulent strain 589 (avir-plant) and virulent strain 602 (vir-plant) were recorded both in agar containers and as whole plants with a Nikon coolpix 4300 (Figure 3.9 and 3.10). In agar containers (Figure 3.9) the morphological differences in growth among the con-plants, avir-plants and vir-plants was prominent from 5 dpi. Typical symptoms of *R. fascians* infection of multiple shoots were apparent at 5 dpi in vir-plants (Figure 3.10 i). At 9 dpi, 80 to 90% of the vir-plants had multiple shoots branching at the crown region of the root and shoot. Root growth was less prolific when compared to avir-plants and con-plants (Figure 3.10 ii). The shrivelling of leaves, stunted shoot growth with multiple shoots, bushy plant growth, shortened and thickened primary roots and lateral root growth was suppressed from 11 dpi to 45 dpi in vir-plants (Figure 3.10 v). By 38 dpi, most of the con-plants started flowering, some avir-plants had flowers but only a few vir-plants had flowers. Leaf senescence was observed in con-plants and avir-plants from 40 dpi but not in the vir-plants (Figure 3.9). The avir-plants and con-plants had similar morphology through all the growth stages (Figure 3.10).

Particularly noticeable on the vir-plants was that cotyledons were intact became bright green and remained robust from 11 dpi to 45 dpi compared to con-plants and avir-plants where the cotyledons were light yellow, and shrivelled and reduced in size as the plants grew (Figure 3.10).

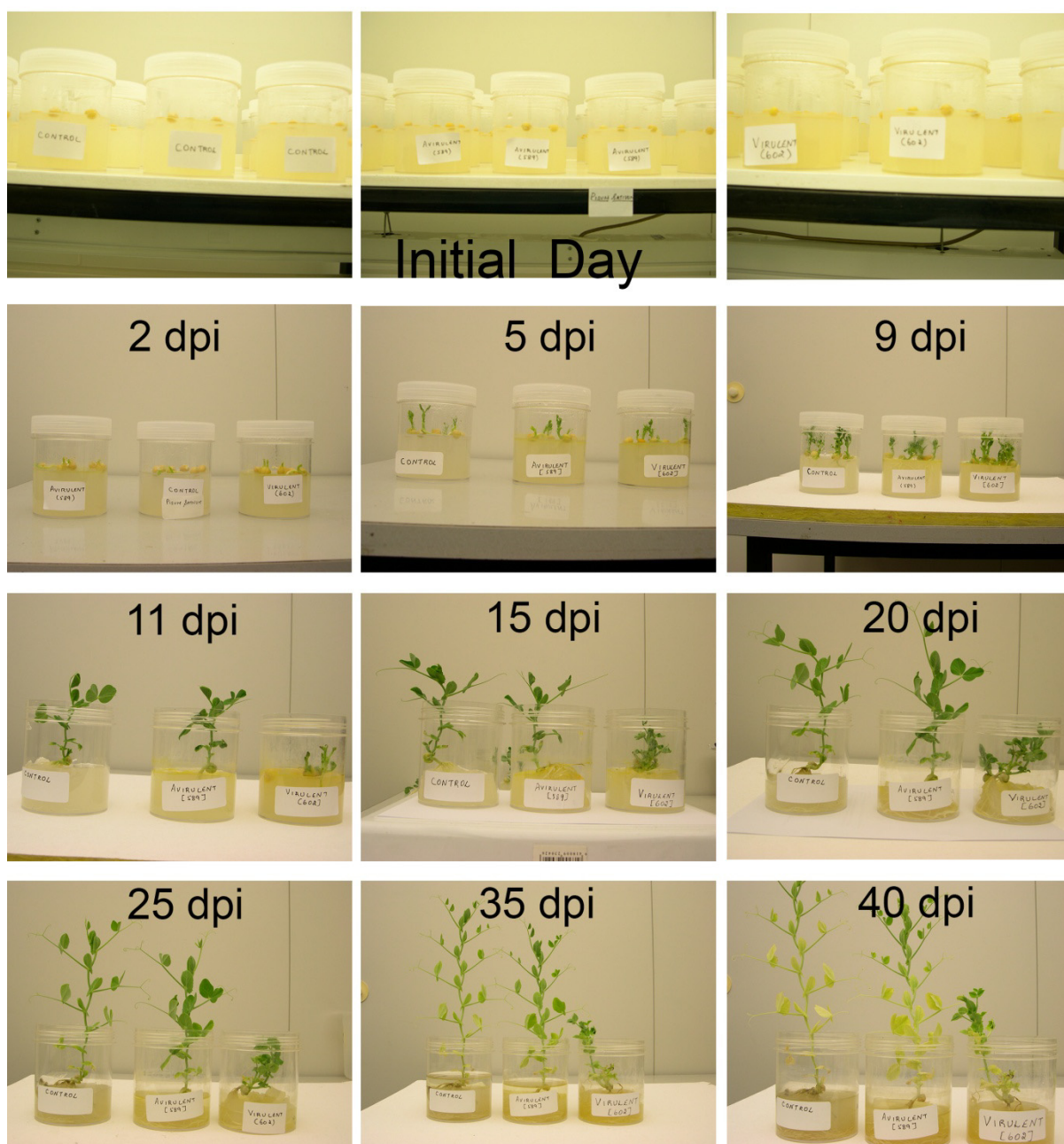


Figure 3.9 Growth stages of *P. sativum* infected with *R. fascians*. The *P. sativum* growth after 4 h of inoculation (hpi) (initial day) to 40 dpi, with mock inoculation (control), *R. fascians* avirulent strain 589 (avirulent) and *R. fascians* virulent strain 602 (virulent) in sterile agar containers.

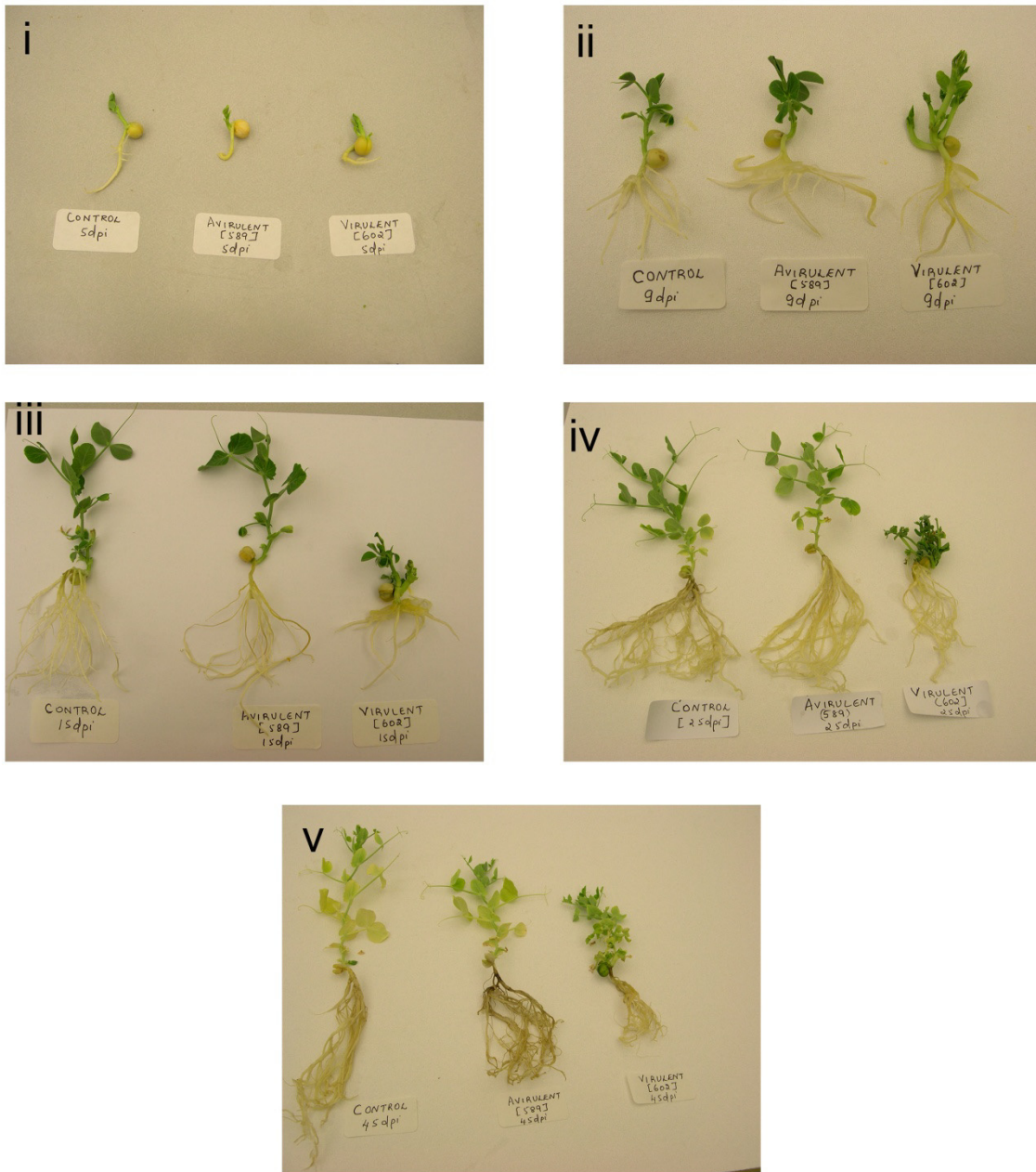


Figure 3.10 Morphology of *P. sativum* plants inoculated with *R. fascians* avirulent strain (589) and virulent strain (602). Effect of *R. fascians* on *P. sativum* at (i) 5 dpi – control plant, avirulent plant and virulent plant (ii) 9 dpi – control plant, avirulent plant and virulent plant (iii) 15 dpi – control plant, avirulent plant and virulent plant (iv) 25 dpi – control plant, avirulent plant and virulent plant (v) 45 dpi – control plant, avirulent plant and virulent plant.

3.3.4 Microbiological traits

3.3.4.1 Detection of *R. fascians* in *P. sativum*

The microbial populations of *R. fascians* from *P. sativum* inoculated with avirulent strain 589 or virulent strain 602 were estimated based on the methodology of Vereecke et al. (2002), where the microbial load on the surface as well as the internal population of *R. fascians* was determined (Section 2.6). The pea seeds infected with the *R. fascians* strains 589 and 602 were sampled from 4 hpi to 40 dpi and the total/ internal populations of a complete plant were determined.

The mock inoculated pea (control) had no *R. fascians* population at any time. There were differences in the total (surface and internal) microbial populations in peas inoculated with the two strains. The total microbial colonies at the time of sowing after 4 h imbibition was higher in seeds inoculated with virulent strain 602 strain (30.0 CFU/ml) compared to those inoculated with avirulent strain 589 (11.6 CFU/ml) (Figure 3.11), whereas, in the case of the internal population, the avirulent strain 589 inoculated seeds had no organisms (0 CFU/ml) compared to virulent strain 602 infected seeds with 15.0 CFU/ml (Figure 3.11).

The microbial populations on and in the pea plants infected with either strain were variable. In general, the *R. fascians* total population was higher in plants inoculated with the virulent strain 602 than with the avirulent strain 589. At 2 dpi the internal population of the avirulent strain 589 was low (6.6 CFU/ml) compared to the virulent strain 602 (10.6 CFU/ml). From 9 to 40 dpi the population of the virulent strain 602 in infected plants, both total and internal microbial load, was higher compared to the avirulent strain 589 infected plants. The whole and internal bacterial population of the virulent strain 602 infected plants was less varied from 2 to 15 dpi. The *R. fascians* whole population was comparatively higher than internal microbial load in the virulent strain 602 infected plants from 20 dpi to 40 dpi (Figure 3.10). The microbes from both the strains were present on the peas until the end of the experiment at 40 dpi. The differences in the internal population and whole population in the avirulent strain 589 infected plants were not high (Figure 3.11).

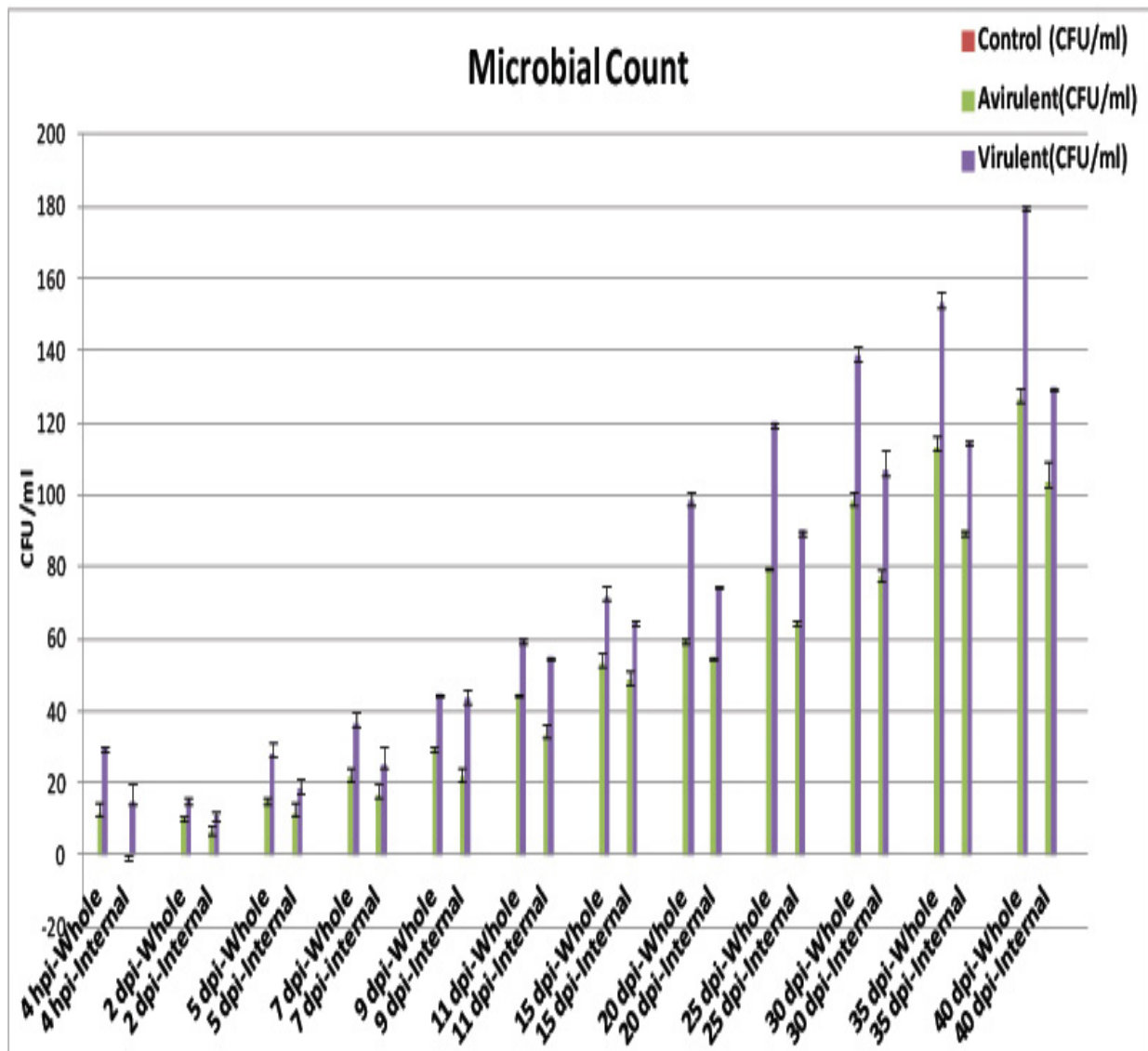


Figure 3.11 Colonisation capacities of *R. fascians* strains 589 (Avirulent) and 602 (Virulent) in *P. sativum*. The whole pea plant was sampled from 4 h post imbibition (hpi) to 40 d post inoculation (dpi). The pour plate technique was done for both whole plants (Whole) and plants surface sterilised (Internal). The error bars are +/- one standard deviation of two biological and three technical replicates.

3.3.4.2 Study of *R. fascians* colonisation in *P. sativum* using scanning electron microscopy

Some of the avirulent and virulent cultures were observed using scanning electron microscopy (SEM) to study their particular characteristics. SEM of *R. fascians* inoculated *P. sativum* plants was performed on samples collected at different time points during growth from 4 h after imbibition to 45 dpi. The SEM analysis of cultures and plant tissues: cotyledons, roots, shoots, leaves, flowers and pods were done based on the procedures mentioned in Chapter 2, Section 2.9.

Cultures of avirulent 589, 590, 593, 670 and 677 strains and the virulent 602, 592, 594 and 603 strains were observed using SEM at seven days of growth (Figure 3.12). There were differences in structure between the free-growing avirulent and virulent strains under SEM. The avirulent strain 589 appeared to be cocci/tiny rods compared to the virulent strain 602 which were prominent rods. However, there were both rods or mixed cocci and rod forms in cultures of virulent strains 592, 594 and 603. Cultures of avirulent strains 590, 593, 670 and 677 appeared rod-shaped (Figure 3.12).

Two methods of inoculation, seed inoculation and brush inoculation were done to select the best method to inoculate the pea with *R. fascians* and also to minimise contamination. The experiment was done twice and two biological replicates from each experiment were observed under SEM. *P. sativum* plants grown aseptically in vermiculite pots for seven days were brush inoculated on the shoots with *R. fascians* avirulent strain 589 and virulent strains 602 grown in flasks with 523 broth. The brush inoculation SEM analysis results are presented in Appendix B. 3.1. The brush inoculation SEM analysis was done on the 7th day (initial) day from germination and then from 3 to 20 days post inoculation (dpi). The control plants which were brushed with sterile Klambt medium (mock inoculation) did not have any organisms from 3 to 20 dpi. Due to brushing of inoculated broth on the shoot portion of the plants, both strains of the organism were detected in the shoots first and later spread to roots and cotyledons from 3 dpi until 20 dpi. Any difference in growth rate was not apparent between the avirulent and virulent strains (Appendix B. Figures 3.1 to 3.5). This type of inoculation led to the problem of not being able to determine the exact scenario as the plants were inoculated on the 7th day of growth in vermiculite pots and during sampling at each stage the

plants were forced out of the pots which lead to loss of organisms and also this type of inoculation led to a cross-contamination problem after 20 dpi. Consequently, seed inoculation and growth of plant in sterile agar containers was selected as the best method to study the interaction of *R. fascians* and *P. sativum* using SEM.

Seed inoculation was performed based on the methodology outlined in Section 2.2 and 2.3. The SEM analysis revealed no organisms in the control treatment from 4 hpi to 45 dpi. After 4 h imbibition (hpi) both the strains of *R. fascians* was present on the cotyledon surface. The virulent strain 602 bacteria were rod-shaped and grouped together compared to the avirulent strain 589 which was spread in a mesh-like structure on the surface of the cotyledon at 4 hpi (Figure 3.13). At 2 dpi, both the avirulent strain 589 and the virulent strain 602 were present on the cotyledon surface (Figure 3.13). The root and shoot were not observed with SEM at 2 dpi stage as they were barely emerged. At 5 dpi, colonies of the virulent strain 602 showed different structures on *P. sativum*: on cotyledons they were rod-shaped, on the root and leaf they were long and hyphal-like forms. The avirulent strain 589 appeared as rods on the cotyledon and leaves and hyphal-like on the root surface (Figure 3.14).

The colonisation of bacteria on each of the pea tissues increased with time. The bacterial colonisation was widely spread on cotyledons by 9 dpi, the virulent strain 602 on the root appeared as a sheath and the avirulent 589 strain as rods meshed together in a network. On both the shoot and leaf surface the bacterial colonies of the avirulent strain 589 were covered by a layer partially concealing them. The virulent strain 602 appeared to be in a thin film containing rods and hyphae-like structures (Figure 3. 15).

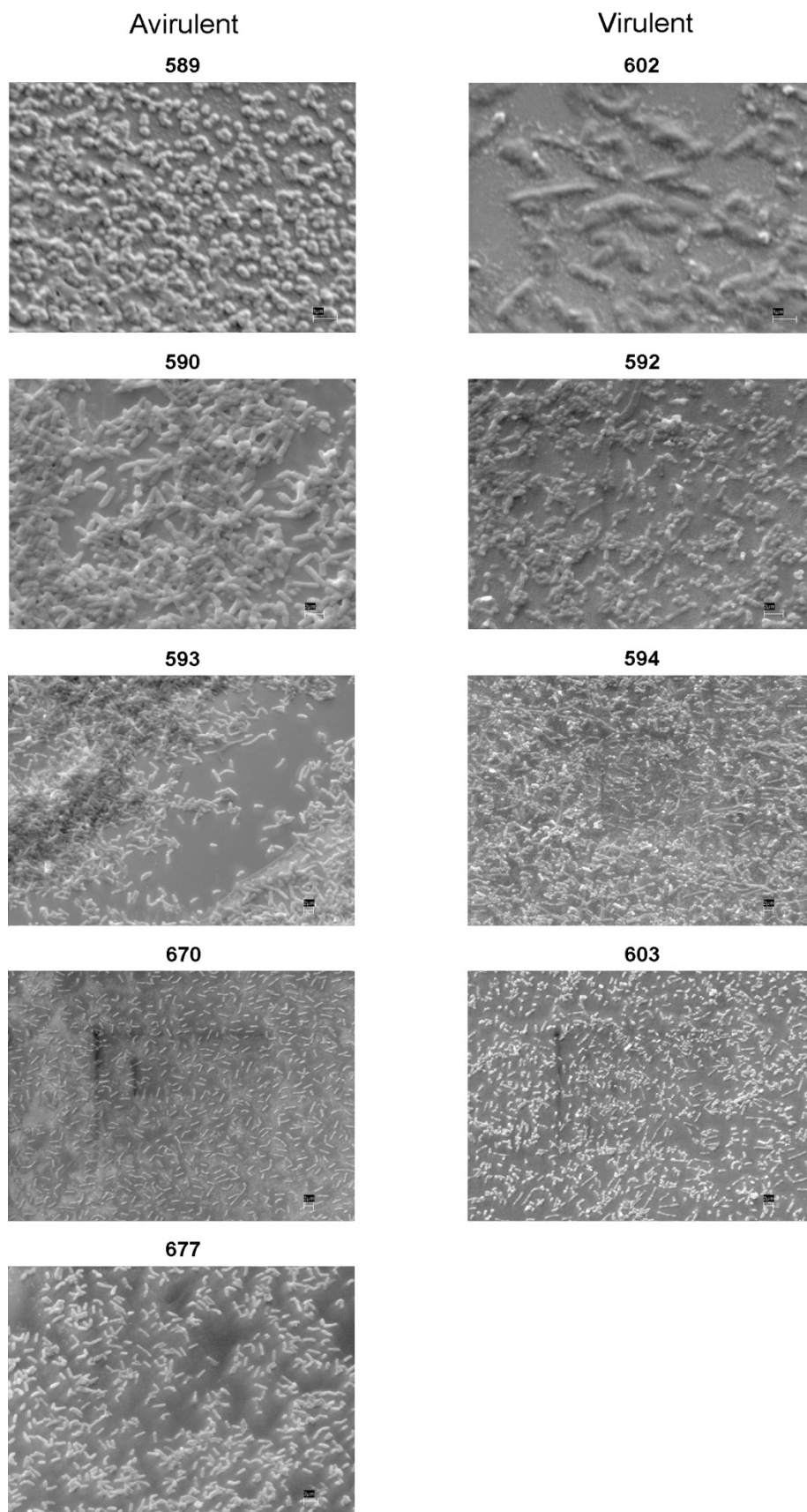


Figure 3.12 Scanning electron micrographs of *R. fascians* avirulent strains 589, 590, 593, 670 and 677 cultures and the virulent strains 602, 592, 594 and 603 cultures at seven days of growth.

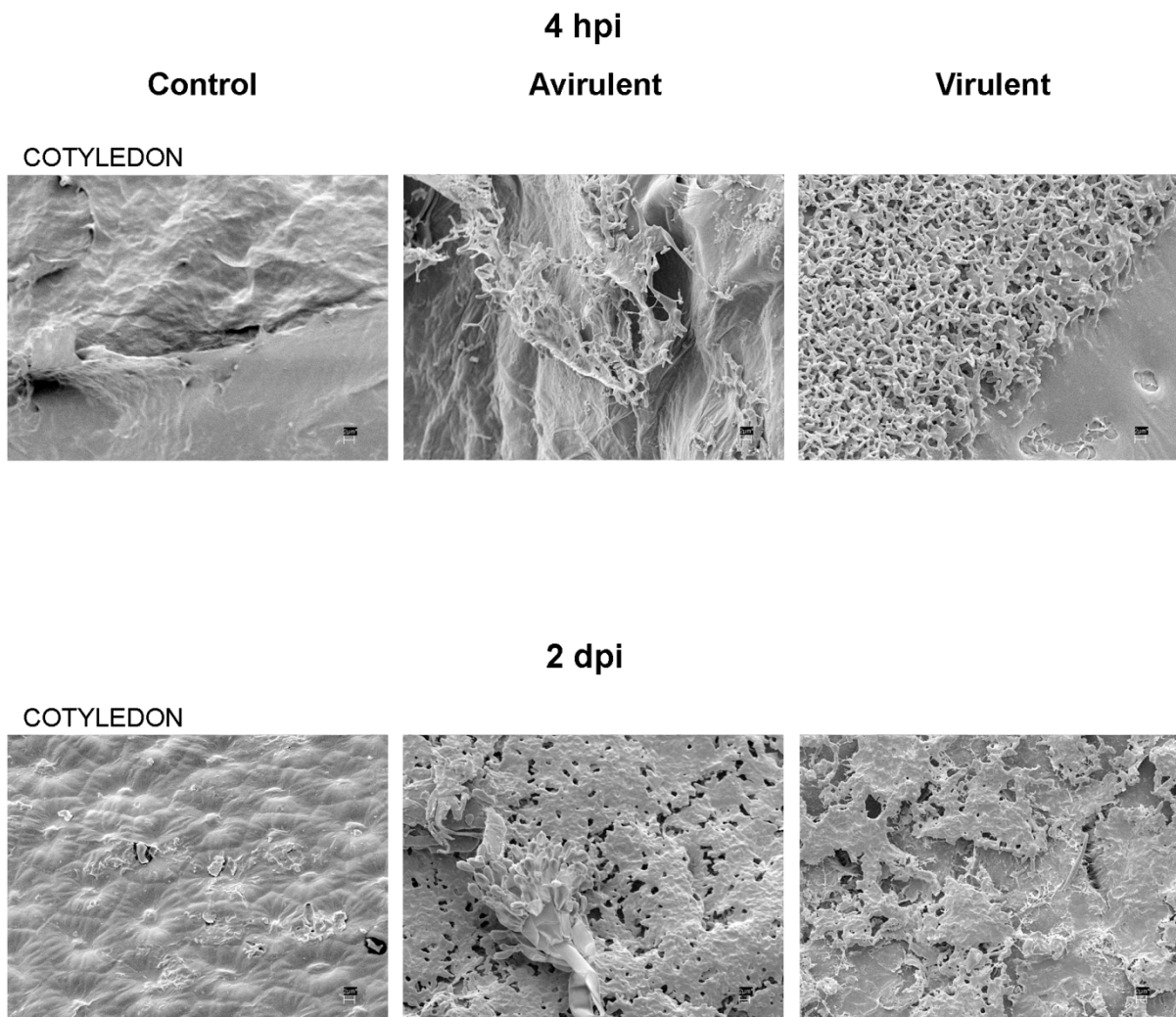


Figure 3.13 **Surface colonisation of *R. fascians* on *P. sativum***. Scanning electron micrographs of the surface of pea cotyledons at 4 h post imbibition (initial day) with Klambt's medium (Control), *R. fascians* avirulent strain 589 (Avirulent) and the virulent strain 602 (Virulent) and at 2 d post inoculation (dpi). Control with uninfected cotyledon without the presence of *R. fascians* on both the initial day and 2 dpi, *R. fascians* avirulent strain 589 infected cotyledon with hyphal-like bacteria forming an interconnected grouping on the initial day; at 2 dpi rod shaped bacteria like a coating. Virulent strain 602 infected cotyledon on the initial day with rod-shaped bacteria and at 2 dpi forming connected rods within a surface coating on the cotyledons.

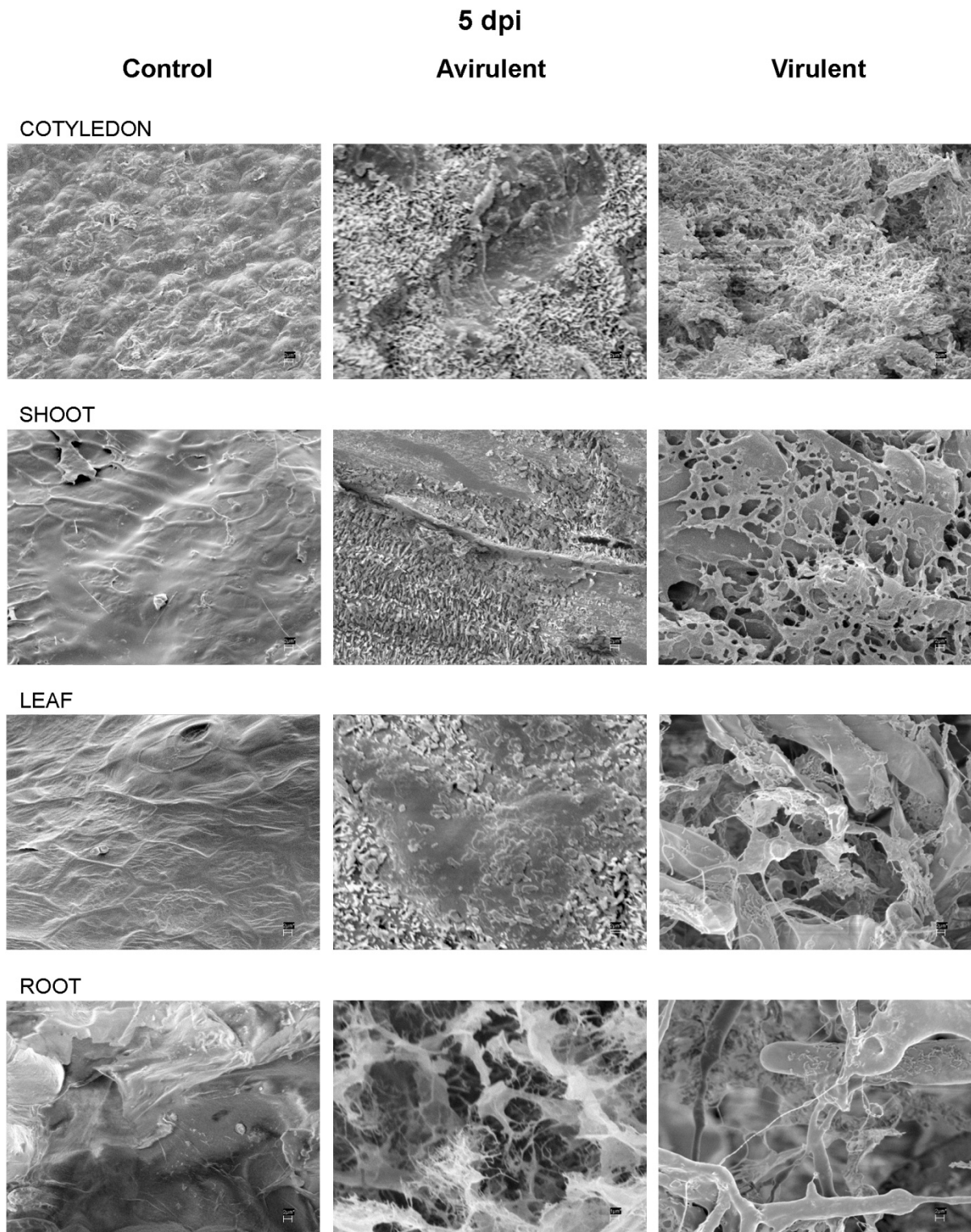


Figure 3.14 **Surface colonisation of *R. fascians* on *P. sativum* at 5 dpi.** Scanning electron micrographs of the surface of the pea cotyledon, root, shoot and leaf. Control uninfected without the presence of *R. fascians* on the surface of cotyledons, root, shoot and leaf. Avirulent strain 589 infected the cotyledon surface with rod shaped bacteria, hyphal –like bacteria on the root and covered by a skin-like coating on the shoot and leaf surface. Virulent *R. fascians* 602 strain infected cotyledon surface showing profuse fine rods, distinct hyphae-like bacteria on the roots, root hairs and on the leaf surface and interconnected rods on the shoot surface.

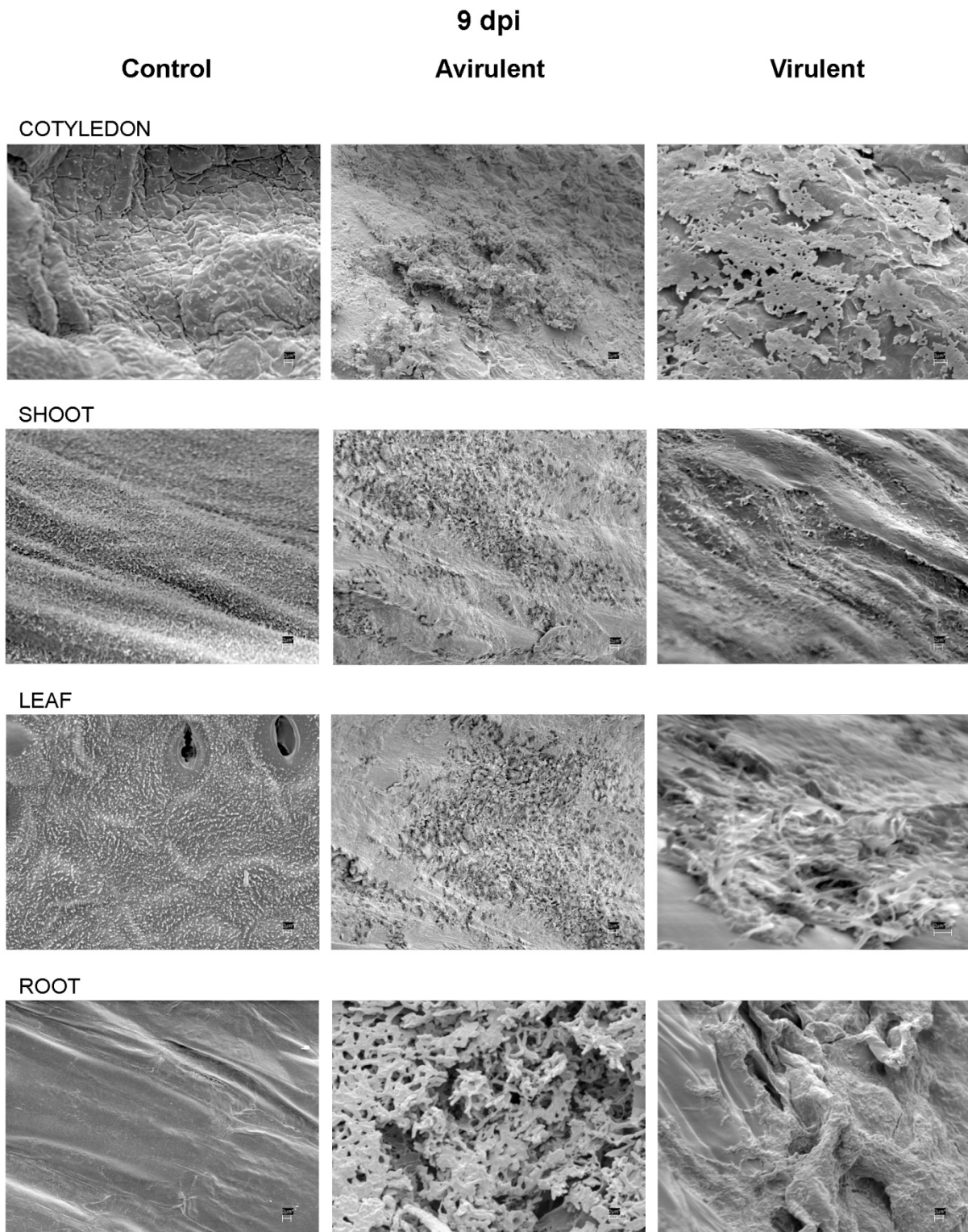


Figure 3.15 **Surface colonisation of *R. fascians* on *P. sativum* at 9 dpi.** Scanning electron micrograph (SEM) of pea cotyledon, shoot, leaf and root surface. Control without the presence of *R. fascians* on the surface of cotyledons, shoot, leaf and root. Avirulent *R. fascians* strain 589 infected cotyledon showing rod shaped microbes, layer covering the bacterial colonies on the shoot and the leaf surface and interconnected rods on the root. Virulent *R. fascians* strain 602 infected cotyledon surface showing profuse bacterial rods encrusted mucilage-like layer, on the shoots surface rods in a thin sheath, hyphae protruding from the leaf surface and on the root surface some rods discernible amongst a coat.

By 11 dpi the surface of the cotyledons and roots was extensively covered with a hyphal mesh of interconnected virulent bacteria similar to avirulent strain 589 (Figure 3.16). Detection of the bacteria on the shoot and leaf surface was not very clear either in the avirulent strain 589 or the virulent strain 602 infected peas at 20 and 25 dpi (Figures 3.17 and 3.18). There were profuse hyphal-like bacterial colonies on the cotyledons and the root surfaces from 30 to 45 dpi for both the avirulent and the virulent strain infected tissues (Figures 3.19, 3.20, 3.21 and 3.22). At 30 dpi, the avirulent bacteria appeared as interconnected short rods on the shoot surface and as rods on the leaf surface (Figure 3.19). The leaf surface had smeared patches of the virulent strain 602 at 30 dpi and distinct localisation of bacteria near stomata at 35 dpi (Figure 3.20). The avirulent strain 589 bacteria showed as darkened patches of bacteria on the leaf surface at 35 and 40 dpi (Figure 3.21).

The avirulent strain 589 bacteria were observed as interconnected rods on the shoot surface at 40 dpi (Figure 3.21). At 45 dpi both the virulent strain 602 and avirulent strain 589 were profusely spread on the cotyledons and root surfaces (Figure 3.22). The surface of the flowers at 45 dpi showed the presence of both the *R. fascians* strains and the pea pod had noticeable rods of the virulent bacteria (Figure 3.22).

In summary, there appeared to be little difference in the surface colonisation of *P. sativum* by either the strains as assessed by SEM. Due to seed inoculation, the cotyledons had profuse bacterial colonisation. *R. fascians* was present on the roots from the time of infection to the last stage of sampling. The extent of colonisation by *R. fascians* on the shoots and the leaf surfaces was sometimes not very clear due to the morphology of the plants where the shoot and leaf surfaces were spongy with a waxy appearance. It is possible that the organisms were removed during processing for SEM.

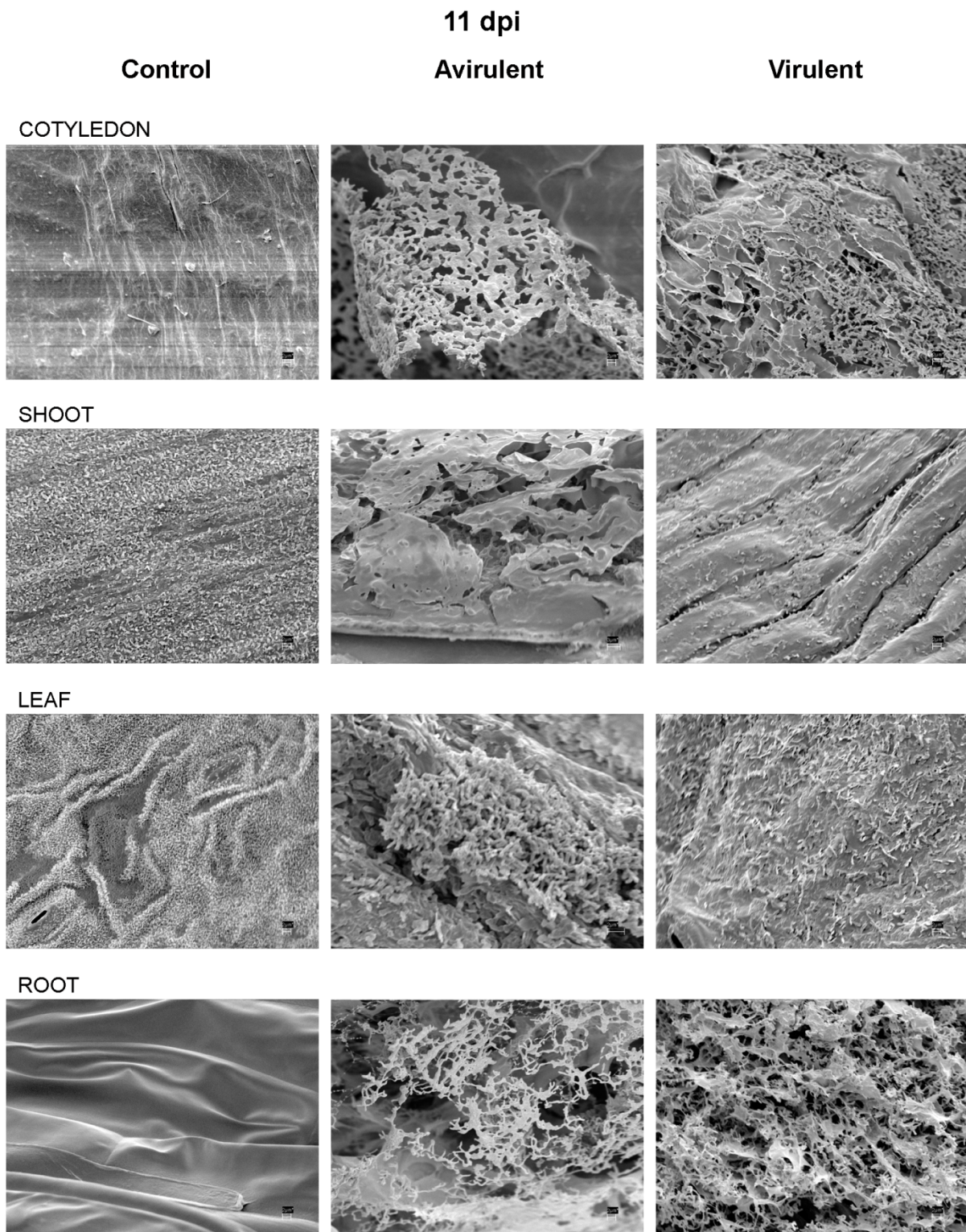


Figure 3.16 **Surface colonisation of *R. fascians* on *P. sativum* at 11 dpi.** Scanning electron micrograph of the pea cotyledon, shoot, leaf and root surface. Control uninfected without the presence of *R. fascians* on the surface of the cotyledons, shoot, leaf and root. Avirulent strain 589 infected cotyledon, leaf and root showing mesh-like patches of interconnected bacteria, on shoot there is a coating overlaying the microbes. Virulent strain 602 infected cotyledon with profuse spread of bacteria; a few rods on shoot and leaf surfaces; and mesh of hyphal-like bacteria on root surface.

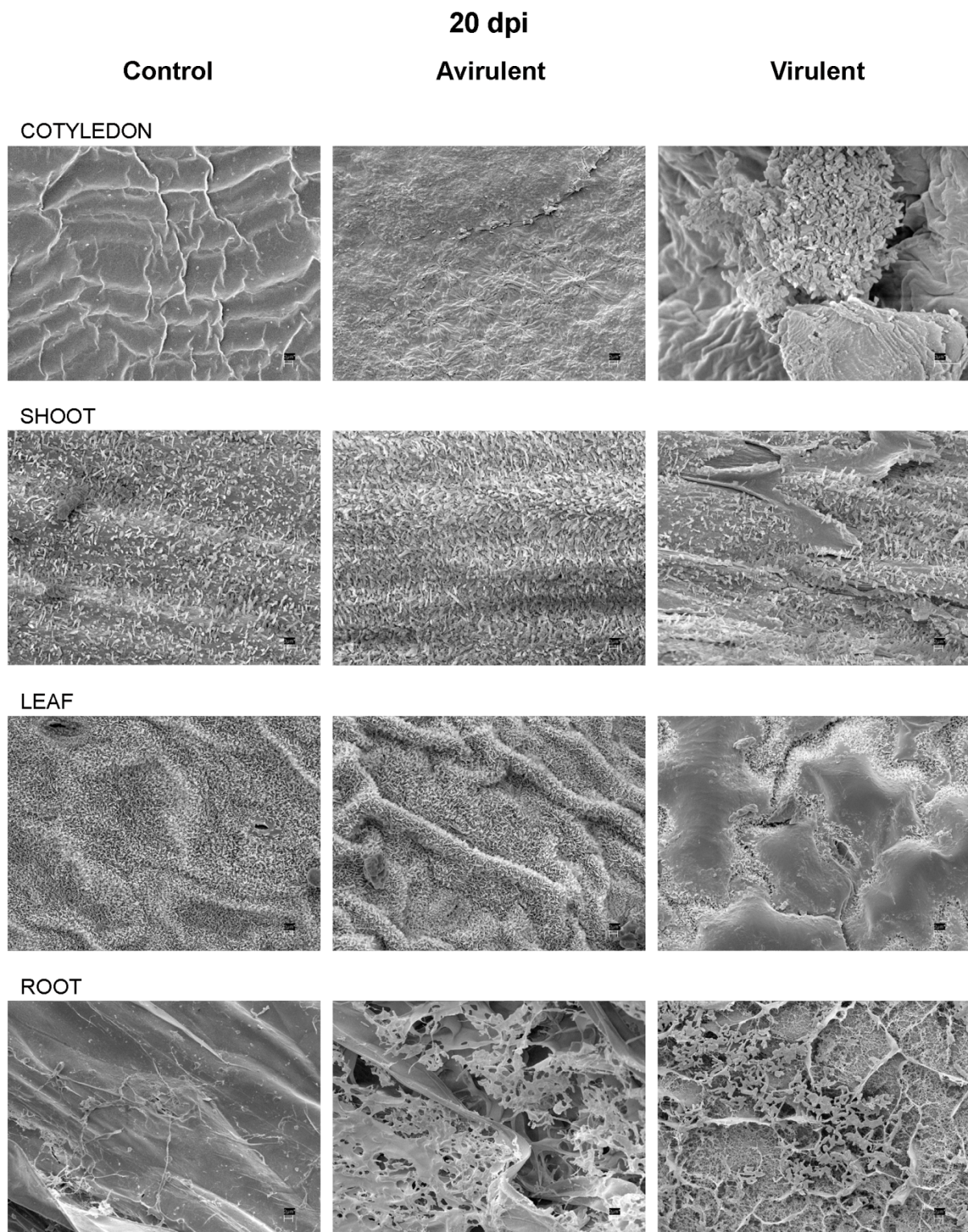


Figure 3.17 **Surface colonisation of *R. fascians* on *P. sativum* at 20 dpi.** Scanning electron micrographs of the pea cotyledon, shoot, leaf and root surface. Control uninfected without the presence of *R. fascians* on the surface of the cotyledon, shoot, leaf and root. Avirulent strain 589 infected cotyledon with rod shaped bacteria; on shoot and leaf bacteria are not prominent; on root surface bacteria are interconnected. Virulent strain 602 infected cotyledon with prominent bunch of bacteria; damaged shoot and the leaf surface with a layer covering pockets of bacteria; hyphal-like network of bacteria on the root surface.

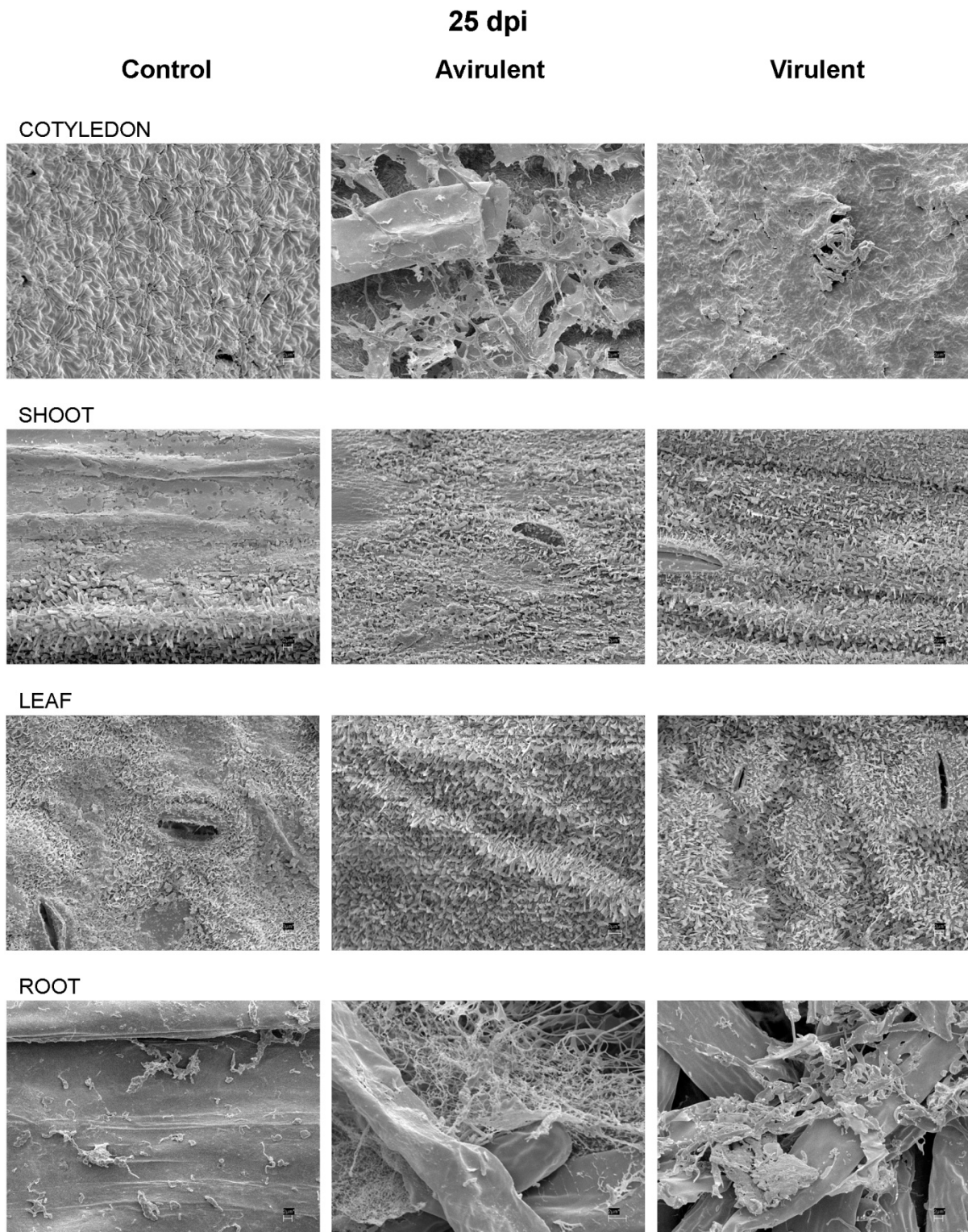


Figure 3.18 **Surface colonisation of *R. fascians* on *P. sativum* at 25 dpi.** Scanning electron micrograph of the pea cotyledon, shoot, leaf and root surface. Control uninfected without the presence of *R. fascians* on the surface of the cotyledons, shoot, leaf and root. Avirulent 589 strain infected cotyledon and root surface with intensive network of hyphal-like bacteria; on shoot and leaf bacteria are not prominent. Virulent strain 602 infected cotyledon with some bacteria within a surface coating; on shoot and leaf bacteria are not clearly visible but are aggregated on the root.

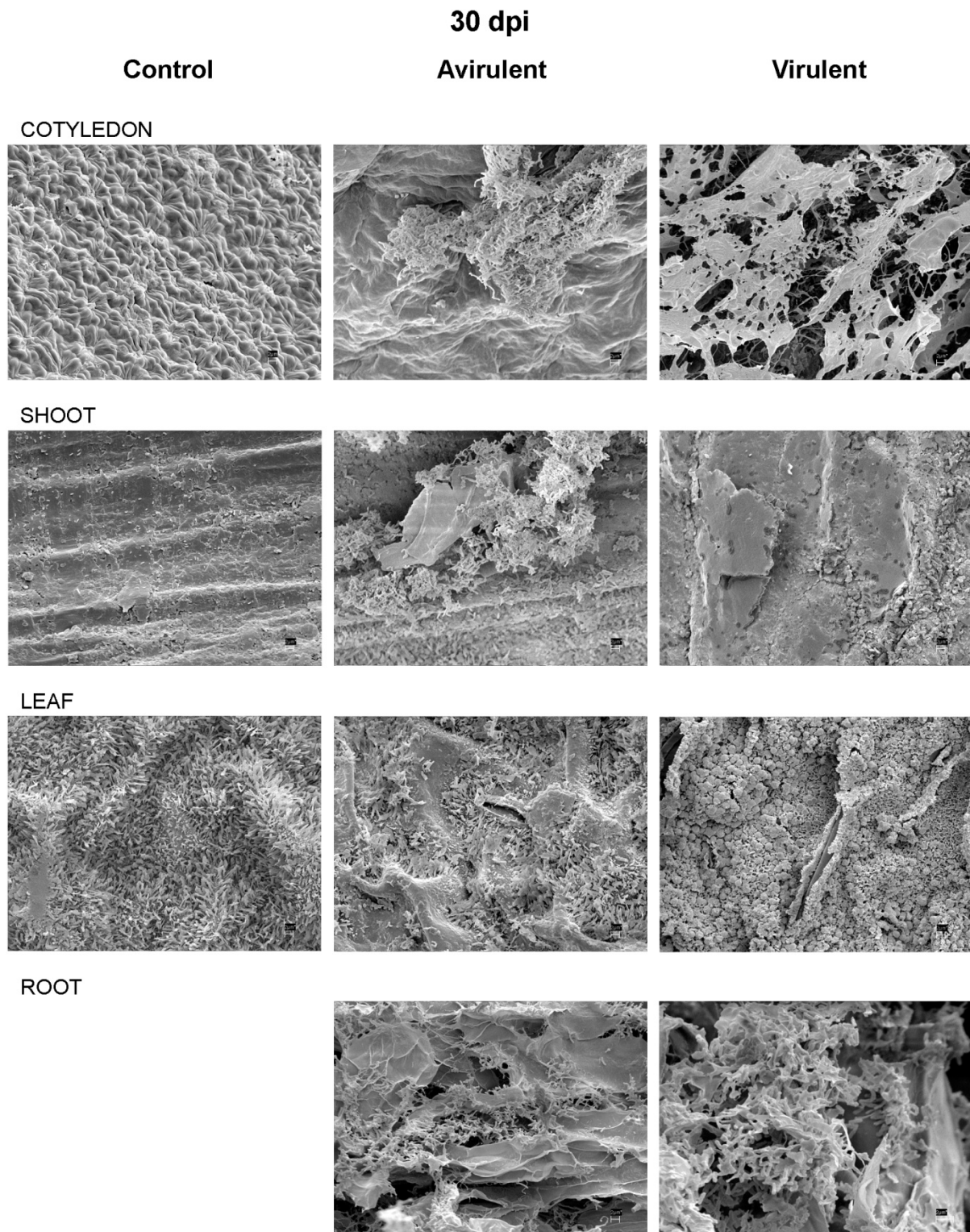


Figure 3.19 **Surface colonisation of *R. fascians* on *P. sativum* at 30 dpi.** Scanning electron micrograph of the pea cotyledon, shoot, leaf and root surface. Control uninfected without the presence of *R. fascians* on the surface of cotyledons, shoot and leaf. Avirulent strain 589 infected cotyledon with rods in network; on shoot and leaf surface tiny rods clumped together; on root surface hyphal-like bacteria. Virulent strain 602 infected cotyledons with prominent bacterial network; damaged shoot with hyphae-like bacteria; prominent clumps of bacteria on leaf surface; hyphal-like network of bacteria on the root surface.

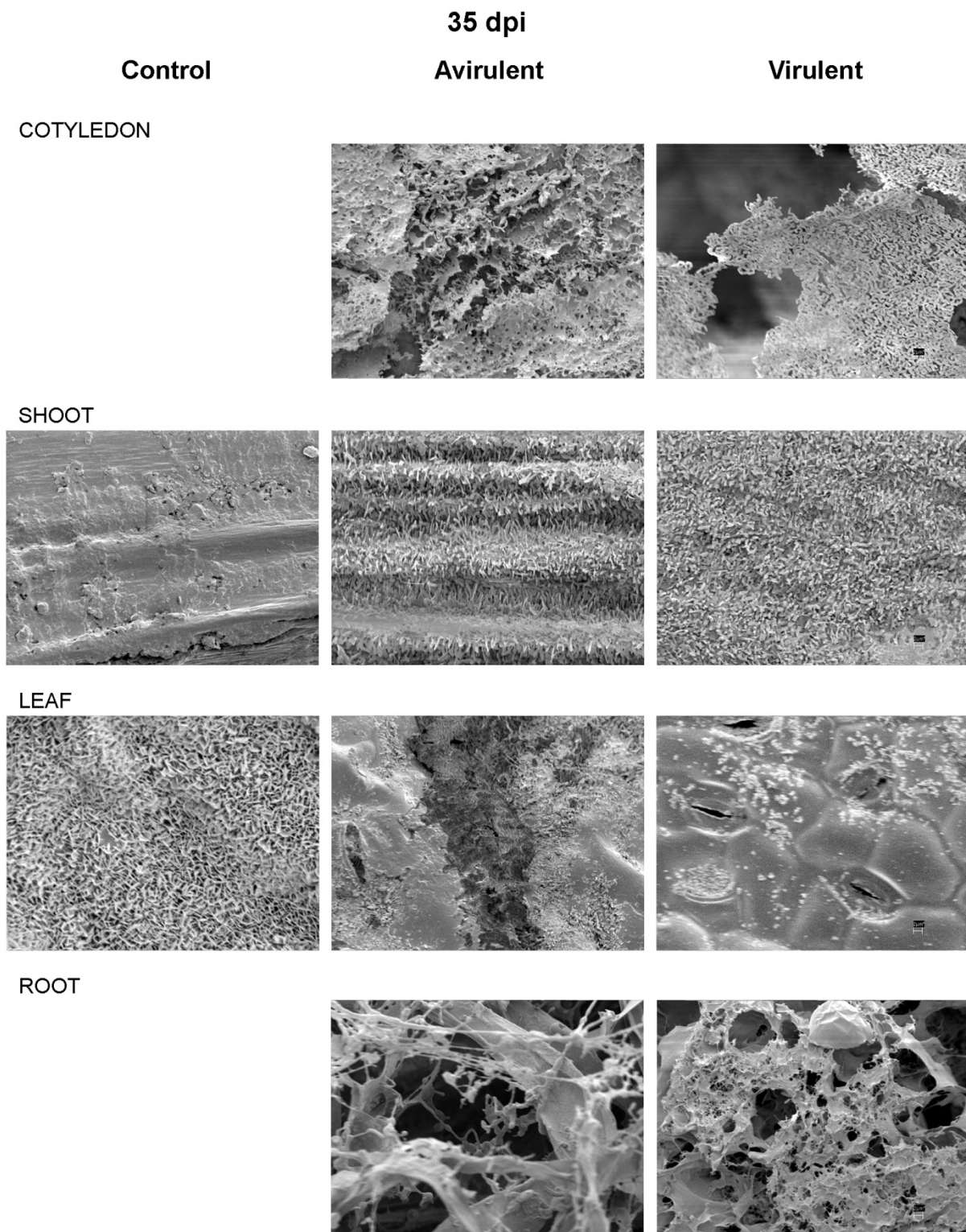


Figure 3.20 **Surface colonisation of *R. fascians* on *P. sativum* at 35 dpi.** Scanning electron micrograph of the pea cotyledon, root, shoot and leaf surface. Control uninfected without the presence of *R. fascians* on the surface of shoot and leaf. Avirulent strain 589 infected cotyledon and root with profuse hyphal-like branched bacteria; on shoot bacteria are not prominent and on leaf surface with darkened patches. Virulent strain 602 infected cotyledon with bacteria as a mesh; hyphal-like network of bacteria on the root surface; shoot bacterial presence is not clear and leaf with some pockets of bacteria.

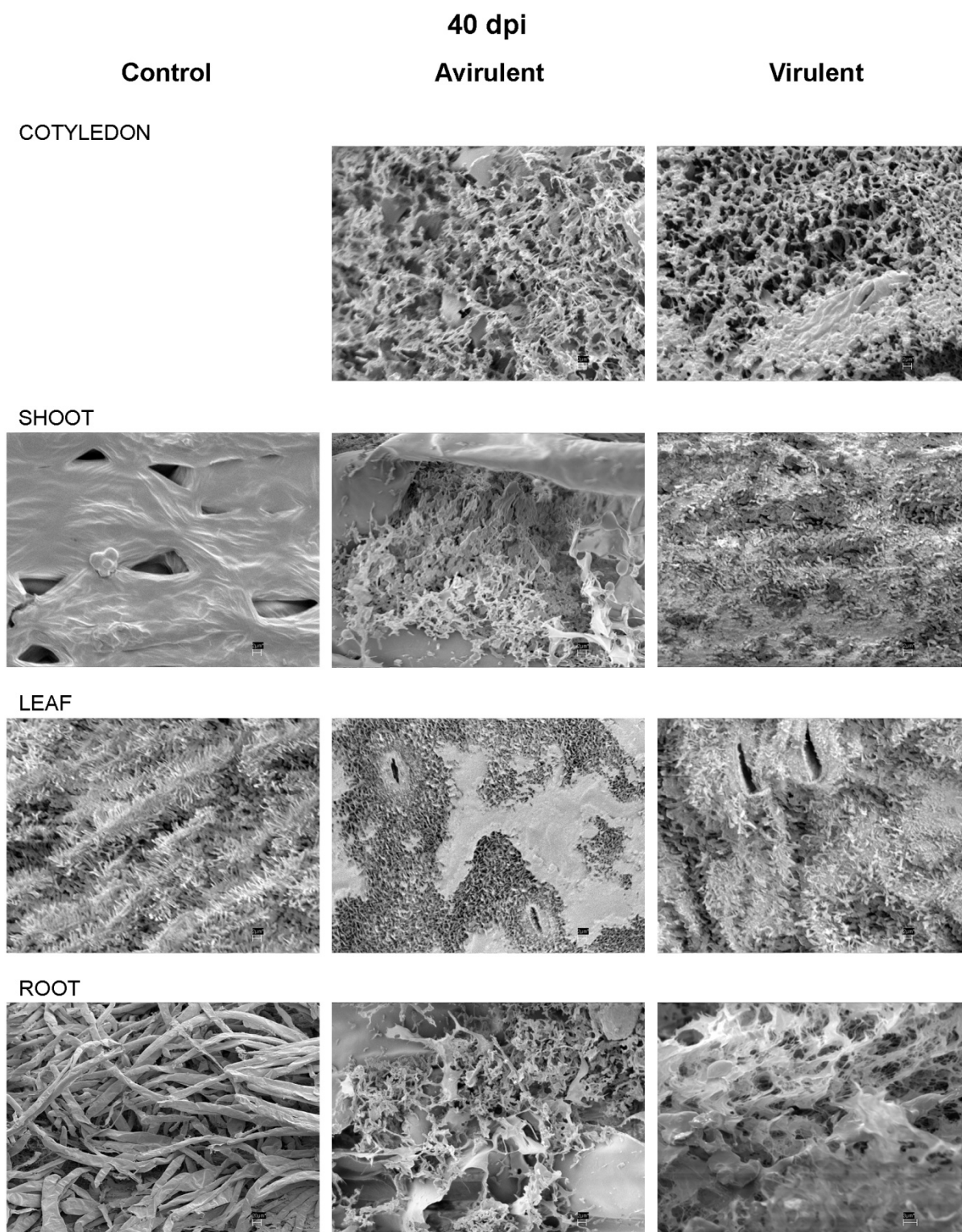


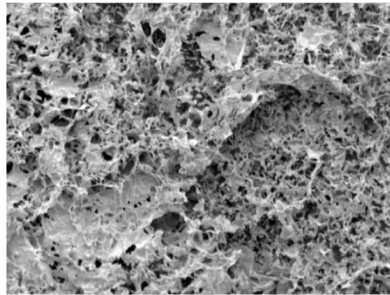
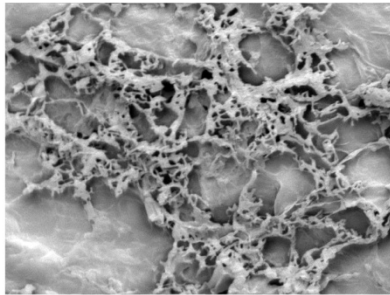
Figure 3.21 **Surface colonisation of *R. fascians* on *P. sativum* at 40 dpi.** Scanning electron micrograph of the pea cotyledon, shoot, leaf and root surface. Control uninfected without the presence of *R. fascians* on the surface of shoot, leaf and root surface (with root hairs). Avirulent strain 589 infected cotyledon fully covered with interconnected rods; on shoot interconnected rods and on the leaf with surface coating; on the root surface profusely branched hyphal-like bacteria. Virulent 602 infected cotyledon covered fully with a layer of bacteria; damaged shoot and leaf with patches of bacteria; hyphal-like network of bacteria on root surface.

45 dpi

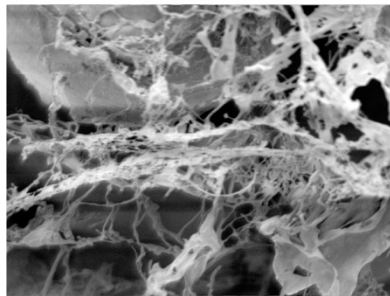
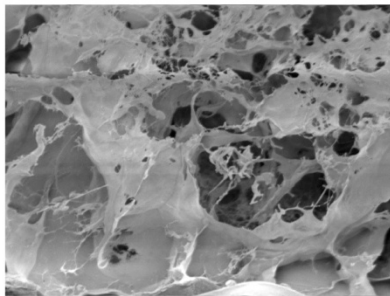
Avirulent

Virulent

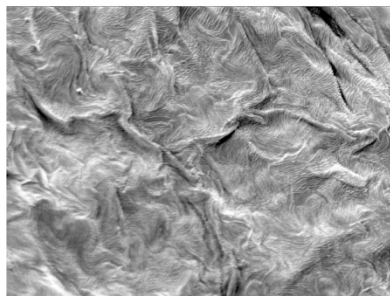
COTYLEDON



ROOT



FLOWER



PEAPOD

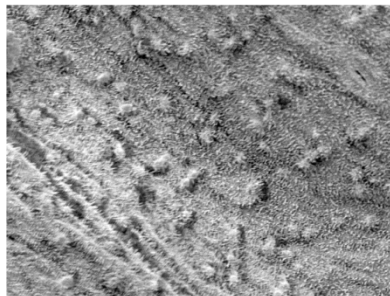
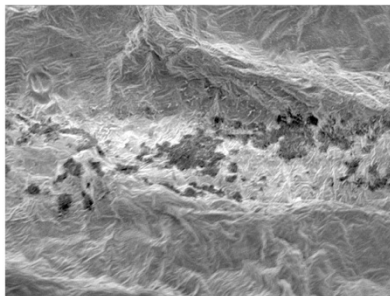


Figure 3.22 **Surface colonisation of *R. fascians* on *P. sativum* at 45 dpi.** Scanning electron micrograph of the pea cotyledon, root, flower and pea pod surface. Avirulent strain 589 infected cotyledon and root with covered interconnected bacterial rods and hyphal-like bacteria; on flower and pea pod surface patches of rods. Virulent strain 602 infected cotyledon fully covered with a layer of bacteria; hyphal-like network of bacteria on root surface; some rods on flower and pea pod surface.

3.3.4.3 Light microscopy study of *P. sativum* plants inoculated with *R. fascians*.

Light microscopy was used to examine the internal colonisation of *P. sativum* infected by *R. fascians*. Cotyledons, roots and shoots were sampled at intervals of 4 hpi and 2, 5, 9, 15, 25 and 35 dpi. Serial transverse sections in the case of the cotyledon and longitudinal thin sections of the roots and shoots, 10 – 13 µm thick, were stained and observed. Some of the *R. fascians* avirulent (589, 590, 593, 676) and virulent (592, 596, 602, 601 and 603) cultures were observed with Gram staining at 2 and 7 d of growth. The procedures for light microscopy are outlined in Section 2.4.2.

Light microscopy of the avirulent and virulent culture strains revealed the gram-positive reaction (Figures 3.23 and 3.24). The avirulent strains 590, 593, 676 and 677 were mainly rods after 2 days of culture. Even though 589 strain appeared to be cocci-like in SEM, they were rods using light microscopy at both 2 and 7 d of growth. The virulent strains 592, 596, and 603 were a mixture of rods and cocci-like bacteria except the virulent 601 and 602 strain which clearly exhibited rod bacteria at 2 d but 602 exhibited both cocci and rods forms at 7 d in their light micrographs (Figure 3.24 e and f).

The staining of sectioned specimens was tested with stains including Sass safranin and fast green, ruthenium red, haematoxylin-eosin and gram staining. The safranin and fast green staining did not differentiate between the bacteria and the plant tissue. The ruthenium red stained everything red so the bacteria were not clearly differentiated. Gram staining formed crystal structures in the cotyledon due to the presence of starch granules. Haematoxylin-eosin (HE) staining was selected as the best due to differential staining of pea and bacteria where the pea tissues stained red and *R. fascians* stained purple.

To enable easy comparison, light micrographs are presented at the same image size for different treatments, except for the digital enlargement of selected areas of micrographs taken using the 100x oil immersion objective. These latter images have variable scale bar lengths. Where *R. fascians* was absent from the tissue sample, micrographs of low magnification (20x and 40x objectives) only are presented in the figures. Where the bacteria were present, higher magnification using the 100x objective and subsequent enlargements are illustrated to show the finer details of the bacteria. There was no *R. fascians* contamination in the control peas at any stage.

AVIRULENT

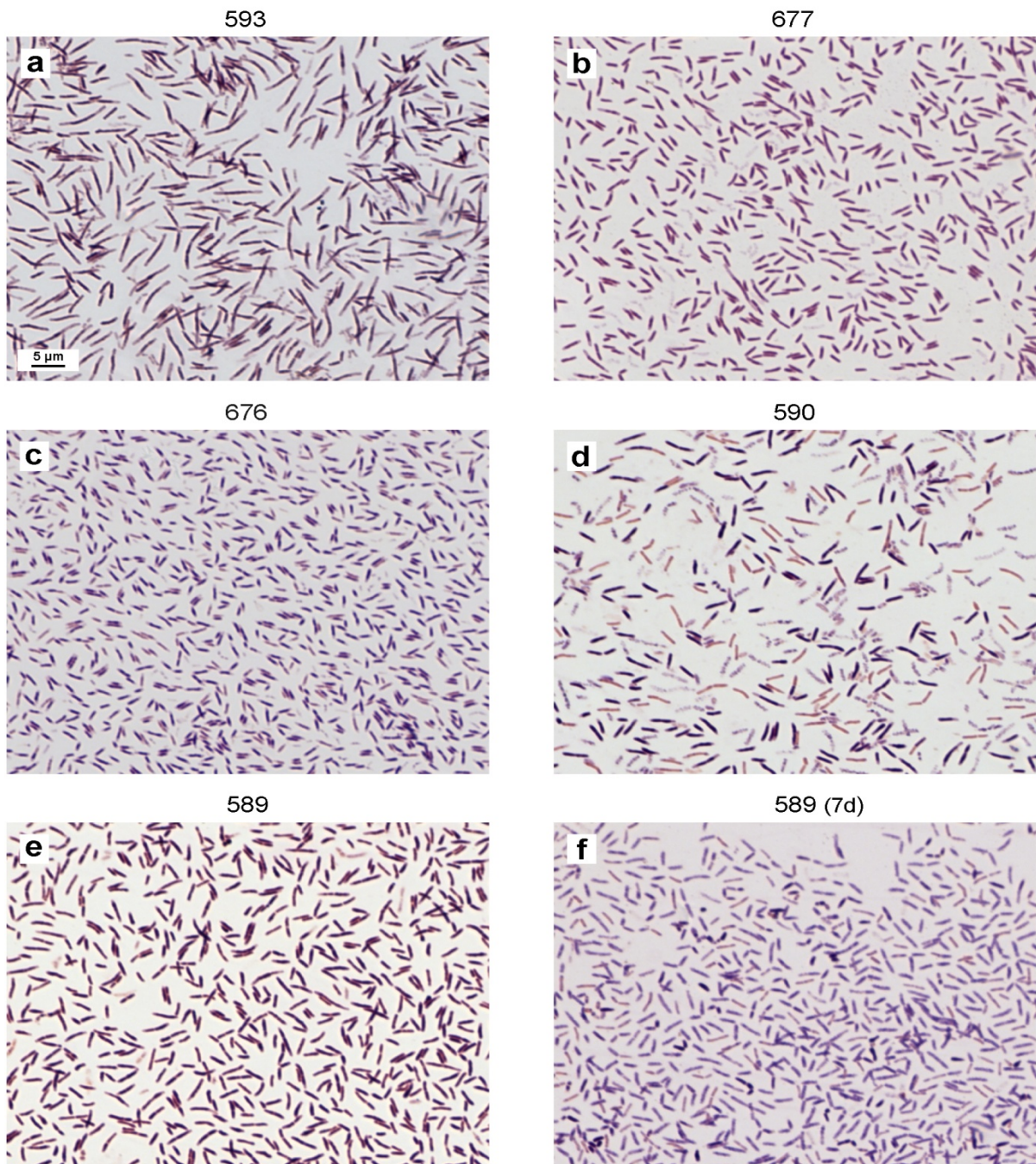


Figure 3.23 Light micrographs showing the gram stained *R. fascians* avirulent isolates at 2 and 7 d growth in 523 media. a) 593 culture isolate at 2 d with prominent rods b) 677 culture isolate at 2 d with short rods c) 676 culture isolate at 2 d with rods d) 590 culture isolate at 2 d with rods e) 589 culture isolate at 2 d with rods f) 589 culture isolate showing very short rods at 7 d of growth in media. Scale bar = 5 µm for all micrographs.

VIRULENT

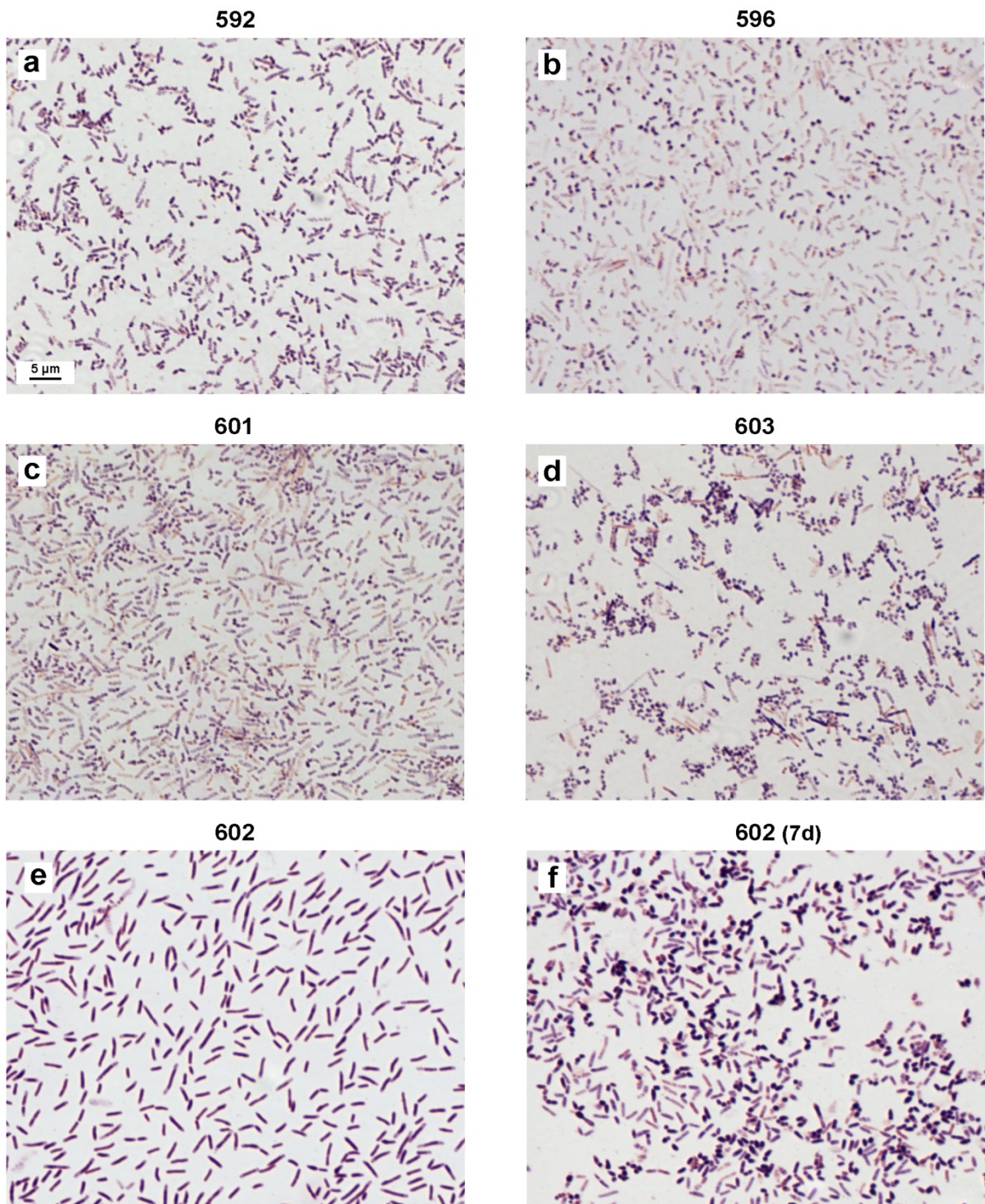


Figure 3.24 **Light micrographs showing the gram stained *R. fascians* virulent isolates at 2 and 7 d growth in 523 media.** a) 592 culture isolate at 2 d with rods and cocci b) 596 culture isolate at 2 d with short rods and cocci c) 601 culture isolate at 2 d with very small rods d) 603 culture isolate at 2d with rods and cocci e) 602 culture isolate with clear rods at 2 d growth f) 602 culture with mix of rods and cocci forms at 7 d growth. Scale bar = 5 µm for all micrographs.

Within 4 h of pea seeds being inoculated with the virulent strain 602 (vir-cot), *R. fascians* colonies were detectable in the intercellular spaces of the sub-epidermal layer of the seed coat, whereas bacteria were not present on the seed coat of seeds inoculated with the avirulent strain 589 (avir-cot) (Figure 3.24). Virulent *R. fascians* was found in groups (Figure 3.25 c, f and g); higher magnification showed the grouping was of small rods or cocci-like bacteria (Figure 3.25 g and h)

At 2 dpi, the avir-cot had *R. fascians* in the intercellular spaces of the subepidermal layer of the seed coat but not on the surface of the cotyledon, compared to the vir-cot which had bacteria present in the parenchyma layer of the seed coat as well as on the surface of the cotyledon (Figures 3.26 and 3.27). Both the strains were detected on the radicle tissue of the pea at 2 dpi (Figure 3.28). The presence of mucilage like material was seen near the surface of the avirulent strain 589 infected radicle root hairs (Figure 3.28 e) and the bacteria were mainly clumped together (Figure 3.28 b, e, g and i). The *R. fascians* virulent strain 602 infected radicle exhibited a layer of the bacteria on the root epidermis and amongst the root hairs (Figure 3.28 c, f and h) which appear as bacterial rods on enlargement (Figure 3.28 j).

At 5 dpi, the seed coat infected with *R. fascians* avirulent 589 strain, the bacteria appeared as clumps in the parenchyma layer of the seed coat (Figure 3.29 a, c and e). Both the vir-cot and avir-cot showed the presence of bacteria spread on the surface of the cotyledon at 5 dpi (Figure 3.30). The colonisation of the avirulent strain 589 infected roots (avir-root) at 5 dpi had clumps of bacteria on the root epidermis and root hairs (Figure 3.31 b, e and g). The *R. fascians* virulent strain 602 infected roots (vir-root) showed significant presence of the bacteria on the root epidermal surface, in particular amongst the root hairs by 5 dpi (Figure 3.31 c, f and h). *R. fascians* was found on the growing the virulent strain 602 infected shoots (vir-shoots) at 5 dpi (Figure 3.32 b, d, e and f).

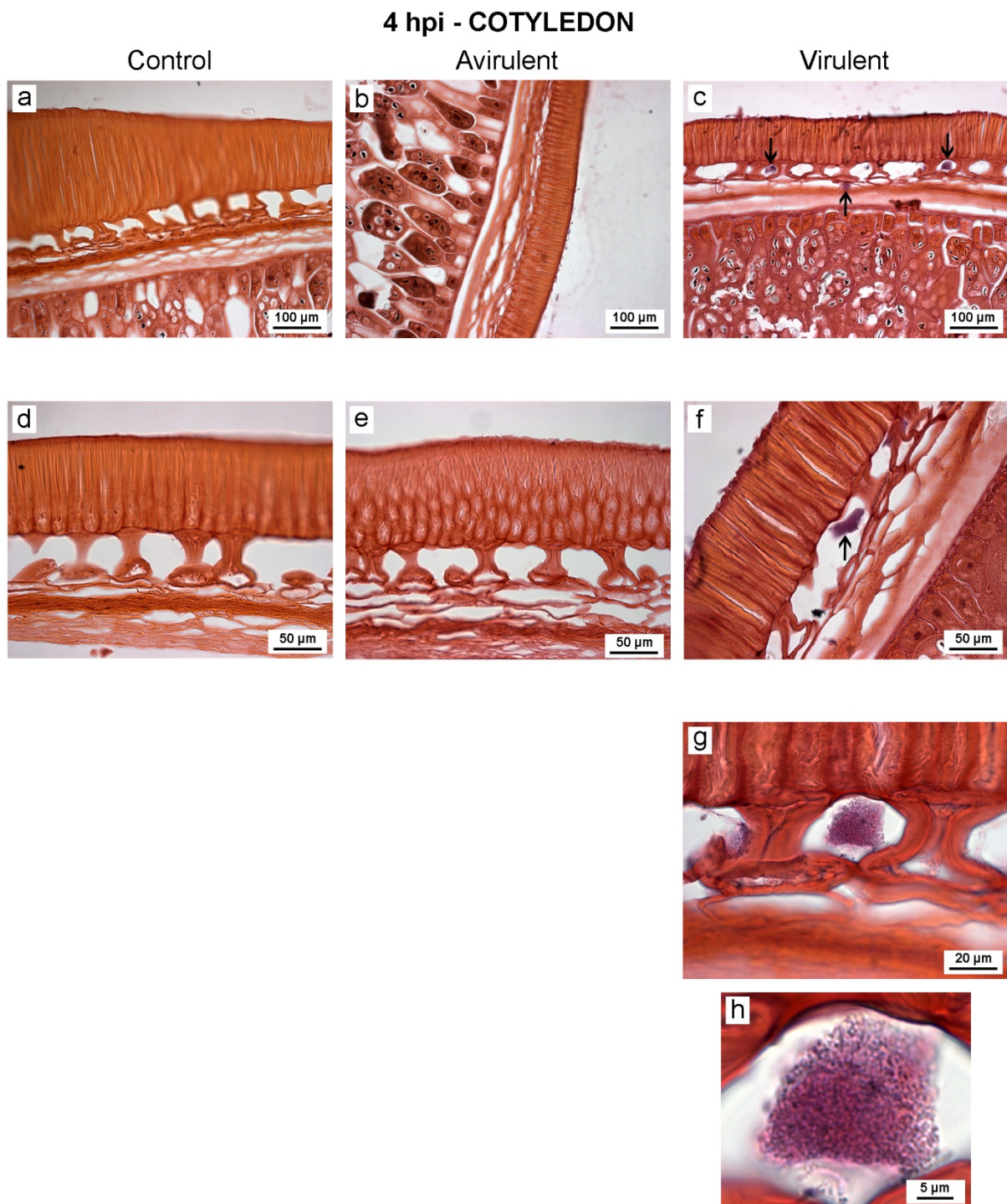


Figure 3.25 Light micrographs of transverse sections of *P. sativum* cotyledon with seed coat after 4 h imbibitions (4 hpi) in Klambt medium or *R. fascians* avirulent strain 589 and virulent strain 602. a) and d) Control cotyledon without *R. fascians* in the seed coat. b) and e) Avirulent strain 589 infected cotyledon without *R. fascians* in the seed coat. c) Virulent strain 602 infected cotyledon with *R. fascians* (arrowed) in the intercellular spaces of the subepidermal layer and parenchyma layer of the seed coat. f) Virulent strain 602 infected cotyledon with purple-stained *R. fascians* (arrowed) clearly visible in the intercellular spaces of the subepidermal layer of the seed coat. g) Virulent strain 602 infected seed coat showing grouping of *R. fascians* in the intercellular space of the subepidermal layer of seed coat. h) Enlargement of (g) highlighting small rods and cocci-like *R. fascians*.

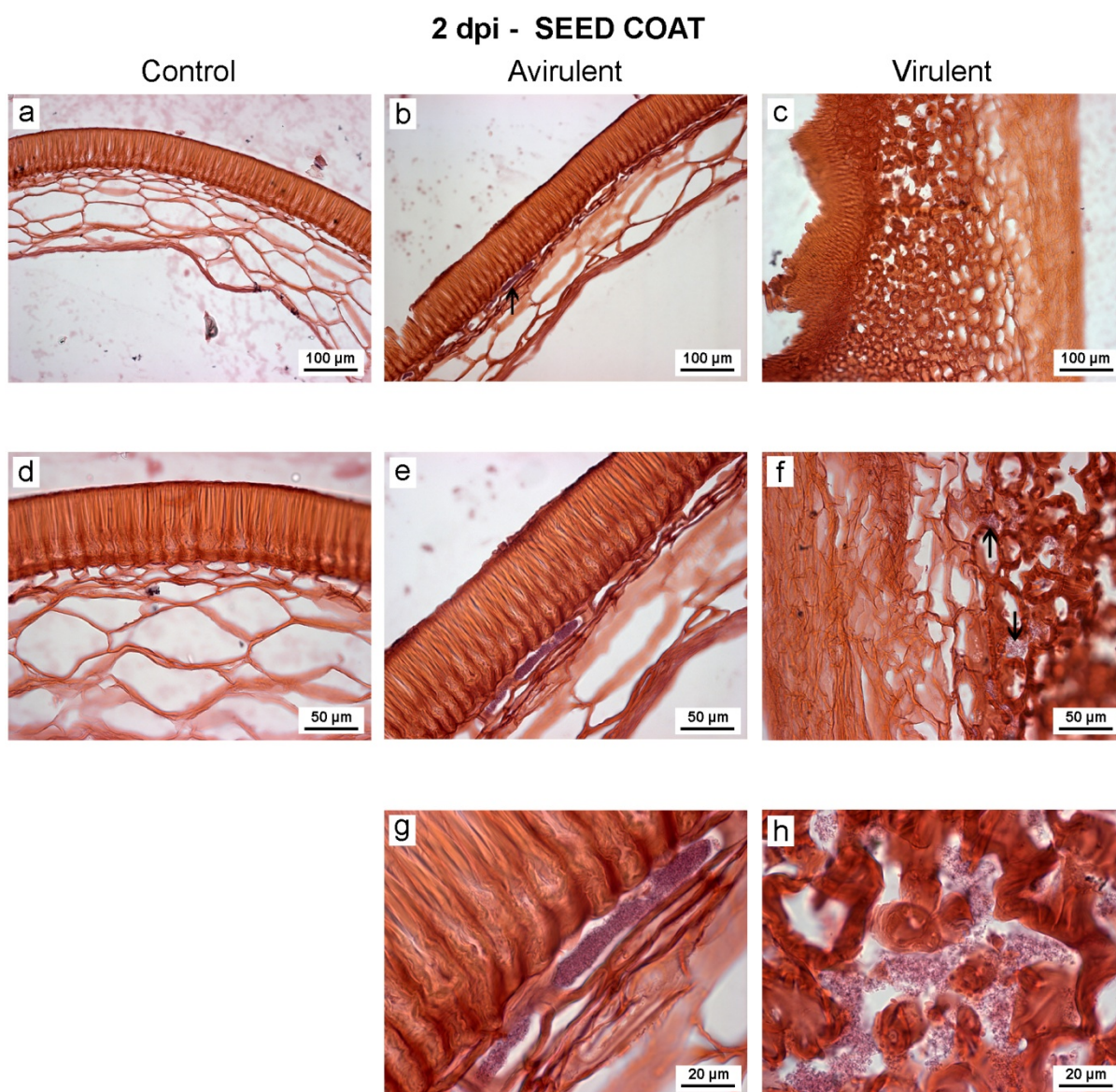


Figure 3.26 **Light micrographs of transverse sections of *P. sativum* seed coat tissue without or with *R. fascians* avirulent strain 589 and virulent strain 602 at 2 d post inoculation (dpi).** a) and d) Control seed coat. b) and e) Avirulent strain 589 infected cotyledon with *R. fascians* (arrowed) in the intercellular spaces of subepidermal layer of the seed coat. c) Virulent strain 602 infected cotyledon with *R. fascians* in the subepidermal layer of the seed coat. f) Virulent strain 602 infected cotyledon with *R. fascians* (arrowed) in the parenchyma layer of the seed coat. g) Higher magnification of the seed coat showing *R. fascians* clumped in the intercellular spaces of the subepidermal layer of the avirulent strain 589 infected cotyledon. h) Virulent strain 602 infected cotyledon with *R. fascians* spread all throughout the parenchyma layer of the seed coat.

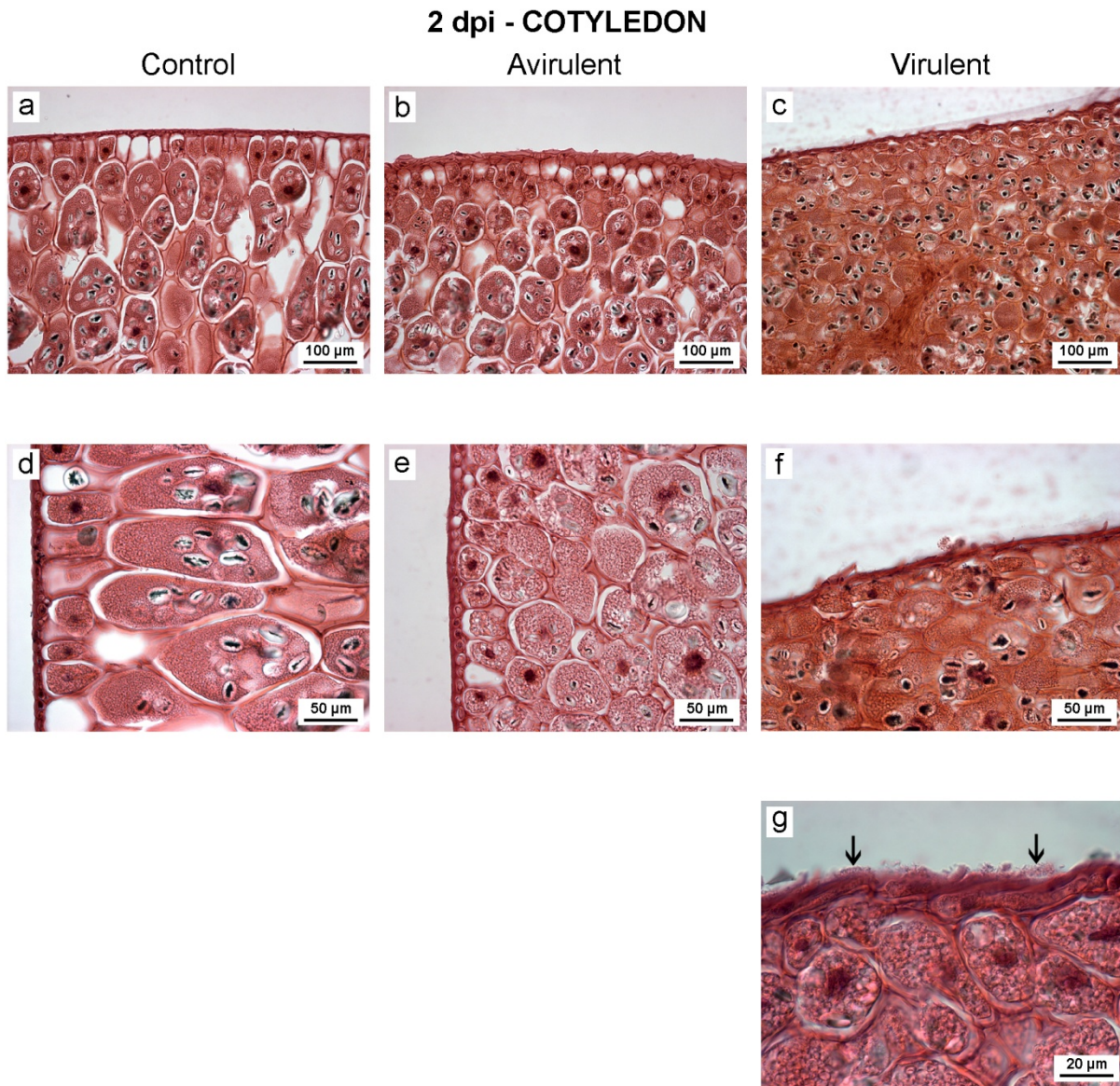


Figure 3.27 **Light micrographs of transverse sections of *P. sativum* cotyledon without or with *R. fascians* avirulent strain 589 and virulent strain 602 at 2 d post inoculation (dpi).** a) and d) Control cotyledon. b) and e) Avirulent strain 589 infected cotyledon with no *R. fascians* on the surface of the cotyledon. c) Virulent strain 602 infected cotyledon with *R. fascians* on the surface of the cotyledon. f) Virulent 602 strain infected cotyledon with *R. fascians* on the cotyledon surface. g) Virulent 602 strain infected cotyledon with a thin layer of *R. fascians* (arrows) visible on the surface of the cotyledon.

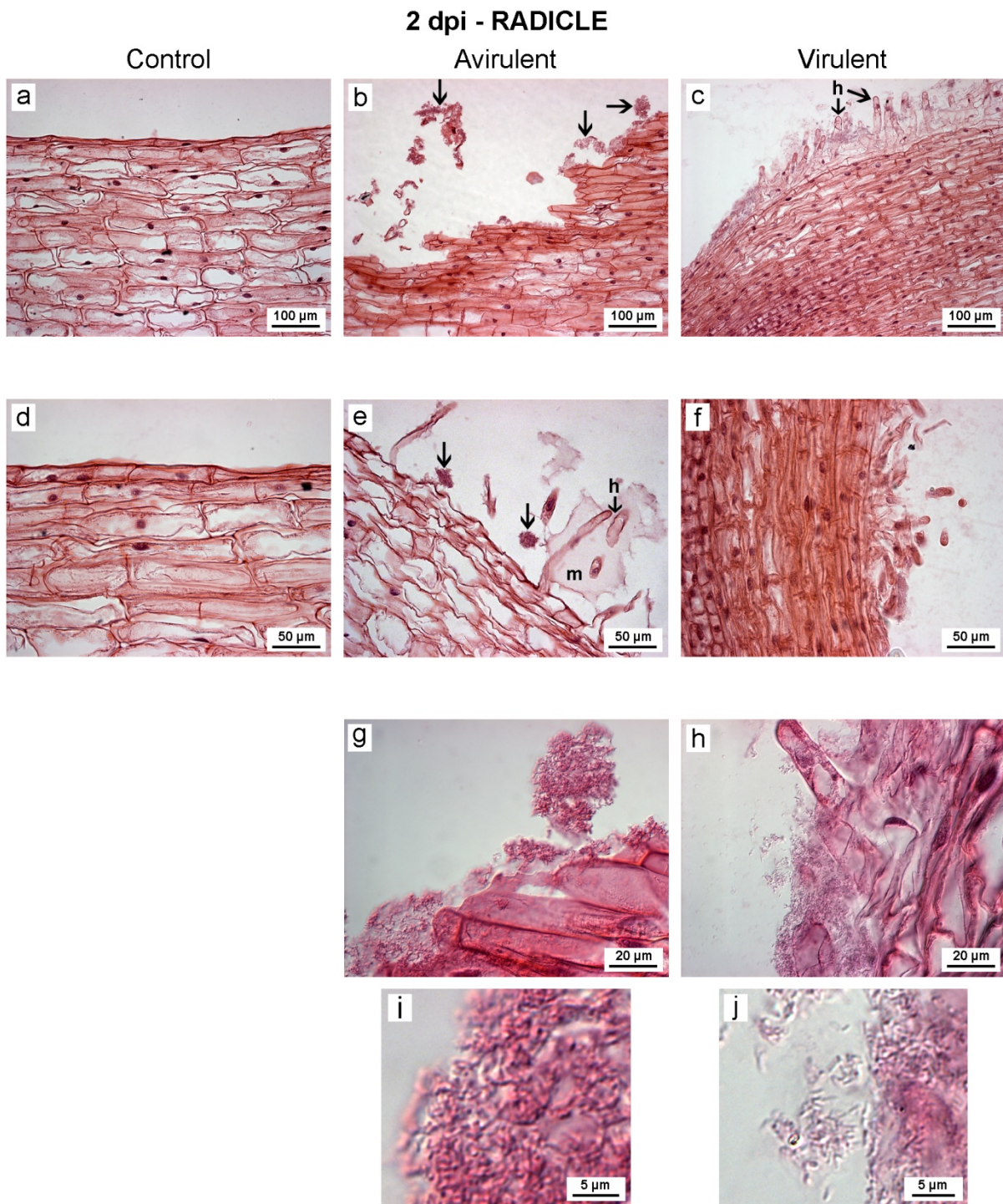


Figure 3.28 Light micrographs of longitudinal sections of *P. sativum* radicle without or with *R. fascians* avirulent strain 589 and virulent strain 602 at 2 d post inoculation (dpi). a) and d) Control radicle. b) Avirulent 589 strain infected radicle with *R. fascians* (arrowed). c) Virulent 602 strain infected radicle with *R. fascians* on the surface of the radicle showing a biofilm of bacteria along the root hairs. h=root hairs. e) Avirulent 589 strain infected radicle with *R. fascians* clumped together (arrowed) and mucilage-like covering over some of the root hairs. h=root hairs, m=mucilage-like material. f) Virulent 602 strain infected radicle with *R. fascians* on the surface of the radicle. g) Avirulent 589 strain infected radicle with *R. fascians* on the surface of the radicle and as a clump. h) Virulent 602 strain infected radicle showing the spread of bacteria on the radicle and root hairs. i) Enlargement of part of (g) highlighting the grouping of bacteria which are cocci-like. j) Enlargement of part of (h) detailing the small, rod shaped bacteria.

5 dpi - SEED COAT

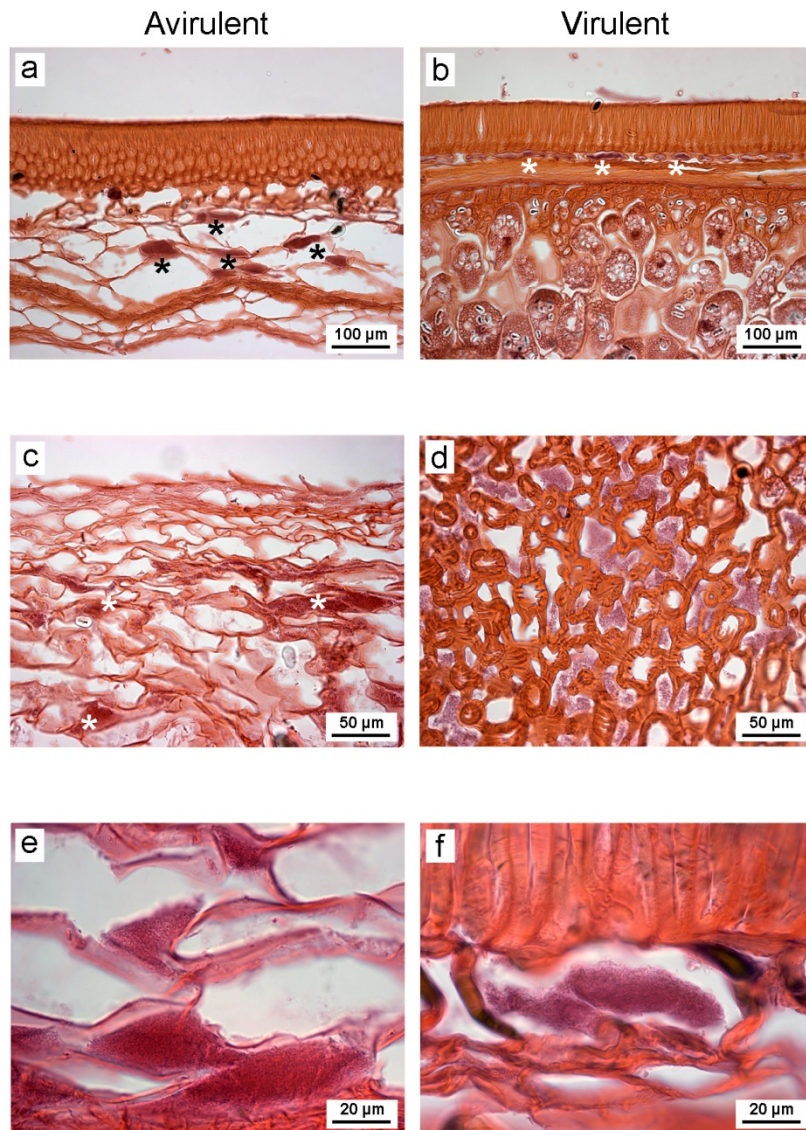


Figure 3.29 **Light micrographs of transverse section of *P. sativum* seed coat tissue with *R. fascians* avirulent strain 589 and virulent strain 602 at 5 d post inoculation (dpi).** a) Avirulent strain 589 infected cotyledon with *R. fascians* clearly visible in clumps (asterisks) in the parenchyma layer of the seed coat. b) Virulent 602 strain infected cotyledon with *R. fascians* (asterisks) in the intercellular spaces of the subepidermal layer of the seed coat. c) Avirulent 589 strain infected seed coat with *R. fascians* (asterisks) in parenchyma layer of seed coat. d) Virulent 602 strain infected cotyledon with *R. fascians* apparent as purple-staining material spread throughout the intercellular spaces of the subepidermal layer of the seed coat. e) Avirulent 589 infected seed coat with *R. fascians* in the parenchyma layer of the seed coat in significant clumps. f) Virulent 602 strain infected cotyledon with *R. fascians* in the intercellular space of the subepidermal layer of the seed coat.

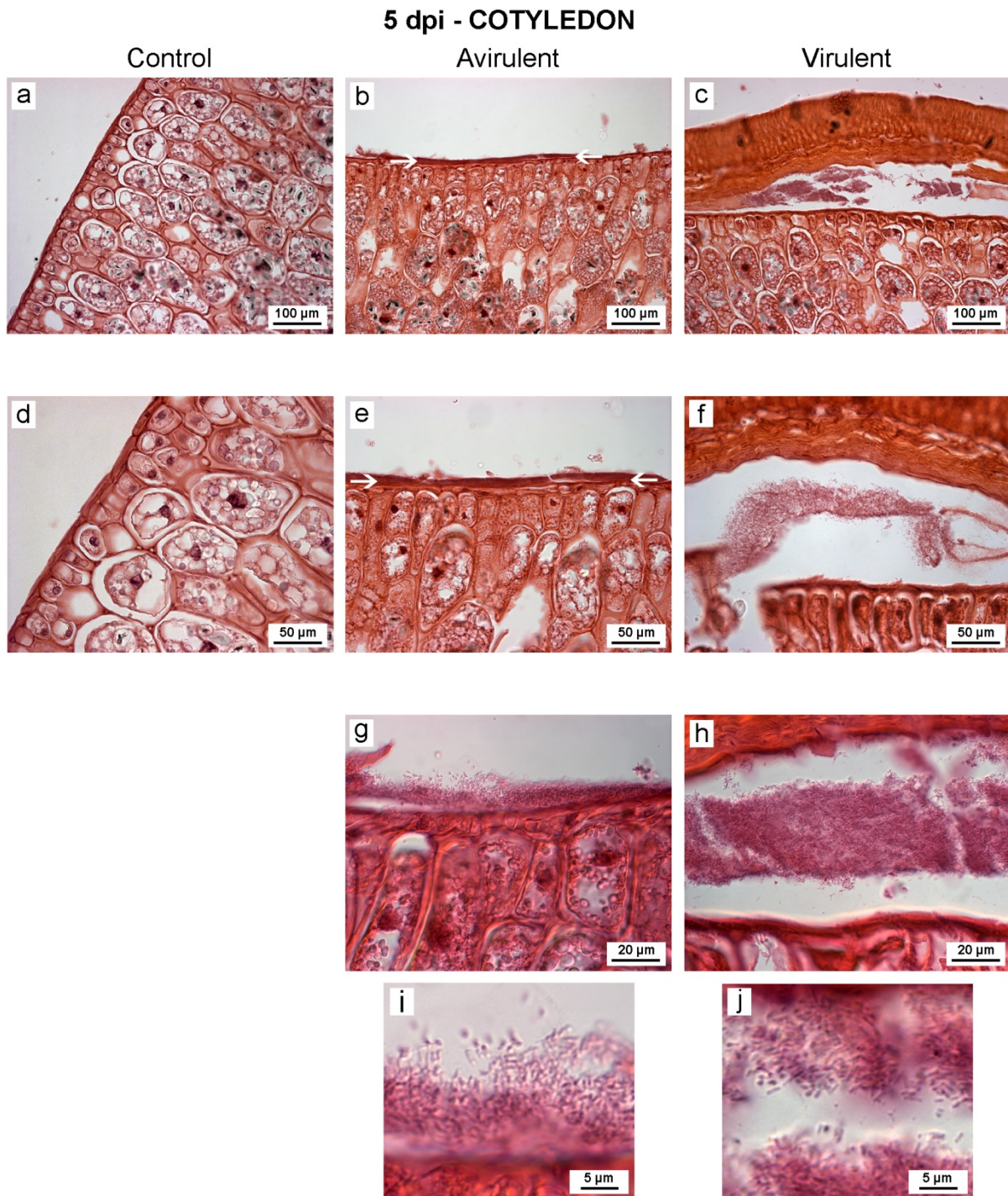


Figure 3.30 Light micrographs of transverse section of *P. sativum* cotyledon tissue without or with *R. fascians* avirulent strain 589 and virulent strain 602 at 5 d post inoculation (dpi). a) and d) Control cotyledon. b), e) and g) Avirulent strain 589 infected cotyledon with a thin layer of *R. fascians* (white arrows) covering the surface of the cotyledon. c) Virulent strain 602 infected cotyledon with the accumulation of *R. fascians* between the endosperm and cotyledon. f) Virulent strain 602 infected cotyledon with *R. fascians* spread between endodermis and cotyledon. h) Virulent strain 602 infected cotyledon with *R. fascians* as significant mat in the region between the endodermis and the cotyledon. i) Enlargement of (g), detailing the rod shape of the bacteria. j) Enlargement of the virulent bacteria illustrating the rod-shaped nature of *R. fascians*.

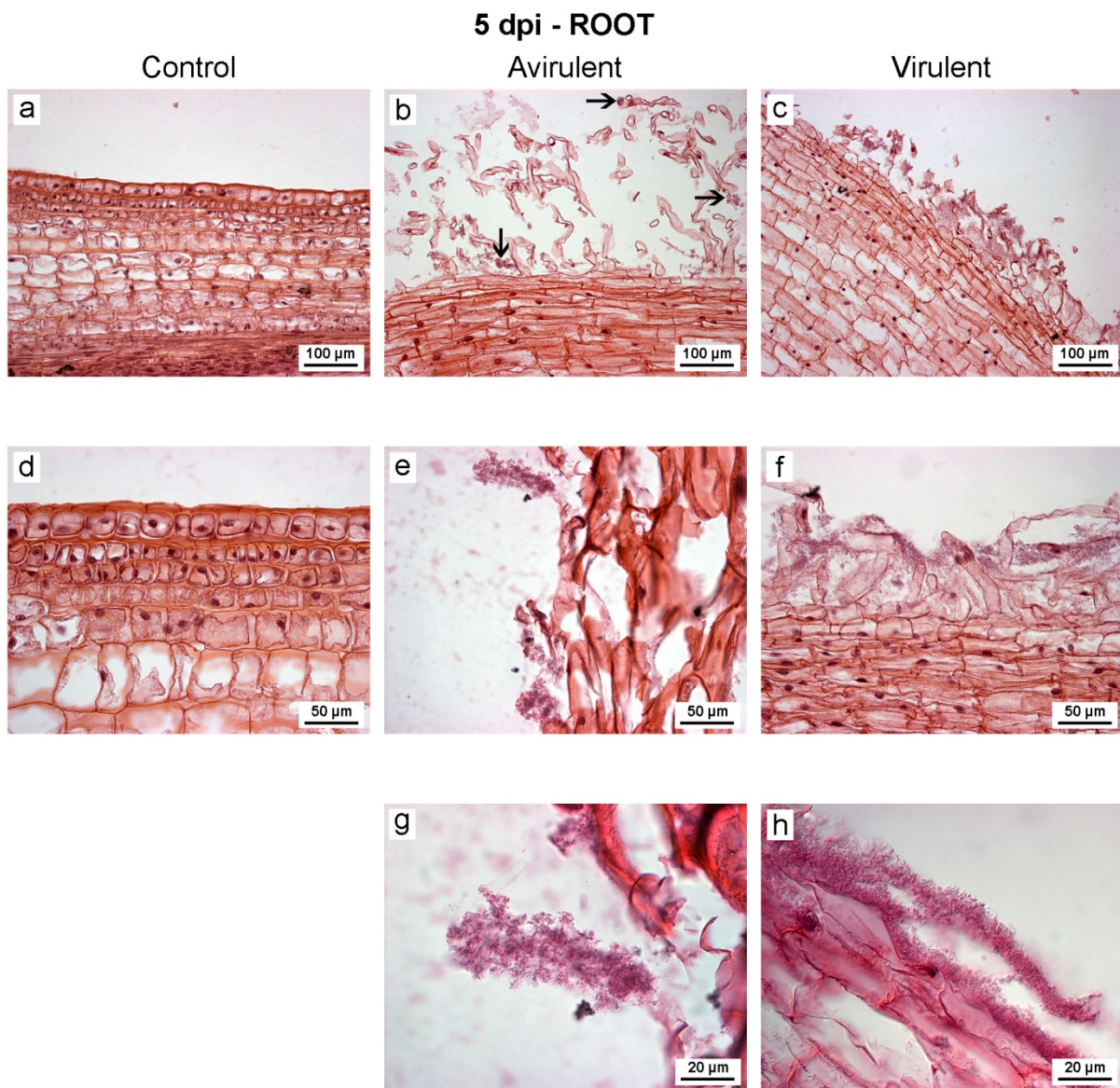


Figure 3.31 Light micrographs of longitudinal section of *P. sativum* root tissue without or with *R. fascians* avirulent strain 589 and virulent strain 602 at 5 d post inoculation (dpi).

a) and d) Control root. b) Avirulent strain 589 infected root with patches of *R. fascians* (arrowed) among the root hairs and near the surface of the root. c) Virulent strain 602 infected root with *R. fascians* spread on the root epidermis and root hairs. e) Avirulent strain 589 infected root with *R. fascians* grouped together on the root epidermis. f) Virulent strain 602 infected root with *R. fascians* entangled amongst the root hairs. g) Avirulent strain 589 infected root with a clump of *R. fascians*. h) Virulent strain 602 infected root showing detail of *R. fascians* spread over the region of the root epidermis.

The colonisation by the virulent strain 602 of cotyledon, shoots and roots appeared to be high compared to avirulent strain 589 infected tissues at 9 dpi (Figures 3.33, 3.34 and 3.35). The avir-roots showed the characteristic feature of small rods clumped together on the root epidermis (Figure 3.34 g and i), which was observed even at 15 dpi (Figure 3.37 b). The bacteria were seen from 9 dpi on the epidermis of shoot surface of the avir-shoots, whereas the typical symptom of multiple shoot with abundant bacterial colonisation was obvious in vir-shoots (Figure 3.35).

The prominence of *R. fascians* avirulent strain 589 as clumps of cells in the subepidermal layer and the parenchyma layer of the seed coat was still evident at 15 dpi (Figure 3.36 a and c). In comparison, the virulent 602 strain was mainly present as a widespread accumulation of cells (Figure 3.35 d and f). The increased mass of colonisation by the *R. fascians* avirulent strain 589 was apparent on the roots and shoots from 15 dpi, but the virulent strain 602 exhibited more diffuse spread of bacteria on roots and as well as noticeable bacterial colonisation on the surface of multiple shoots (Figures 3.37 and 3.38).

For the *R. fascians* avirulent strain 589, the most extensive colonisation was observed on 25 dpi roots and shoots (Figures 3.40 and 3.41) and also on 35 dpi roots (Figure 3.43). The colonisation of *R. fascians* in the vir-cots was apparent from 15 to 35 dpi, whereas in the avir-cots it became more significant in later stages of growth mainly at 25 and 35 dpi (Figures 3.39 and 3.42). Both virulent and avirulent infected tissues showed profuse *R. fascians* colonies on the surface of the root at 15 dpi (Figure 3.37).

By 35 dpi, both strains of *R. fascians* appeared to colonise the shoot tissue in a similar manner (Figure 3.44). Higher magnification revealed both the virulent and avirulent bacterial strains were mainly rod-shaped forms, but cocci-like morphology was also apparent (e.g. Figures 3.25 h, 3.33 i, 3.34 i, 3.37 j). Where the bacteria were densely clumped or grouped together, it was sometimes difficult to differentiate the two forms, except around the periphery of the colonies (e.g. Figures 3.30 i, 3.35 i and j, 3.41 g and h).

5 dpi - SHOOT

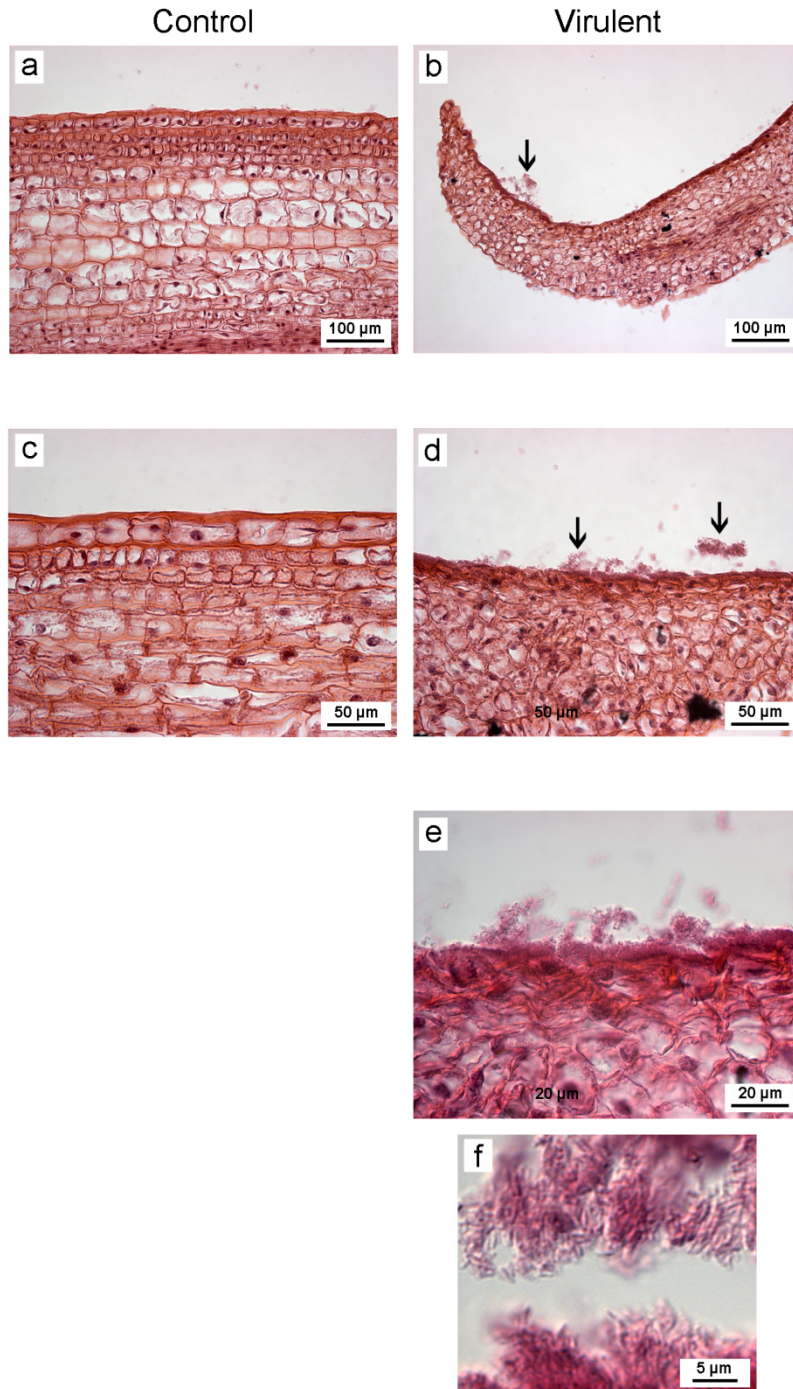


Figure 3.32 Light micrographs of longitudinal section of *P. sativum* shoot tissue without or with *R. fascians* avirulent strain 589 and virulent strain 602 at 5 d post inoculation (dpi).

a) and c) Control shoot. b) Virulent strain 602 infected shoot with *R. fascians* as patches near and on the epidermis of the shoot (arrowed). d) Virulent strain 602 infected shoot with *R. fascians* on the epidermis of the shoot.(arrowed) e) Virulent strain 602 infected shoot with *R. fascians* on the surface of the shoot epidermis. f) Enlargement of *R. fascians* virulent strain 602 revealing rod and V-shaped forms of bacteria.

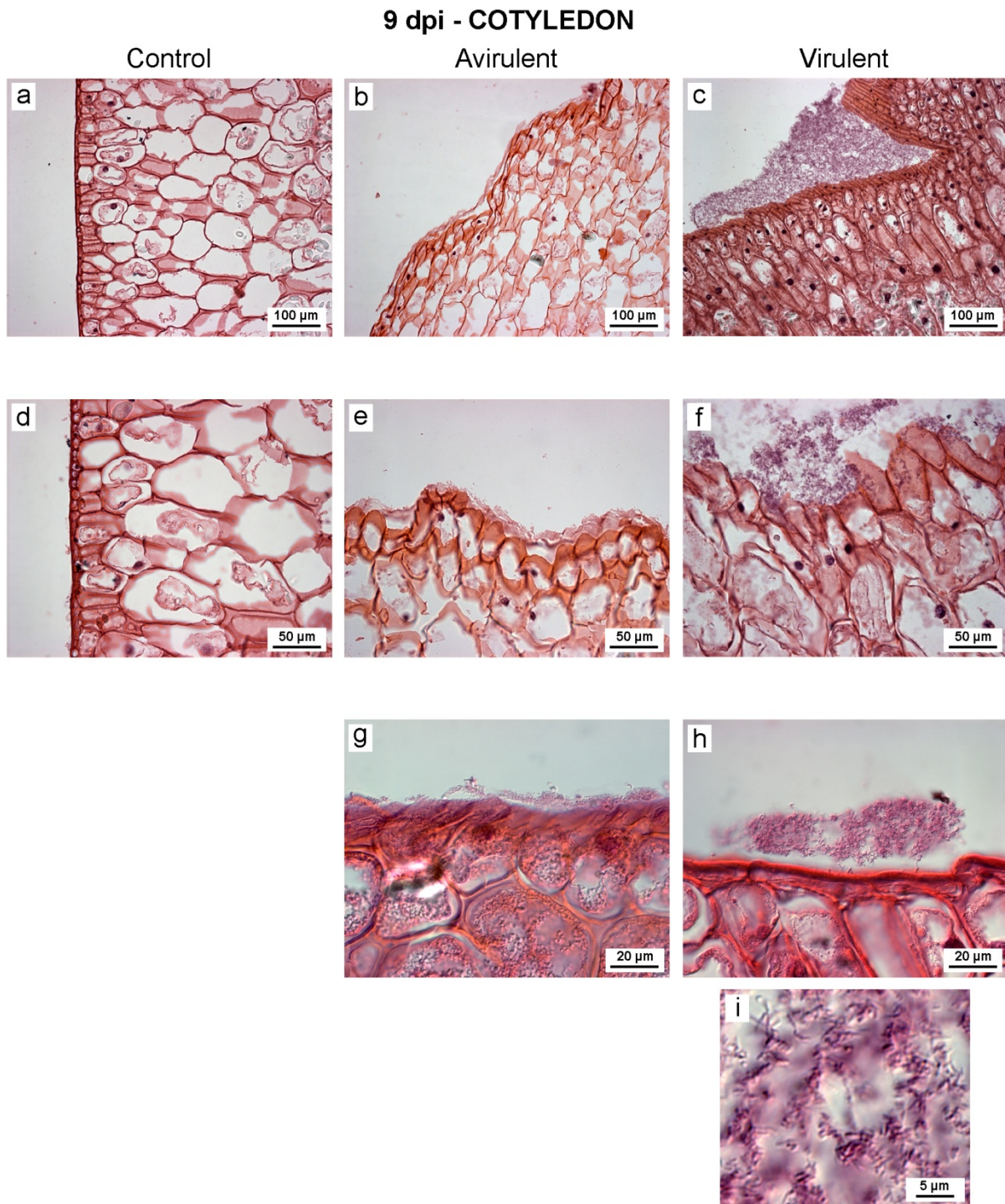


Figure 3.33 **Light micrographs of transverse section of *P. sativum* cotyledon tissue without or with *R. fascians* avirulent strain 589 and virulent strain 602 at 9 d post inoculation (dpi).** a) and d) Control cotyledon. b), e) and g) Avirulent strain 589 infected cotyledon with *R. fascians* spread all over the surface of the cotyledon. c) and f) Virulent strain 602 infected cotyledon with dense patch of *R. fascians* on the surface of the cotyledon. h) Virulent strain 602 infected cotyledon with *R. fascians* near the surface of the cotyledon. i) Enlargement of *R. fascians* strain 602 infected cotyledon illustrating small rod shaped bacteria.

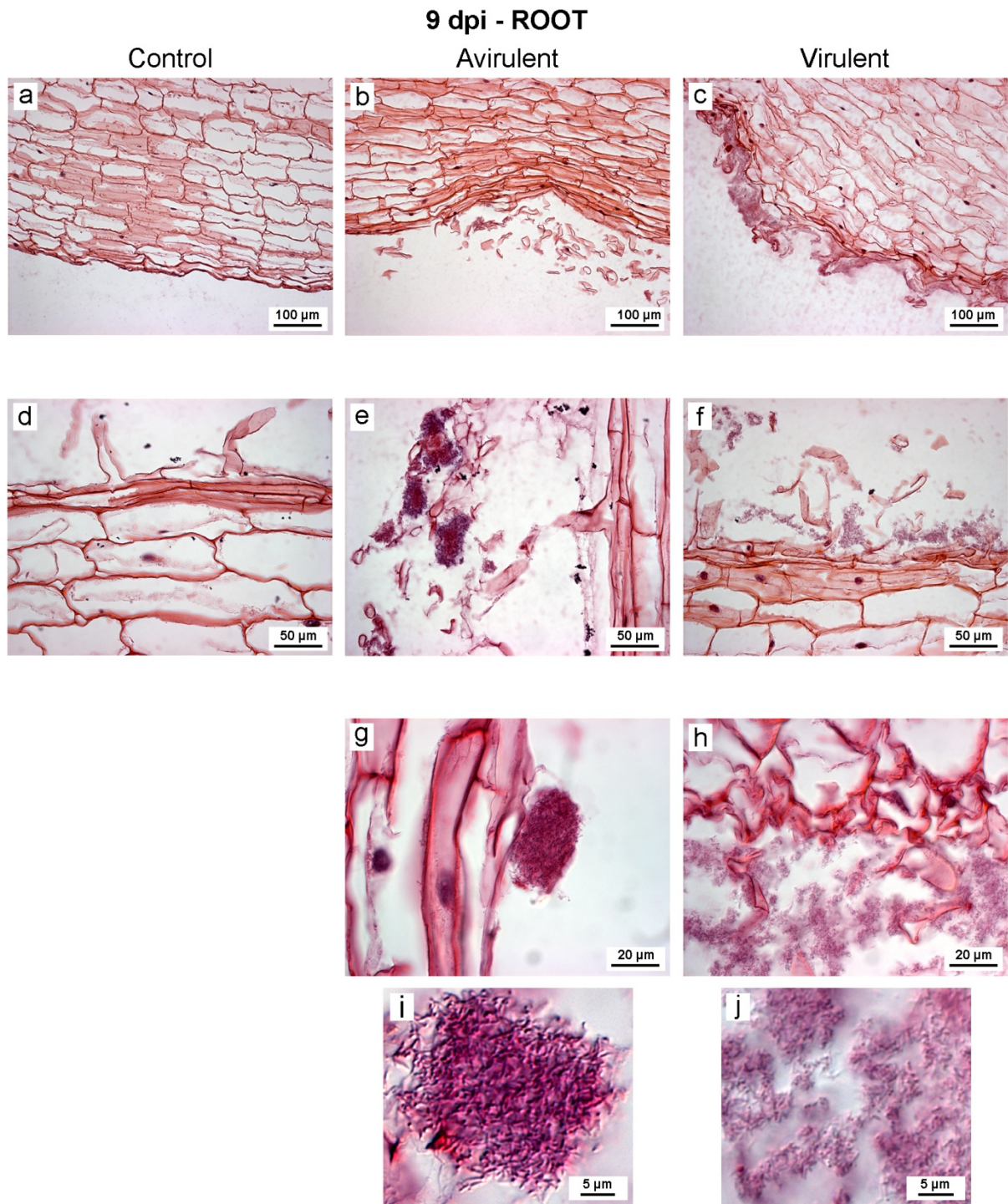


Figure 3.34 Light micrographs of longitudinal section of *P. sativum* root without or with *R. fascians* avirulent strain 589 and virulent strain 602 at 9 d post inoculation (dpi).

a) and d) Control root. b) Avirulent strain 589 infected root with *R. fascians*. c) Virulent strain 602 infected root with *R. fascians* on the surface of the root which showing wide-spread colonisation of the bacteria. e) Avirulent strain 589 infected root with *R. fascians* distinctly clumped together amongst the root hairs. f) Virulent strain 602 infected root with *R. fascians* on the surface of the root. g) Avirulent 589 strain infected root with *R. fascians* as a dense clump of bacteria on the surface of the root. h) Virulent 602 strain infected root showing spread of bacteria on the root and sloughing of root tissues i) Enlargement of *R. fascians* strain 589 clearly revealing its rod-shaped form. j) Enlargement of part of (h) highlighting *R. fascians*.

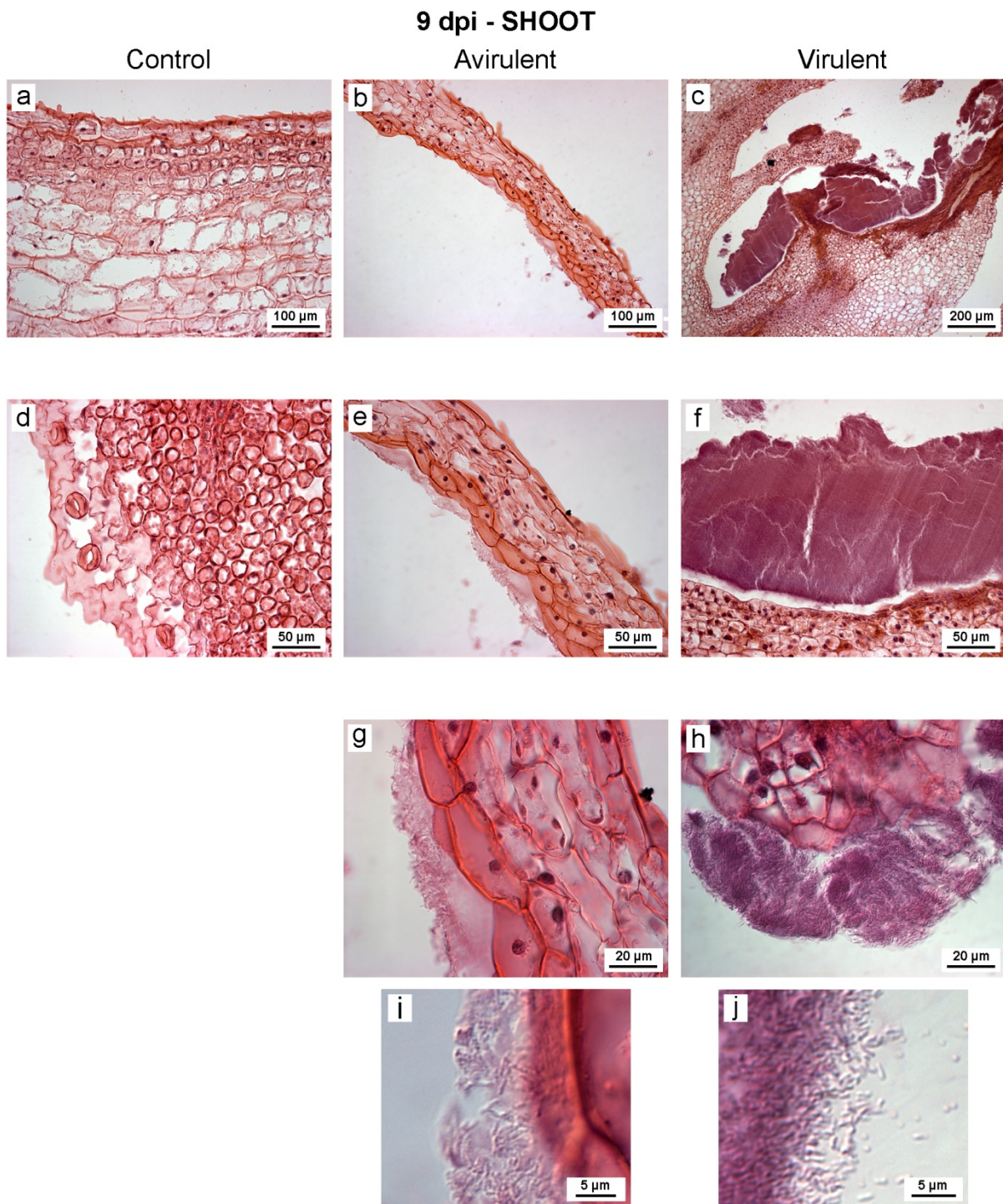


Figure 3.35 **Light micrographs of longitudinal section of *P. sativum* shoot without or with *R. fascians* avirulent strain 589 and virulent strain 602 at 9 d post inoculation (dpi).** a) and d) Control shoot. b), e) and g) Avirulent strain 589 infected growing shoot tip with *R. fascians* spread on the shoot surface. c) Low magnification of multiple shoot tips of a virulent strain 602 infected shoot with *R. fascians* present on the surface as an extensive dense mass. (Note: scale bar = 200 μm). f) Higher magnified view of part of (c) showing the distinct purple-stained virulent strain 602 infected shoot with distinct purple-stained *R. fascians* accumulated on the shoot surface. g) Avirulent strain 589 infected shoot with *R. fascians* on the surface shoot epidermis. h) Virulent strain 602 infected shoot showing spread of bacteria on the shoot epidermis. i) Enlargement of *R. fascians* avirulent strain 589 infected shoot clearly recognisable rod-shaped *R. fascians*. j) Enlarged view of prominent *R. fascians* virulent strain 602 rods.

15 dpi - COTYLEDON

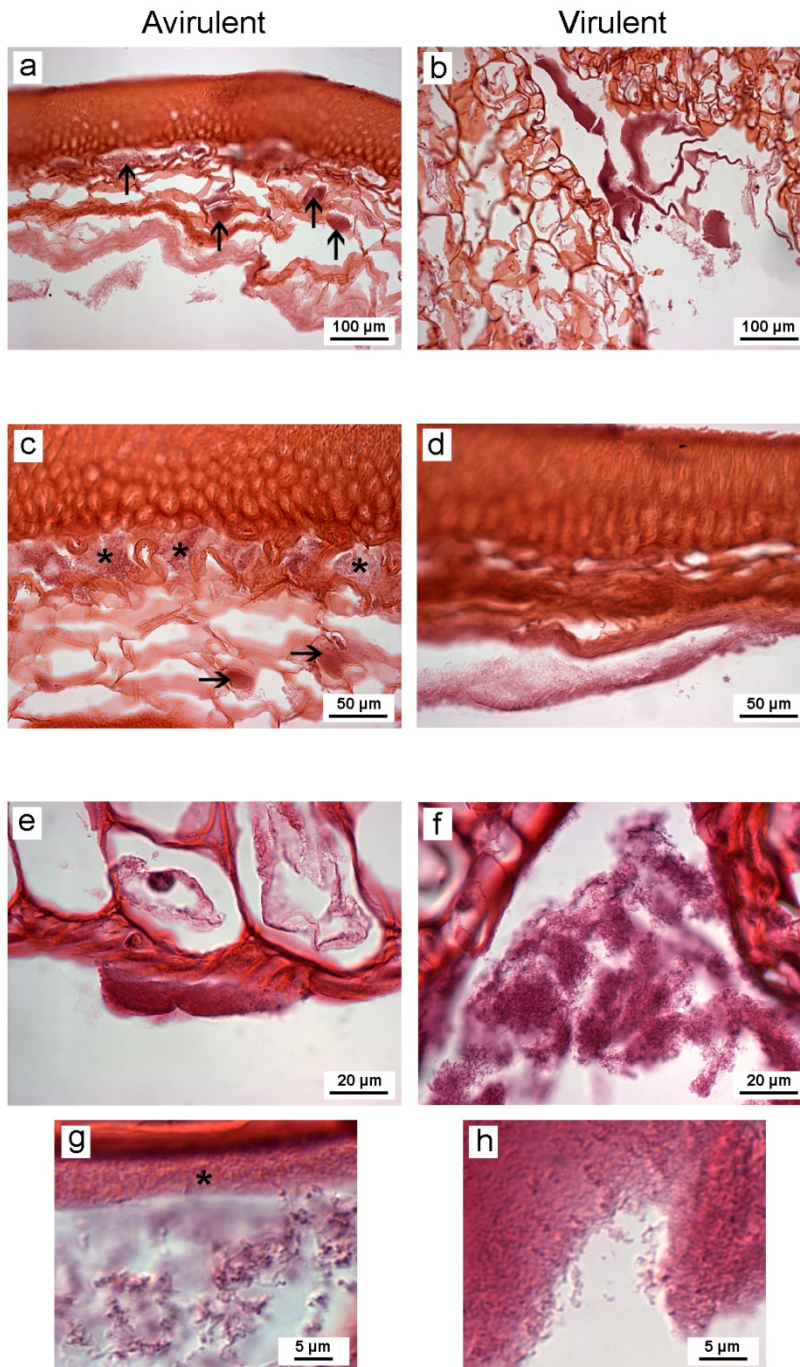


Figure 3.36 **Light micrographs of transverse section of *P. sativum* cotyledon tissue without or with *R. fascians* avirulent strain 589 and virulent strain 602 at 15 d post inoculation (dpi).** a) Avirulent strain 589 infected cotyledon with various clumps of *R. fascians* (arrows) on the parenchyma layer and in the intercellular spaces of the subepidermal of the seed coat. b) Virulent strain 602 infected cotyledon with dense spread of *R. fascians* between the cotyledon and root initiation. c) Avirulent strain 589 infected cotyledon showing extensive colonisation of *R. fascians* (asterisks) in the intracellular spaces of subepidermal layer and as clumps on the parenchyma layer of the seed coat. d) Virulent strain 602 infected cotyledon having a layer of *R. fascians* spread underneath seed coat. e) Avirulent strain 589 infected cotyledon with dense patch of *R. fascians* on the surface of the cotyledon. f) Virulent strain 602 infected cotyledon showing dense spread of *R. fascians* between the cotyledon and root arising area. g) Enlargement of avirulent strain 589 infected cotyledon illustrating *R. fascians* as thick layer on the cotyledon surface (asterisk) and more diffused peripherally. h) Enlargement of *R. fascians* virulent strain 602.

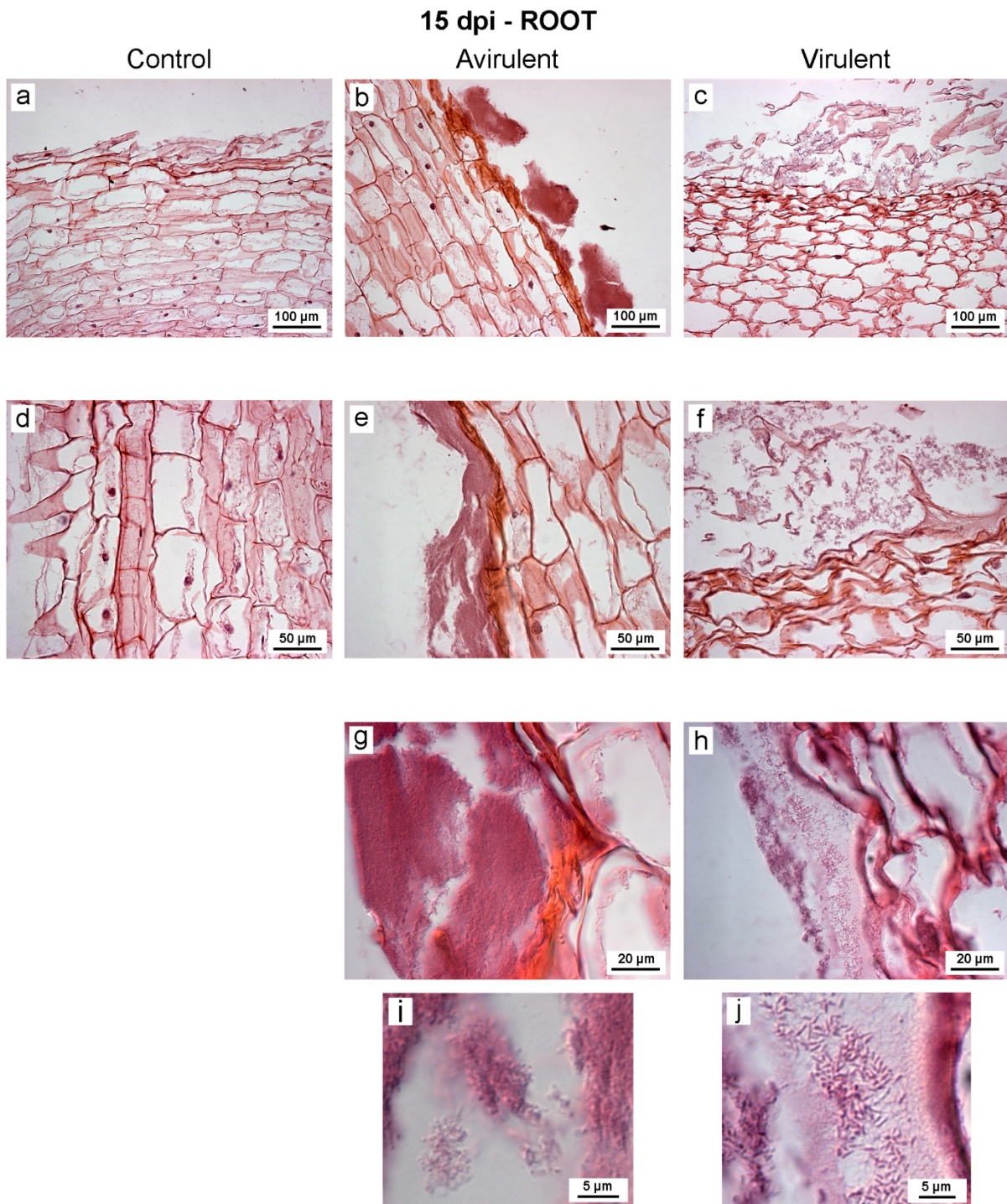


Figure 3.37 Light micrographs of longitudinal section of *P. sativum* root without or with *R. fascians* avirulent strain 589 and virulent strain 602 at 15 d post inoculation (dpi).

a) and d) Control root. b) Avirulent strain 589 infected root with distinct dense clumps of *R. fascians* on the root surface. c) Virulent strain 602 infected root with *R. fascians* on the surface of the root showing wide diffuse spread of the bacteria. e) Avirulent strain 589 infected root with *R. fascians* spread on the root surface. f) Virulent strain 602 infected root with *R. fascians* on the root. g) Avirulent strain 589 infected root with *R. fascians* as a dense mass of bacteria on the surface of the root. h) Virulent strain 602 infected root showing diffuse spread of bacteria on the root i) Enlargement of *R. fascians* strain 589. j) Enlargement of part of (h) with *R. fascians* strain 602 as clearly distinct rods.

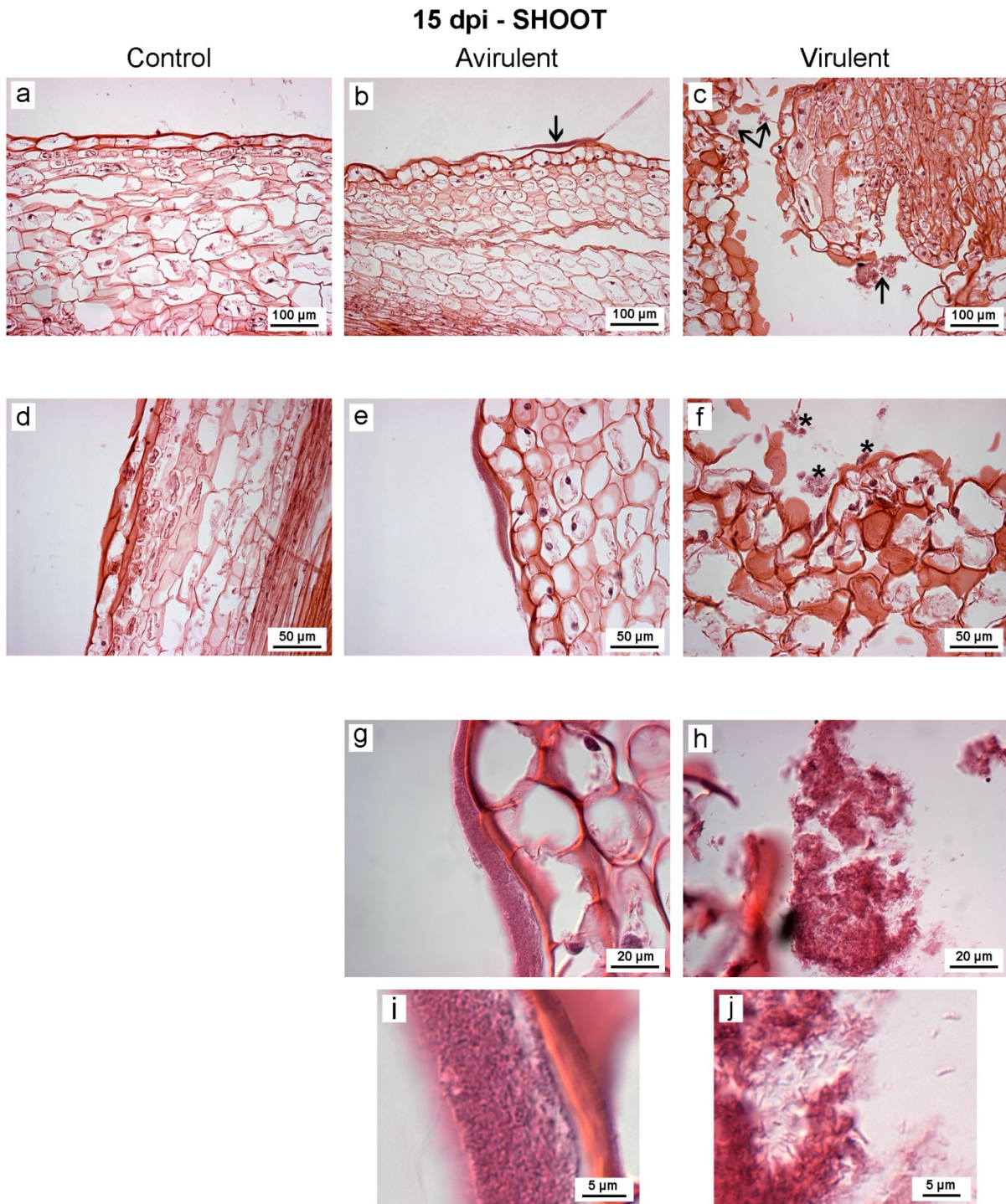


Figure 3.38 Light micrographs of longitudinal section of *P. sativum* shoot without or with *R. fascians* avirulent strain 589 and virulent strain 602 at 15 d post inoculation (dpi).

a) and d) Control shoot. b) Avirulent strain 589 infected shoot with *R. fascians* as thin layer (arrowed) on the shoot surface. c) Virulent strain 602 infected shoot with multiple shoots (ms) with patches of *R. fascians* (arrowed). e) and g) Avirulent strain 589 infected shoot with *R. fascians* as a layer on shoot surface. f) Virulent strain 602 infected shoot with pockets of *R. fascians* (asterisks) accumulated on the surface of the damaged shoot. h) Virulent strain 602 infected shoot showing a cluster of bacteria on the shoot surface. i) Enlargement of part of (g) detailing the distinct dense layer of *R. fascians* avirulent strain 589 on the shoot surface. j) Enlargement of part of (h) highlighting rod-shaped *R. fascians*.

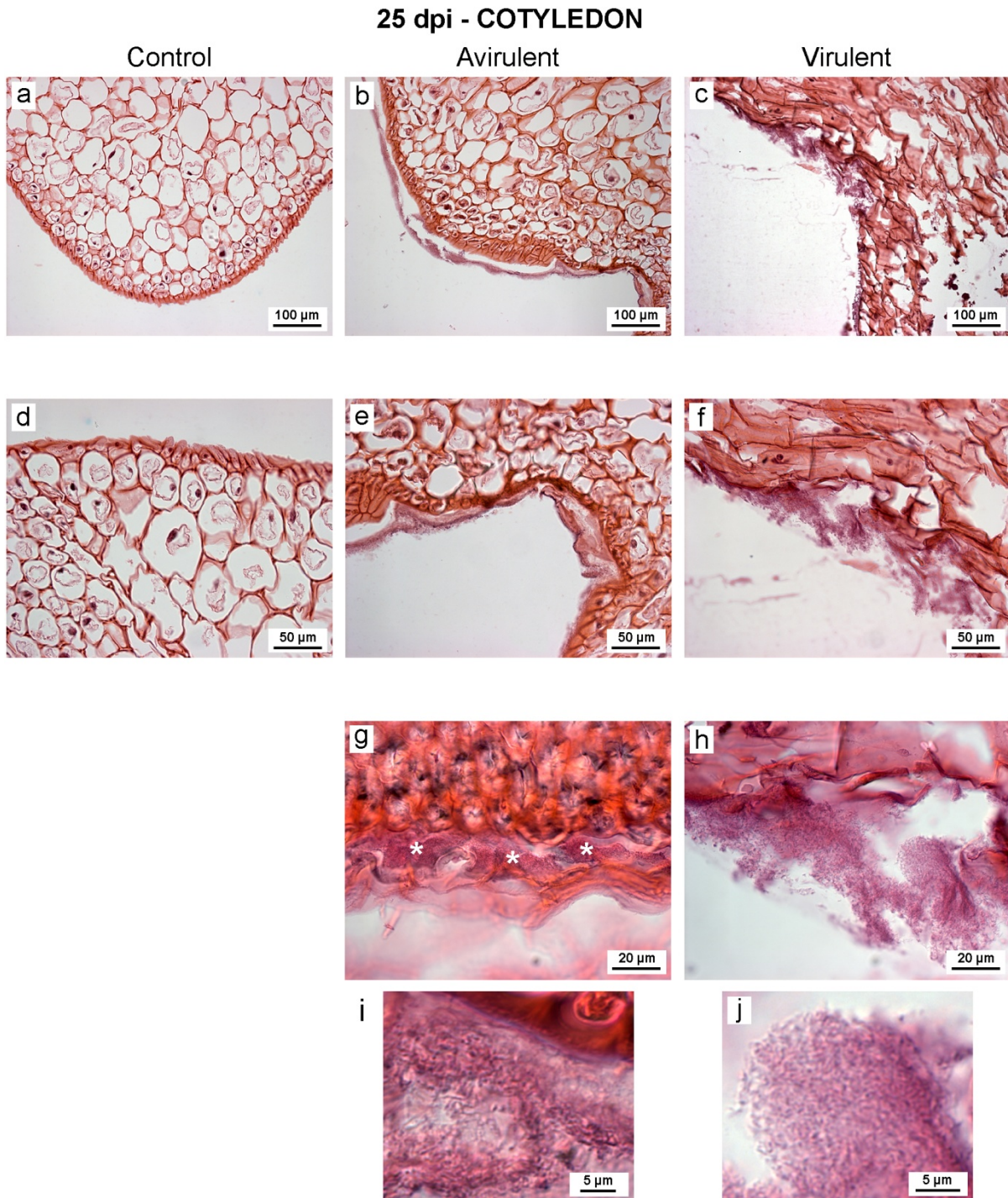


Figure 3.39 Light micrographs of transverse section of *P. sativum* cotyledon tissue without or with *R. fascians* avirulent strain 589 and virulent strain 602 at 25 d post inoculation (dpi).

a) and d) Control cotyledon. b) Avirulent strain 589 infected cotyledon with a thin layer of *R. fascians* along the cotyledon surface. c) Virulent strain 602 infected cotyledon showing the presence of purple-stained *R. fascians* and also the cotyledon cells damaged due to the pathogen. e) Avirulent strain 589 infected cotyledon with *R. fascians* showing bacterial colonisation on the surface of the cotyledon. f) Virulent strain 602 infected cotyledon with cells affected due to *R. fascians* along the surface. g) Avirulent 589 strain infected cotyledon with mass spread of *R. fascians* (asterisks) underneath the palisade layer of the seed coat. h) Virulent strain 602 infected cotyledon with *R. fascians* on the cotyledon surface. i) Enlargement of avirulent strain 589 cotyledon highlighting clear presence of the bacteria. j) Enlargement of part of (h) with *R. fascians*.

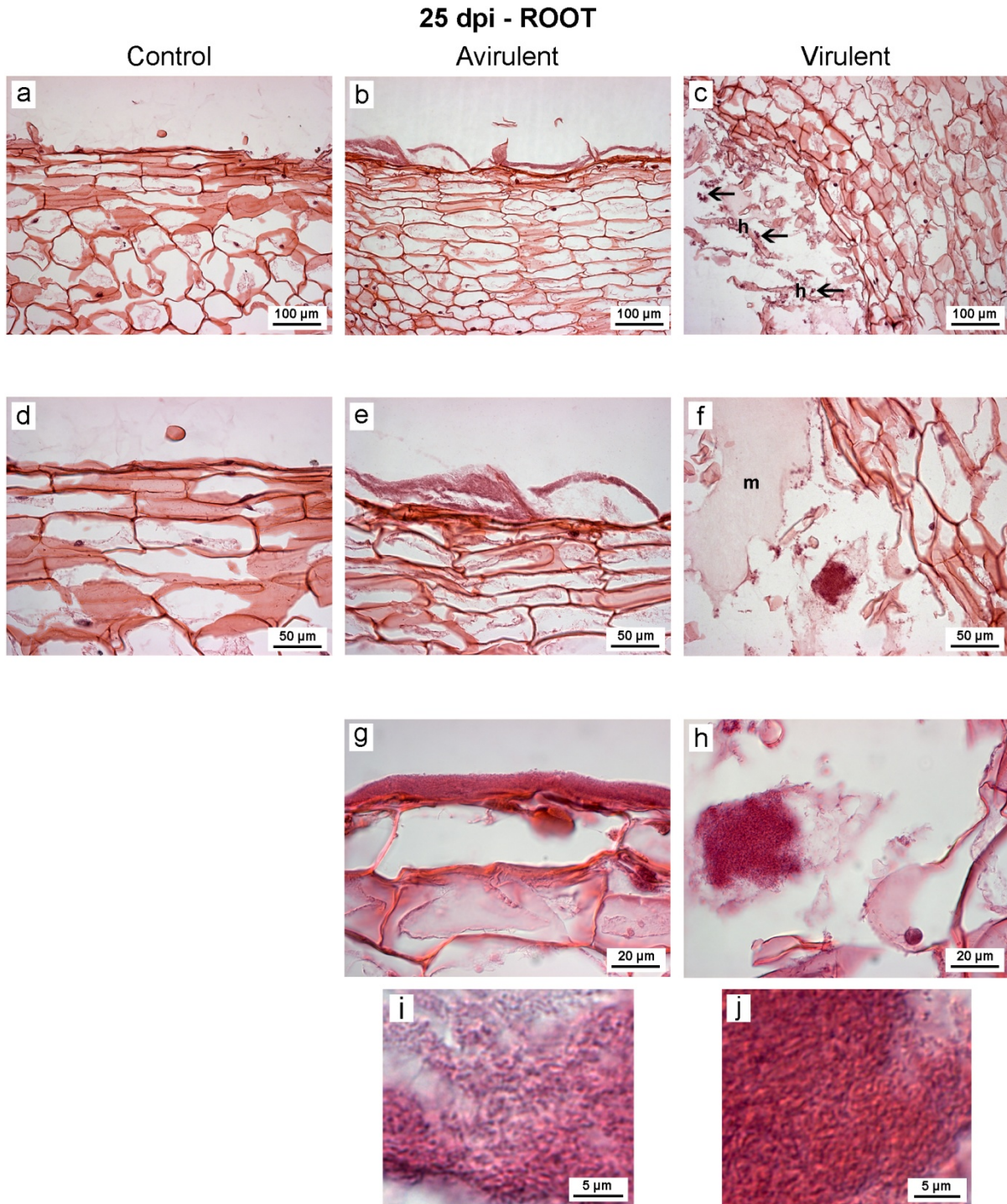


Figure 3.40 Light micrographs of longitudinal section of *P. sativum* root without or with *R. fascians* avirulent strain 589 and virulent strain 602 at 25 d post inoculation (dpi).

a) and d) Control root. b) and e) Avirulent strain 589 infected root with distinct presence of *R. fascians* on the root epidermis. c) Virulent strain 602 infected root with small pockets of *R. fascians* (arrowed) amongst the root hairs (h). f) Virulent strain 602 infected root with *R. fascians* as a patch (arrowed) with presence of mucilage-like material (m). g) Avirulent strain 589 infected root with *R. fascians* as a dense mass of bacteria on the surface of the root epidermis. h) Magnification of virulent 602 strain showing grouping of bacteria.

i) Enlargement of *R. fascians* strain 589. j) Enlargement of part of (h) with *R. fascians* strain 602 as cocci-like and rods forms.

25 dpi - SHOOT

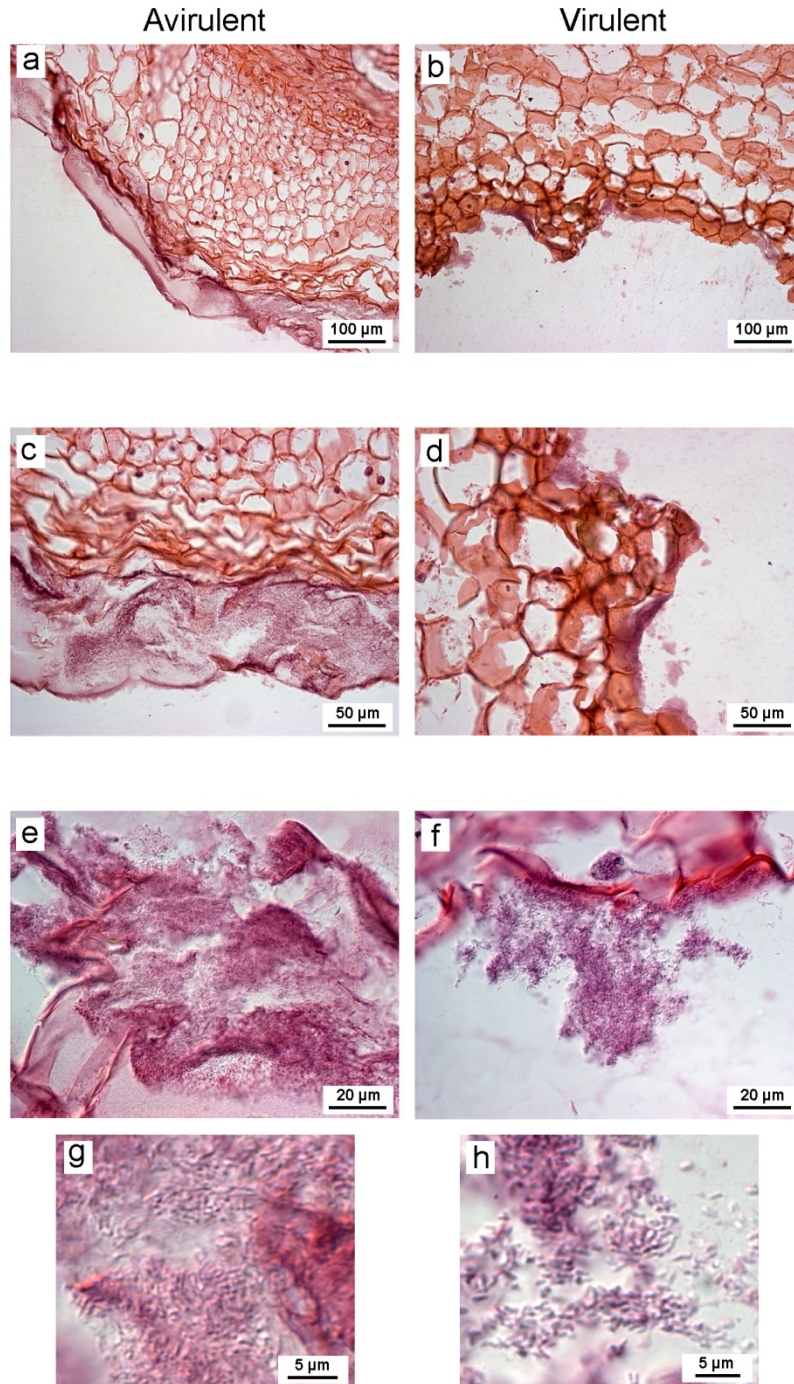


Figure 3.41 **Light micrographs of longitudinal section of *P. sativum* shoot without or with *R. fascians* avirulent 589 strain and virulent 602 strain at 25 d post inoculation (dpi).** a) Avirulent 589 strain infected shoot with *R. fascians* as thick extensive layer on the shoot. b) Virulent 602 strain infected shoot having patches of *R. fascians*. c) Avirulent 589 strain infected shoot with *R. fascians* as a widespread layer on shoot surface. d) Virulent 602 strain infected shoot with pockets of *R. fascians* accumulated on the surface of the damaged shoot. e) Avirulent 589 strain infected shoot with clear thick mass of *R. fascians* f) Virulent 602 strain infected shoot showing a cluster of bacteria on the shoot surface. g) Enlargement of (e) with distinct dense mat of *R. fascians* avirulent 589 strain highlighting rods. h) Enlargement of (f) with *R. fascians*.

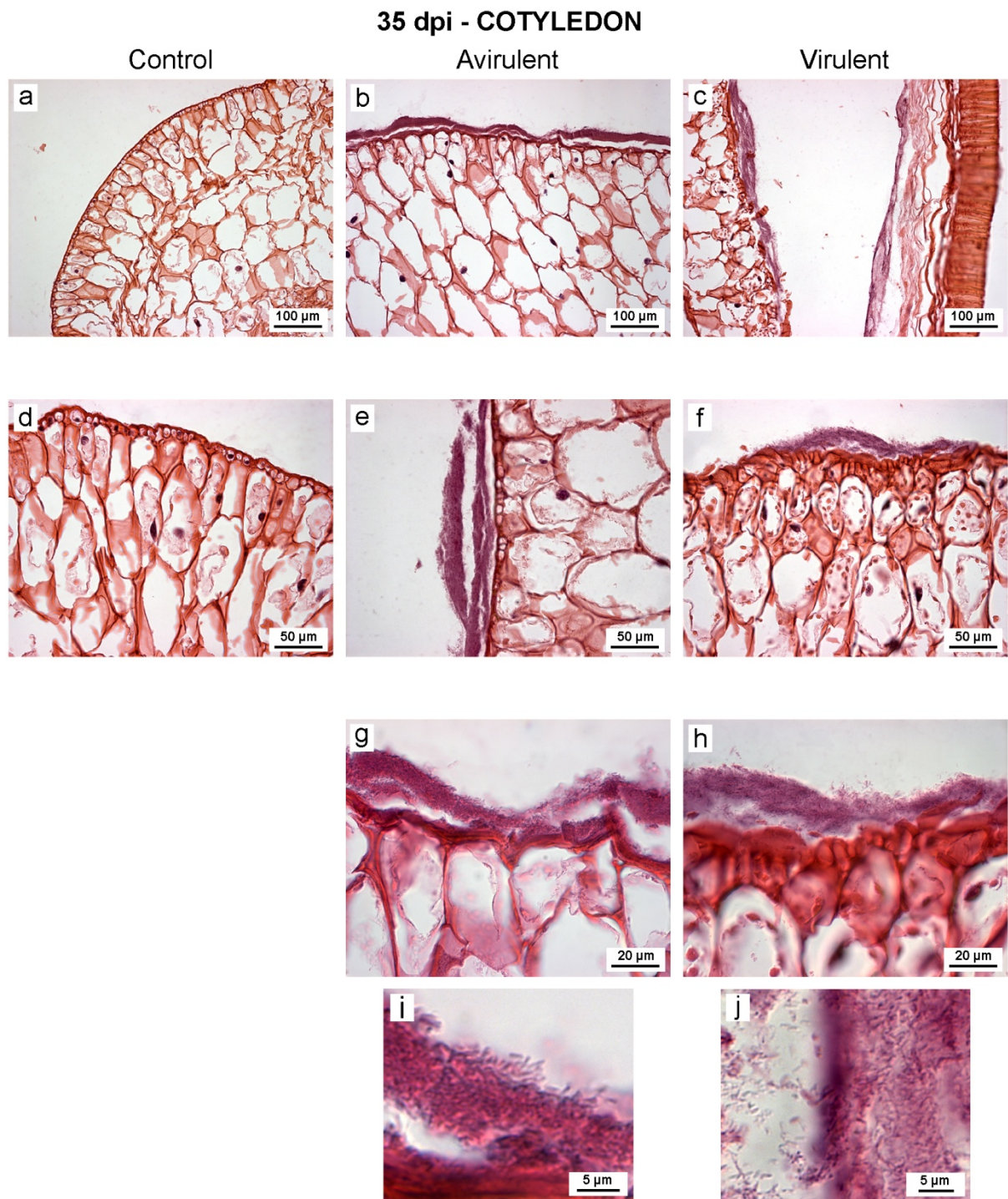


Figure 3.42 **Light micrographs of transverse section of *P. sativum* cotyledon tissue without or with *R. fascians* avirulent strain 589 and virulent strain 602 at 35 d post inoculation (dpi).** a) and d) Control cotyledon. b) e) and g) Avirulent strain 589 infected cotyledon with a layer of *R. fascians* on the cotyledon surface. c) Virulent strain 602 infected cotyledon showing the presence of *R. fascians* on cotyledon (cot) surface and underneath the parenchyma layer of the seed coat (sc). f) Virulent 602 strain infected cotyledon with *R. fascians*. h) Higher magnification of (f) with *R. fascians* on the cotyledon surface. i) Enlargement of a part of (g) illustrating the dense colonisation of avirulent strain 589. j) Enlargement of *R. fascians* virulent strain 602 showing variable densities of the bacteria.

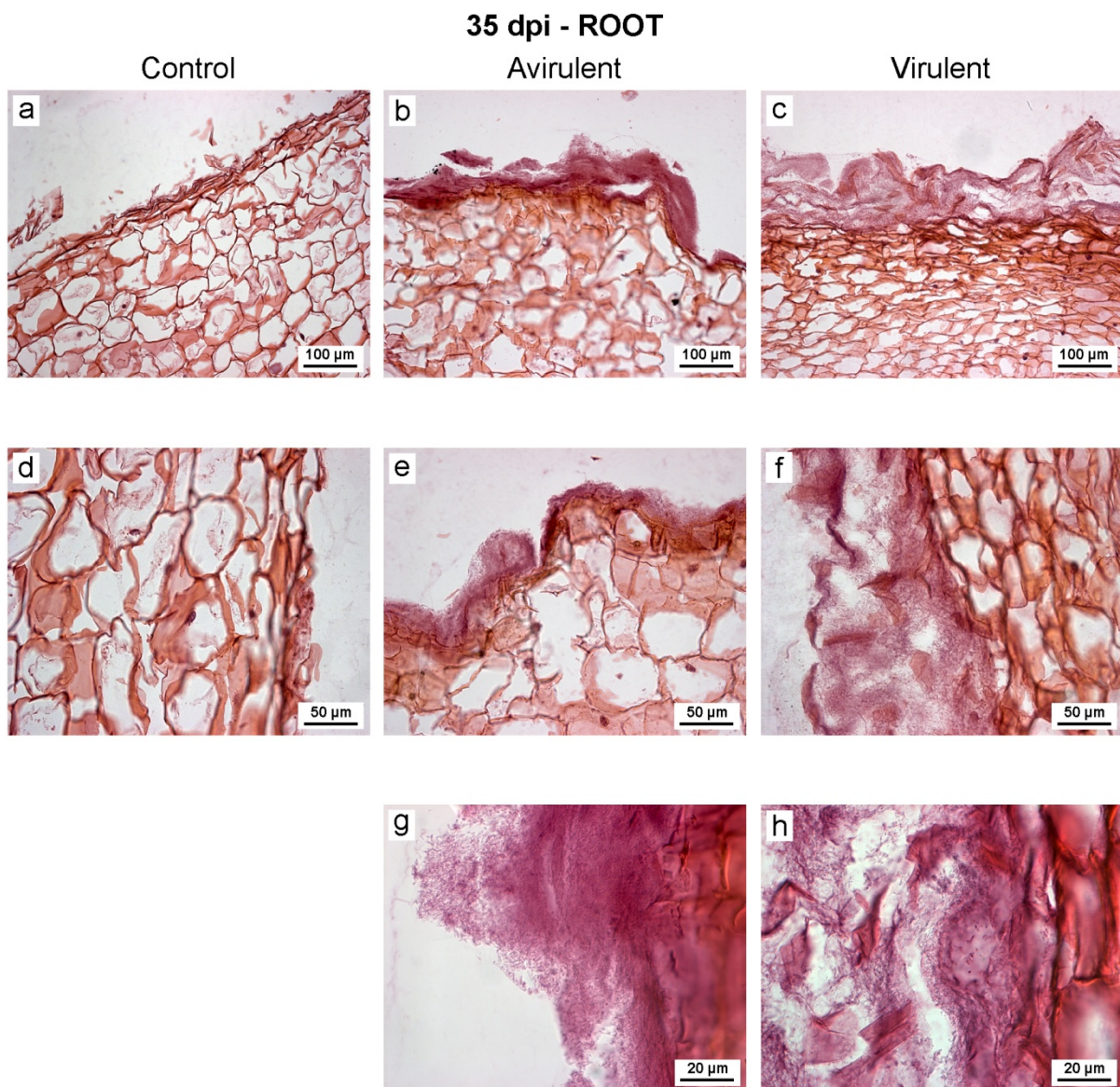


Figure 3.43 **Light micrographs of longitudinal section of *P. sativum* root without or with *R. fascians* avirulent strain 589 and virulent strain 602 at 35 d post inoculation (dpi).** a) and d) Control root. b) and e) Avirulent strain 589 infected root with distinct layer of *R. fascians* on the root surface. c) and f) Virulent strain 602 infected root with *R. fascians* on the surface of the root showing wide disperse extend of the bacteria. e) Avirulent 589 strain infected root with *R. fascians* showing extensive colonisation of the bacteria on the root epidermis. g) Avirulent strain 589 infected root with *R. fascians* as a dense mass of bacteria on the root epidermis. h) Virulent 602 strain infected root showing spread of bacteria and sloughed of the root surface.

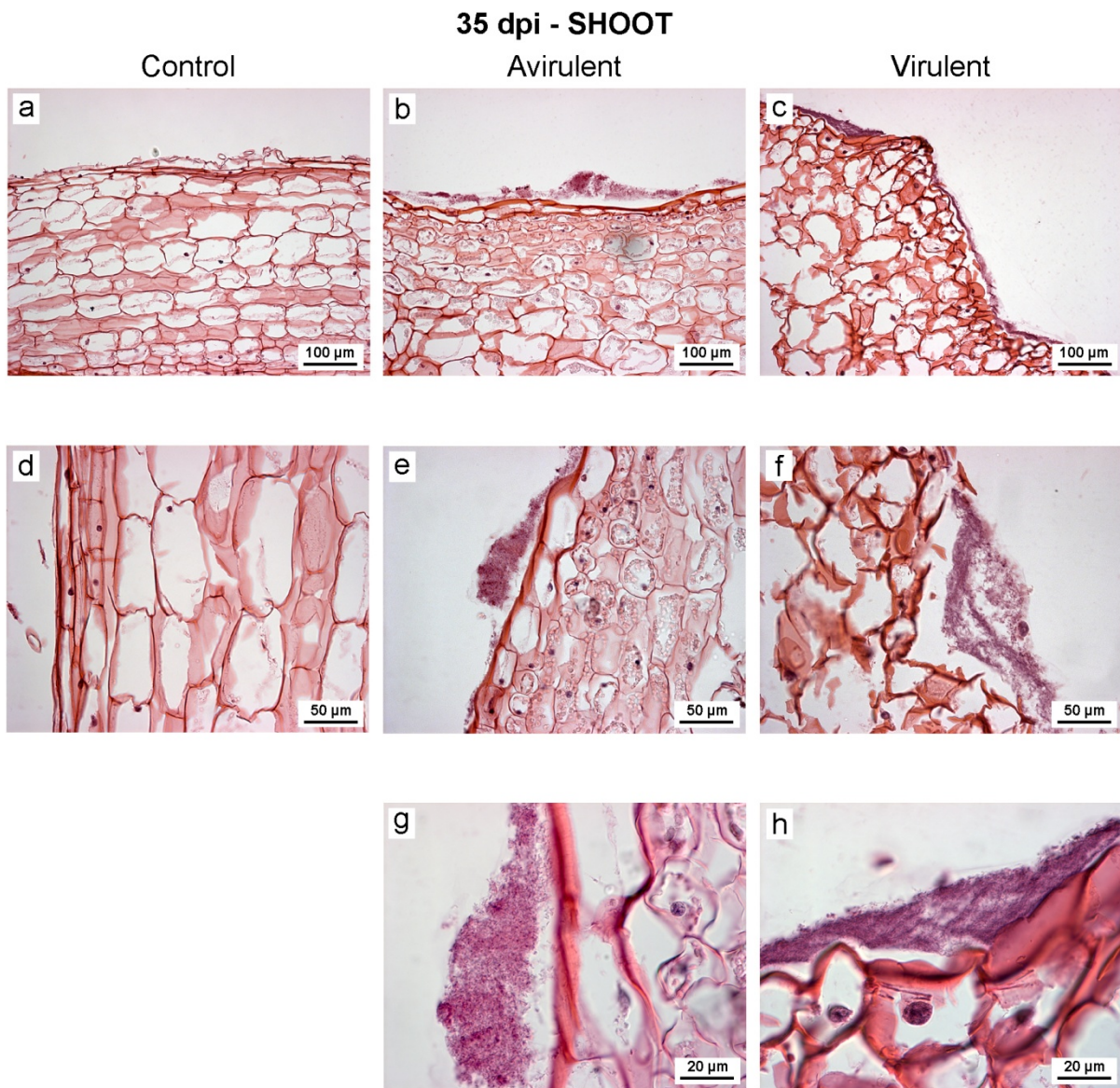


Figure 3.44 Light micrographs of longitudinal section of *P. sativum* shoot without or with *R. fascians* avirulent strain 589 and virulent strain 602 at 35 d post inoculation (dpi). a) and d) Control shoot . b) and e) Avirulent strain 589 infected shoot with *R. fascians* visible on the shoot surface. c) and f) Virulent strain 602 infected shoot with *R. fascians* coating on the shoot epidermis. g) High magnification of (e) showing avirulent strain 589 *R. fascians*. h) Virulent strain 602 infected shoot with bacteria on the shoot surface.

3.4 Discussion

The association of cytokinin genes *fasD* and *fasE* with virulence of *R. fascians* has been extensively studied in recent years (Crespi et al. 1992, 1994, Stange et al. 1996, Galis et al. 2005b). It was not until the advent of pulsed-field gel electrophoresis (which was required to mobilise large linear plasmid into gels) was a large linear plasmid positively correlated with virulence in multiple wild-type strains (Stange et al. 1996). Initially, in this project the primers designed by Galis et al. (2005b) were used to detect *fasD* and *fasE* genes in the 36 strains previously classified by Stange et al. (1996) as avirulent or virulent. Stange et al. (1996) had revealed that there is a strong relationship between the presence of the large linear plasmid and cytokinin genes *fasD* and *fasE*. The initial work carried out in this project for screening the presence of both *fasD* and *fasE* genes confirmed the integrity of the 18 strains previously confirmed as virulent by Stange et al. (1996).

Pertry et al. (2010) showed the presence of the LOG gene within the Fas locus through the study of the activity of FasF (LOG) and FasF-MBP (maltose binding protein) on 5'-monophosphate (5'-MP) nucleosides of iP, tZ and cZ. These three substrates were converted into their respective free bases implying that FasF potentially contributes to the bioactive cytokinin bases produced by *R. fascians* during their interaction with the host (Pertry et al. 2010). The *RfIPT*, *RfCKX* and *RfLOG* genes were isolated with the primers designed to discriminate their sequences from the host pea *IPT*, *CKX* and *LOG* genes sequences. This study showed, as expected, that *RfLOG* as well as *RfIPT* and *RfCKX* were present on the 18 wild-type virulent strains of *R. fascians*.

The phylogenetic analysis of the *RfIPT*, *RfLOG* and *RfCKX* revealed bifurcation between the plant and microbe cytokinin genes based on their protein sequences. The analysis showed that the isolated *RfIPT*, *RfLOG* and *RfCKX* protein sequences grouped with *R. fascians* (D188) *FasD*, *FasE* and *FasF*, strongly supporting the likelihood that the primers were designed specifically. The *R. fascians* (G+ve) *IPT* grouped with other actinomycetes, *R. fascians* D188 *FasD* and *Streptomyces turgidiscabies* (G+ve) *FasD*, and all the other gram negative gall-forming bacteria formed a separate group. This may be due to substrate specificity and pathology differences between actinomycetes and gram negative bacteria.

In the case of RfIPT phylogenetic tree analysis, the homologous sequences between plant AtIPT2, LjIPT5 and *Streptomyces turgidiscabies* FasD and *R. fascians* FasD reveal that plants have IPPT (tRNA isopentenyltransferase) activity as in AtIPT2 (Takei et al. 2001). The alignment is similar to the tree observed by Golovko et al. (2002), where *A. thaliana* IPPT had sequence similarities with the prokaryote *Saccharomyces cerevisiae* and they suggested that higher eukaryotes IPPTs were derived from the microbial IPPTs.

The RfCKX formed a clade with the other gram positive actinomycetes and *Legionella pneumophila* (G-ve) FasE separated out from the main group. There are differences in sequences of FasD and FasE between the actinomycete (G+ve) microbes and other gram negative bacteria but this phenomenon was not seen in the case of FasF proteins.

The phylogenetic analysis also confirms sequence differences between the isolated RfIPT, RfLOG and RfCKX and the isolated pea IPT, LOG and CKX proteins. This strongly supports the likelihood that the primers were correctly designed to discriminate the *R. fascians* and pea cytokinin (*IPT*, *LOG* and *CKX*) gene sequences, an essential of this project.

The morphological changes upon infection of *P. sativum* plants with the virulent strain 602 of *R. fascians* gave rise to a distinct phenotype. Phenotypic changes occurred by 5 dpi. The abnormal growth parameters of plants inoculated with *R. fascians* strain 602 were multiple branching of shoots with thicken shoot bases, stunted growth of plants, thickening of primary roots and the cotyledons were bright green, intact and robust until 40 dpi. These morphological changes were similar to the observations made by Eason et al. (1995) in *P. sativum* cv. Novella infected with virulent strains of *R. fascians*. Eason et al. (1995) noted that pea plants infected with virulent strains of *R. fascians* exhibited swollen shoot bases, short fleshy stems, small leaves and swollen short primary roots at 14 days after inoculation. Manes et al. (2004) observed upon infection by *R. fascians* through vacuum-infiltration of two-week-old *A. thaliana* multiple phenotypic alterations after three weeks of infection including overall stunted and bushy appearance, increased number of rosettes and inflorescences, abnormal flowers and serrated/ curly leaves. In this project, the pea plants infected with *R. fascians* displayed phenotypic symptom malformation as seen in other plant species, including shoot proliferation and stunted growth. Root growth in pea plants infected with the virulent strain 602 was altered: the main roots increased in thickness with inhibition

of secondary root growth, resulting in reduced root growth. Similar root morphological changes were observed in pea and *A. thaliana* plants inoculated with *R. fascians* (Eason, 1993, Vereecke et al., 2000, Vereecke et al., 2003). The effects of *R. fascians* on host plants including shoot proliferation and inhibition of root growth along with delayed senescence were considered to be typical cytokinin-like effects (Davies, 1995, Vereecke et al., 2000). Manes et al. (2004) proposed that the morphological abnormalities (symptoms) observed in *A. thaliana* infected with *R. fascians* was likely to be due to the colonisation and associated production of specific signals by the bacteria.

The control plants and plants infected with the avirulent strain 589 showed signs of senescence by 40 dpi but not in plants infected with the virulent strain 602, agreeing with the suggestion of Vereecke et al. (2000) that infected plants outlive the non-infected plants. The phenotypes of plants infected by *R. fascians* virulent strain 602 had a bushy appearance with a delay in the senescence of leaves compared to the control and the avirulent strain 589 infected plants. Cytokinins are key components in the regulation of plant senescence (Nam, 1997). The delay in senescence of leaves due to infection of *R. fascians* strain 602 may be due to the elevated cytokinin in the infected plants as the exogenous application of cytokinin or the ectopic expression of IPT gene decreases senescence of plant tissues (Noodén et al., 1997).

The number of bacteria in pea infected by *R. fascians* was measured as colony forming units (CFUs) which showed quantitative differences between the *R. fascians* avirulent 589 and virulent 602 strains. But the difference in colonisation between whole plant (without bleach) and internal (with bleach) was not particularly great. This may be due to improper surface sterilisation of the infected pea plants. The surface sterilisation procedure may have needed standardisation in terms of time of exposure to bleach as surface:area ratio increases with the growth of plant. The procedure followed was possibly not adequate to remove the surface organism effectively so the interior population level was shown to be greater than might have been expected from the literature (Cornelis et al. 2001).

Both virulent 602 and avirulent 589 strain formed both epiphytic and endophytic colonies. This result is similar to the observations made by Cornelis et al. (2001) and Vereecke et al. (2002) in tobacco infected with *R. fascians* strains D188 and D188-5 or mutant X798.

Vereecke et al. (2002) showed that the mutant X798 can colonise tobacco plants as well as the pathogenic *R. fascians* strain D188. The differences between the number of bacteria in plants infected with virulent strain 602 was not higher than the plants infected with avirulent strain 589 at all stages of growth with both bleach and without bleach treatment. Similar result was observed by Cornelis et al. (2001) that there was no differences between the virulent strain D188 and the avirulent strain D188-5 in the number of CFUs per gram of plant tissue without bleach treatment in tobacco plants infected with *R. fascians* strains D188 or D188-5 after three to four weeks post infection. The *R. fascians* avirulent strain 589 bacterial number increased with time but initially (from 4 hpi to 11 dpi) the microbial load was lower compared to the virulent strain 602 indicating that the virulent bacteria grows more rapidly with the host at the time of infection compared to the avirulent strain 589.

The visualisation of *R. fascians* using scanning electron microscopy (SEM) revealed the epiphytic characteristics of *R. fascians* colonisation pattern on the host, morphology of the bacteria and the spread of the bacteria on the host surface. There was little difference between the *R. fascians* virulent strain 602 and avirulent strain 589 surface colonisation on pea cotyledons, shoots, leaves and roots but there were differences in the morphology of both the bacteria on different parts of the plant at different time points. Initially, at the time of infection, the virulent strain 602 was more prevalent on the cotyledon compared to the avirulent strain 589. Both the strains mainly possessed similar morphological characteristics with a few exceptions. With the growth of both the host and the bacteria, *R. fascians* exhibited more elongated interconnected rods and, by end of the experiment, the bacteria appeared as hyphal-like structures forming a mesh covering the organs, especially on the cotyledons and roots. This indicates that *R. fascians* are both rods and hyphae which are a known characteristics of an actinomycete. As reported by Cornelis et al. (2001) for *Arabidopsis* and tobacco plants, the variable morphology of *R. fascians* was explained to be pleomorphic by Miller et al. (1980) cited from Cornelis et al. (2001) which was noticed when the bacterium was grown in a synthetic medium. On pea cotyledons, shoots and roots the bacteria often appeared to be encased in a raised mesh-like coating which may be similar to the slime layer mentioned by Cornelis et al. (2001) which covered the virulent D188 bacteria on the leaf surface of tobacco. Francis et al. (2012) reported the formation of an epiphytic biofilm of *R. fascians* on a tobacco leaf infected with virulent strain D188.

The similarity of the colonisation pattern on the surface of the pea tissues by both *R. fascians* virulent and avirulent strains shows that this feature may not be related to symptom development. This was also observed in the leaf tissue of tobacco plants by Manes et al. (2001) and they stated that both virulent and non-virulent strains have comparable surface colonisation capacities. The fact that the continuous presence of *R. fascians* is needed for symptom persistence (Lacey 1936) was supported by the SEM analysis where *R. fascians* was shown to be present on the surface of all the symptomatic tissues until the last stage of sampling. Similarly the avirulent strain 589 was present on the surface of the pea organs until the end of the experiment. However, in other reports it appears that an avirulent strain was not observed along with virulent strains at different time points (Cornelis et al., 2001, Goethals et al., 2001b, Manes et al., 2001). So the observation that both strains were present as epiphytic populations on the host may be novel.

To examine the epiphytic as well as endophytic colonisation by *R. fascians* in infected *P. sativum*, light microscopy was performed. The bacteria were only ever visualised on the surface of plant tissues except for the endophytic population which was present within the seed coat. The purple-stained bacteria were readily distinguishable from plant tissues which were stained red using haematoxylin-eosin stain (H&E). Endophytic bacterial colonisation in the infected cotyledons, roots and shoots was not observed even with the use of differential interference contrast (DIC) microscopy techniques. There was some evidence of disruption and sloughing of the epidermal layer of root and shoot cells in plants infected with the virulent strain 602 compared to the control and the avirulent strain 589 infected plants. Even though the microscopic studies with infected *A. thaliana* and *N. tabacum* showed the presence of *R. fascians* in the intercellular spaces of inner cell layers of leaves and the inflorescence (Cornelis et al. 2001, Manes et al. 2004), no such results were observed in the cotyledon, roots and shoots of pea in this study. Cornelis et al. (2001) used *Arabidopsis* and tobacco seedling infection, dipping, vacuum infiltration of *R. fascians* two-day old culture for their SEM analysis. Studies so far have found fewer bacteria in the interior than on the surface of hosts such as sweet pea seedlings (Lacey 1936), *A. thaliana* and *N. tabacum* (Cornelis et al. 2001). The review by Goethals et al. (2001) reported that *R. fascians* only occasionally invades the epidermal cell layer and most of the bacteria are present on the exterior of the fasciations. So, the surface bacteria may produce signals to initiate the symptom development as suggested by Cornelis et al. (2001) describing the model of

infection for the production of the leafy gall. Internal colonisation by *R. fascians* was demonstrated by Cornelis et al. (2001) using *in situ* hybridisation, through a probe linked to the fluorophore rhodamine targeted to the conserved region of 16S rRNA of bacteria.

However, other studies found no bacterial cells in stomata, hydathodes and vascular tissues of tobacco and *Arabidopsis* (Cornelis et al. 2001, Putnam and Hiller 2007). But Manes et al. (2004) found *R. fascians* colonisation in the internal tissues of the stem, leaves, floral organs, sepals (mainly in substomatal cavities), and in the intercellular spaces of the subepidermal cortical cell layers by applying a droplet of a highly concentrated *R. fascians* culture on *A. thaliana* two-week old seedlings. All these previous works have studied leaves, stem and floral parts but not other parts of the plant such as cotyledons and roots.

In the seed coat and cotyledon, the virulent strain 602 colonisation was profusely spread from 9 dpi to 35 dpi compared to the avirulent strain 589. The avirulent strain 589 appeared to colonise pea tissues later than the virulent 602 strain. The virulent strain 602 colonisation was most pronounced on the epidermal layer of shoots, mainly on the multiple shoots, at 9 dpi compared to the avirulent strain 589 which was more abundant at 25 dpi. The colonies of the avirulent strain 589 were clumped together more densely on the epidermal layer of roots which may be due to greater production of extra cellular matrix compared to the virulent strain 602 which showed more widespread expanse of the bacteria with profuse growth.

The two microscopy techniques provided a complimentary insight into the morphology and colonisation characteristics of *R. fascians* on pea tissues. The light microscopy analysis highlighted some of the features of *R. fascians* which were not revealed clearly with SEM. The use of DIC enabled a more refined view of the individual shape of the rods and cocci and the specific colour staining of the bacteria allowed for easier recognition of the bacteria compared to plant cells. However, the fine hyphal-like forms were more apparent with SEM. The advantage of the fast speed of preservation with the cryo-preparation and freeze-drying SEM technique provided images with possibly fewer artefacts compared to those associated with light microscopy fixation, wax embedding and knife sectioning. However, a three-dimensional view of the bacteria was often hindered by the smothering effect of the mesh-like coating.

The virulent strain 602 of *R. fascians* was microscopically detected before the onset of the symptom development in the pea plant. Although the virulent bacterial strain was visualised in the seed coat within 4 h of seed imbibition and on the cotyledon and radicle surface by 2 dpi, the typical *R. fascians* symptom of multiple shoot growth was not apparent until 5 dpi. The colonisation by the virulent bacteria preceded symptom visualisation at 5 dpi, which agrees with the concept that the presence of bacteria externally causes the initial symptom development through production of virulence factors (Crespi et al. 1992).

The virulent strain 602 colonised the pea tissues at an earlier time period compared to the avirulent strain 589. The avirulent strain 589 in *P. sativum* was detected later than the virulent strain 602, and colonisation generally appeared to increase with growth of the plant mainly at 25 and 35 dpi. The epiphytic and endophytic colonisation of both the virulent and avirulent strains of *R. fascians* on the *P. sativum* indicate that the virulence factor is not necessary for colonisation capability (Cornelis et al. 2001). On the roots of the pea plant *R. fascians* was found to be associated with a slime or mucilage-like layer near the surface of the pea roots which was seen in both the avirulent strain 589 and the virulent strain 602. Francis et al. (2007) explained that *R. fascians* when it contacts a host plant, forms large epiphytic colonies embedded in a protective slime layer.

This study highlighted the colonisation behaviour of both *R. fascians* avirulent and virulent strains on *P. sativum* plants through its course of growth from germination to 35 dpi. The epiphytic and endophytic colonisation capacity of both the strains indicates that the virulence plasmid pFiD188 does not play a role in the colonisation capacity of *R. fascians*. The virulent strain 602 colonisation preceded the manifestation of symptoms in pea. Particularly noticeable were the dark green intact cotyledons when infected with the virulent strain 602. This observation is investigated further in Chapter 5. The occurrence of multiple shoots, shortened roots and delayed onset of senescence due to *R. fascians* virulent strain 602 infection are all indicative of elevated cytokinins in the infected tissues.

CHAPTER 4 Identification, isolation and expression of cytokinin genes in *P. sativum* and *R. fascians*

4.1 Introduction

Cytokinins are plant hormones involved in promoting and regulating growth and developmental processes in plants and they have emerged as a major factor in plant-microbe interactions. Pertry et al. (2009) suggested the continuous presence of cZ and 2MeScZ in *Arabidopsis* infected with *R. fascians* virulent strain D188 (due to ineffective degradation by *AtCKX*) enables continuous tissue proliferation. They explained the *R. fascians* phytopathology as the 'trick-with-the-cytokinin-mix' concept. However, the cytokinin profile of *Arabidopsis* infected with an avirulent strain was not compared with virulent infected tissues by Pertry et al. (2009) to determine whether cZ and 2MeScZ accumulated in the avirulent infected tissues. Eason et al. (1996) and Galis et al. (2005b) have shown that cytokinin levels in pea shoots inoculated with nonvirulent strains were higher than virulent strain inoculated tissues but symptoms were not manifested. So, the strategy by which the virulent *R. fascians* causes shooty malformations is still obscure.

The more recent studies have mainly been done on the aerial parts of *A. thaliana* and *tobacco*, particularly stems and leaves. However, investigations of the expression of cytokinin genes in host and *R. fascians* at different growth stages in other plant parts including cotyledons and roots is lacking. Previous studies have not clearly explained the correlation of cytokinin levels, virulence and symptom development of plants infected with *R. fascians* (Eason et al., 1996, Galis et al., 2005b, Goethals et al., 2001a, Manes et al., 2001, Murai et al., 1980).

The cytokinin biosynthetic and metabolic multigene families have been analysed in a number of plant species including *Arabidopsis*, maize, rice, wheat, *Brassica* and soybean, but not in pea. The key aim of this project was an analysis of these genes simultaneously with the expression of *R. fascians* *fas* genes (*RfIPT*, *RfLOG* and *RfLOG*) in multiple tissue types at different development stages, using the primers designed specifically to discriminate between the plant and microbial cytokinin genes.

Most often the reports on *R. fascians* and plant interaction are with the host seedlings infected after 72 h or 2 weeks of normal growth, so the microbe is introduced after the establishment

of the host (Depuydt et al., 2008, Eason et al., 1996, Galis et al., 2005b, Pertry et al., 2009). These studies do not reveal the early interplay between the host and pathogen when they are grown together at the same time.

In the current study, the polymerase chain reaction (PCR) and real-time quantitative PCR (RT-qPCR) were used to isolate and analyse the *in planta* expression of pea cytokinin (*PsIPT*, *PsLOG* and *PsCKX*) genes simultaneously with the isolated *fas* genes of *R. fascians*, *RfIPT*, *RfLOG* and *RfCKX*. Pea inoculated with *R. fascians* avirulent strain 589 and virulent strain 602 and gene expression monitored in different organs and at different stages of growth. The expression of *P. sativum* response regulators (*PsRRs*) were monitored as an indirect measure of the level of endogenous cytokinins in pea plants.

4.2 Materials and Methods

The materials and methods used in this chapter have already been given in Chapter 2 and any additional information is provided below.

4.2.1 Identification and isolation of cytokinin biosynthesis, metabolism and response regulator genes

For the identification of putative *IPT*, *LOG*, *CKX* and *RR* genes, orthologue sequences in pea (Section 2.7), all annotated family members of these multigene families from *Arabidopsis thaliana* and the available legume homologues from *Glycine max*, *Medicago truncatula*, *Lotus japonicas* and *Pisum sativum* were used as query sequences to BLAST search the GenBank database (<http://blast.ncbi.nlm.nih.gov>). In the case of *R. fascians* the same procedure was followed to identify *IPT*, *LOG* and *CKX* genes with other microbial sequences homologues were selected and used for alignment. The alignment was done using ClustalX program (Thompson et al. 1997) and MEGA4 program (Tamura et al., 2007). The identification of the genes was also done by Dr Jianchen Song based on a pea transcriptome sequence analysis.

For isolation of the genes of interest from pea, the sequencing of PCR products was done using the cDNA template from mixed tissue samples of pea, containing cotyledon, shoot, root and whole plant at various development stages (4 hpi to 35 dpi) along with PCR primers

designed based on pea transcriptome sequence analysis and GenBank database sequence information. In case of *R. fascians* the virulent strain (602) was used as template and primers designed from the NCBI database.

4.2.2 Plant Material and *R. fascians* strains

Pisum sativum variety Bohatyr was used as host plant, which was inoculated with two strains of *R. fascians*, virulent (602) and avirulent (589) by seed inoculation. Virulent strain 602 was considered highly virulent (Eason et al. 1996), and contains *IPT*, *LOG* and *CKX* whereas avirulent strain 589 lacked these genes (Figure 3.4).

The cultures of *R. fascians* 589 and 602 were cultured as mentioned in Section 2.2. The pea seeds were inoculated with *R. fascians* avirulent and virulent strains and grown in sterilised agar containers in growth room (Section 2.3).

4.2.3 Polymerase Chain Reaction (PCR)

The Polymerase Chain Reaction (PCR) reactions were conducted based on the manufacturer instructions. PCR amplification was done in a 20µl master mix containing 2 µl of 10 x Tag buffer, 1µl of 2 mM MgCl₂, 1 µl of 10 pmol of each forward and reverse primer, 2 µl of 5-fold diluted cDNA, 2.5 µl of 2mM dNTPs and 0.2 µl of 5U Taq polymerase with water to make up 20 µl. The designed primers were first run in Temperature Gradient PCR program, with 35 cycles of 94 °C for 5 min, 40 °C for 5 min, 72 °C for 5min followed by 94 °C for 30 s, then to temperature gradient of lower temperature of 50 °C to upper temperature of 60 °C for 30s, 72 °C for 30s, followed by one cycle of 72 °C for min then held at 4 °C. Each column in the PCR plate had a temperature gradient of which 50 °C, 51.7 °C, 54.3 °C, 56 °C, 58.5 °C and 60 °C were selected to assess the annealing temperature of the primers designed in a BIORad DNA Engine Peltier Thermal Cycler or a MJ Research PTC-200 Peltier Thermal Cycler.

Based on the result from the temperature gradient PCR cycling, the standard PCR program to amplify the DNA fragments was carried out as outlined in Section 2.10. Nested PCR was done for sequencing when the normal PCR did not work to isolate some of the genes of interest.

4.2.4 Cloning of PCR amplification of target gene

In order to isolate genes which were not able to be done by the standard procedure, cloning was done. The cloning was performed by TOPO®TA cloning kit based on the manufacturer's protocol.

The PCR products from standard PCR run were purified by using Ultraclean™15 purification kit (Section 2.12). The TOPO® cloning reaction was set up with following reagents: PCR product- 4 µl, salt solution-1 µl, TOPO vector-1 µl. The reaction mixture was gently mixed and incubated for 5 min at room temperature then placed on ice and transforming competent cells was performed. To a vial containing one shot chemically competent *E. coli*, 2 µl of TOPO cloning reaction was added and mixed gently by tapping the tip, incubated on ice for 30 min. Then the cells were heat shocked at 42 °C for 90 s and immediately transferred to ice. The S.O.S medium (250 µl) was added to the vial capped tightly and shaken horizontally at 200 rpm, 37 °C for 1 h. From each transformation 10 -50 µl was spread on two pre-warmed plates containing LB media with ampicillin and incubated at 37 °C overnight. To analyze the positive transformants 2-6 colonies were cultured overnight in 4 µl LB broth containing ampicillin in a shaker. The plasmid DNA was isolated with the Charges Switch –Pro plasmid isolation protocol. To check the plasmids for the insert, restriction digestion was done with EcoR1. The plasmid DNA was then sequenced.

4.2.5 Expression analysis of cytokinin biosynthesis and metabolic genes

The relative expression of the genes of interest was done as described in Chapter 2 (Section 2.13).

4.3 RESULTS

4.3.1 Cytokinin biosynthesis, metabolism and response regulator genes identification and isolation

4.3.1.1 Isopentenyl transferase (*PsIPT*)

A thorough search in the NCBI website, BLAST search using *A. thaliana* and pea *IPT* genes as query sequences, various multigene families of *IPT* from in rice, maize, other legumes

(*M. truncatula*, *G. max* and *L. japonicas*) were identified. A number of legume EST sequences similar to *IPT* were also identified.

Based on the alignment and phylogenetic analysis, specific and degenerate primers were designed with Primer Premier 5.00. PCR primers (Table 4.1) were used to amplify a mixture of pea cDNA from mixed tissues. The PCR products which were of approximately the expected size were sequenced (Figure 4.1).

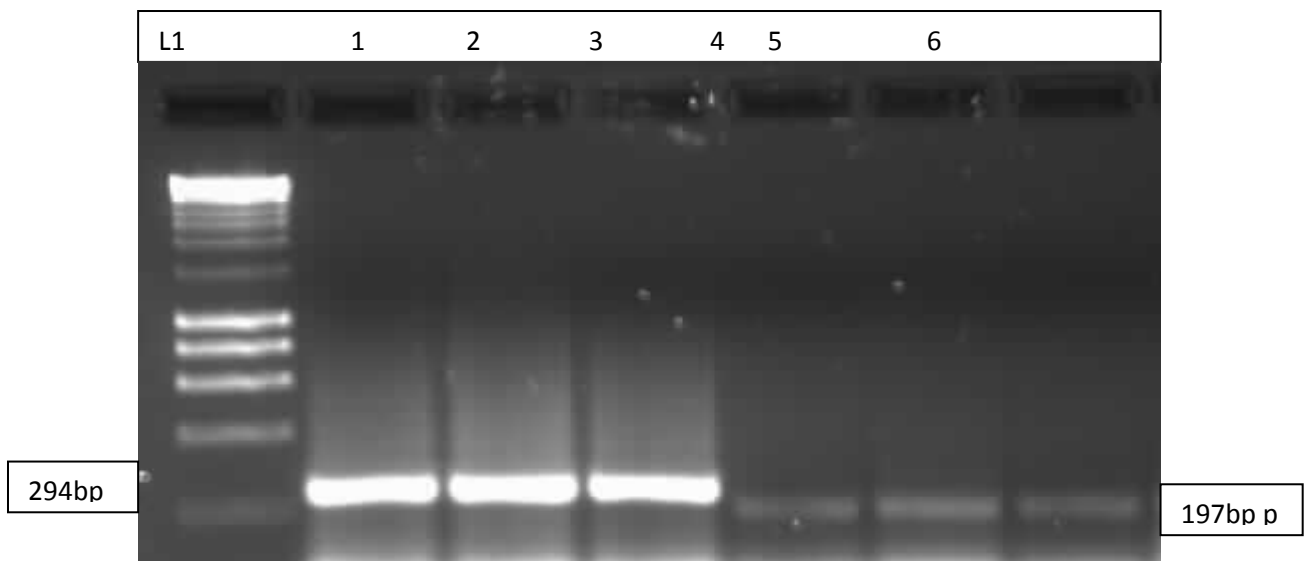


Figure 4.1 **PCR products for *PsIPT1* and *PsIPT2***. The PCR reaction performed with *PsIPT1F1R1* and *PsIPT2F4R5* primers. L1: DNA hyper ladder; 1, 2, 3: *PsIPT2F4R5* product length 294 bp and 4, 5 and 6: *PsIPT1F1R1* product length 197 bp.

Table 4.1 Specific PCR *PsIPT* primers

Gene	Primer name	Sequences
<i>PsIPT1</i>	PsIPT1 F1	5' TTACACGAGAGGGATACGAAGA
	PsIPT1 R1	5' TCTTCCACATAACCATAAAGCCTA
	PsI1F1	5' GAAGAGCCATTGGTGTACCTGA
	PsIPT1 F2	5' ACCGCCACTAATGGATAATGA
	PsIPT1 F3	5' AGTTGGCGATAGACTTAGCGAA
	PsIPT1 R3	5' TTTGATTCTTCTCTTGCTGGCT
	PsIPT1 F4	5' CGAAAGGGGAGTGGAGTGAT
<i>PsIPT2</i>	PsIPT2 F1	5' AAGATGGGTTGCCTATTATTGC
	PsIPT2 R1	5' TCCCTTTAGTATAATCACCCGA
	PsIPT2 F2	5' AAGATGGGTTGCCTATTATTGC
	PsIPT2 R2	5' AAGAATGAAGGACAGGAAGTGC
	PsIPT2 F3	5' GGTGGTAGTGATAATGGGGGC
	PsIPT2 R3	5' GCGACCGCCGACAATGTTAGT
	PsIPT2 F4	5' CAACAAACTTCACTGCCAATG

From the above designed primers, the PCR products from PsIPT1F1R1, PsI1F1R1, PsIPT2F4R1 were sequenced, which were verified to be *IPT* gene family members of *P. sativum*. The PCR products from RfIPTF1R1, RfIPTF2R2, RfIPTF4R5 of *R. fascians* which were sequenced and identified to be *RfIPT* gene (Chapter 3) was used.

In order to isolate the other family members of *PsIPTs*, degenerate primers were designed (Table 4.2) and tested. When these did not work the pea transcriptome sequence analysis was done.

Table 4.2 Degenerate *PsIPT* PCR primers

Gene	Primer name	Sequences	Remarks*
<i>TDIPT1</i>	TDIPT1F1	5' RHGCWACMGGRACAGGCAAGTC	AtIPT3, LjIPT3, Mtbl- CT146865
	TDIPT1R1	5' AAYTCMGGGAAMHCCRATBGC	
	TDIPT1R2	5' CCWCCRRCGATGATYGGAAG	
<i>TDIPT2</i>	TDIPT2F1	5' CATCCGAGATCATCAATTCAGAC	MtblCT96307 4
	TDIPT2R1	5' ATTCTCTTATCTCATCTACCATCCC	
<i>TDIPT3</i>	TDIPT3F1	5' AARGTRGTDGTSATMATGGG	LjIPT2, 4, GmIPT, PsIPT2
	TDIPT3R1	5' RTCRACCCARAGRAARCARC	

[Note: * the degenerative primers were designed based on these sequences; N = ATGC, M = AC, R = AG, Y = CT, W = AT, K = GT, S = GC, H = ACT, B = CGT, V = CG, D = AGT]

Based on pea transcriptome sequence analysis, Dr Jiancheng Song identified and designed *IPT* primers (Appendix C. 4.1). Through this, PsI604F2R2, PsI605F1R1, PsI605F2R2 primers were identified and verified as *PsIPT1* (PsI604F2R2) and *PsIPT2* (PsI605F1R1, PsI605F2R2). Through TOPO®TA cloning, PsI421F1R1 was sequenced and identified as *PsIPT3*. The remaining *PsIPT* multi gene families were not isolated with cloning. So, only three *PsIPT* gene families were isolated and studied.

For phylogenetic analysis, along with the sequenced nucleotides, the homologues *IPT* gene sequences of monocot (*Z. mays* and *O. sativa*), *A. thaliana*, legumes (*G. max*, *L. japonicus*, *P. sativus*) and *R. fascians* from the BLAST GenBank database were aligned. The phylogenetic tree analysis (Figure 4.2) showed three main clades. The dicot and monocot formed into two main clades. The monocots *O. sativa* and *Z. mays* *IPTs* grouped together mostly as clade II (Bootstrap value 42) with high bootstrap values among the gene families. The *AtIPT2*, 9, *ZmIPT1* and *LjIPT5* were grouped into clade III (Bootstrap value 65). The newly isolated *PsIPTs* : *PsIPT1*, *PsIPT2* and *PsIPT3* formed the clade I along with *A. thaliana* *IPTs* and legume *IPTs*. *PsIPT3* grouped along with *CaIPT1* (Bootstrap value 83), and sub grouped with *LjIPT1* (bootstrap value 99) along with a broad group of *AtIPT1*, 4, 6 and 8. *PsIPT1* branched alone and came under *AtIPT5* and 7, and other legume *IPTs* such as

LjIPT2, *GmIPT5* (2), *PsIPT2* and *LjIPT4*. *PsIPT2* grouped together with *LjIPT4* with high bootstrap value of 99. So, *PsIPT1* and *PsIPT2* grouped together with legumes and *AtIPT5* and 7. The isolated *RfIPT* formed an out group along with *Rf(D188)IPT* (Figure 4.2).

4.3.1.2 The Lonely Guy (*PsLOG*)

In 2007, the gene *LOG* was identified as a novel cytokinin-activating enzyme that catalyses the final step of bioactive cytokinin synthesis (Kurakawa et al. 2007) in rice. Nine rice *LOG* and nine *AtLOGs* have been identified (Kurakawa et al., 2007, Kuroha et al., 2009). With *AtLOG1* to 9 amino acid sequences as query the GenBank database search was done. The clones and EST sequences of legume *LOGs*, in *G.max*, *M. trunculata* and *Phaseolus vulgaris*, were also identified through BLAST search. The degenerative primers for *PsLOG* were designed (Table 4.3) based on the alignment in ClustalX with Primer Premier 5.00. In the case of *R. fascians*, *fasf* was used as query and all homologous sequences through which other microbes *FasF* were identified (Chapter 3).

Table 4.3 Degenerate *PsLOG* PCR primers

Gene	Primers	Sequences
<i>PsLOG</i>	PsLOGF1 PsLOGR1 PsLOGF2 PsLOGR2	5' GGTCTATGGAGGTGGTAGCGTG 5' AAATCTTTGGCTGTGGGTGCTG 5' TTGGGGAAGTGAGAGCAGTATC 5' GAAATAAAGCCTTCATCAACGG

When the above designed *LOG* primers were amplified with mixed cDNA of all tissues of pea in PCR, RfLOGF1R1 and RfLOGF2R2 were identified as *RfLOG* (Chapter 3) but all the *PsLOGs* PCR products when sequenced did not identify the *LOG* gene.

The transcriptome sequence analysis of pea was used by Dr Jiancheng Song and *PsLOG* primers were redesigned (Appendix C. 4.3). This analysis revealed that the PCR products of *PsLOG1F1R1*, *PsLOG1F2R2*, *PsLOG6F1R1*, *PsLOGF2R2*, *PsLOG8F1R1* and *PsLOG8F2R2* belonged to *LOG* family genes of legumes through BLAST GenBank search.

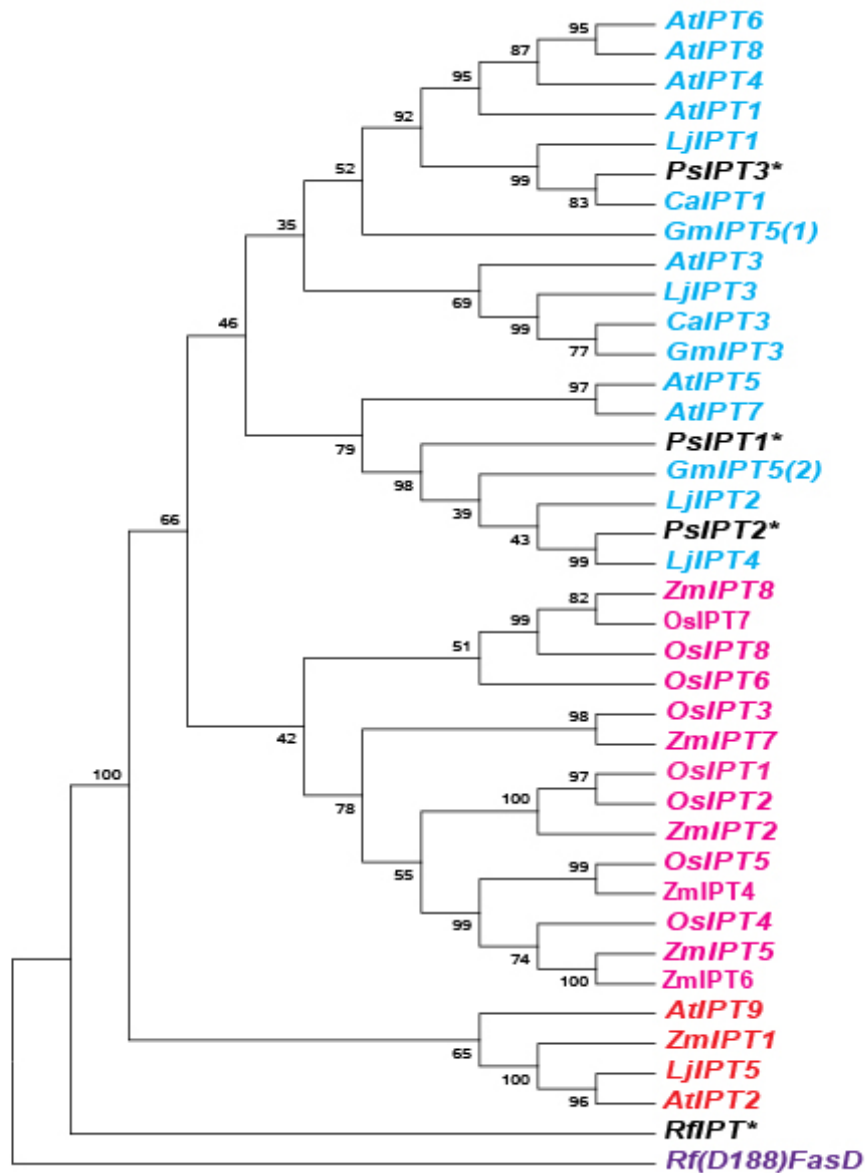


Figure 4.2 Phylogenetic tree of IPT. The Maximum Parsimony phylogenetic tree showing the relationship between *P. sativum* IPT (*PsIPT*): *PsIPT1*; *PsIPT2*; *PsIPT3*, *Arabidopsis thaliana* IPT (*AtIPT*): *AtIPT1*(AB062607.1); *AtIPT2*(NM_128335); *AtIPT3*(BT001075.1); *AtIPT4*(AB062611.1); *AtIPT5*(AB062608.1); *AtIPT6*(AB062612.1); *AtIPT7*(AB062613.1); *AtIPT8*(AB062614.1); *AtIPT9*(NM122011), *Cicer arietinum* IPT (*CaIPT*): *CaIPT1* (XM00497026); *CaIPT3* (XM004495166), *Lotus japonicus* IPT (*LjIPT*): *LjIPT1*(DQ436462); *LjIPT2*(DQ436463); *LjIPT3*(DQ436464); *LjIPT4*(DQ436465); *LjIPT5* (EU195535), *Glycine max* IPT (*GmIPT*): *GmIPT3* (XM003518882), *GmIPT*(1) (XM0035504612), (*GmIPT5* (2) (XM003530866), *Zea mays* IPT (*ZmIPT*): *ZmIPT1*(EU263125); *ZmIPT2*(EU263126); *ZmIPT4*(EU263127); *ZmIPT5*(EU263128); *ZmIPT6*(EU263129); *ZmIPT7*(EU263130); *ZmIPT8*(EU263131), *Oryza sativa* IPT (*OsIPT*): *OsIPT1*(AB239797); *OsIPT2*(AB239798); *OsIPT3*(AB239799); *OsIPT4*(AB239800); *OsIPT5*(AB239801); *OsIPT6*(AB239803); *OsIPT7*(AB239804); *OsIPT8*(AB239805). The node values are bootstrap values generated with 10, 000 bootstrap replicates. The tree was rooted by using *Rhodococcus fascians* IPT: *Rf(D188)FasD*(Z29635.1). *The isolated sequences of *PsIPT1*, *PsIPT2* and *PsIPT3* and *RfIPT* in this project.

Note: Recent realignment indicate that *PsIPT3** is in fact *PsIPT4*.

For phylogenetic analysis, along with the sequenced nucleotides, the homologous *LOG* gene sequences of *A. thaliana*, *G. max*, *O. sativa* and *R. fascians* from the BLAST GenBank database were aligned. The phylogenetic analysis and phylogenetic tree with Maximum Parsimony in MEGA4 (Figure 4.3) was prepared with 10,000 bootstrap replicates. The phylogenetic tree grouped *OsLOGs* together with subgroups except *OsLOGL7*. The isolated *PsLOG1* grouped with *GmLOG3*, belonged to a clade consisting of *AtLOG6*, 3, 4 and *GmLOG1*. *PsLOG6* had high bootstrap value (100) with *GmLOG6* and belonged to the clade consisting of *PsLOG8*, *GmLOG8*, *AtLOG8* and 9 along with *OsLOGL7*. The *PsLOG8* had high sequence similarity with *GmLOG8*, *AtLOG8* and 9. The isolated *R. fascians LOG* was shown to be an out group orthologue.

4.3.1.3 Cytokinin oxidases/dehydrogenases (*PsCKX*)

The *CKX* gene specific primers were designed (Table 4.4) with the published *P. sativum* sequences which were identified as coding sequences similar to *PsCKX1* and *PsCKX2* gene family members in BLAST GenBank database.

Table 4.4 Specific *PsCKX* primers

Gene	Primer	Sequences
<i>PsCKX1</i>	PsCKX1F1	5' ATCCTCAAACCTTTACACCCTCAA
	PsCKX1R1	5' TCGGTCAGTTTGGTATCATCAC
	PsCKX1R2	5' AATTGAATCCCTTATTGTAGCAGA
	PsCKX1F2	5' ATTATCTCGGGCTAACGGTG
	PsCKX1R2	5' CCTCAAACCTTTACACCCTCAAC
	PsCKX1F3	5' TATGGTGAGATGGATAAGGGTGA
	PsCKX1R3	5' ATTGAATCCCTTATTGTAGCAGA
<i>PsCKX2</i>	PsCKX2F1	5' GTGCTTCATCCAAATCAGTCTCT
	PsCKX2R1	5' GGAAACTCTCCATCATAACCTTA
	PsCKX2R2	5' TGTCTCATTCAAAACATTTATCCA

The above primers were amplified and sequenced, of which only PCR products of PsCKX1F3R3, PsCKX2F1R2, RfCKXF1R1 and RfCKXF2R2 were identified as *PsCKX1*

(PsCKX1F3R3), *PsCKX2* (PsCKX2F1R2) . The *RfCKX* (RfCKXF1R1, RfCKXF2R2) was used for gene expression studies.

Again pea transcriptome sequence analysis was used to design primers (Appendix C.4.2) by Dr Jiancheng Song in order to isolate the other gene family members of *PsCKX*. Through this process, three more gene family members were isolated: PsC910F1R1, Ps910F2R2 as *PsCKX1*, PsC627F1R1, *PsCKXF2R2* as *PsCKX2*, Ps942F1R1, Ps942F2R2 as *PsCKX3*, PsC930F1R1, PsC930F2R2 as *PsCKX4* and PsC131F1R1, PsC131F2R2 as *PsCKX5* gene family members.

The phylogenetic analysis of isolated *PsCKX* gene family members and *RfCKX* with other homologous gene sequences of *CKX* genes of *Z. mays*, *A. thaliana* and other legumes was assessed, aligned and phylogenetic tree with Maximum Parsimony in MEGA4 software with 10,000 bootstrap replicates drawn (Figure 4.4). In case of *CKXs* it was noticed that the monocot *ZmCKXs* gene families formed to one clade (Bootstrap value 89) except *ZmCKX3*. The pea *CKX* gene families which were isolated in this study grouped with the dicots. *PsCKX1* had high bootstrap value of 99 with *GmCKX7*, *AtCKX5* and 7. *PsCKX2* grouped with *GmCKX6* (bootstrap value 99) and *PsCKX4* with *GmCKX1* (bootstrap value 80). The *PsCKX4* had bootstrap value of 99 with *GmCKX1*. Both *PsCKX2* and *PsCKX4* formed a group along with *AtCKX1* and *ZmCKX3*. *PsCKX3* formed a group with *GmCKX5* and *AtCKX6* (high bootstrap value 98). The last gene family of *PsCKX5* isolated had bootstrap value of 49 with *MtCKX* and *GmCKX3*. The *R. fascians CKX* grouped with high bootstrap value of 100 with *RfCKX* (D188) gene as an out group.

4.3.1.4 Pea Response regulators (*PsRR*)

The A- type and B-type response regulator genes were identified through use of *Arabidopsis* Response Regulators (*ARR*) sequences as query sequences in BLAST search through Genbank database. Except for *Phaseolus vulgaris PvRR1* there were no legume response regulators available, so ESTs and cloned legume sequences were identified and aligned.

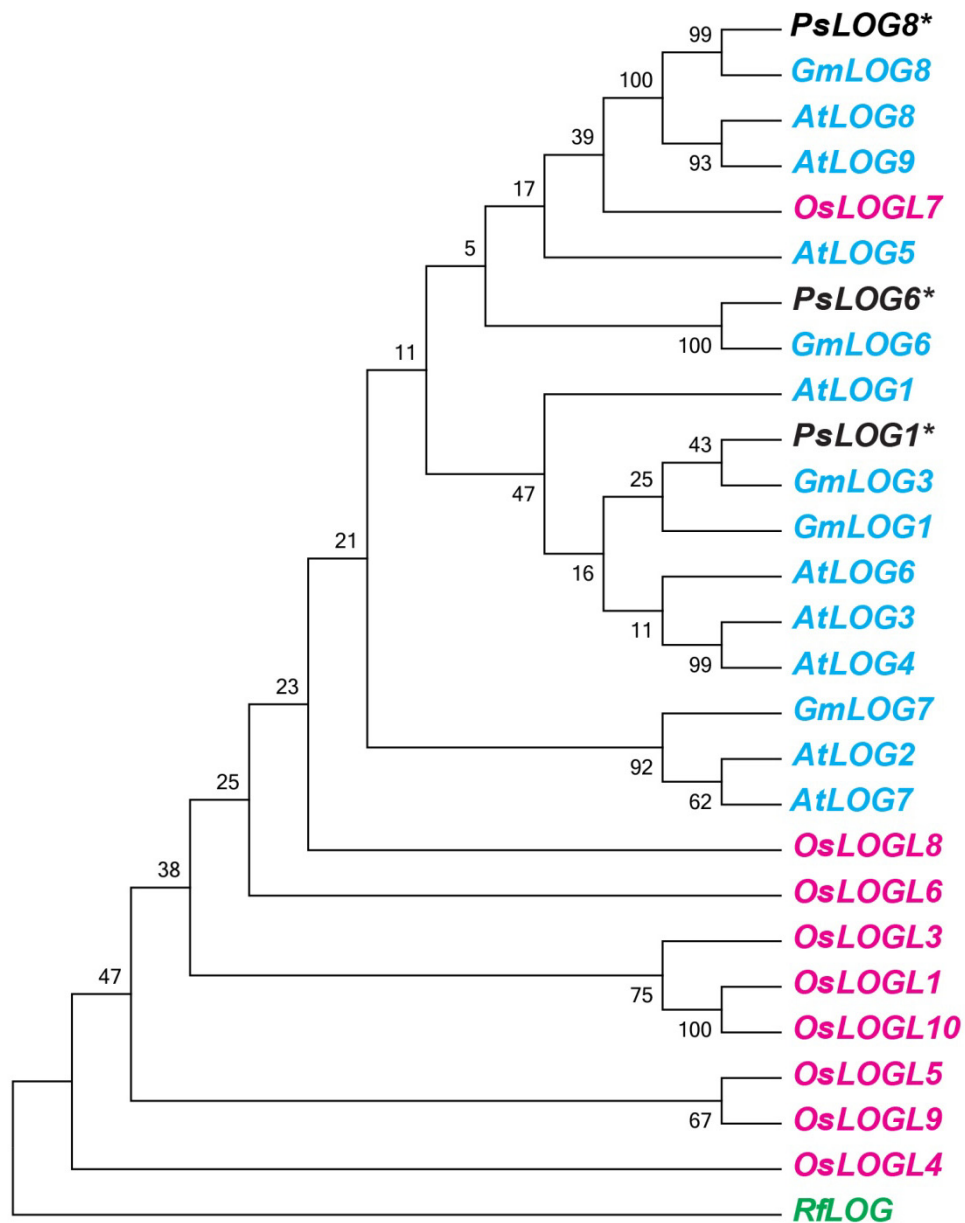


Figure 4.3 **Phylogenetic tree of LOG.** The Maximum Parsimony phylogenetic tree showing the relationship between *Pisum sativum* LOG: *PsLOG1*, *PsLOG6* and *PsLOG8*, *Arabidopsis thaliana* LOG (*AtLOG*): *AtLOG1* (At2g28305); *AtLOG2* (At2g35990); *AtLOG3* (At2g37210); *AtLOG4* (At3g53450); *AtLOG5* (At4g35190); *AtLOG6* (At5g03270); *AtLOG7* (At5g06300); *AtLOG8* (At5g11950); *AtLOG9* (At5g26140); *Glycine max* LOG (*GmLOG*): *GmLOG1* (XM003538129); *GmLOG3* (NM001253269); *GmLOG6* (XM003527643); *GmLOG7* (XM003519078); *GmLOG8* (XM003550217); *Oryza sativa* LOG (*OsLOG*): *LOG* (Os01g0588900); *LOGL1* (Os01g0708500); *LOGL2* (Os02g0628000); *LOGL3* (Os03g0109300); *LOGL4* (Os03g0697200); *LOGL5* (Os03g0857900); *LOGL6* (Os04g0518800); *LOGL7* (Os05g0541200); *LOGL8* (Os05g0591600); *LOGL9* (Os09g0547500); *LOGL10* (Os10g0479500). The tree was rooted using *Rhodococcus fascians* LOG (*RfLOG*). The node values are the bootstrap values generated with 10,000 bootstrap replicates. *The sequences of *P. sativum* LOGs, *PsLOG1*, *PsLOG6*, *PsLOG8* and *R. fascians* LOG: *RfLOG* isolated in this project.

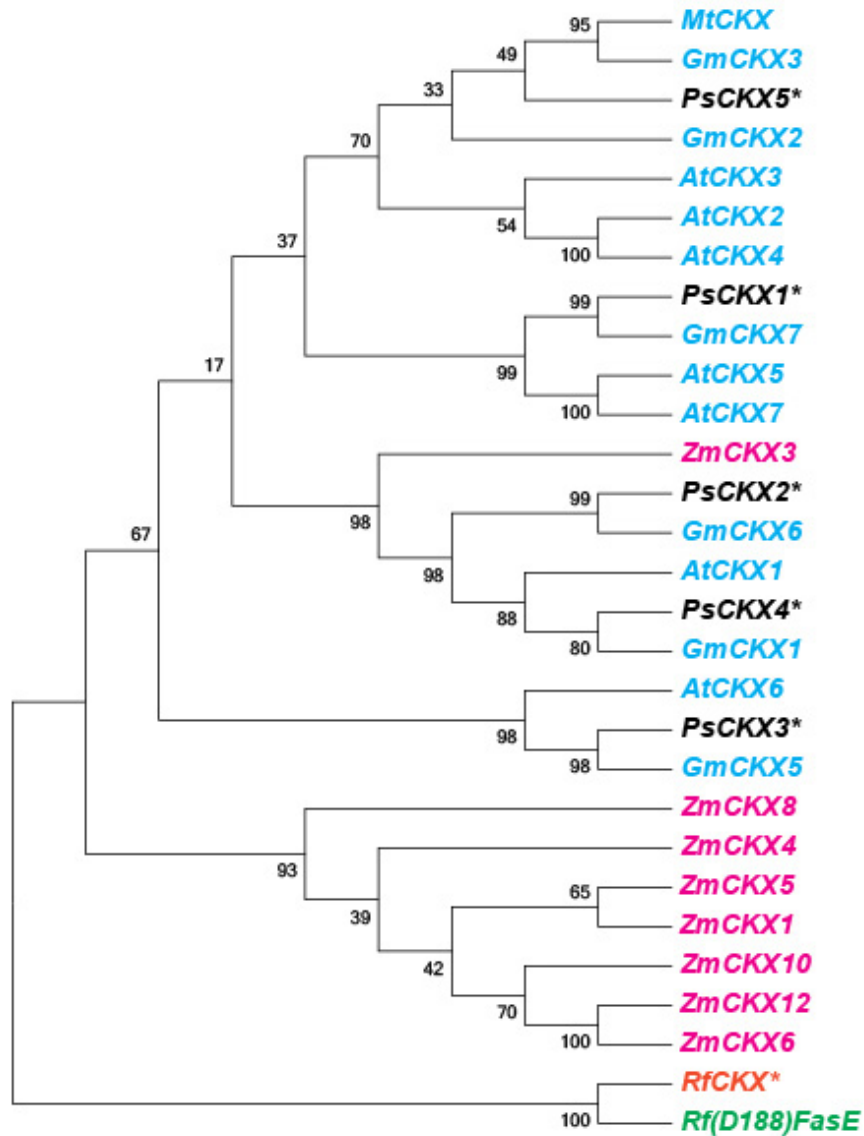


Figure 4.4 **Phylogenetic tree of CKX.** The Maximum Parsimony phylogenetic tree showing the relationship between *P. sativum* CKX (PsCKX): *PsCKX1*, *PsCKX2*; *PsCKX3*; *PsCKX4*; *PsCKX5*, *Arabidopsis thaliana* CKX (*AtCKX*): *AtCKX1* (NM129714.2); *AtCKX2* (NM127508.2); *AtCKX3* (NM125079.2); *AtCKX4* (NM179139.1); *AtCKX5* (NM106199.5); *AtCKX6* (NM116209.3); *AtCKX7* (NM180532.2), *Zea mays* CKX (*ZmCKX*): *ZmCKX1* (AF044603); *ZmCKX3* (NM001111693); *ZmCKX4* (GU160398.1); *ZmCKX5* (NM001199029.1); *ZmCKX6* (NM001199030.1); *ZmCKX8* (NM001198880.1); *ZmCKX10* (NM001153366.1), *ZmCKX12* (NM001199032.1), *Glycine max* CKX (*GmCKX*): *GmCKX1*(NM001257274.1); *GmCKX2* (XM003547425), *GmCKX3* (NM001256884.1), *GmCKX5* (XM003523516), *GmCKX6* (XM003539871), *GmCKX7*(XM003522248), *Medicago trunculata* CKX (*MtCKX*); *MtCKX* (XM003595136.1). The tree was rooted using *Rhodococcus fascians* *Rf*(D188)*FasE* (Z29635). The node values are the bootstrap values generated with 10,000 bootstrap replicates. *The sequences of *P. sativum* CKXs, *PsCKX1*, *PsCKX2*; *PsCKX3*; *PsCKX4*; *PsCKX5* and *RfCKX* isolated in this project. **Note:** Recent realignment indicate that *PsCKX3** is in fact *PsCKX5* and *PsCKX5** is *PsCKX3*.

The specific and degenerative primers were designed initially focussing on the A-type response regulators *ARR5* and *ARR15*.

>*ARR5* F1: 5' TATCTACTCGCAGCTAAAACGC
> *ARR5* R1: 5' TTCTACGAAAAGCCATGTAAAGT
> *ARR5* F2: 5' TGATATCTACTCGCAGCTAAAACG
> *ARR5* R2: 5' TAGCTTGTCTTCGTGTAATGAACG
> *ARR5* R3: 5' TGGATTCGATTCATGTAGACAGC
>*ARR15* F1: 5' TCGTAAAGTTATTGAGAGATTGC
>*ARR15* R1: 5' CAGAAGACATTATCACTACTGGGA
>*ARR15* F2: 5' GTGACGACTGTTGAGAGTGGGA
>*ARR15* R2: 5' AGTGTCGTCATCAAGGGAGGAA

When the above designed *ARR5* and 15 primers amplified with mix of pea tissue cDNA in PCR the sequenced products did not reveal the *RR* sequences, so all the primers failed to isolate the *RR* gene family. When pea transcriptome sequence analysis was done then the *PsRR* gene family primers were designed by Dr Jiancheng Song (Appendix C.4.1.4). Four *PsRR* gene families were isolated with these primers, PsRR3FR1 as *PsRR3*, PsRR5F1R as *PsRR5*, PsRR6F1R and PsRR6F2R as *PsRR6* and PsRR9FR1 and PsRR9FR2 as *PsRR9*.

The phylogenetic analysis was done with A-type *RR* and B-type *RR* gene families of *Arabidopsis* and legumes *G. max*, *M. trunculata* and *P. vulgaris* with isolated *PsRR* gene families by Maximum Parsimony in MEGA4 program with 10,000 bootstrap replicates (Figure 4.5). The analysis revealed that B-type *RRs* and A-type *RRs* grouped to two different clades. The A-type *RRs* grouped with legumes and the newly isolated *PsRRs*. *PsRR3* grouped with *MtRR3*, *PvRR1* and *GmRR3* with bootstrap value of 93 to 56. *PsRR5* and *PsRR6* aligned in a clade containing *GmRR6*, *GmRR5* and *MtRR5*. *PsRR5* had high bootstrap value of 98 and 97 with *MtRR5* and *GmRR5* respectively. *PsRR6* had high sequence similarity with *GmRR6* (bootstrap value 97). The isolated *PsRR9* grouped in a clade with *GmRR9* (bootstrap value 89), A-type *ARR9* and *ARR16*. The tree was rooted with *O. sativa* OsRR5 as an out group.

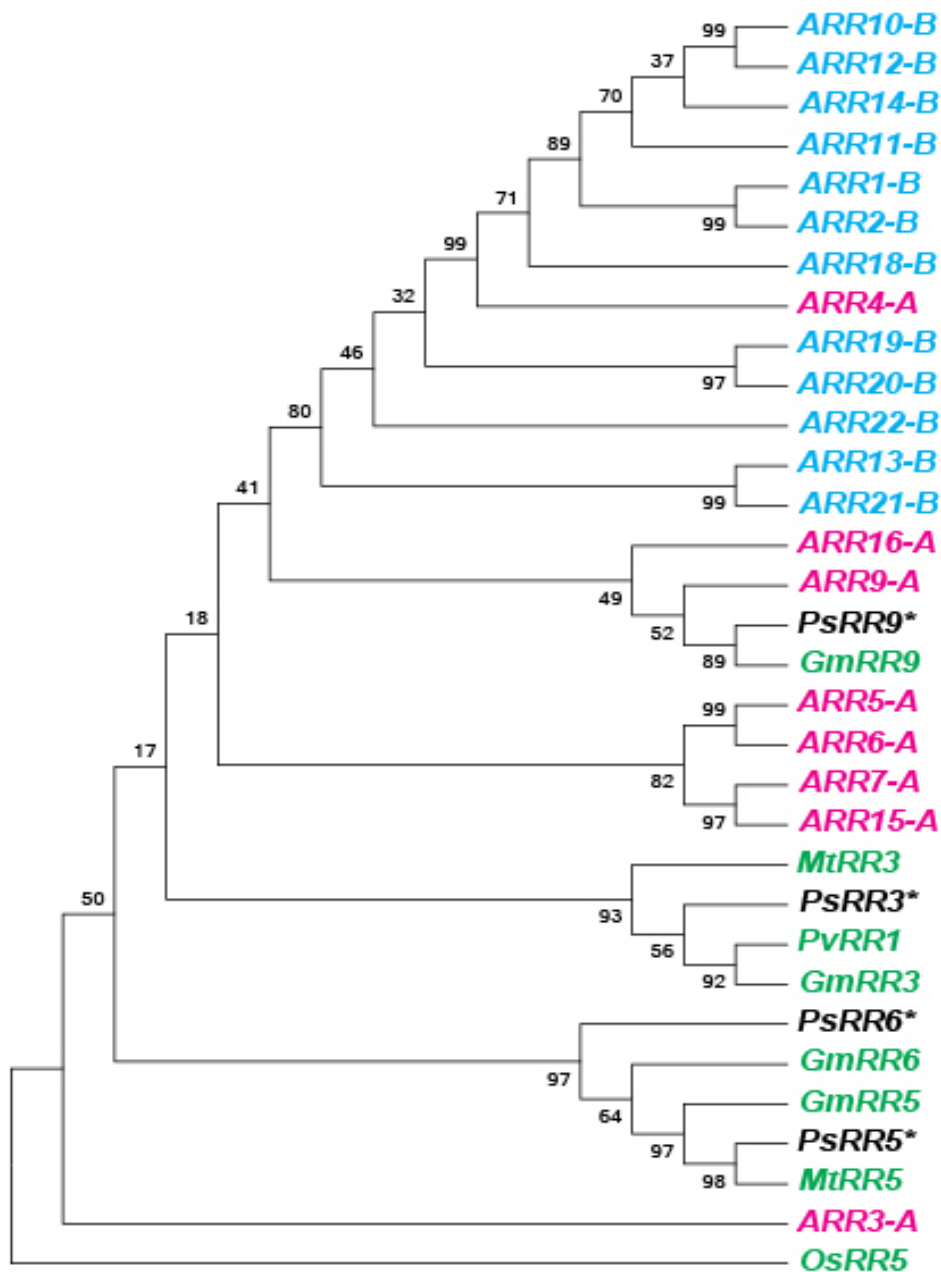


Figure 4.5 **Phylogenetic tree of RR**. The maximum parsimony phylogenetic tree showing the relationship between *P. sativum* RR (PsRR): *PsRR3*, *PsRR5*, *PsRR6*, *PsRR9*; *P. vulgaris* RR (PvRR): *PvRR1* (EF078889); *Glycine max* RR: *GmRR3* (XM003517698), *GmRR5* (XM003549599), *GmRR6* (XM003526992), *GmRR9* (NM0012555250); *Medicago trunculata* RR: *MtRR5* (XM003608889); *Arabidopsis* RR: *ARR3-A* (NM104686), *ARR4-A* (NM 100921), *ARR5-A* (AB008488), *ARR6-A* (NM125686), *ARR7-A* (NM101763), *ARR9-A* (NM115563), *ARR15-A* (NM106147), *ARR16-A* (NM129629), *ARR1-B* (NM112561), *ARR2-B* (NM117704), *ARR10-B* (NM119343), *ARR11-B* (NM105439), *ARR12-B* (NM128075), *ARR13-B* (NM128265), *ARR14-B* (NM126237), *ARR18-B* (NM125193), *ARR19-B* (NM103809), *ARR20-B* (NM1116132), *ARR21-B* (NM120803). The node values are the bootstrap values generated with 10,000 bootstrap replicates. The tree was rooted with *Oryza sativa* RR: *OsRR5* (AJ938074). *The sequences of *P. sativum* RRs, *PsRR3*, *PsRR5*, *PsRR6* and *PsRR9* isolated in this project.

4.3.2 Housekeeping/ reference genes identification and isolation

The putative sequences of 18S rRNA (*U18S*), β -actin (*ACT*), GAPDH (*GAP*) and elongation factor (*EP*) for *P. sativum* were identified through BLAST search Genbank database. They were named as *U18S*, *PsACT*, *PsGAP* and *PsEF*. These reference genes were used for further gene expression studies as internal controls for normalisation of RT-qPCR.

The following primer sequences for the reference genes were:

U18S

U18SF1: 5' CGATCAGATACCGTCCTAGTCTCAAC

U18S R1: 5' CAGAACATCTAAGGGCATCACAGAC

U18SF2: 5' GCTGAAACTTAAAGGAATTGACGGAAG

U18SR2: 5' TTGAAGACCAACAATTGCAATGATCTATC

***PsACT*(ref: *P. sativum actin X67666, X90378*)**

PsACT F1:5' TTGGATTCTGGTGATGGTGTG

PsACT R1: 5' CATAGATGGCTGGAAAAGGAC

PsACT F2: 5' TTGCCTATGTTGCTGTGGATTA

PsACT R2: 5' ATCTCCTTGCTCATAACGGTCAG

PsACT F3: 5' AATCAACAATGGCAGAAGC

PsACT R3: 5' ATCACCAACATACGCATCTT

***PsGAP* (ref: *P. sativum GAPC1 X73150*)**

PsGAPF: 5' GGTATGTCATTCCGTGTCCCA

PsGAPR: 5' CCCTCAGACTCTTCCTTGATAGC

***PsEF* (ref: *PsEF-6555*)**

PsEFF1: 5' ACAATGTTSGATTCAATGTTAAGAATGTTG

PsEFF2: 5' AGAATGTTGCAGTCAAGGATCTCAAG

PsEFR1: 5' CTTACCAGATCGCCTGTCAATCTTG

PsEFR2: 5' CTCCTTCTCAAKCTCCTTACCAGATC

The above primers were all used in PCR amplification with pea tissue cDNA and the best primers were selected for the studies.

4.3.3 Optimisation of RT-qPCR

Total RNA isolated from all the tissue samples using TRIzol reagent generally yielded good quality RNA with a 260/280 ratio of 1.8 to 1.9 in TE buffer. The integrity of RNA extracted was assessed by gel electrophoresis. Good quality RNA showed two major bands of 18S and 28S ribosomal RNA which were selected for cDNA synthesis (Figure 4.6). The RNAs without two distinct bands and high degradation were discarded and the extraction of RNA was redone for these samples.

The quality of cDNA synthesised was assessed by RT-qPCR. For each cDNA, two reference genes and one target gene were used to test the quality of cDNA. The best cDNAs were selected based on the amplification and melting curve analysis of RT-qPCR. For example: the RT-qPCR performed with control cotyledon cDNAs at different growth stages (5, 9 and 15 d after imbibition) (Figure 4.7) with the two reference genes, *UI8S* and *PsEF* and the target gene *PsIPT1* showed distinct single sharp peak with specific product. The melting curve graph of the cDNAs from the different growth stages are shown to be the same concentration (Figure 4.7A). The amplification graph reveals that all the cDNAs tested come out at more or less the same cycle (Ct value) depending on the gene (Figure 4.7B) which shows that the similar concentration of RNAs extracted were translated to cDNAs .

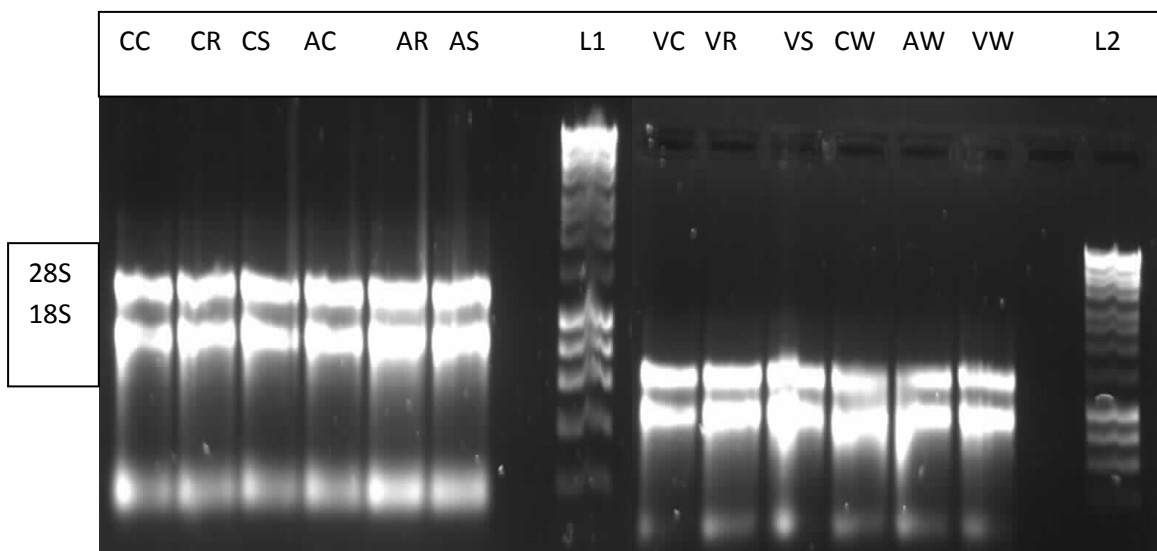


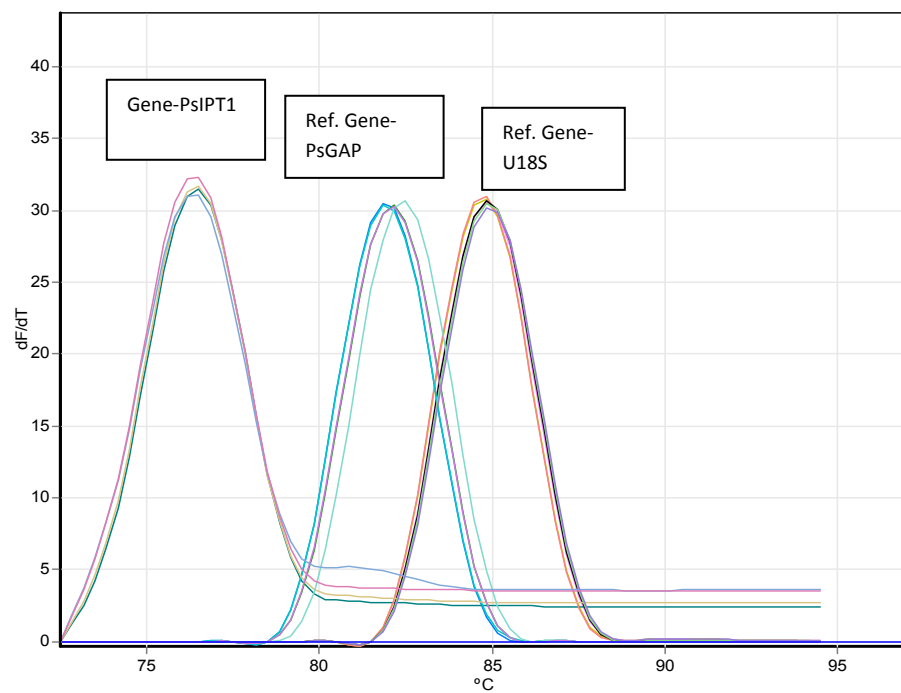
Figure 4.6 Total RNAs isolated using TRIzol reagent. Lane CC: control- cot, CR: control-root, CS: control-shoot, AC: avir-cot, AR: avir-root, AS: avir-shoot, L1: DNA ladder, VC: vir-cot, VR: vir-root, VS: vir-shoot, CW: control-whole plant, AW: avir-whole plant, VW: Vir-whole plant, L2: DNA ladder.

The quality of all cDNAs synthesised was assessed using RT-qPCR. Good quality cDNAs with relatively constant Ct values across all tissues for the target and reference genes were selected for the gene expression studies. The cDNAs with variations in their Ct values and melting curves differences (more than one peak) were discarded and resynthesised.

Optimisation of primers was performed by determining the optimal annealing temperature of all the target primers and reference genes at 52°C, 55°C, 58°C and 60°C annealing temperatures. As judged by the amplification, melt curve and gel analysis the primers best suited for a temperature of 58°C were selected for the RT-qPCR runs (Figure 4.8 and 4.9). It can be seen that the target gene *PsIPT1*, reference genes *UI8S* and *PsGAP* had different peaks and similar Ct values. The primer pairs best suitable for a temperature (58°C) had sharp peak with single product and similar Ct values. The primers used for RT-qPCR for all the target genes and reference genes are given in Table 4.5.

A duplicate, no template control (NTC) was included in every run for each primer pair to test buffers and solutions for DNA contamination and to assess for primer-dimers.

A.



B.

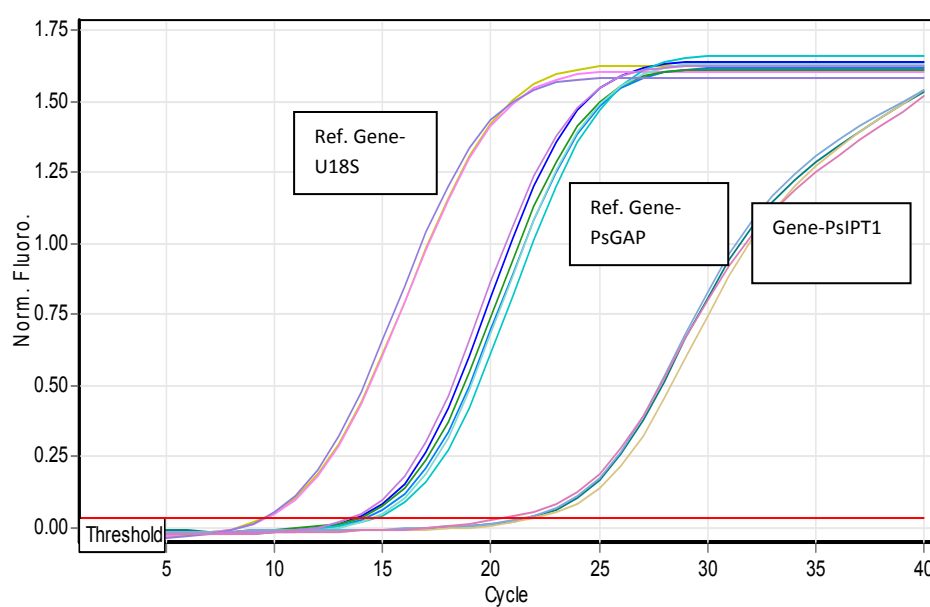


Figure 4.7 Rotor-Gene Q quantification of cDNA from pea tissues: assessment with two reference genes *U18S* and *PsGAP* and one target gene *PsIPT1*. A- melting curves; B- amplification curve.

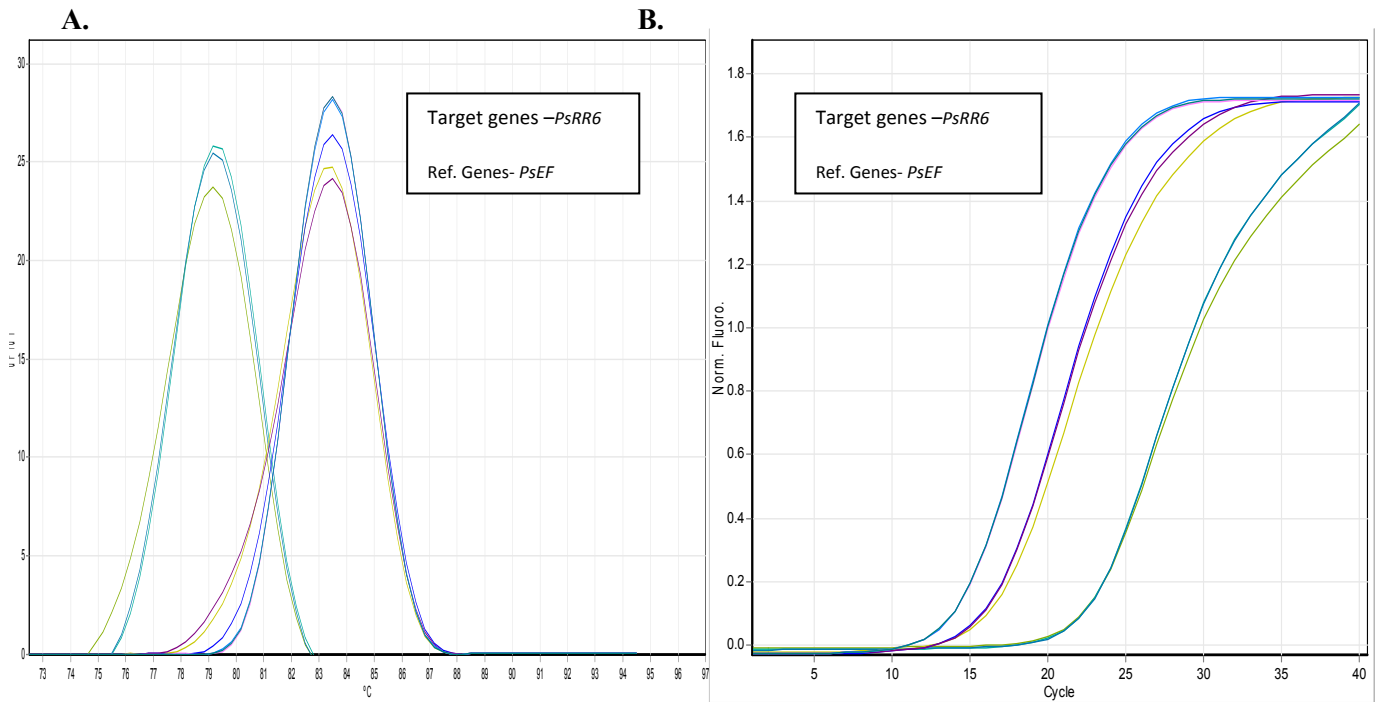


Figure 4.8 **The RT-qPCR performed at 58°C annealing temperature.** A. The melt curve and B. amplification profile of target gene *PsRR6* and reference gene *PsEF*, indicates that most efficient expression would occur at 58°C and the analysis indicates a single PCR product.

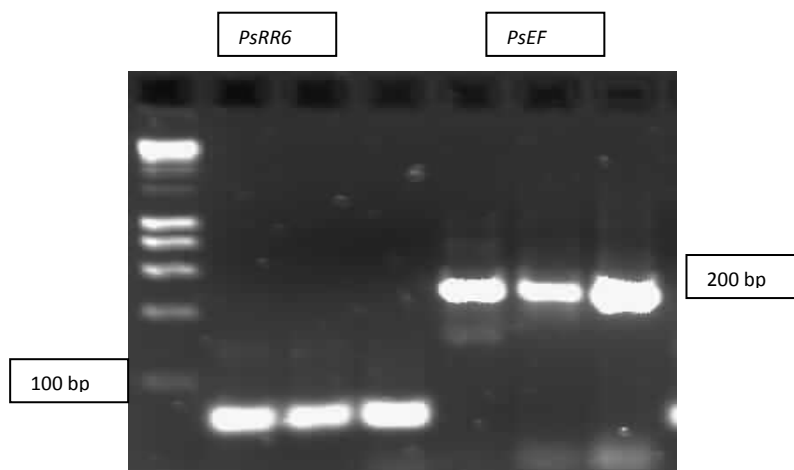


Figure 4.9 **Gel analysis of PCR products.** Gel electrophoresis analysis of the PCR product confirms the presence of a single fragment of expected size.

Table 4.5 Sequences of the selected RT-qPCR primers for expression analysis of *P. sativum* and *R. fascians* genes of interest and reference genes

Gene/primer	Species	Forward(F)/reverse (R) primer sequences
<i>PsIPT1</i> -PsI1	<i>P. sativum</i>	F1: 5' GAAGAGCCATTGGTGTACCTGA R1: 5' TCTTCCACATAACCATAAAGCCTA
<i>PsIPT2</i> - PsI605	<i>P. sativum</i>	F1: 5' GGGTTGATGTTGCACTTCCTGTC R1: 5' ATCGGCTGAATTTGCTTCTGCAG
<i>PsIPT3</i> - PsI421	<i>P. sativum</i>	F1: 5' GCTGAAACGAGTCGACGACATGT R1: 5' CCTTCACTGCTTCCTGGTATGCAC
<i>PsLOG1</i>	<i>P. sativum</i>	F: 5' TSARCTTGGAAMGAATTGGTKTCAAG R: 5' AAWGCATCWGARTGYTAGCCATYTCAG
<i>PsLOG6</i>	<i>P. sativum</i>	F1: 5' ATAAACCKGTGGGGTTRTTGAACGTG R: 5' TGACTTTGCWGTGTTAACYAACGTGTTG
<i>PsLOG8</i>	<i>P. sativum</i>	F2: 5' GCGGCAATGGCTCAAGAAGCTG R2: 5' TTCCGAGCACCAGGCTTAATGAAG
<i>PsCKX1</i> - PsC910	<i>P. sativum</i>	F1: 5' GGGATGATAGACTCAGTAGTGGTAC R1: 5' TCTCTGAACAAATCTATTCCATTTATCTCCA
<i>PsCKX2</i> - PsC627	<i>P. sativum</i>	F1: 5' TTTACAGTGTACTTGGAGGCTTAGGA R1: 5' AGTTCTTCCATCTGATTTGAACTTGCT
<i>PsCKX3</i> - Ps942	<i>P. sativum</i>	F1: 5' TGTTTTACCTGGTGGCATTCTGAG R1: 5' GAATTGCATCTTCATGGCATTGAATTG
<i>PsCKX4</i> - PsC930	<i>P. sativum</i>	F1: 5' GGTCCCATACTCATTTACCCTGTCA R1: 5' GGCATGGGTGCAGAAATCTAAGATC
<i>PsCKX5</i> - PsC131	<i>P. sativum</i>	F2: 5' ATGGGGTKGTGKTGAAYATGACT R1: 5' GTAACAACATCCAATTCAWGAACATTGG
<i>RfIPT</i>	<i>R. fascians</i>	F4: 5' GAGTTCGCCTTCTCCCATTTTC R5: 5' CGACAGCACCGCATCTAAAC

<i>RfLOG</i>	<i>R. fascians</i>	F1: 5' GAACCGTCGTTGGCGTGAT R1: 5' GAGAGCAAGGGGCGGTAATA
<i>RfCKX</i>	<i>R. fascians</i>	F2: 5' ACAATCCGTCTGACCGCTG R2: 5' CCGAAGTGCGTACACCAATC
<i>PsRR3</i>	<i>P. sativum</i>	F: 5' TCCCGGGTTTGAAGGTGGATCTAG R1: 5' TGCACCTTCCTCCAAACATCTGTC
<i>PsRR5</i>	<i>P. sativum</i>	F1: 5' RAARCCRGTCARTTGTGAGATGTAAG R:5' ATTTCTTRGAKGATAATGKTGATGGTGAGAGTGGTGAG
<i>PsRR6</i>	<i>P. sativum</i>	F1: 5' GTGGTTATGTCSTCTGAGAAATCTTG R: 5' RGWCGATAGAGATGRAATGSAATCATCTG
<i>PsRR9</i>	<i>P. sativum</i>	F: 5' CAGRAATGACAGGYTATGATCTGCTG R2: 5' WWCATTCTTAACTTTTGWYTTCAACAAATGTG
<i>UI8S</i>		F2: 5' GCTGAAACTTAAAGGAATTGACGGAAG R2: 5' TTGAAGACCAACAATTGCAATGATCTATC
<i>PsEF</i>	<i>P. sativum</i>	F2: 5' AGAATGTTGCAGTCAAGGATCTCAAG R2: 5' CTCCTTCTCAAKCTCCTTACCAGATC
<i>PsGAP</i>	<i>P. sativum</i>	F: 5' GGTATGTCATTCCGTGTCCCA R: 5' CCCTCAGACTCTTCCTTGATAGC
<i>PsACT</i>	<i>P. sativum</i>	F1:5' TTGGATTCTGGTGATGGTGTG R1: 5' CATAGATGGCTGGAAAAGGAC

[Note: N = ATGC, M = AC, R = AG, Y = CT, W = AT, K = GT, S = GC, H = ACT, B = CGT, V = CG, D = AGT].

4.3.3.1 Reference genes normalisation

To normalise the target gene expression in RT-qPCR, the commonly used housekeeping genes, *UI8S*, actin (*ACT*), elongation factor (EF) and glyceraldehyde-3 phosphate dehydrogenase (GAPDH) were used as reference genes.

The melting curve of all the four reference genes produced a single sharp peak. Figure 4.10 shows that *PsEF* had a single peak at 83°C with only one product and the Ct values of all stages of growth of the three treatments were in the range of 12.0 to 15.0 in cotyledon tissue cDNA.

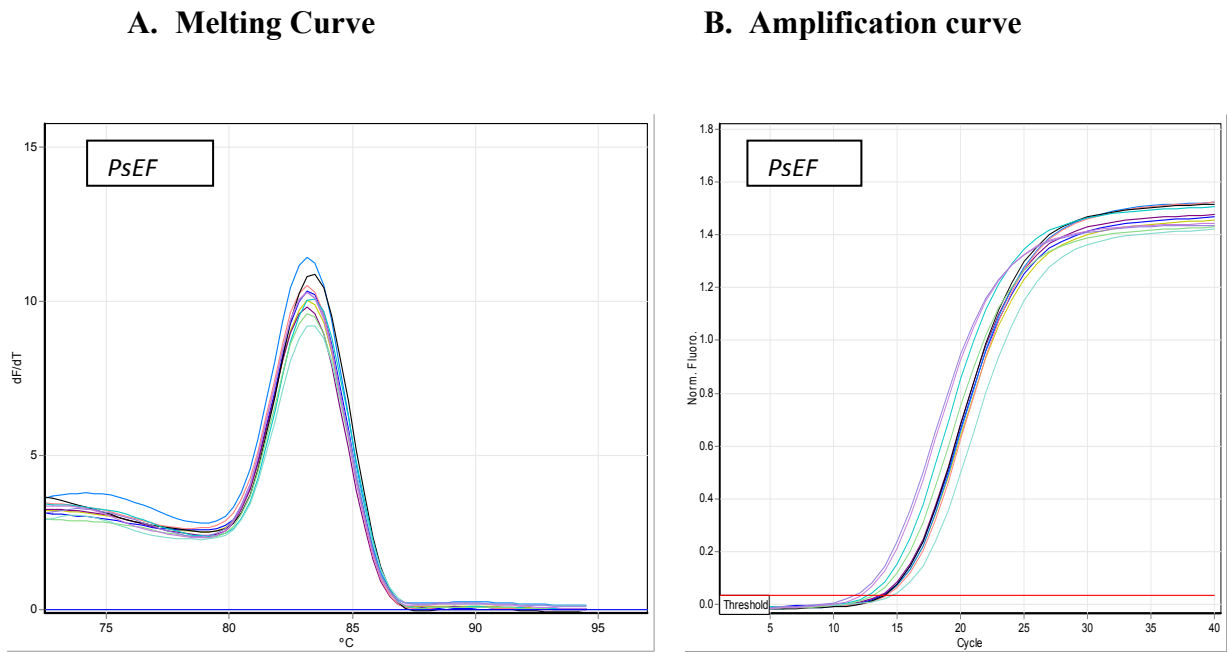
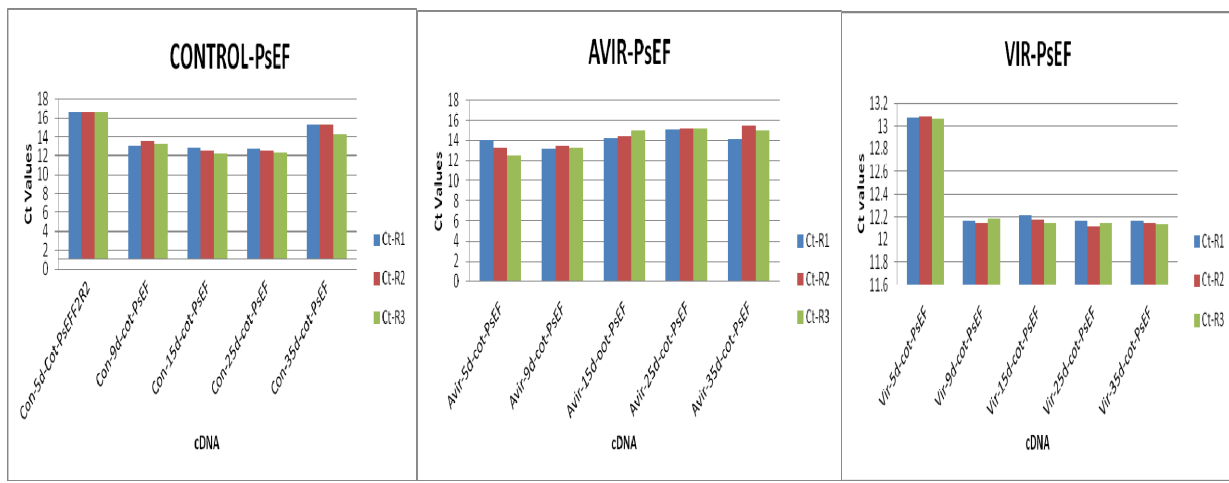


Figure 4.10 The RT-qPCR reaction of reference gene *PsEF* with PsEFF1R1 primer. A. melting curve and B. amplification curve of pea cotyledon cDNA from control, avirulent and virulent treatments at different stages of growth.

Each of the reference genes was tested for their expression stability. Based on the Ct values the reference genes were selected. As an example the expression of all four reference genes in cotyledons from the three treatments (control, avirulent and virulent), is shown in Figure 4.11. The graphs for shoot and root are given in Appendix C.4.2.



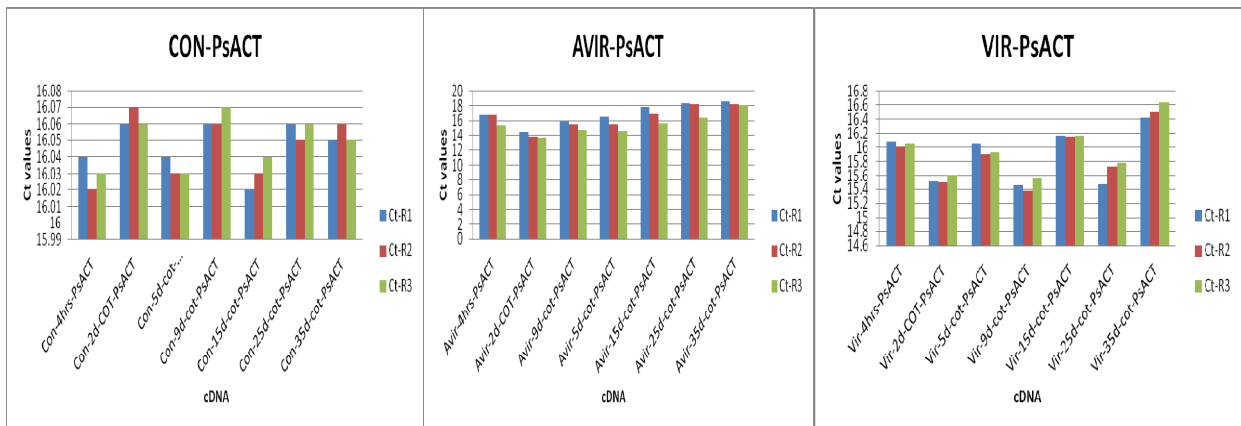
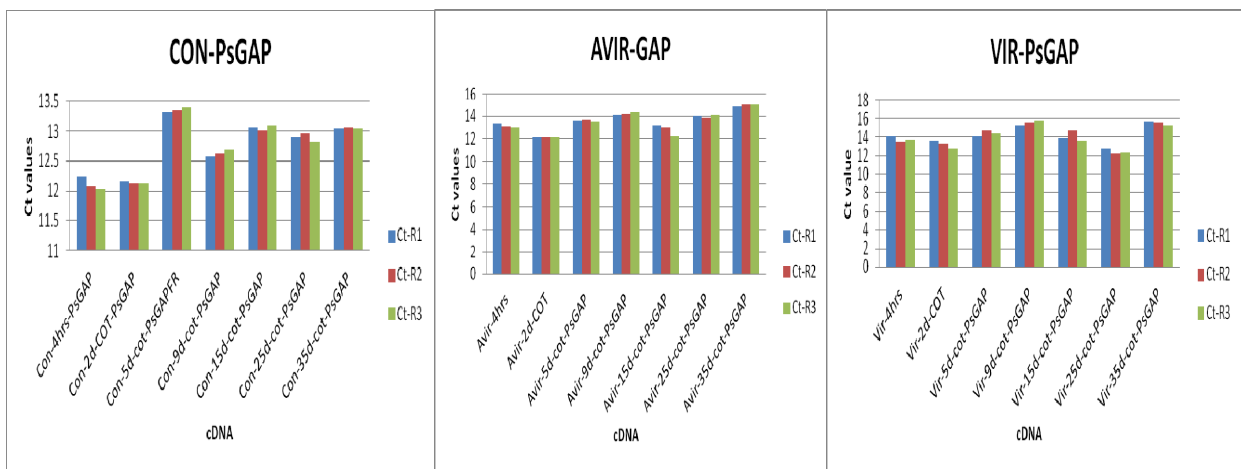
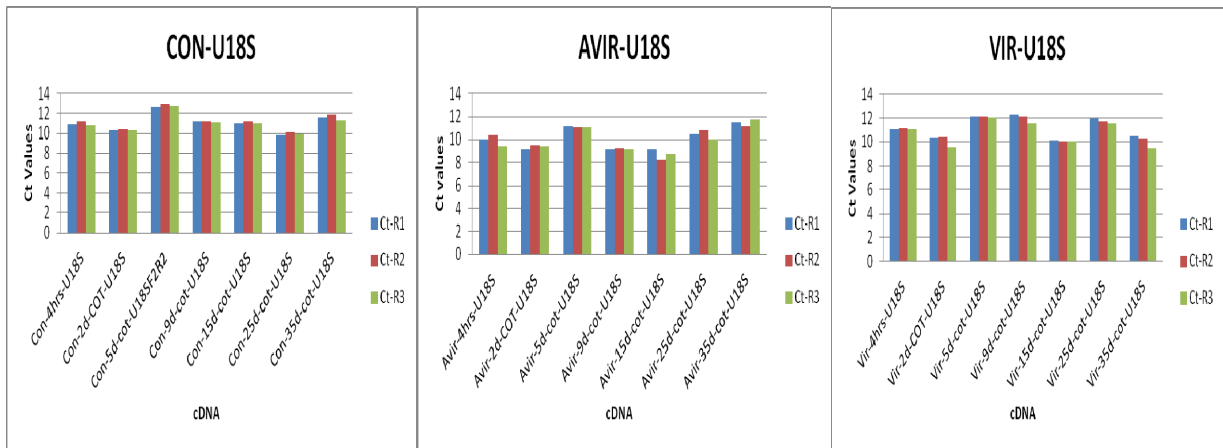


Figure 4.11 The expression (Ct values) of four reference genes. *PsEF*, *U18S*, *PsGAP* and *PsACT* in pea cotyledon tissue from the three treatments (control (CON), inoculated with avirulent (AVIR) and virulent (VIR) strains of *R. fascians*) at different stages of growth period.

The results based on the Ct values of the four reference genes, *PsEF*, *UI8S*, *PsGAP* and *PsACT* (Figure 4.11) showed that the range of Ct values among the reference genes was narrow where *UI8S* had lower Ct values and *PsACT* had maximum Ct values. Variation between the replicates was not more than +/- 1 Ct value. So, all four reference genes were selected for inclusion in the gene expression studies, as the variation in expression was much smaller across the different tissues.

Even though all the reference genes did not express at the same level as expected theoretically, the expression of all the four reference genes was adjusted. For each reference gene, a correction factor (CF) for each cDNA was calculated; the values of three technical replicates were averaged to form the CF for each biological replicate of each reference gene. The final CF value for each biological replicate was done by averaging the CF values of the four reference genes as described by Song et al. (2012).

4.3.4 Relative expression of cytokinin biosynthesis, metabolic and response regulator genes in different tissues of *P. sativum* inoculated with *R. fascians*.

The relative expression of cytokinin biosynthesis, metabolic and response regulator genes were studied in *P. sativum* inoculated with a virulent strain (602) and an avirulent strain (589) of *R. fascians*. Samples were collected through a time series post inoculation from four hours post-imbibition to 35 days post inoculation (dpi). Whole plants or plants separated into cotyledon, root and shoot tissues were analysed. The cDNAs from these tissues were used for gene expression studies, with *PsEF*, *PsGAP*, *PsACT* and *UI8S* as reference genes.

The following gene families which have been identified, isolated and sequenced from *P. sativum* (Section 4.2.2.1) and *R. fascians* (Section 3.3.2) were used for the study of relative gene expression in pea cotyledons, roots and shoots tissues:

1. *PsIPT1*, 2 and 3
2. *PsCKX1* to 5
3. *PsLOG1*, *PsLOG6* and *PsLOG8*
4. *PsRR3*, *PsRR5*, *PsRR6* and *PsRR9*
5. *RfIPT*, *RfCKX* and *RfLOG* identified, isolated and sequenced from virulent strain 602.

Expression is stated as fold-change relative to the relevant tissues (cotyledon or root or shoot) at 4 hpi or 5 dpi (initial stage) for the three treatments (control, avirulent and virulent).

4.3.4.1 Relative expression of *Rhodococcus fascians* cytokinin biosynthesis and metabolic genes in *P. sativum* and in *R. fascians* cultures

The relative expression of *R. fascians IPT*, *LOG* and *CKX* varied in cotyledon, root and shoot tissue at 4 h, 2, 5, 9, 15, 25 and 35 d post inoculation (Figure 4.12). The *RfIPT*, *RfLOG* and *RfCKX* expression profiles in control and the avirulent strain 589 infected cotyledons, roots and shoots tissue were negligible which confirms that the primers designed for the *R. fascians IPT*, *LOG* and *CKX* genes discriminated against the *P. sativum* cytokinin genes (*PsIPT*, *PsLOG* and *PsCKX*).

Among the tissues (cotyledon, root and shoot) inoculated with virulent strain 602, *RfIPT*, *RfLOG* and *RfCKX* expression were relatively high either generally at 9 or 15 dpi except for vir-cot (Figure 4.12). In vir-cot *RfIPT* expression peaked at 4 hpi and 9 dpi then decreased to a steady level; the expression of *RfLOG* and *RfCKX* was high at 5 and 9 dpi and then reduced (Figure 4.12a, b and c).. In vir-root, *RfIPT*, *RfLOG* expression peaked at 15 dpi, *RfCKX* expression was high at 15 and 25 dpi (Figure 4.12d, e and f). The vir-shoot *RfIPT* expression peaked at 15 dpi and level of expression was steady until 35 dpi, whereas, *RfLOG* and *RfCKX* expression was similar with high level at 15 dpi and reduction later (Figure 4.12g, h and i).

The comparison between the pea cytokinin genes, *PsIPT*, *PsLOG* and *PsCKX* with *RfIPT*, *RfLOG* and *RfCKX* was done by studying the relative expression of control, the avirulent strain 589 and the virulent strain 602 infected pea cotyledons, roots and shoots, along with *R. fascians* culture cDNAs of the avirulent strain 589 and the virulent strain 602. In the cultures of *R. fascians* avirulent strain 589 and virulent strain 602, *RfIPT*, *RfLOG* and *RfCKX* expression was very high in the virulent strain 602 culture whereas in avirulent strain 589 culture the expression was not detected (Figure 4.12j, k and l).

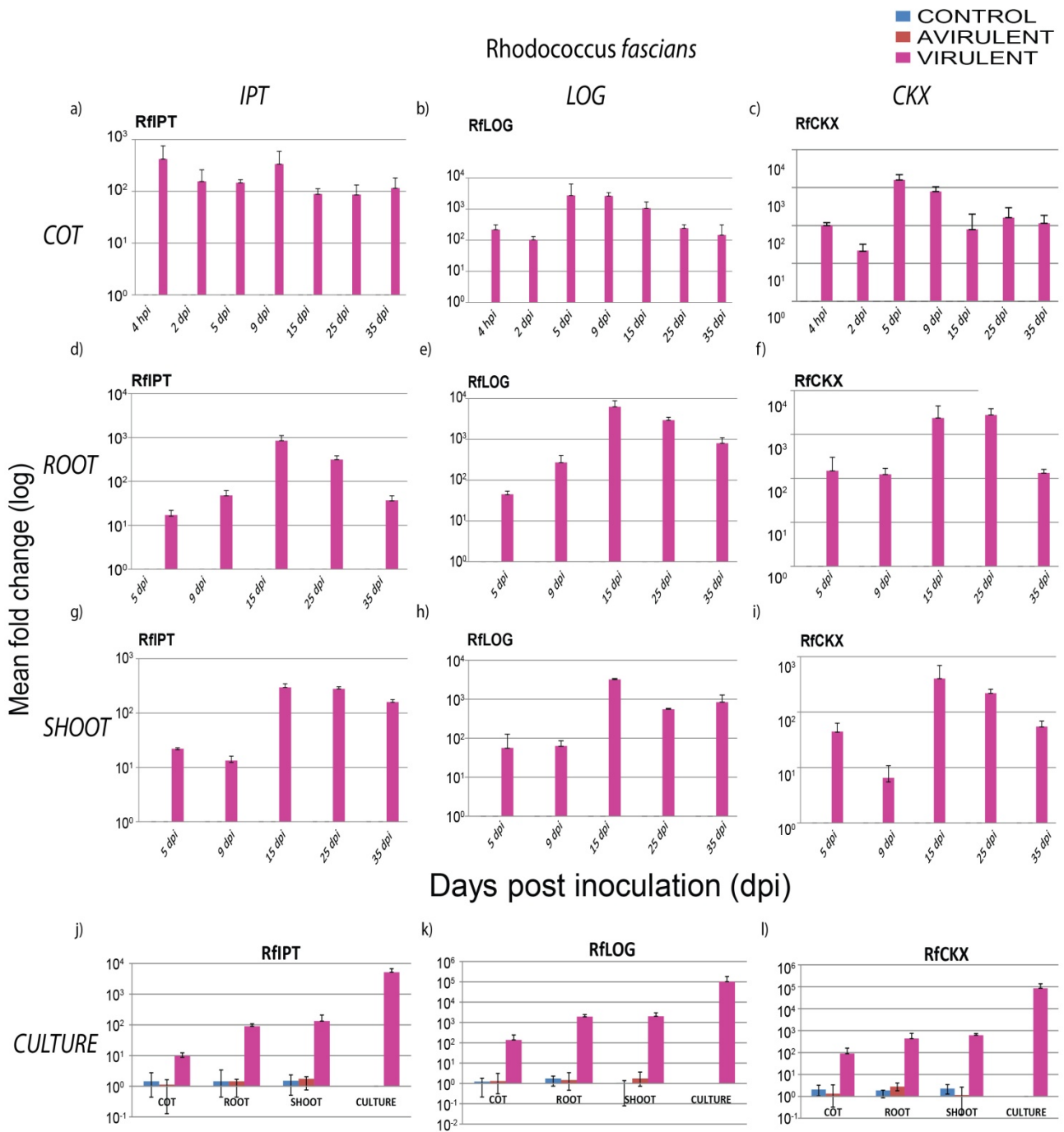


Figure 4.12 **Relative expressions of *RfIPT*, *RfLOG* and *RfCKX* in *P. sativum* cotyledon, shoot tissue and *R. fascians* cultures.** a) *RfIPT* in cotyledon b) *RfLOG* in cotyledon c) *RfCKX* in cotyledon d) *RfIPT* in root e) *RfLOG* in root f) *RfLOG* in shoot g) *RfIPT* in shoot h) *RfLOG* in shoot i) *RfCKX* in shoot j) *RfIPT* in cotyledon, root, shoot, *R. fascians* cultures 589 and 602 k) *RfLOG* in cotyledon, root, shoot, *R. fascians* cultures 589 and 602 l) *RfCKX* in cotyledon, root, shoot, *R. fascians* cultures 589 and 602. Data are means of relative mRNA levels in fold changes (log) detected using three technical replicates for each of two biological replicates. *PsEF*, *UI8S*, *PsGAP* and *PsACT* were used as internal controls. Before quantification of the expression level of each target genes the Ct numbers for each internal control and target gene were corrected with an internal calibrator and also by using the average correction factor determined for each of the four reference genes. Error bars represent the +/- one SD calculated for the combined technical and biological replicates.

No expression was detected in control and the avirulent strain 589 infected cotyledons, roots and shoots. *RfIPT*, *RfLOG* and *RfCKX* expressions was undetectable, whereas the expression was high in virulent strain 602 infected tissues (Figure 4.12j, k and l). The expression profile and level of *RfIPT*, *RfLOG* and *RfCKX* is explained in the subsequent sections.

4.3.4.2 Relative expression of cytokinin biosynthesis, metabolic and response regulator genes in tissues of *P. sativum* infected with *R. fascians*

4.3.4.2.1 Isopentenyl Transferase (*PsIPT*)

Cotyledon: The relative expression level was low in the three *PsIPT* gene family members in the seeds imbibed with Klambt broth (mock inoculated; con-cot) compared to the later growth stages. *PsIPT1* was most highly expressed in cotyledons at 5 dpi which was 65.3-fold higher than the baseline expression (4 hpi). This reduced to 9.2-fold at 9 and 6.3-fold at 15 dpi but by 35 dpi had increased to 16.67-fold relative to 4 hpi (Figure 4.13a). The expression patterns of *PsIPT2* and *PsIPT3* were similar to that of *PsIPT1* but with a much lower range of expression. The expression of *PsIPT3* was highest at 2 dpi (Figure 4.13c).

The expression of *IPT* gene family members in pea seeds inoculated with the virulent strain 602 (vir-cot) was elevated following four hours of imbibition in the *R. fascians* culture compared to the expression of control cotyledons. However, the expression reduced at 2 and 5 dpi. The expression of *PsIPTs* in the vir-cot only exceeded the con-cot at around at 9 to 15 dpi. This was particularly noticeable in *PsIPT2* (Figure 4.13b).

The pattern of expression of the *PsIPTs* in seeds inoculated with the avirulent *R. fascians* strain 589 (avir-cot) was similar to the con-cot except at 25 and 35 dpi where the level of expression was higher (Figure 4.13a, b, c). Avir-cot had high expression in *PsIPT1*, 2 and 3 at 25 and 35 dpi when compared to the con-cot and vir-cot. But expression depressed compared to con-cot at mostly in the three *PsIPTs*.

Significant *RfIPT* expression was detected only in cotyledons infected with the virulent strain (Figure 4.13d). The con-cot and avir-cot had least expression (with Ct values ranging from 33 to 35) which confirmed that the primers were discriminating between *PsIPTs* and *RfIPT*. The *RfIPT* relative expression was initially high which decreased at 2 dpi then peaked at 9 dpi

but reduced by 15 dpi. At later stages (25 dpi to 35 dpi) there was little change in *RfIPT* expression (Figure 4.13d).

Root: Root growth was evident only from 5 dpi, so expression studies on root tissue were limited from 5 to 35 dpi (Figure 4.14a, b, c, d). The expression patterns of the three *PsIPT* gene family members were similar from 5dpi to 35 dpi in con-root. *PsIPT1*, 2 and 3 were highly expressed at 5 dpi, reduced at 9 and 15 dpi then highest at 25 dpi after which the expression level decreased in control roots.

In contrast to con-root, *PsIPT1*, 2 and 3 expression in vir-root was relatively low at 5 dpi, increased at 9 dpi and was highest at 15 dpi and 25 dpi. There was reduced expression in vir-root at 35 dpi. The pattern of expression in all three *PsIPTs* was similar in vir-root (Figure 4.14a, b, c). The vir- root had high *PsIPTs* gene expression mainly at 15 dpi compared to con- root and avir-root.

The avir-root at 5 dpi had low expression in *PsIPT1*, 2 and 3 and gradually increased at 15 to 25 dpi then reduced at 35dpi. With the exception of the con-root, *PsIPTs* gene expression across all treatment was highest at 15 and 25 dpi in root tissue. On the whole, there was similar expression profile of the three members of the *PsIPT* gene family investigated in all the three treatments in roots.

The *R. fascians IPT* gene expression in roots (Figure 4.14d) gradually increased from 5 dpi to 15 dpi and then decreased from 15 to 35 dpi in vir-root.

Shoot: The pattern of expressions of the three *PsIPTs* in con-shoot was similar with highest expression at 5 dpi. There was discernible reduction by 9 dpi and slight increase at 15 and 25 dpi until 35 dpi (Figure 4.15a, b, c). The expression patterns of the *PsIPTs* were similar although *PsIPT2* and 3 relative expression levels were lower than *PsIPT1*.

The *PsIPTs* expression in vir-shoot was high from 15 to 35dpi. *PsIPT1* and 3 expressed highly at 15 and 25 dpi in vir-shoot compared to con-shoot and avir-shoot (Figure 4.15a, c). The *PsIPTs* showed increased expression in vir-shoot with growth.

The avir-shoot in the three *PsIPTs* had high expression at 9 dpi compared to con-shoot and vir-cot and low at 15 dpi. The expression of avir-shoot was lower than vir-shoot at most time points except at 9dpi in all three *PsIPTs* and at 25dpi with *PsIPT2* (Figure 4.15a, b, c). The *RfIPT* gene expression in vir-shoot from 5 dpi increased to 14.4-fold at 15 dpi and 13.3-fold at 25 dpi then decreased by 35dpi (7.5-fold) (Figure 4.15d).

When a calibrator (internal control) is used between RT-qPCR runs, the relative expression of a target gene can be compared across the tissues. *PsIPT1* expressed highly in shoots (182,469-fold) and cotyledons (163,661-fold) compared to roots (1,858- fold). In contrast, *PsIPT2* expressed most highly in roots (10,957-fold), and lowest in cotyledons (1,268-fold). *PsIPT3* expression was highest in roots (15,448-fold) followed by cotyledons and was least in shoots (1,664-fold).

4.3.4.2.2 The Lonely Guy (*PsLOG*)

Cotyledon: The relative expression level was very low in *PsLOG1*, 6 and 8 in the mock inoculated cotyledon at 4 hpi compared with other sampled growth stages. *PsLOG1* expression in con-cot was highest at 2 dpi (132-fold) reduced to 117-fold at 9 dpi and to 48-fold at 15 dpi but increased at 25 dpi (89-fold) and 35 dpi (116-fold). The expression profile of *PsLOG6* and 8 was similar (Figure 4.16).

The vir-cot exhibited high level of expression in all three *LOG* families at 4 hours post inoculation (hpi), decreased at 2 dpi then up regulated at 5 and 9 dpi and steady decrease from 15 to 35 dpi (except *PsLOG8*) than con-cot and avir-cot. The vir-cot had highest *LOG* expression at 5 and 9 dpi in the three gene families (Figure 4.16). *PsLOG8* expression level was noticeably increased in the vir-cot at all time points compared to con-cot and avir-cot (Figure 4.16).

The expression level of the three *PsLOG* gene families was lower in avir-cot during initial growth stages (2 to 15 dpi). Similar to *PsIPT1* and 3 in avir-cot the *PsLOG1* and 6 expression increased at later stage of growth (25 and 35 dpi) (Figure 4.16).

The *R. fascians LOG* expression was similar to *RfIPT* gene in their expression pattern in vir-cot with gradual increase from 2 dpi to 5 dpi and steady decrease from 9 to 35dpi (Figure 4.16).

COTYLEDON-IPT

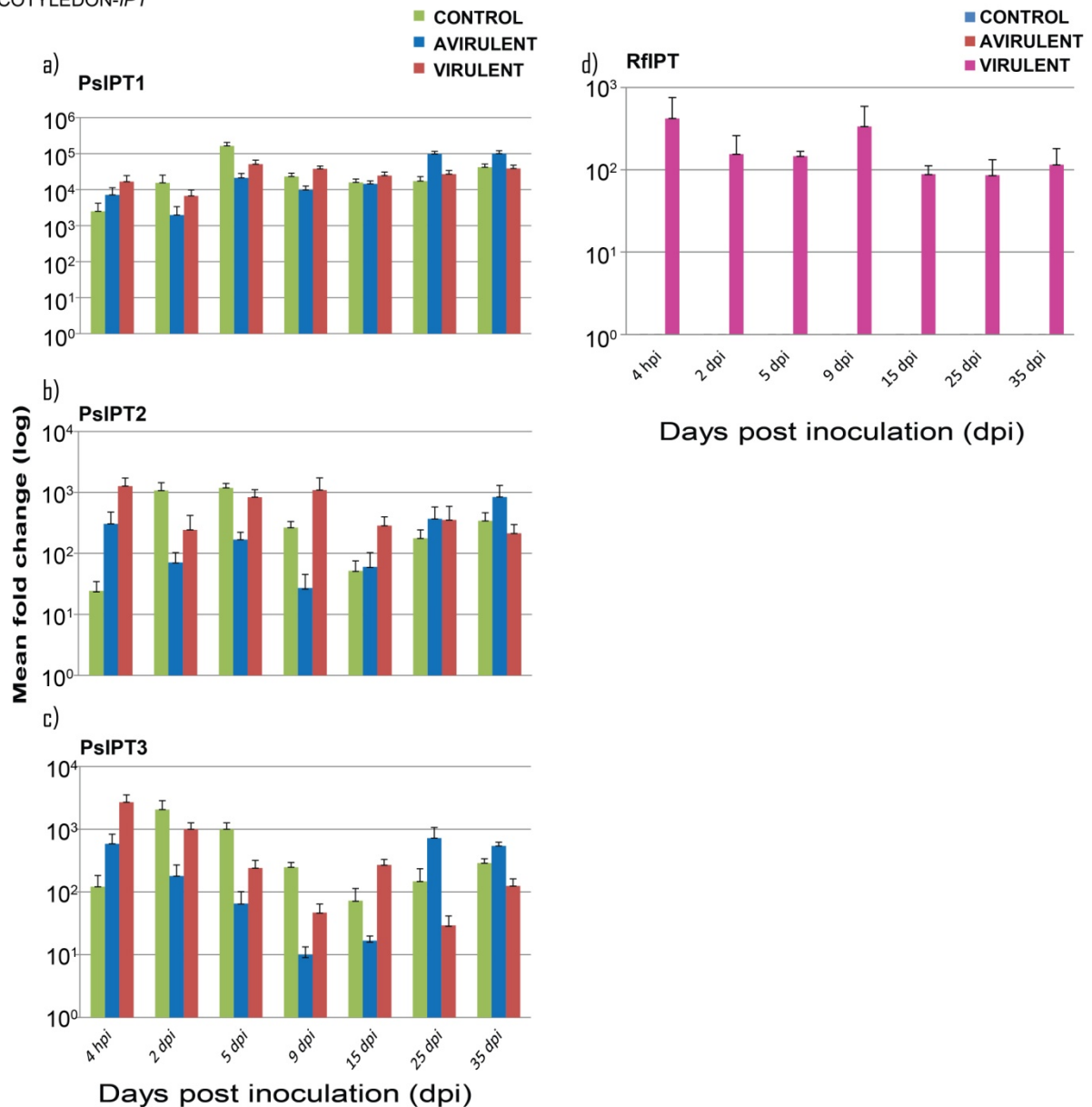


Figure 4.13 Relative expression of *PsIPT1*, 2, 3 and *RfIPT* in *P. sativum* cotyledon tissue. a) *PsIPT1* gene b) *PsIPT2* gene c) *PsIPT3* gene d) *RfIPT* gene. Data are means of relative mRNA levels in fold changes (log) detected using three technical replicates for each of two biological replicates. *PsEF*, *U18S*, *PsGAP* and *PsACT* were used as internal controls. Before quantification of the expression level of each target genes, the Ct numbers for each internal control and target gene were corrected with an internal calibrator and also by using the average correction factor determined for each of the four reference genes. Error bars represent the +/- one SD calculated for the combined technical and biological replicates.

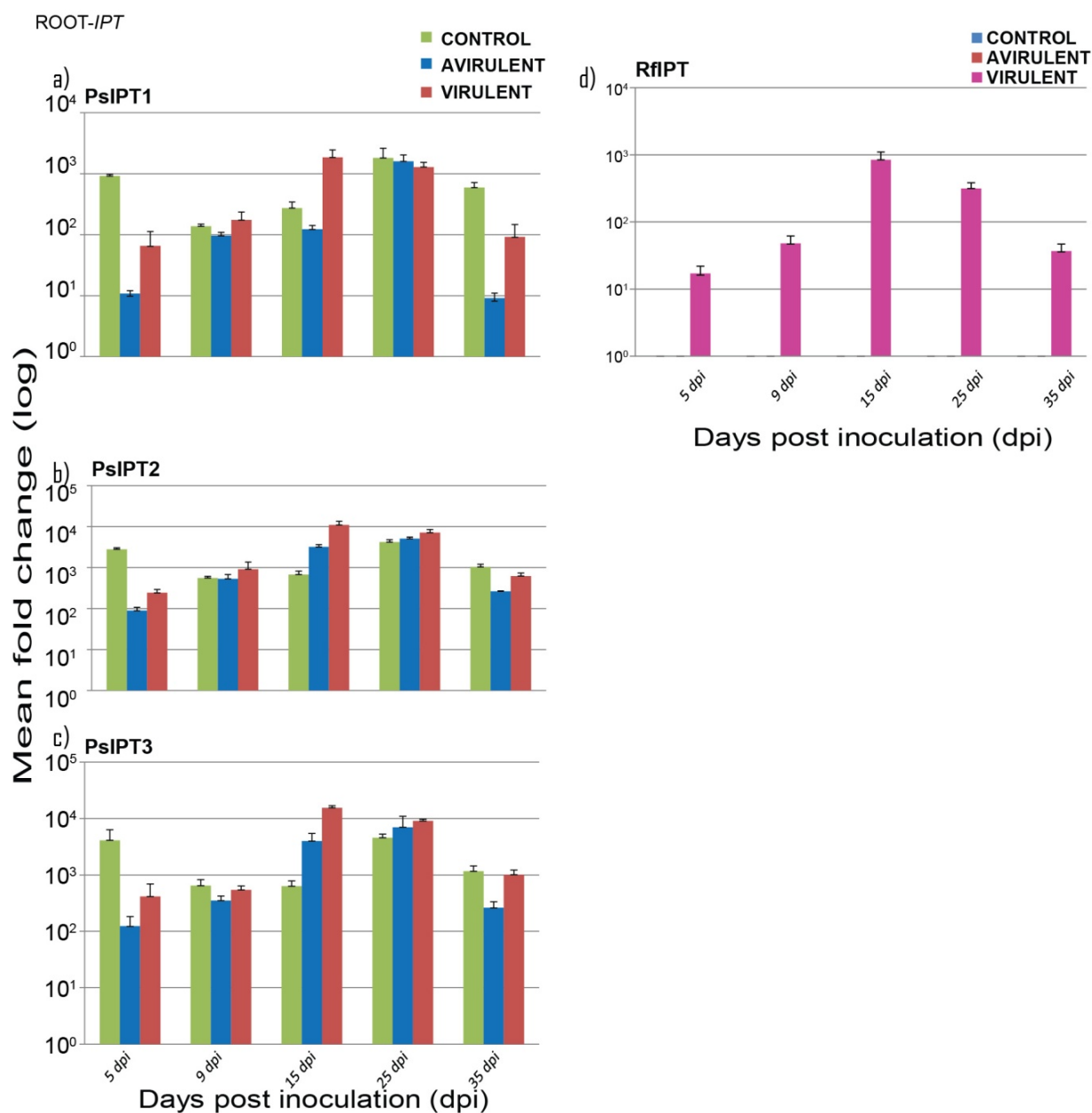


Figure 4.14 Relative expression of *PsIPT1*, 2, 3 and *RfIPT* in *P. sativum* root tissue. a) *PsIPT1* gene b) *PsIPT2* gene c) *PsIPT3* gene d) *RfIPT* gene. Data are means of relative mRNA levels in fold changes (log) detected using three technical replicates for each of two biological replicates. *PsEF*, *U18S*, *PsGAP* and *PsACT* were used as an internal control. Before quantification of the expression level of each target genes, the Ct numbers for each internal control and target gene were corrected with internal calibrator and also by using the average correction factor determined for each of the four reference genes. Error bars represent the +/- one SD calculated for the combined technical and biological replicates.

SHOOT-IPT

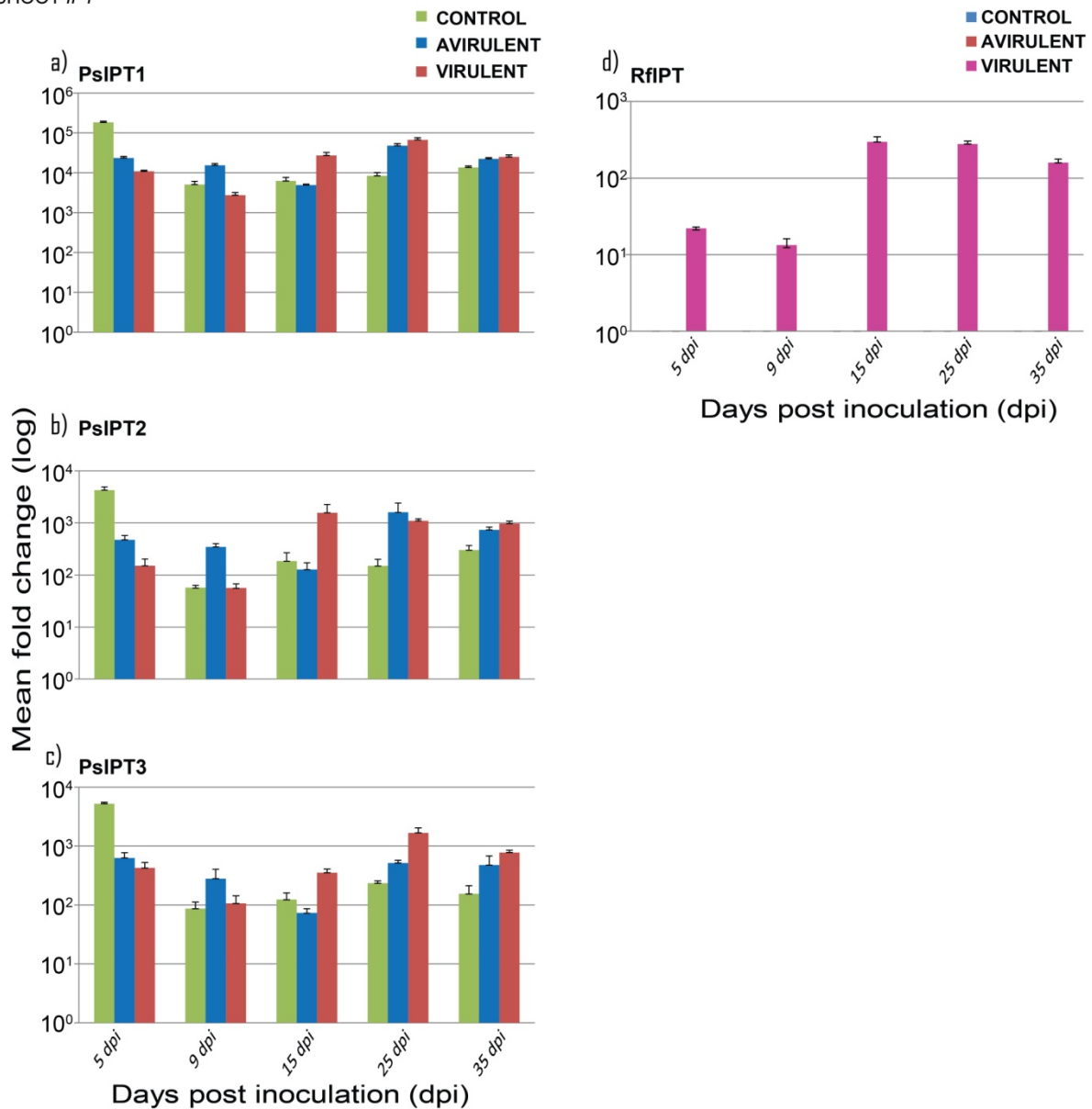


Figure 4.15 Relative expression of *PsIPT1*, 2, 3 and *RfIPT* in *P. sativum* shoot tissue. a) *PsIPT1* gene b) *PsIPT2* gene c) *PsIPT3* gene d) *RfIPT* gene. Data are means of relative mRNA levels in fold changes (log) detected using three technical replicates for each of two biological replicates. *PsEF*, *U18S*, *PsGAP* and *PsACT* were used as internal controls. Before quantification of the expression level of each target genes, the Ct numbers for each internal control and target gene were corrected with an internal calibrator and also by using the average correction factor determined for each of the four reference genes. Error bars represent the +/- one SD calculated for the combined technical and biological replicates.

When the expression pattern of plant *LOG* and microbial *LOG* are compared, it was noticed that *PsLOG* expression was higher than *RfLOG* in all treated cotyledons (Figure 4.16). But *RfLOG* expression was high at 5 to 25 dpi compared to *PsLOG1* in vir-cot (Figure 4.16). On the whole *PsLOGs* and *RfLOG* had high level of expression at 5 and 9 dpi in the vir-cot. This phenomenon was observed only with *LOG* gene but not with *IPT* gene expression.

Root: The three *PsLOG* gene family members had high expression at 5 dpi in con- root (Figure 4.17). This decreased in *PsLOG6* and 8 at 9 dpi and gradually increased from 15 to 25 dpi but reduced at 35 dpi. *PsLOG1* expression was very low at 15 dpi but increased at 25 dpi in con-cot (Figure 4.17).

Except at 5dpi, the vir-root had high or similar *PsLOG1*, 6 and 8 genes expression at 9 and 15 dpi and at 15 dpi the highest level of expression was noticed.

PsLOG1, 6 and 8 expressions were least initially (5dpi), increased until 25dpi with striking reduction at 35dpi. The avir-root showed very low *PsLOG1*, 6 and 8 expressions compared with con-root and vir-root in most growth stages except in *PsLOG1* at 25 dpi (similar level as vir-root).

The pattern of *RfLOG* expression was such that there was gradual increase from 5 dpi (203-fold) to 15 dpi (28, 410-fold) and slow decrease at 25 dpi (13, 488-fold) to 35 dpi (3,693-fold) in vir-root (Figure 4.17).

In case of *PsLOG1*, 6, 8 and *RfLOG* genes expression (Figure 4.17) comparison data revealed that microbial *LOG* gene expression was higher from 9 to 35 dpi in vir-root than plant *LOGs* (mainly *PsLOG1* and 6).

Shoot: In shoots, the *PsLOG* gene expression had a pattern similar to that of *PsIPT*. The control shoot had higher level of *PsLOG1*, 6 and 8 expressions at 5 dpi compared to avir-shoot and vir-shoot (Figure 4.18). At 9 and 15 dpi the con-shoot had least expression in *PsLOG1* (15dpi) and *PsLOG6* (9dpi) later increased for all three *PsLOG* gene family members at 25 and 35 dpi.

COTYLEDON-LOG

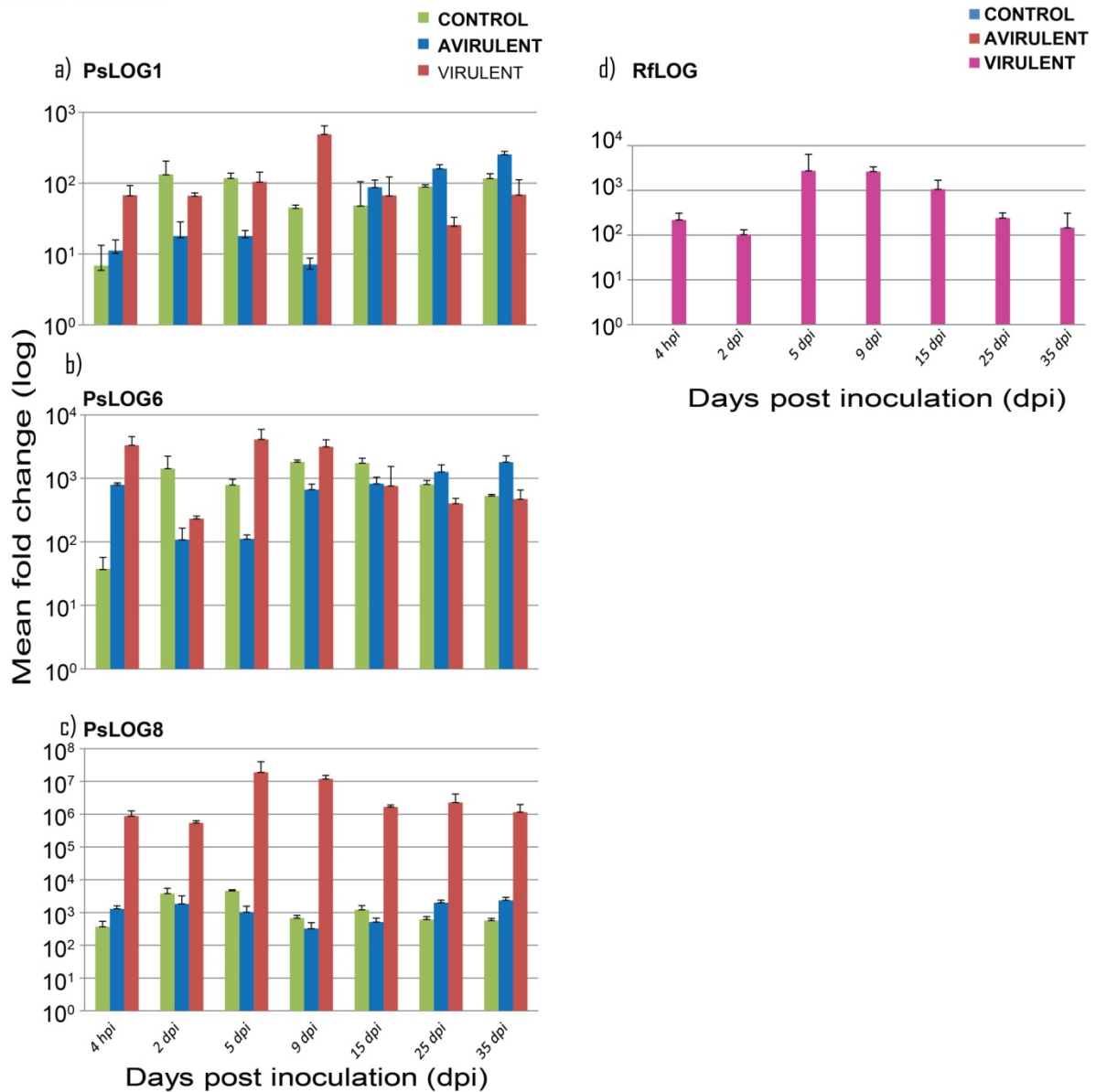


Figure 4.16 Relative expression of *PsLOG1*, 6, 8 and *RfLOG* in *P. sativum* cotyledon tissue. a) *PsLOG1* gene b) *PsLOG6* gene c) *PsLOG8* gene d) *RfLOG* gene. Data are means of relative mRNA levels in fold changes (log) detected using three technical replicates for each of two biological replicates. *PsEF*, *UI8S*, *PsGAP* and *PsACT* were used as internal controls. Before quantification of the expression level of each target genes, the Ct numbers for each internal control and target gene were corrected with an internal calibrator and also by using the average correction factor determined for each of the four reference genes. Error bars represent the +/- one SD calculated for the combined technical and biological replicates.

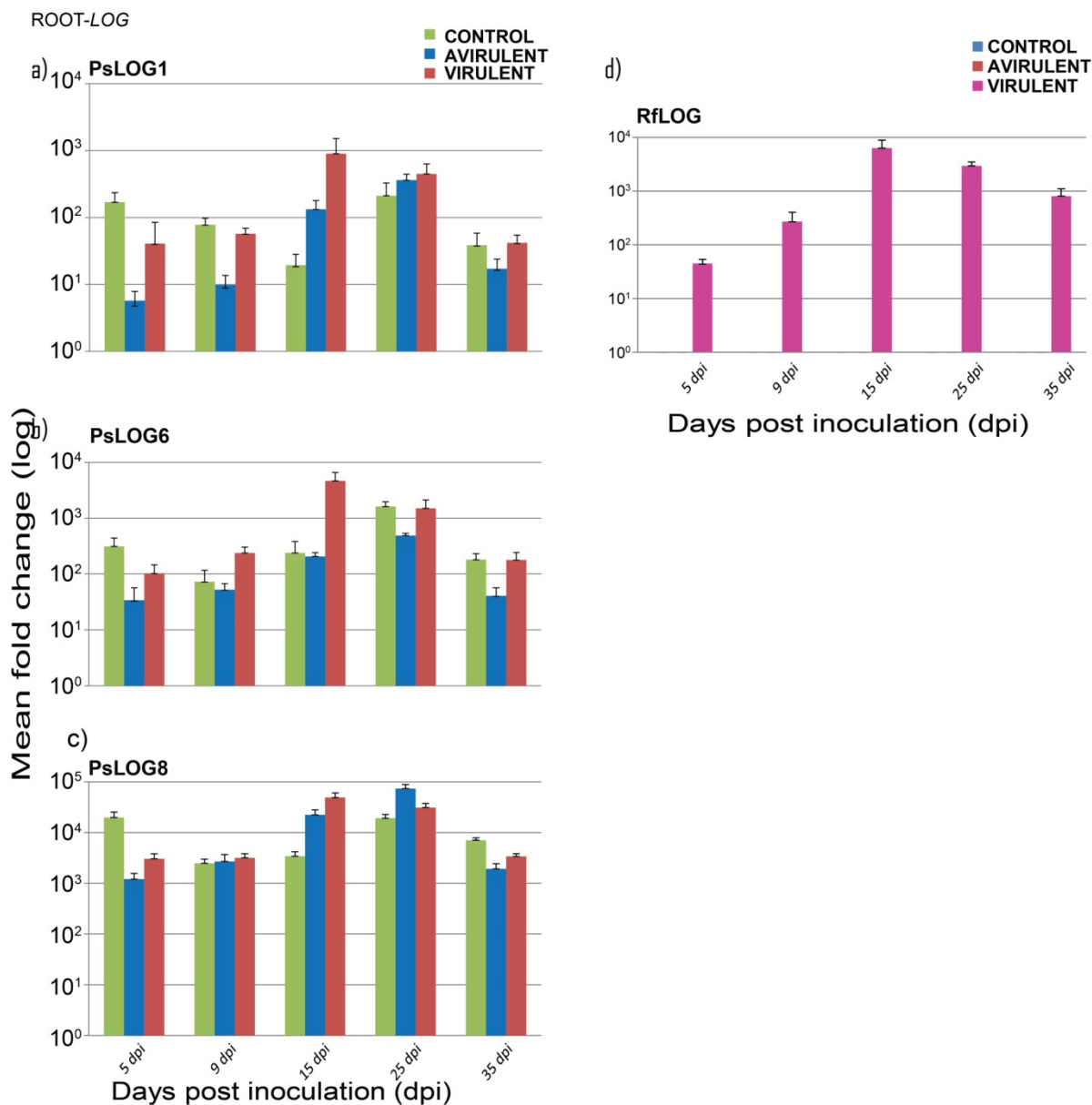


Figure 4.17 Relative expression of *PsLOG1*, 6, 8 and *RfLOG* in *P. sativum* root tissue. a) *PsLOG1* gene b) *PsLOG6* gene c) *PsLOG8* gene d) *RfLOG* gene. Data are means of relative mRNA levels in fold changes (log) detected using three technical replicates for each of two biological replicates. *PsEF*, *UI8S*, *PsGAP* and *PsACT* were used as internal controls. Before quantification of the expression level of each target genes, the Ct numbers for each internal control and target gene were corrected with an internal calibrator and also by using the average correction factor determined for each of the four reference genes. Error bars represent the +/- one SD calculated for the combined technical and biological replicates.

The expression of *PsLOG1*, 6 and 8 was shown to be high in vir-shoot at 15dpi. The vir-shoot mostly had low or same level of expression as con-shoot and avir-shoot in the three *PsLOG* gene family members in all growth stages except at 15 dpi.

Mainly the avir-shoot had high level of expression in later stage of growth (25dpi-35dpi) in *PsLOG1*, 6 and 8. *PsLOG6* expression was high at 9 dpi in avir-shoot (Figure 4.18).

As expected the *RfLOG* had low level of expression in con-shoot and avir-shoot at all growth stages (4.18d). *RfLOG* expression was high at 15 dpi in case of vir-shoot. The expression increased to 56.8-fold at 15 dpi and reduced to 9.8-fold at 25 dpi then later increased at 35 dpi (14.9-fold) than baseline expression at 5 dpi in vir-shoot (Figure 4.18).

Even in shoots it was noticed that the *RfLOG* expression in vir-shoot was higher than *PsLOG1* and 6 at 15 dpi (Figure 4.18). On other growth stages the three *PsLOG* genes expression was higher compared with *RfLOG* in vir-shoot.

In general, when the three *PsLOGs* are compared for their expression in the pea tissues, it was seen that mainly *PsLOG1* and 6 genes expressed most highly in shoots (4578-fold and 7738-fold respectively), whereas, *PsLOG8* expressed highly in cotyledons (1,912,771-fold) in vir-cot.

4.3.4.2.3 Cytokinin oxidases/ dehydrogenases (*PsCKX*)

Cotyledons: Of the five *PsCKX* gene family members isolated, *PsCKX2* expression was highest at 4 hpi (initially) (399-fold), but in *PsCKX1*, 3, 4 and 5 expressions were relatively low (40 to 175-fold) in con-cot (Figure 4.19). This level increased from 2 to 5 dpi in *PsCKX1*, 2 and 5 but mainly the *PsCKX* genes had low expression from 15 to 35 dpi in con-cot. The expression level of *PsCKX5* was high relative to the other *PsCKX* genes in con-cot.

PsCKX1 and 3 was most highly expressed in all growth stages (except at 2dpi) in vir-cot compared to avir-cot and con-cot. The *PsCKX* gene families had high level of expression in most of the growth stages in vir-cot (Figure 4.19). Except at 2 dpi, *PsCKX3* expression in vir-cot was noticeable at all other time points.

SHOOT-LOG

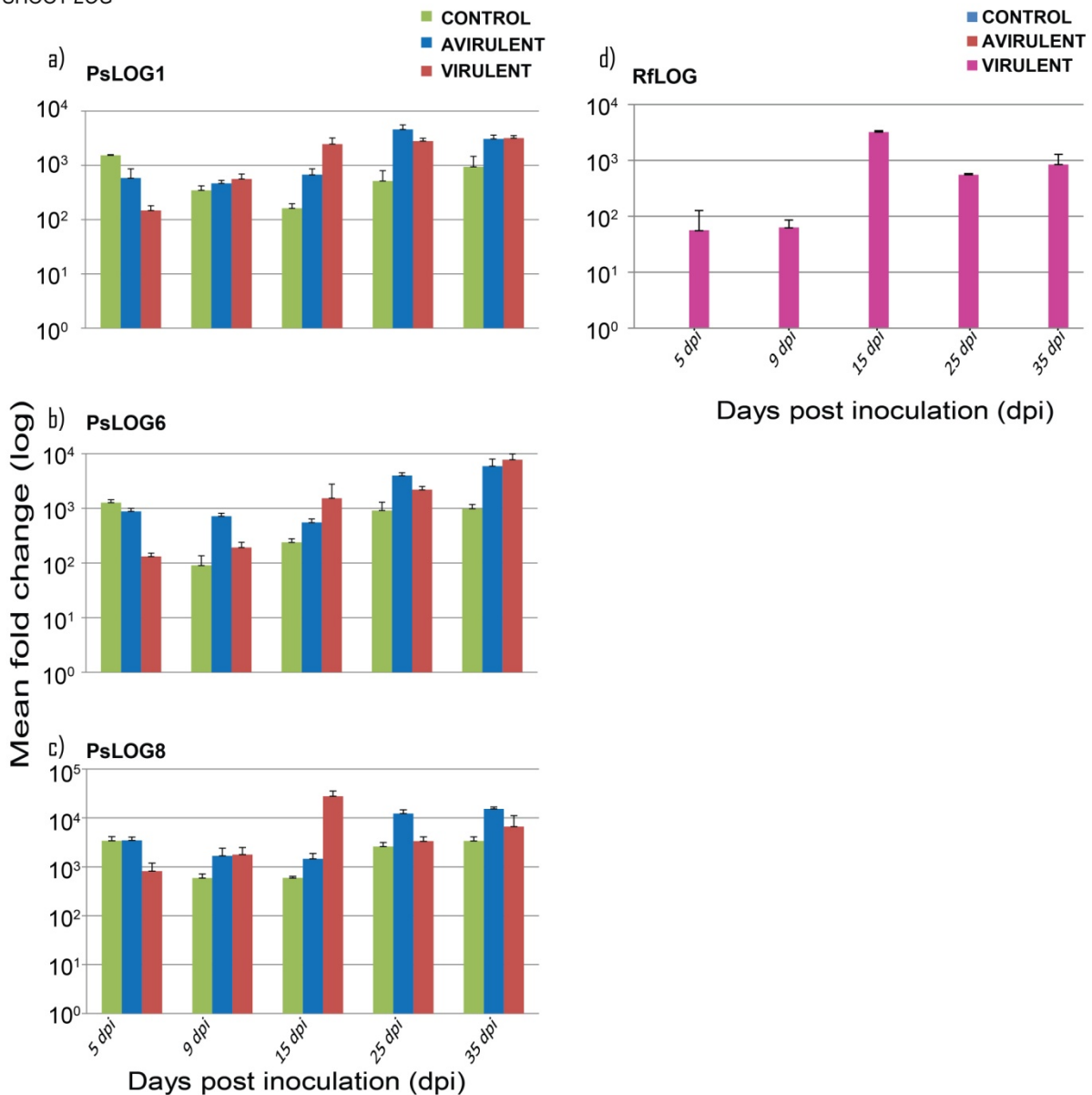


Figure 4.18 **Relative expression of *PsLOG1*, 6, 8 and *RfLOG* in *P. sativum* shoot tissue.** a) *PsLOG1* gene b) *PsLOG6* gene c) *PsLOG8* gene d) *RfLOG* gene. Data are means of relative mRNA levels in fold changes (log) detected using three technical replicates for each of two biological replicates. *PsEF*, *UI8S*, *PsGAP* and *PsACT* were used as internal controls. Before quantification of the expression level of each target genes, the Ct numbers for each internal control and target gene were corrected with an internal calibrator and also by using the average correction factor determined for each of the four reference genes. Error bars represent the +/- one SD calculated for the combined technical and biological replicates.

The expression of *PsCKX4* and 5 in avir-cot was higher at 25 and 35 dpi compared to other growth stages (Figure 4.19). In other *PsCKX* gene families the level of expression was low in avir-cot from 4 hpi to 35 dpi compared to vir-cot and con-cot.

The *RfCKX* expression was highest at 5 dpi, with steady decrease until 15 dpi and slight increase was observed at 25 dpi. The expression of *RfCKX* in con-cot and avir-cot was slightest (Figure 4.19).

Root: The five *PsCKX* genes expression was high at 5 dpi (Figure 4.20) relatively decreased at 9 dpi (except *PsCKX1*) and gradually increased at 25 dpi, but by 35 dpi decreased in con-root. *PsCKX1* had high expression at 25 dpi compared to avir-root and vir-root.

The vir-root had high expression level at 15dpi -25dpi which was mostly higher at 15dpi compared to con-root and avir-root in all *PsCKX* gene families.

The avir-root had lowest expression at 5dpi in all *PsCKX* gene family members then increased with growth and highest at 25dpi, (except *PsCKX1*) and reduced considerably at 35dpi. The expression profile of *PsCKX* gene families revealed high expression in vir-root compared to con-root and avir-root, in most of the growth stages with few exceptions.

The microbial *CKX* (*RfCKX*) expression was high at 25 dpi (18.57-fold) than the baseline expression at 5 dpi and reduced at 35 dpi in vir-root. The expression was slight in case of con-root and avir-root (Figure 4.20).

The phenomenon of similar or increased *RfCKX* expression than *PsCKX* was noticed in all the *PsCKX* gene families except in *PsCKX5* (Figure 4.20) in most of the growth stages in vir-root.

Shoot: The relative expression of the five *PsCKX* gene family members isolated was low at all growth stages in con-shoot. *PsCKX5* expressed highly at 5dpi compared to avir-shoot and vir-shoot (Figure 4.21).

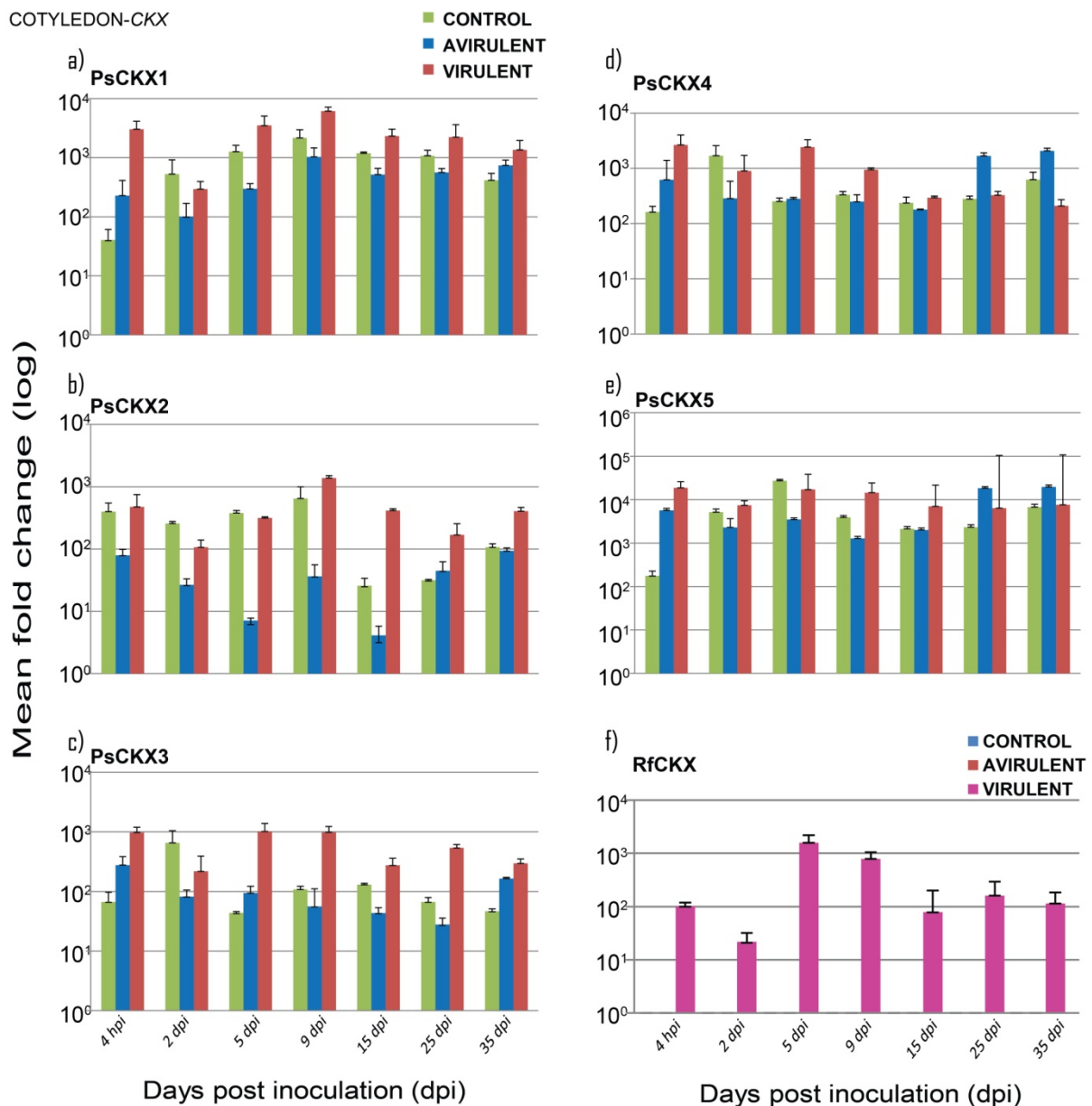


Figure 4.19 **Relative expression of *PsCKX1*, *2*, *3*, *4*, *5* and *RfCKX* in *P. sativum* cotyledons tissues.** a) *PsCKX1* gene b) *PsCKX2* gene c) *PsCKX3* gene d) *PsCKX4* gene e) *PsCKX5* gene f) *RfCKX* gene. Data are means of relative mRNA levels in fold changes (log) detected using three technical replicates for each of two biological replicates. *PsEF*, *U18S*, *PsGAP* and *PsACT* were used as internal controls. Before quantification of the expression level of each target genes, the Ct numbers for each internal control and target gene were corrected with an internal calibrator and also by using the average correction factor determined for each of the four reference genes. Error bars represent the +/- one SD calculated for the combined technical and biological replicates.

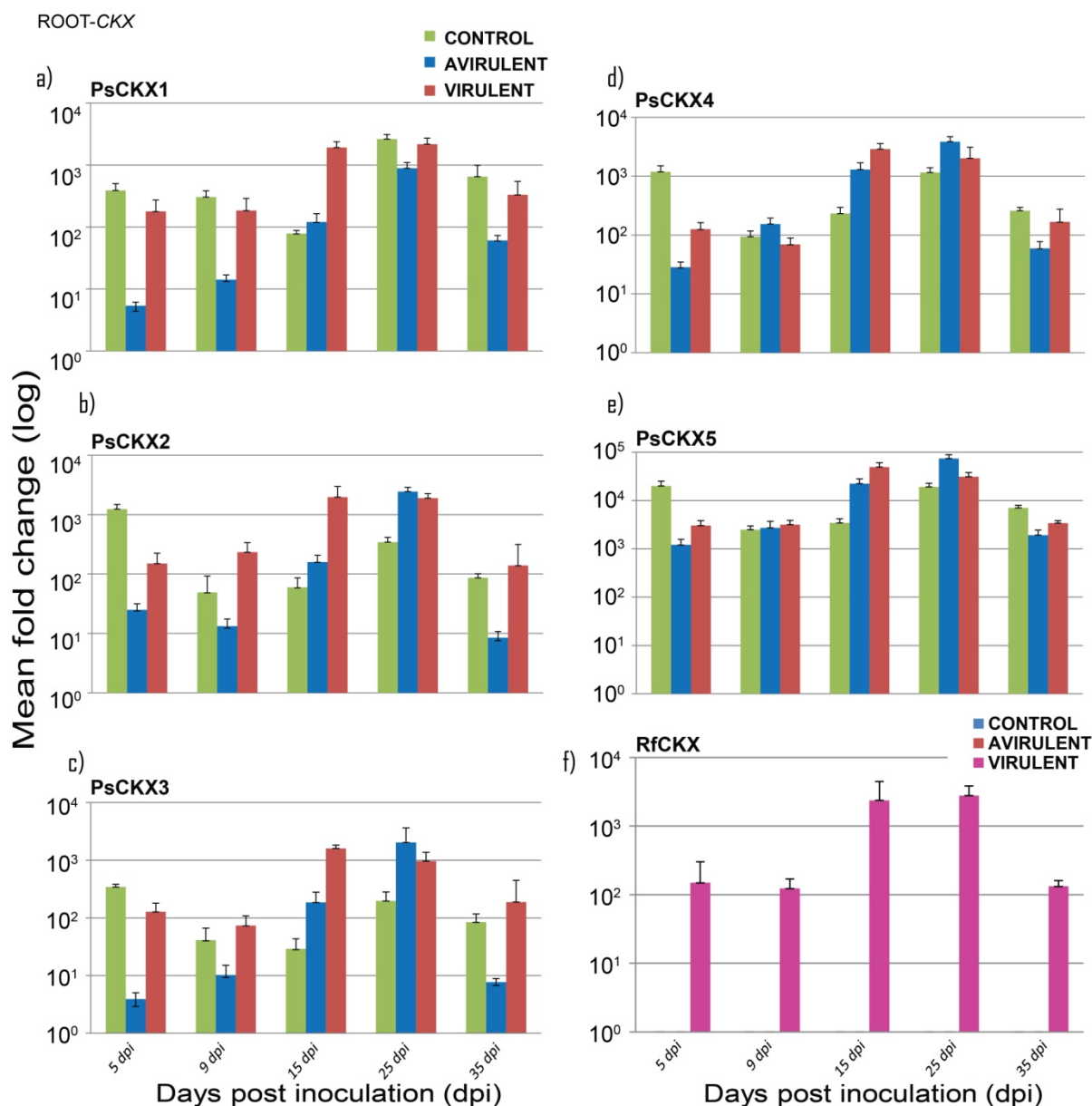


Figure 4.20 **Relative expression of *PsCKX1*, 2, 3, 4, 5 and *RfCKX* in *P. sativum* root tissues.** a) *PsCKX1* gene b) *PsCKX2* gene c) *PsCKX3* gene d) *PsCKX4* gene e) *PsCKX5* gene f) *RfCKX* gene. Data are means of relative mRNA levels in fold changes (log) detected using three technical replicates for each of two biological replicates. *PsEF*, *U18S*, *PsGAP* and *PsACT* were used as internal controls. Before quantification of the expression level of each target genes, the Ct numbers for each internal control and target gene were corrected with an internal calibrator and also by using the average correction factor determined for each of the four reference genes. Error bars represent the +/- one SD calculated for the combined technical and biological replicates.

The five *PsCKX* genes expressed highly in vir-shoot compared to con-shoot and avir-shoot at most of the growth stages, especially in later stages of growth (15dpi-35dpi).

Except *PsCKX5*, all the other *PsCKX* genes expression was high at 5 dpi in avir-shoot. In all the other sampling stages the avir-shoot had low or similar expression level compared to vir-shoot in the five *PsCKX* genes studied (Figure 4.21).

The *RfCKX* expression in vir-shoot reduced considerably at 9 dpi (0.13-fold), increased at 15 dpi (9.11-fold) and later reduced at 35 dpi (1.22-fold) than the baseline expression at 5 dpi. As in previous cases, the control and avir-shoot had least *RfCKX* expression in all time points (Figure 4.21).

The *PsCKX* gene family members isolated exhibited differential expression in the pea tissues: *PsCKX1*, 2 and 4 expressed highly in shoots whereas *PsCKX3* and 5 expressed prominently in root. The five *PsCKXs* studied had least expression in cotyledon, except *PsCKX1* which was relatively higher.

4.3.4.2.4 Pea Response Regulators (*PsRR*)

Cotyledon: Generally, *PsRR3*, 5, 6 and 9 genes were most highly expressed at 2 dpi but in most of other growth stages the expression was relatively low compared to vir-cot and avir-cot. *PsRR9* expression noticeably reduced in con-cot from 9 d post imbibitions (Figure 4.22).

The expression level of the three response regulators *PsRR3*, 5 and 9 was high at 5 and 9 dpi in vir-cot. Based on the expression profile, it was seen that *PsRR3*, 5 and to some extent *PsRR9* had highest level of expression in vir-cot compared to con-cot and avir-cot. In case of *PsRR6*, the expression was relatively very high at 4 hpi (initial) in vir-cot then decreased at later time points (Figure 4.22).

With avir-cot it was noticed that the expression was generally lower than vir-cot in most of the days in all *PsRR* gene families except in *PsRR6* where it was higher at 25 and 35 dpi. *PsRR9* expression was depressed in avir-cot at 5, 9 and 15 dpi (Figure 4.22).

SHOOT-CKX

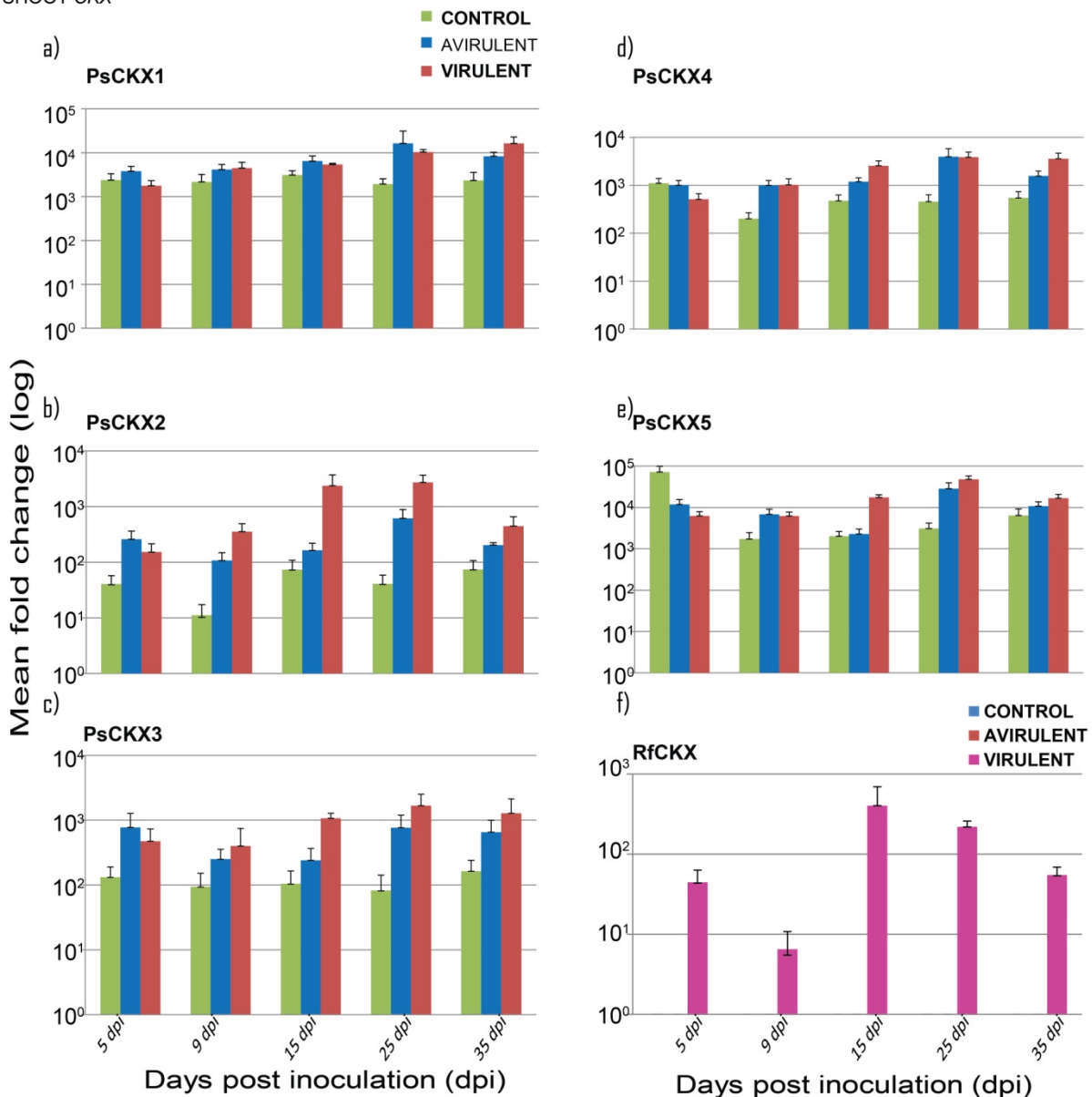


Figure 4.21 **Relative expression of *PsCKX1*, 2, 3, 4, 5 and *RfCKX* *P. sativum* shoot tissues.** a) *PsCKX1* gene b) *PsCKX2* gene c) *PsCKX3* gene d) *PsCKX4* gene e) *PsCKX5* gene f) *RfCKX* gene. Data are means of relative mRNA levels in fold changes (log) detected using three technical replicates for each of two biological replicates. *PsEF*, *U18S*, *PsGAP* and *PsACT* were used as internal controls. Before quantification of the expression level of each target genes, the Ct numbers for each internal control and target gene were corrected with an internal calibrator and also by using the average correction factor determined for each of the four reference genes. Error bars represent the +/- one SD calculated for the combined technical and biological replicates.

Root: The *PsRR* genes exhibited fluctuating expression in con-root over the 35 days (Figure 4.22). In general, in most of the growth period the expression level of the *PsRR* genes in con-root was lower than vir-root, except in *PsRR6* and 9 expressions was high at 5 dpi (Figure 4.23). *PsRR3* and 9 had higher level of expression in con-root at 35 dpi compared to avir-root and vir-root.

Similar to cotyledon tissues, the four *PsRR* genes expression was elevated in vir-root among the three treatments studied (Figure 4.23). The four *PsRRs* mainly expressed highly in vir-root t 15 and 25 dpi.

In case of avir-root, *PsRRs* genes expression level was mainly very low in most of the time points. Sometimes the *PsRRs* expression was negligible. The avir-root had lower *PsRRs* genes expression compared to con-root and vir-root at all time points (Figure 4.23).

Shoot: The response regulators (*RR*) in shoot had low expression in con-shoot at all growth stages. (Figure 4.24).

Similar to cotyledons and roots, the expression of the four *PsRR* gene families in the vir-shoot was elevated at most growth stages compared to con-shoot.

The *PsRR3*, 5 and 6 showed high expression level at 5 dpi in avir-shoot compared to con-shoot and vir-shoot and then reduced their expression in all other stages of growth in the four *PsRR* gene families.

In general across the tissues the *PsRR* gene family members had elevated level of expression in *R. fascians* virulent strain (602) inoculated tissues compared to control and avirulent plant tissues.

Of the four isolated *PsRR* gene family members, *PsRR3* and 5 expressed highly in cotyledon. *PsRR6* and 9 expressions were high in shoot and *PsRR6* expression was high also in cotyledon. Mainly *PsRR* regulators expression was relatively very low in roots (192-fold to 1,348-fold) (Figure 4.23) compared to cotyledon (440- fold to 13,016-fold) and shoot (1,980-fold to 14,569-fold) (Figures 4.22 and 4.24).

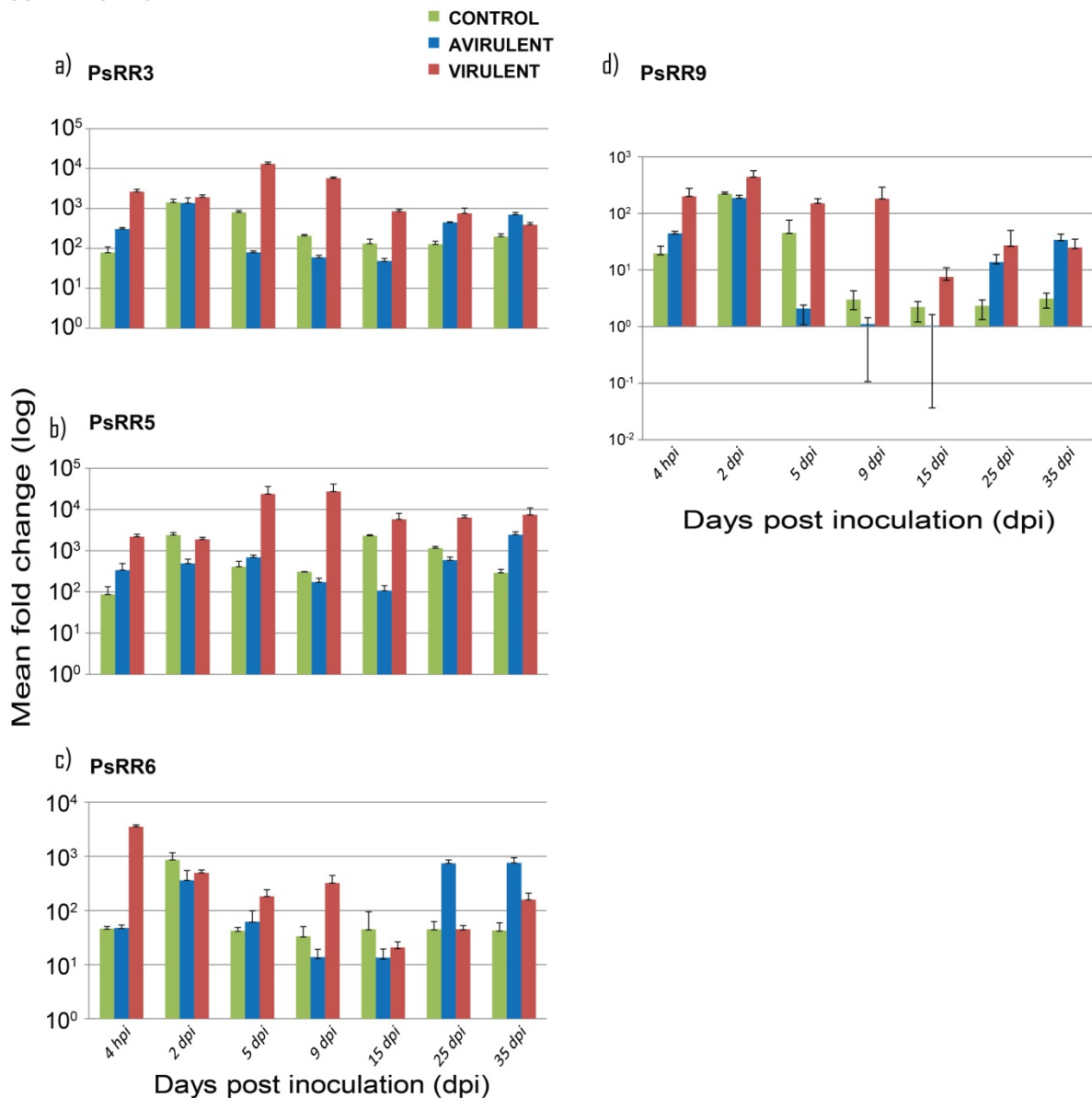


Figure 4.22 **Relative expression of *PsRR3*, *5*, *6* and *9* in *P. sativum* cotyledon tissues.** a) *PsRR3* gene b) *PsRR5* gene c) *PsRR6* gene d) *PsRR9* gene. Data are means of relative mRNA levels in fold changes (log) detected using three technical replicates for each of two biological replicates. *PsEF*, *UI8S*, *PsGAP* and *PsACT* were used as internal controls. Before quantification of the expression level of each target genes, the Ct numbers for each internal control and target gene were corrected with an internal calibrator and also by using the average correction factor determined for each of the four reference genes. Error bars represent the +/- one SD calculated for the combined technical and biological replicates.

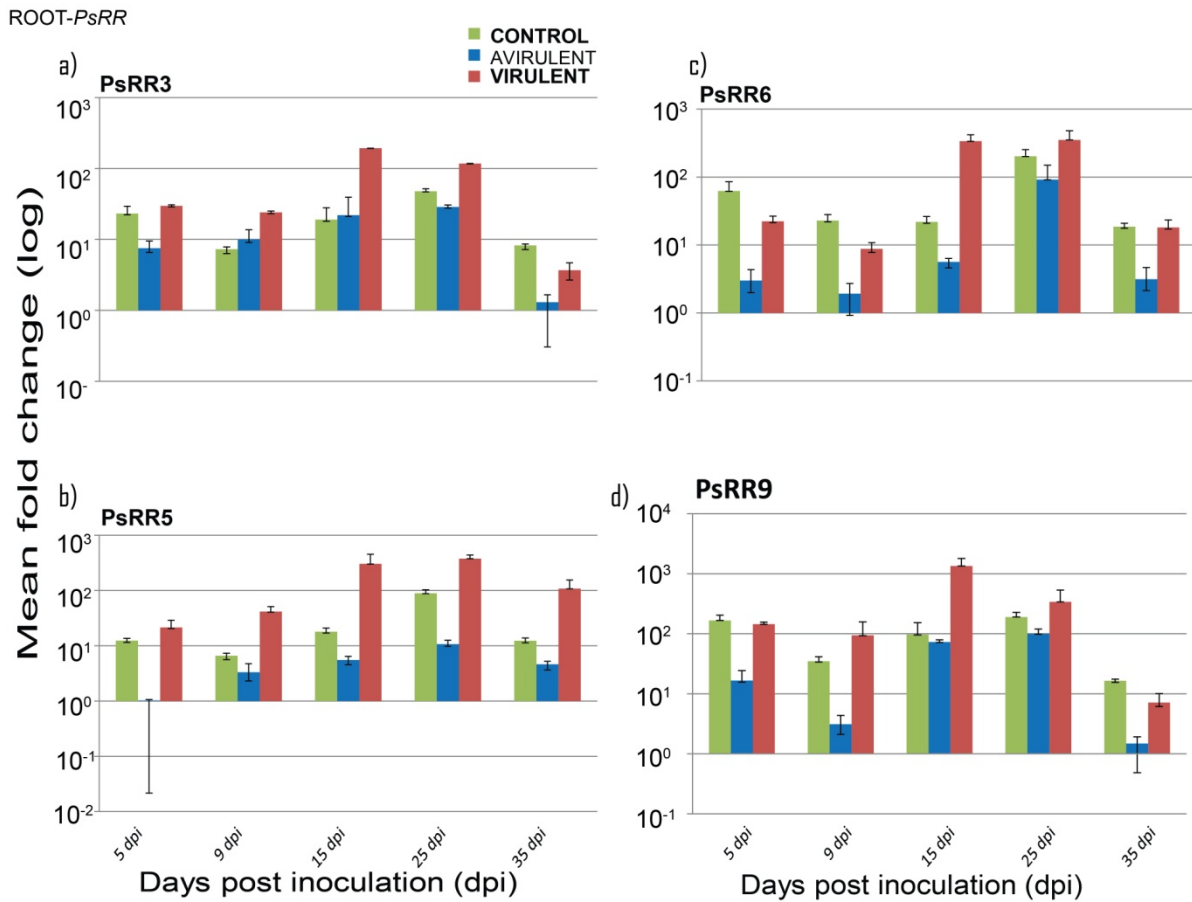


Figure 4.23 **Relative expression of *PsRR3*, *5*, *6* and *9* in *P. sativum* root tissues.**

a) *PsRR3* gene b) *PsRR5* gene c) *PsRR6* gene d) *PsRR9* gene Data are means of relative mRNA levels in fold changes (log) detected using three technical replicates for each of two biological replicates. *PsEF*, *U18S*, *PsGAP* and *PsACT* were used as internal controls. Before quantification of the expression level of each target genes, the Ct numbers for each internal control and target gene were corrected with an internal calibrator and also by using the average correction factor determined for each of the four reference genes. Error bars represent the +/- one SD calculated for the combined technical and biological replicates.

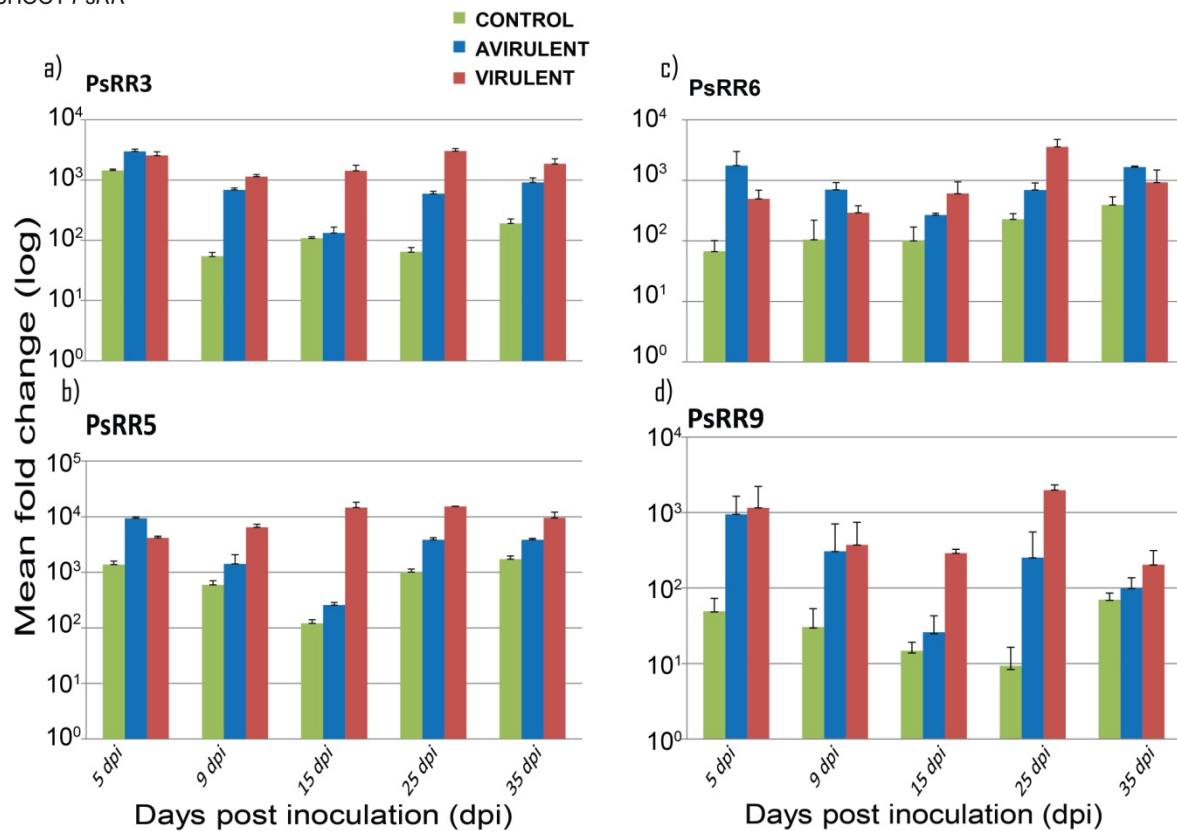


Figure 4.24 **Relative expression of *PsRR3*, 5, 6 and 9 in *P. sativum* shoot tissues.** a) *PsRR3* gene b) *PsRR5* gene c) *PsRR6* gene d) *PsRR9* gene Data are means of relative mRNA levels in fold changes (log) detected using three technical replicates for each of two biological replicates. *PsEF*, *U18S*, *PsGAP* and *PsACT* were used as internal controls. Before quantification of the expression level of each target genes, the Ct numbers for each internal control and target gene were corrected with an internal calibrator and also by using the average correction factor determined for each of the four reference genes. Error bars represent the +/- one SD calculated for the combined technical and biological replicates.

4.4 Discussion

4.4.1 Cytokinin synthesis, metabolic and response regulator gene identification and characterisation

In this project, multi-gene family members of key cytokinin genes involved in biosynthesis, metabolism and response were isolated from *P. sativum* and their relative expression was studied to understand the spatial and temporal expression pattern of the multi-genes which has been confirmed in number of plant species. The key genes *IPT*, *LOG*, *CKX* and *RR* multi-gene families were isolated from the pea transcriptome analysis. But not all the gene family members could be isolated because the cDNA mix of pea tissues used for isolation were from pea plants grown until 35 days. Due to differential expression pattern of members of the cytokinin multi-genes not all genes expressed within this time period.

As expected the phylogenetic analysis of the *IPT* gene family members showed a clear split between the monocot and dicot *IPT* genes. The dicot genes had two distinct clades, one containing *AtIPT5*, *AtIPT7* along with legumes *PsIPT1*, *PsIPT2*, *LjIPT2*, *LjIPT4* and *GmIPT5(2)* and a second clade containing *AtIPT1*, *AtIPT3*, *AtIPT4*, *AtIPT6*, *AtIPT8* along with legumes *PsIPT3*, *CaIPT1*, *CaIPT3*, *GmIPT3*, *GmIPT5*, *LjIPT1* and *LjIPT3*. This result indicates that the isolated *PsIPT1*, *PsIPT2* and *PsIPT3* are homologous with *AtIPTs* and other legume *IPTs*. Additionally, the isolated *PsIPT* gene family members isolated represent both the clades of dicot. The phylogenetic tree was rooted with *R. fascians FasD (Rf(D188))* shows the sequence dissimilarities between *PsIPTs* and *RfIPT*. The isolated *RfIPT* revealed sequence similarity with *Rf(D188)FasD* but not with isolated *PsIPTs*. The result of sequence analysis through phylogenetic tree construction is consistent with Takei et al. (2001), Kakimoto (2001), Miyawaki et al. (2004), Sakamoto et al. (2006) and Brugière et al. (2008).

The plant *LOG* genes diverged into dicot and monocot as the two clades except *OsLOGL7* differing to the observation made by Kuroha et al. (2009). The dicot *LOG* genes had three clades, one containing *AtLOG1*, *AtLOG3*, *AtLOG4* and *AtLOG6* along with legumes *GmLOG1*, *GmLOG3* and isolated *PsLOG1* with subgroups. The second clade consisted of *AtLOG8*, *AtLOG9*, *AtLOG5* with *PsLOG6*, *PsLOG8* and *GmLOG6* and 8 along with monocot *OsLOGL7*. The third clade had *AtLOG2*, *AtLOG7* and *GmLOG7*. This result was not similar to the phylogenetic tree analysis of Kuroha et al. (2009) as the *AtLOGs* and legume *LOGs*

separated from the rice *LOGs* separately except *OsLOGL7*. The isolated *PsLOG1*, *PsLOG6* and *PsLOG8* had high sequence similarities with *GmLOG3*, *GmLOG6* and *GmLOG8* respectively. The isolated *RfLOG* was used to root the tree due to its sequence dissimilarities from the isolated *PsLOGs*.

The *CKX* genes show relatively high level of sequence similarity and contain several conserved domains (Schmülling et al., 2003). The phylogenetic analysis grouped the monocot *ZmCKXs* to one clade and dicot *AtCKXs* with legume *CKXs* to another clade. The *AtCKX2*, *AtCKX3*, *AtCKX4* grouped to one clade and *AtCKX5* and *AtCKX7* to another clade as predicted by Schmülling et al. (2003) and Ashikari et al. (2005). The five *PsCKX* genes had sequence similarities with *AtCKXs* and legumes *CKX*. The whole phylogenetic analysis was rooted with *Rf*(D188) *fasE*. The *RfCKX* gene had high sequence dissimilarity with the *PsCKXs* highlighting the discrimination between pea *CKX* and *R. fascians* *CKX*.

The *Arabidopsis* response regulators (*ARR*) and Pea response regulators (*PsRR*) based on phylogenetic analysis formed two major clades with type A-RRs and type B-RRs in agreement with Hutchison and Kieber (2002) and To et al. (2004). *PsRR6* grouped with *GmRR6* and *PsRR5* with *MtRR5*. The *PsRR3* had sequence similarities with *MtRR3*, *GmRR3* and *PvRR1* formed a clade. *PsRR9* grouped with A –types *ARR9* and *ARR16*, and had high sequence similarity with *GmRR9* (Figure 4.4). It is highly likely that the *PsRR3*, *PsRR6*, *PsRR5* and *PsRR9* isolated in this project are of the type-A RR. Each of the isolated *PsRRs* had high sequence homology with their respective *GmRR* and *MtRRs* gene families. The monocot rice *RR* formed an out group highlighting the monocot and dicot sequence dissimilarity in response regulator genes.

4.4.2 Quantitative expression of cytokinin biosynthesis, metabolic and response regulator genes in *P. sativum* infected with *R. fascians*.

To gain a picture of the interplay between *R. fascians* cytokinin genes (*RfIPT*, *RfLOG* and *RfCKX*) and the multi-gene family members of pea *IPT*, *LOG* and *CKX* during the infection of pea by *R. fascians*, a key factor was to be able to differentiate the expression of *R. fascians* *IPT*, *LOG* and *CKX* from *P. sativum* *IPT*, *LOG* and *CKX* genes. To achieve this target, the primers were designed to discriminate the expression of the microbe and the plant.

The primers designed to discriminate the pea and *R. fascians* cytokinin genes was confirmed by testing the expression in pea tissues, *R. fascians* avirulent strain 589 culture and the virulent strain 602 culture cDNAs in RT-qPCR. *RfIPT*, *RfLOG* and *RfCKX* expressions were negligible in cotyledons, roots, shoots in control and infected by the avirulent strain 589 and the avirulent 589 culture cDNA, but were very high in cotyledons, roots, shoots infected by the virulent strain 602 and the virulent strain 602 culture cDNA. This confirmed that the designed primers discriminated between the microbial (*R. fascians*) cytokinin genes and plant (*P. sativum*) cytokinin genes. The *RfIPT*, *RfLOG* and *RfCKX* expressions were higher in the virulent strain 602 culture compared to the virulent strain 602 infected plant tissues (Figure 4.14 j, k and l). The *RfIPT*, *RfLOG* and *RfCKX* expressions were insignificant in mock inoculated control and the avirulent strain 589 inoculated pea plant tissues which confirmed that the avirulent strain 589 did not possess the *fasD* (Crespi et al., 1992, Galis et al., 2005b, Stange et al., 1996) and *fasE* genes (Galis et al., 2005a, Galis et al., 2005b). So, through both *R. fascians* and pea *IPT*, *LOG* and *CKX* genes expression profile the fact of discrimination in expression between plant and microbe was established in this project.

Generally, in cotyledons infected by the virulent strain 602 *RfIPT*, *RfLOG* and *RfCKX* expressions were up-regulated initially at 4 hpi or 5 dpi but decreased with time, whereas, in the roots and shoots there was gradual increase from 5 dpi, peaked at 15 dpi and later decreased. Pertry et al. (2010) noted similar response of *fasE* and *fasF* expression through GUS activity in tobacco which peaked mainly between 7 and 14 dpi then decreased gradually to a steady state. They suggested that *fas* gene expression is necessary at the beginning of the interaction to trigger symptom development and, subsequently, much lower activity, mediated by both FasA-FasD and FasF pathways is sufficient to maintain the hyperplasia.

The understanding of cytokinin biosynthesis and metabolism has greatly progressed in the past few years due to the identification and isolation of key genes involved in these processes (Kieber and Schaller, 2010). In this study, members of *IPT*, *LOG*, *CKX* and *RR* multi-gene families of *P. sativum* were isolated and their expression in various tissues studied following inoculation of *P. sativum* with *R. fascians*. Initially, the discussion will focus on the expression of multi-gene family members in the control (normal) plants.

The three *IPT* gene family members used in this study, *PsIPT1*, *PsIPT2* and *PsIPT3* showed specific, but similar expression patterns in roots and shoot development of mock-inoculated control pea plants with few exceptions. In cotyledons, *PsIPTs* genes expressed highly at an early stage of seed germination indicating a role of cytokinin in germination as suggested by Mok and Mok (2001). The three *PsIPTs* expressed highly at 5 dpi, in all the three tissues tested and reduced at 9 dpi. Takei et al. (2001a) through analysis of nine *AtIPT* gene expression profiles indicated that not only root meristem but also young leaves, phloem tissues, embryos and nodal stem, were sites of cytokinin synthesis. The striking low expression of *IPT* genes in pea shoots at 9 dpi may indicate reduced cytokinin synthesis. This was also noticed by Tanaka et al. (2006), who suggested that the low *PsIPT1* and *PsIPT2* expression in 7 day old seedlings might lead to suppression of pea axillary bud growth. The pea roots exhibited lower *PsIPTs* expression at 9 dpi. A similar situation was observed by Chang et al. (2013) in *Arabidopsis* at 6 d after germination who suggested that the cytokinin deficiency might allow the initiation of root primordia and lateral root development. *PsIPTs* expression varied in cotyledons, roots and shoots during growth of plant.

The tissue specificity of *PsIPT1*, *PsIPT2* and *PsIPT3* was observed in the tissues tested for expression. *PsIPT1* expressed highly in shoots and cotyledon compared to root, *PsIPT2* and *PsIPT3* in roots and shoots than cotyledons indicating spatial and temporal expression pattern in the *PsIPT* gene families. The expression profiles of *AtIPT* genes exhibit considerable discrimination within the diverse range of plant tissues and organs (Miyawaki et al. 2004). The *PsIPT1* and *PsIPT2* identified and isolated from the pea transcriptome was most similar to *PsIPT1* and *PsIPT2* from BLAST GenBank sequences with respect to its sequence alignment (Tanaka et al. 2006). In terms of expression profile, Tanaka et al. (2006) showed that *PsIPT1* and *PsIPT2* have been associated with breaking of apical dominance in axillary buds with low expression in roots. This pattern of expression was noticed in *PsIPT1* but did not agree with *PsIPT2* expression which was high in roots. Even though *PsIPT1* and *PsIPT2* sequence similarities were close to *AtIPT5* and *AtIPT7* the tissue specificity expression varied, where *PsIPT2* expression was more similar to *AtIPT5* and *PsIPT1* expression similar to *AtIPT7* expression, which was high in trichomes of young leaves and the root elongation region (Miyawaki et al. 2003). *GmIPT5* exhibited transcript abundance in the leaves of soybean (Le et al., 2012).

The *PsIPT3* grouped with *CaIPT1* and *LjIPT1* with high degree of sequence similarity and formed into the clade containing *Arabidopsis IPTs*: *AtIPT1*, 4, 6 and 8. *PsIPT3* expressed highly in roots and germinating cotyledon compared to shoot which compares well with *AtIPT1* expression in primary roots and cotyledons in seedlings soon after germination, as well as *AtIPT4* and *AtIPT8* expression patterns in seeds and early stage of seed development (Miyawaki et al. 2004).

PsLOG1, *PsLOG6* and *PsLOG8* expression pattern was similar in cotyledons, roots and shoots which had the same profile as the three *PsIPTs*. Initially (4 hpi) the *PsLOGs* expression was low, increased at 2 and 5 dpi, reduced at 9 dpi and 15 dpi and higher at 25 dpi mainly which was similar to the expression profile of *PsIPTs*. *PsLOGs* and *PsIPTs* expression similarity in cotyledon, root and shoot tissues in this study supports the statement made by Kuroha et al. (2009) that the expression of *IPT* and *LOG* might also overlap. This can be seen in *AtLOGs* (Kuroha et al. 2009) and *AtIPTs* (Miyawaki et al. 2004 and Takei et al. 2004 a) expression in lateral root primordia, ovules, root and leaf vascular tissues. Of the three *PsLOGs* isolated, *PsLOG1* and *PsLOG6* predominant expression in shoots supports the Kurakawa et al. (2007) work showing strong expression localisation of *LOGs* in shoot meristem tips, and activation of cytokinins in a specific development domain

The isolated *PsLOG1* formed a subgroup in the clade with *AtLOG1*, 3, 4 and 6. The *AtLOG3*, *AtLOG4* and *AtLOG1* through *LOG_{pro}*: GUS fusion staining was seen to be mainly expressed in root tips, primary roots, root primordia, shoot apical meristem and cotyledons (Kuroha et al. 2009). *PsLOG1* expression was predominantly in shoots compared to roots and cotyledons. Tokunaga et al. (2012) using multiple mutants of *AtLOG* showed the importance of *AtLOG7* for maintenance of shoot apical meristem size and normal root growth together with *AtLOG3* and *AtLOG4*. *PsLOG8* grouped with *GmLOG8*, *AtLOG8* and *AtLOG9* with high sequence similarity and expressed predominantly in cotyledons. Interestingly, *OsLOGs* were localized in shoot meristem tips (Kurakawa et al. 2007) and *AtLOG8* were shown to be expressed in cotyledons, mature roots, flowers and stems. *PsLOG6* grouped with *GmLOG6* indicating sequence similarity to *AtLOG8* and *AtLOG9*. The *PsLOG6* expressed highly in shoot compared to root and cotyledon revealing differential expression of *LOGs* in various pea tissues during plant growth as shown by Kuroha et al. (2009). The predominate expression of *PsLOG8* in cotyledons highlights the potential of *LOG* gene, where recently,

Eviatar-Ribak et al. (2013) showed that activation of *TLOG1* ectopic expression in tomato led to the outgrowing of tomato buds to generate aerial minitubers and suggested that cytokinins may function in storage-organ formation as universal regulators.

The pattern of expression of the five *PsCKXs* isolated in this study was similar at most of the time points tested in cotyledons, roots and shoots. In the case of cotyledons, the five *PsCKXs* expression was low initially except in *PsCKX2*, increased until 5 dpi in *PsCKX1*, *PsCKX2* and *PsCKX5*. With growth of plant the *PsCKXs* expression decreased or remained steady in cotyledons. In roots, *PsCKXs* expression was mainly high at 5 dpi, reduced with growth and peaked at 25 dpi. But in conr-shoot *PsCKXs* expression was low at all tested time points except with *PsCKX5* (high at 5 dpi). Vaseva-Gemisheva et al. (2004) observed fluctuating profiles of *CKX* levels during the vegetative development in two cultivars of pea with 90% activity in roots, but *PsCKXs* expression was in general low in control roots and shoots at most of the time points tested in this study.

The relative expression differed in cotyledons, roots and shoots, agreeing with differential expression of *AtCKXs* reported by Werner et al. (2003) from a promoter-GUS fusion analysis of individual *AtCKX* multi-genes. The *AtCKX* genes were localised to specific domains in the root and shoot (Werner et al. 2006). *PsCKX1*, *PsCKX2* and *PsCKX4* expressed highly in shoots, *PsCKX3* and *PsCKX5* predominately in roots and *PsCKX1* expression was also in cotyledons. Vaseva-Gemisheva et al. (2005) showed high expression levels of *PsCKX1* and *PsCKX2* in the leaves with RT-qPCR analysis and also differential expression in the leaf and root tissues of control plants similar to the result of this study. The five *PsCKXs* isolated were homologous to *AtCKXs* and legume *CKXs* (*M. truncatula* and *G. max*). Even with sequence similarities between *PsCKXs* and *AtCKXs* the expressions in tissues were not similar to Werner et al. (2006) observation, except *PsCKX3* expression resembled *AtCKX6* expressions in roots and *PsCKX4* resembled *AtCKX1* expressions in shoots. The isolated *PsCKX* gene family members had high sequence similarities with *GmCKX* gene family members. Based on Le et al. (2012) observation of 14 *GmIPTs* and 17 *GmCKXs* expression in RT-qPCR under normal and drought conditions, *GmCKX3* and *GmCKX5* expression was hardly detected, *PsCKX3* and *PsCKX5* with high sequence similarity with *GmCKX3* and 5, expressed mainly in roots in this study.

The isolated pea response regulators *PsRR3*, 5, 6 and 9 revealed to be type-A *RRs* through phylogenetic analysis. *PsRR3* was homologous to *PvRR1* and *GmRR3*, *PsRR3* expression was high in pea cotyledon. *PsRR5* had sequence similarity with *MtRR5* (98%) and high level of expression in pea cotyledon tissue. *PsRR6* was homologous to *GmRR6* (97%) and *PsRR9* had sequence similarities with *GmRR9* (89%). *PsRR6* and *PsRR9* expressions were high in pea shoot. Among the pea tissues, *PsRRs* expression was higher at 2 dpi in cotyledon and at 5 dpi in root but in shoot the *PsRRs* expression was low in all growth periods tested. The expression of the four *PsRRs* isolated were not prominent in roots. This may be due to low cytokinin levels, as the type-A *RRs* are negative regulators of cytokinin and are up-regulated in response to cytokinin presence (To et al. 2007). Most of the reports on the type-A response regulators are mainly from maize, rice and *Arabidopsis* (Asakura et al., 2003, Jain et al., 2006, To et al., 2004), so far there are no reports available on response regulators (*RR*) expression in legumes. Op den Camp et al. (2011) showed type-A *MtRR9* and *MtRR11* involved in root nodule symbiosis and the expression is induced by *Rhizobium* spp. Nod factor signaling.

The discussion is now based on the comparison the expression of cytokinin (*PsIPT*, *PsLOG* and *PsCKX*) multi-gene family members in control, *R. fascians* avirulent strain 589 and virulent strain 602 infected pea plants.

The expression profile of *PsIPTs* in pea seeds imbibed in *R. fascians* avirulent strain 589 and virulent strain 602 were varied in cotyledons, roots and shoots. *PsIPT1*, *PsIPT2* and *PsIPT3* expression exhibited similar pattern in cotyledons, roots and shoots of both avirulent and virulent strain inoculated plants with varied level of expression between the two treatments. The *PsIPTs* expression pattern in vir-cot were high initially (4 dpi) decreased until 9 dpi (except *PsIPT2*) peaked at 15 dpi then decreased or steady level with growth of plant. *PsIPTs* expression in avir-cot was lower compared vir-cot in most of time points except at later stages of growth (25 and 35 dpi). This does not agree with Galis et al. (2005b) result that the total cytokinin content in pea cotyledons inoculated with *R. fascians* virulent strain (602) was lower than nonvirulent strain (589) at 3, 6 and 9 dpi. The contradicting result may be due to the fact that not all gene family members of pea *IPT* were used for the expression study there might be other *PsIPTs* gene family members expressing at this time point. Depudyt et al. (2008) in transcript profiling data showed the differential expression of the 9 *AtIPT* genes on

R. fascians virulent strain D188 inoculated *Arabidopsis* leaves at 30 dpi, *AtIPT7*, *AtIPT5* were switched off, *AtIPT3* was down-regulated and *AtIPT1*, 4, 6 and 8 were not expressed in virulent D188 symptomatic tissue but in case of nonvirulent strain D188-5 infected *Arabidopsis* aerial tissues *AtIPT2*, 3 and 7 were up-regulated. The three *PsIPTs* expression in the vir-root was generally higher compared to the avir-root, but lower or same to con-root except at 15 dpi. The three *PsIPTs* expression in the avir-shoot were higher compared to the vir-shoot from 5 to 9 dpi, indicating similar to the result of Galis et al. (2005b), where the levels of cytokinin free bases, ribosides, O-glucosides and nucleotides were decreased within 6 days in pea shoots inoculated with the virulent strain compared to the avirulent strain infected shoots.

The *PsIPTs* expression result indicates that virulent strain inoculated plants had variation in the *PsIPTs* expression in cotyledon, root and shoot without a set pattern. On the whole the *PsIPTs* expression was up-regulated from 4 hpi until 15 dpi and decreased from 25 to 35 dpi compared to the avirulent strain 589 inoculated pea plants (except in roots). Similar observation was seen in *Brassica rapa* infected with *Plasmodiophora brassicae* where the expression of *BrIPT1*, 3, 5 and 7 in roots through northern blotting was increased at 20 dpi then it repressed in later growth stages of clubroot disease development (Ando et al. 2005). Eason et al. (1996) observed only slightly higher levels of non-hydroxylated cytokinins (iP and ms-iPA) but lower levels of cytokinin nucleotides in the *P. sativum* cv. Novella plants inoculated with *R. fascians* virulent strains than those inoculated with the avirulent strains at 15 dpi. The initial increase in three *PsIPTs* expression soon after inoculation and decrease in later stages of growth (25-35 dpi) in the virulent strain 602 inoculated plant tissues may be due to the fact that the cytokinin accumulated in the infected plants at the onset of plant-microbe interaction, but thereafter cytokinin level decreases distinctly as plant activates its homeostatic mechanism (Stes et al., 2013). The decrease of cytokinin biosynthesis genes (*PsIPT*) expression in the tissues infected with the virulent strain 602 at later stages of growth after reaching a peak mainly at 9 to 15 dpi might be due to decrease cytokinin content in *R. fascians* infected plants due to the mechanism of homeostasis which has been demonstrated in previous studies (Eason et al. 1996, Galis et al. 2005b, Depuydt et al. 2008).

The three *PsLOGs* studied had similar expression profile in the virulent strain 602 inoculated cotyledons, roots and shoots which resembled *PsIPTs* expression. *PsLOGs* and *PsIPTs* expressions pattern were similar in the cotyledon, root and shoot inoculated with both strains. On the whole, the virulent strain inoculated plants had *PsLOGs* expression decreased with development of plant compared to the avirulent strain inoculated plants which had high *PsLOGs* expression with growth in cotyledon and shoot. This might be due to the conversions of nucleotides to its bases by *fasF* (Pertry et al. 2009) immediately after inoculation by the bacteria. Eason et al. (1996) and Galis et al. (2005b) have showed high level of nucleotides in the pea shoots infected with avirulent strains compared to the shoots infected with virulent strains. It was also noticed that *PsLOG8* expressed with high impact in virulent strain 602 inoculated cotyledons compared to control and the avirulent strain 589 inoculated cotyledons at all time points. This may be due to the fact that *R. fascians* infection leads to multiple shoots in peas which might be due to cytokinin activation predominantly mediated by *LOG*- dependent pathway in the vegetative growth stage (Tokunaga et al. 2012). The *PsLOG* expression profile in the virulent strain 602 infected tissues is down regulated with growth by 25 dpi compared to the avir-shoot which resembles the *PsIPT* expression agreeing with the previous reports that cytokinin production is relatively not high or low in the virulent infected shoots (Eason et al. 1996, Jameson 2000, Galis et al. 2005b). Depudyt et al. (2009 b) using microarrays data suggested that *AtIPT3* was down regulated in *R. fascians* virulent D188- infected *Arabidopsis* shoots due to the onset of cytokinin homeostatic mechanism in plants.

The cytokinin biosynthesis *PsIPT* and *PsLOG* genes expression was mostly either low or same level in the virulent strain 602 cotyledons, roots and shoots at 2, 5 and 9 dpi (except in *PsLOG8* in cotyledons) compared to the control tissues. The virulent strain 602 cotyledons, roots and shoots had *PsIPTs* and *PsLOGs* expression up-regulated mostly at 15 dpi compared to control. This result of down-regulation of *PsIPTs* expression in vir-shoot from 2 to 9 dpi compared to con-shoot, confirms the data reported by Depudyt et al. (2008) that cytokinin content in *Arabidopsis* leaves were affected due to infection with virulent strain D188, reduction in the level of three cytokinin monophosphates was seen over time with the down-regulation of *AtIPT* genes compared to mock inoculation and the cytokinin biosynthesis in the plant is reduced early upon infection. This pattern of cytokinin biosynthetic genes (*PsIPT* and *PsLOG*) expression contradicts with the result of Pertry et al.

(2009) where the cytokinin bases iP, cZ, 2MeSiP, 2MeScZ, 2MeStZ except tZ were more abundant initially (2 dpi) in the virulent strain D188 infected *Arabidopsis* shoot than in mock-inoculated controls.

All the five *PsCKX*s expressed more highly in vir-cot, but in vir-root and vir-shoot there was fluctuations in their expression pattern at most of the time points. The *PsCKX*s expressions were low in avir-cot except in *PsCKX4* and *PsCKX5* it was higher in 25 and 35 dpi compared to the vir-cot and control-cots. *PsCKX*s expression pattern in the vir-root were highest at 15 dpi, but in other time points it was lower compared to con-root and avir-root. The avir-root had high expression of *PsCKX2*, *PsCKX3*, *PsCKX4* and *PsCKX5* at 25 dpi. Mainly among the five *PsCKX* gene family members, *PsCKX1*, *PsCKX3* and to some extent *PsCKX2* expressions were up-regulated in vir-cot compared to con-cot and avir-cot. This supports the transcript data of Depuydt et al. (2009b) where two *AtCKX* genes were up-regulated in virulent D188 *Arabidopsis*.

In shoots, *PsCKX*s expression was up-regulated in the vir-shoots at most of growth stages compared to the avir-shoot except at 5 dpi (reduced). *PsCKX*s expression was up-regulated at most of the time points in the virulent strain 602 infected tissues which was similar to the observation made by Galis et al. (2005a) with the *AtCKX* promoter 3::GUS fusion which was induced with tobacco infected with *R. fascians* virulent strain but not with the avirulent strain. This result also supports Depuydt et al. (2008) suggestion that the up-regulation of the *CKX* genes might be due to the compensatory mechanism of the plant to restore the mechanism of cytokinin homeostasis in response to bacterial cytokinin secretion. There was differential expression pattern among the five *PsCKX*s expression, with prominent increase in *PsCKX2* and *PsCKX3* expression in vir-shoot compared to avir-shoot and con-shoot. *AtCKX3* expression was highly up-regulated than other *AtCKX* gene family members in *R. fascians* virulent strain D188 infected *Arabidopsis* compared to nonvirulent D188-5 infected plants (Depuydt et al. 2008). The micro array data of Depuydt et al. (2009b) also confirms the up-regulation of *AtCKX* expression due to *R. fascians* virulent strain D188 infection in *Arabidopsis*. Pertry et al. (2009) report on substrate specificities of apoplastic *CKX* enzymes, where *CKX* enzymes did not effectively degrade *cis*-derivatives and 2MeS-type cytokinins which were accumulated in the virulent infected shoots of *Arabidopsis*. They suggested this accumulation was the cause of shoot malformation. In case of tobacco leafy galls, iP was

found to accumulate rather than cis-derivatives and 2MeS-type cytokinins through cytokinin profiling, so Pertry et al. 2009 suggested that the accumulation of specific bacterial cytokinins depends on the type of host. Le et al. (2012) indicated that the levels of cZ-type of cytokinins were lower compared to tZ and iP-type of cytokinins in almost all of the soybean tissues/ organs. The up-regulation of *PsCKXs* in vir-shoot indicates that effectively the cytokinins are degraded with rapid metabolism which may be the reason for detection of low levels of cytokinins in virulent strain infected plants.

The expression study of cytokinin genes *IPT*, *LOG* and *CKX* in peas, in *R. fascians* and in peas infected with the avirulent strain 589 and the virulent strain 602 in cotyledon, root and shoot tissues revealed that the *PsIPTs* and *PsLOGs* expression followed generally similar expression profile in all the tissues. In case of the avir-cot *PsIPTs* and *PsLOGs* expression was similar to con-cot, low at the time of inoculation (4 hpi) peaked at 5 dpi then reduced until 15 dpi. But was up-regulated in later stages of 25 to 35 dpi compared to con-cot. In contrast the vir-cot had high *PsIPTs* and *PsLOGs* expression at time of inoculation (4 hpi) down regulated until 5 dpi with a peak at 9 to 15 dpi then reduced with growth. *PsLOG8* expressed strongly up-regulated in the vir-cot at all time points tested. There were variations in the expression pattern of the five *PsCKX* gene families in the cotyledons. *PsCKX1*, 2 and 3 expressions in virulent strain 602 infected cotyledons was up-regulated at all stages of growth except at 2 dpi, whereas *PsCKX4* and 5 expressions had fluctuations. Mainly, *PsCKXs* expression was down regulated at all times in control and the avir-cot, but *PsCKX4* and 5 expressions were up-regulated in the avir-cot at 25 and 35 dpi. So far the effect of plant cytokinin gene (*IPT*, *LOG* and *CKX*) expression due to *R. fascians* virulent infection on *A. thaliana* or *N. tabacum* studied on the aerial part (shoots or leaves) but not in cotyledons, this data cannot be compared with other findings.

The avirulent strain 589 inoculated and control cotyledons, roots and shoots level of *PsIPTs*, *PsLOGs* and *PsCKXs* genes expression was not similar in most of the time points. In some cases there was depressed or very low cytokinin synthetic and metabolic genes expression observed in avirulent strain 589 inoculated tissues. *PsIPTs* and *PsLOGs* expression pattern in the avir-root and con-root was not similar at all time points except at 25 dpi. The avir-shoot and con-shoot had variations initially but was normally lower than the vir-shoot in all stages tested. These results indicates that cytokinin biosynthetic genes (*IPT* and *LOG*) was reduced

in control and the pea roots and shoots infected with avirulent strain 589 with growth development agreeing with the concept that the host cytokinin biosynthetic genes are down regulated in an attempt to maintain the cytokinin homeostasis (Depuydt et al. 2008). The *PsCKXs* expression was reduced in normal and roots and shoots infected by the avirulent strain 589 at the majority of the growth stages but in shoots and roots infected by the virulent strain 602 it was up-regulated throughout the growth period except at initial stage. Similar results was observed by Galis et al. (2005a) where *AtCKX3* expression was induced with tobacco infected with a virulent strain of *R. fascians* but not in plant infected by an avirulent strain, so low cytokinin levels were observed in the virulent strain infected tissues. Global transcriptomics using microarrays on infected *A. thaliana* with *R. fascians* revealed the up regulation of two *CKX* genes and *IPT3* down regulation confirms the mechanism of cytokinin homeostasis and central position of cytokinin in pathology (Depuydt et al., 2009b).

Recently, reports relating the cytokinin receptors and response genes in *Arabidopsis* infected by *R. fascians* to correlate the role of cytokinin in infection process have been published (Depuydt et al. 2008, Depuydt et al. 2009b, Pertry et. al. 2009) (Section 1.2.3.2). So, in this study pea response regulators (*PsRR3*, 5, 6 and 9) were isolated and their expression levels monitored to use them as indicators for measures of endogenous cytokinin levels in pea tissues infected by *R. fascians*.

The expression of pea response regulators (*PsRR*) in the vir-cot and avir-cot revealed the impact of cytokinin presence in the infected cotyledons. The *PsRR3*, 5, 6 and 9 up-regulation in cotyledons, roots and shoots infected by the virulent strain 602 indicates the presence of cytokinin in the infected pea tissues higher than control and pea tissues infected by the avirulent strain 589. The up-regulation of *PsRRs* expression in pea tissues infected by virulent strain 602 agrees with the data reported by Depuydt et al. (2008) where *ARR5* was up-regulated due to infection by *R. fascians* in *Arabidopsis* at 30 dpi. Depuydt et al. (2009b) through microarray analysis showed that *A. thaliana* with a virulent strain showed that six *ARR* genes (*ARR4*, 7, 16 18 and 9) were up-regulated due to cytokinins and mediate a feedback regulation of the cytokinin response. *PsRR3*, 5, 6 and 9 expressions in avir-cot was down regulated at most growth stages compared to the vir-cot and control-cot except at 35 dpi (*PsRR3*,6 and 9). *PsRR9* expression in the avir-cot was very low or not detected from 5 to 15 dpi, as well down regulated in all time points tested except at 35 dpi. In the avir-root, the

four *PsRR* gene families expression was least or not detected at all growth stages. These results confirm the cytokinin biosynthetic genes *PsIPTs* and *PsLOGs* expression pattern signifying low level of biologically active cytokinins in tissues infected by the avirulent strain 589 in most of growth and development except at later stage of growth. As indicated by Galis et al. (2005b) the pea shoots inoculated with avirulent strains had high levels of O-glucosides, the storage forms of cytokinins which might not have been detected by the *PsRRs*. The result of *PsRR* up-regulation in pea shoots infected by the virulent strain 602 agrees with Pertry et al. (2009) observation of high induction of AHK4 expression in shoot due to presence of increased cytokinin levels in *Arabidopsis* infected with *R. fascians* virulent strain D188.

Chapter 5 SOURCE-SINK TRANSITIONS IN *PISUM SATIVUM* COTYLEDONS INFECTED WITH *RHODOCOCCUS FASCIANS*

5.1 INTRODUCTION

Apart from multiple shoots, the most noticeable morphological feature of pea cotyledons infected with the virulent strain of *R. fascians* were intact and dark green in colour. This observation led to the investigation of source-sink transitions. The cotyledons were used to study the expression of transporter gene, *PsSUTs* and *PsAAPs* to determine if there were differences between the control cotyledons and those inoculated with an avirulent and virulent strains of *R. fascians* during germination of the seed.

Cytokinins play a major role in the regulation of various processes associated with the supply of nutrients to growing tissues of plants. Cytokinin responses are associated with active growth or activation of a possible link to the carbohydrate supply (Kuiper, 1993). Sucrose and protein are major forms of storage, so sucrose transporters and amino acid transporters play a prominent role in plant nutrient transport. The long-distance transport of carbohydrates, mainly sucrose takes place in the sieve elements of the phloem through differences in pressure potential (Evert (1982) cited from Roitsch and Ehneß (2000)). Sucrose is released from the sieve elements into the apoplast by sucrose transporters. Sucrose transporters (SUTs or SUCs) are membrane proteins that facilitate the uptake of sucrose into the cytoplasm. The genes catalysing Suc/H⁺ symport are called as Suc transporters (*SUT*) or suc carriers (*SUC*) and those participating in passive transport are Suc facilitators (*SUF*) (Ayre, 2011).

The first *SUT* genes were identified and sequenced from spinach (*SoSUT1*; *Spinacia oleracea*) and potato (*StSUT1*; *Solanum tuberosum*) through cDNA-expression libraries screened in yeast (Riesmeier et al., 1993, Riesmeier et al., 1992). Since then *SUT* genes have been isolated from numerous species through sequence homology and analysis of sequenced genomes and EST libraries (Ayre 2011). Nine *SUTs* or *SUCs* have been described in *Arabidopsis* (2000) and five *SUT* genes found in rice genome (Aoki et al., 2003). Zhou et al.

(2007) isolated sucrose transporter genes, *PsSUF1*, *PsSUF4* (suc facilitators), *PvSUT1* and *PvSUF1* from the seed coats of *Phaseolus vulgaris* and *P. sativum*.

The *SUTs* or *SUCs* are possessed by all plants involved in long distance transport of sucrose from source to sink sites where sugars are used or stored (Doidy et al., 2012). The *SUTs* latest classification has five distinct clades: *SUT1-SUT5* (Kühn and Grof, 2010). The *SUT1* clade is found only in dicots and is the largest. It is responsible for phloem loading of sucrose and includes *PsSUF1* and *AtSUT1*. The *SUT3* and *SUT5* are monocot specific and *PsSUT3* appears to be functionally orthologous to *SUT1* members. *SUT2* clade members are described as sugar sensors and members of the *SUT4* clade have both monocot and dicot members (Doidy et al., 2012, Kühn and Grof, 2010).

Tegeeder et al. (1999) isolated *PsSUT1* from a pea cotyledon cDNA library and through northern blot analyses showed *PsSUT1* expression in non-seed tissues, including sucrose sinks and sources. Sucrose transporter genes, *PsSUF1*, *PsSUF4*, *PvSUT1* and *PvSUF1* were isolated from pea and bean seed coats of developing seed, all sub grouped into Clade I except *PsSUF4* which grouped to Clade II. The sucrose transporters were expressed throughout the plant and in developing seeds (Zhou et al., 2007).

Kühn and Grof (2010) reviewed that sucrose transporters are not only in phloem loading processes but also in exchange of sucrose between beneficial symbionts such as mycorrhiza and *Rhizobium*, pathogens and parasitic fungi. They are also integral components of signal transduction between sink and source metabolism. Recently, Li-Qing et al. (2010) has identified sugar transporter, SWEET from pathogens or mycorrhizal fungi, which plays a role not only in pollen development and senescence, but also in the nutrition of plant-interacting fungi and in resistance against pathogens. Doidy et al. (2012) reviewed the essential role of sugar transporters for the carbohydrates distribution inside plant cells and the mechanisms with sugar exchange between fungi and their hosts.

Seeds of grain legumes are nutritionally important due to their relatively high content of amino acids, which accumulate in cotyledons as storage proteins (Muntz (1982) cf. Tegeeder et al. (2000). A number of amino acid transporter genes have been identified in *Arabidopsis* and based on sequence homology, they were classified into two major families: the ATF

(Amino acid transporter family) and APC (amino-acid-polyamine-choline facilitator) (Fischer et al., 1998). The ATF family consists of the broad-specificity AAP transporters (Amino acid permease), the basic amino acid LHT (lysine-histidine-like) transporters, the compatible solute ProT (proline) transporters and the putative AUX (auxin) transporters (Tegeger and Ward, 2012).

The *AAPs* are encoded by multigene families which display temporal and spatial expression patterns (Okumoto et al., 2002). Eight *Arabidopsis* *AAPs* were isolated. Of these *AtAAP8* and *AtAAP6* have been identified as high affinity amino acid transport systems. *AtAAP6* functions in uptake of amino acids from xylem. *AtAAP6* is expressed in xylem parenchyma and *AtAAP8* is expressed in siliques and developing seeds, indicating its role in supplying organic nitrogen to developing seeds (Okumoto et al., 2002). Tegeger et al. (2000) isolated *PsAAP1* and *PsAAP2* from cDNA library of pea cotyledons. *PsAAP1* expressed in seed coats and cotyledons, whereas *PsAAP2* expression could not be detected. *PsAAP1* expression patterns was similar to *AtAAP1* expression and the cellular localisation in phloem functions in loading of amino acid for translocation to sinks and in seed development and protein storage (Tegeger et al., 2007).

Many micro-organisms secrete cytokinin analogues or activate plant cytokinin production to divert nutrients from the host towards the growth of infected tissues (Robert-Seilaniantz et al., 2007, Walters and McRoberts, 2006). Extensive studies with transporter genes have been done on developing seeds but not on germinating seeds. Depuydt et al. (2009b) reported the effect of *R. fascians* infection in *Arabidopsis* shoots through profiling of primary metabolites and microarrays and reported that the expression of sugar transporter gene family are up-regulated and amino acid transporter family expression are down regulated with higher levels of sugars and amino acids in shoots infected with virulent strain D188, but other parts of plant were not studied. In the current study, the *in planta* expression of transporter genes, *SUT* and *AAP*, was analysed in pea cotyledons and shoots inoculated with virulent and avirulent strains of *R. fascians* to assess the effect of *R. fascians* on sucrose and amino acid transporters during the germination of the seed.

5.2 MATERIALS AND METHODS

The materials and methods used in this chapter are outlined in Chapter 2 and 4. The same plant samples and cDNAs previously used for cytokinin gene expression were used for this study.

5.3 RESULTS

5.3.1 Chlorophyll content of *P. sativum* infected with *R. fascians*.

The cotyledons of plants inoculated with *R. fascians* virulent strain 602, was that their cotyledons remained dark green and intact during the growth of plant from 15 to 45 dpi (Figure 5.1). The amount of chlorophyll in pea cotyledons, roots and shoots was measured as they progressed in growth from 4 h to 40 dpi.

With growth of plants it was observed that the mock inoculated (con-cot) and avirulent strain 589 inoculated cotyledons (avir-cot) reduced in size and shrivelled from 25 dpi to 45 dpi compared to *R. fascians* virulent strain 602 inoculated (vir-cot) cotyledons (Figure 5.1 c and d). The vir-cot from 15 dpi started greening and at 45 dpi the cotyledons were dark green in colour and were intact (Figure 5.1 b, c and d). This can clearly be seen in Figure 5.1, where the cotyledons were removed to show the clear greening effect at 15 dpi (Figure 5.1 e) and at 25 dpi (Figure 5.1 f). The greening of vir-cot was seen until the plants were harvested at 45 dpi (Figure 5.1 d).

The chlorophyll content of cotyledons, roots and shoots at different growth stages from 4 hpi to 40 dpi was determined (Figure 5.2, 5.3 and 5.4). In general the total chlorophyll content of con-cot was 0.035 mg/g tissue (4 hpi) to 0.23 mg/g tissue (11 dpi) compared to vir-cot (0.12 mg/g tissue at 4 hpi to 1.13 mg/g tissue at 35 dpi) (Figure 5.2). The chlorophyll content in con-cot increased until 11 dpi (0.2334 mg/g tissue) but later decreased to 0.046 mg/g tissue at 40 dpi. The chlorophyll content of cotyledons inoculated with *R. fascians* virulent strain 602 increased with growth of the pea plant. Chlorophyll content increased markedly from 11 dpi to 40 dpi in vir-cot compared to con-cot and avir-cot.

The chlorophyll content in con-root, avir-root and vir-root did not vary until 7 dpi. From 9 dpi to 40 dpi the total chlorophyll content increased in vir-cot compared to con-cot and

avir-cot. The increase of chlorophyll content was prominent in vir-cot from 20 dpi to 40 dpi (Figure 5.3). The vir-roots from 30 dpi to 40 dpi revealed a much higher content of chlorophyll than the con-root and avir-root.

Until 5 dpi, there was little shoot growth in pea, so total chlorophyll estimation was determined from 5 dpi (Figure 5.4). The chlorophyll content was higher in shoots compared to cotyledons and roots. Chlorophyll content in con-shoot increased to a maximum at 15 days (9 mg/g tissue) then reduced strikingly between 35 and 40 dpi (1.250 mg/g tissue). The chlorophyll content was lower from 11 dpi to 20 dpi in vir -shoot compared to con-shoot and avir-shoot. The chlorophyll content of vir-shoot had increased considerably by 35 dpi (14.096 mg/ g tissue). The chlorophyll content in avir-shoot was high at 9 dpi (8.165 mg/g tissue) and at 15 dpi (9.873 mg/g tissue) compared to con-cot and vir-cot.

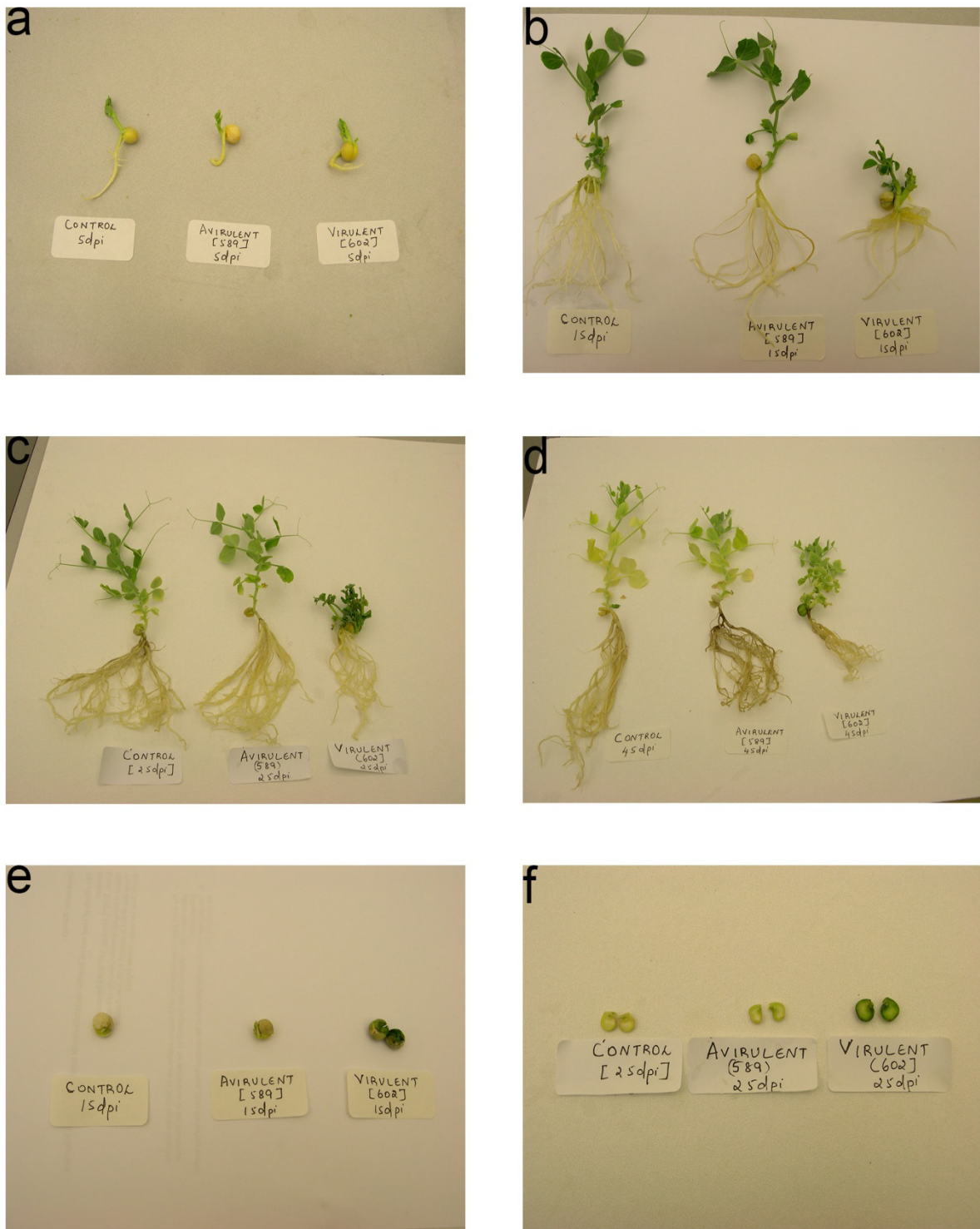


Figure 5.1 **Morphology of *P. sativum* plants and cotyledons infected with or without *R. fascians*.** a) pea plants at 5 dpi showing control, *R. fascians* avirulent strain 589 infected and virulent strain 602 infected seedlings b) 15 dpi - control, avirulent and virulent infected pea plants c) 25 dpi – control, avirulent and virulent infected pea plants d) 45 dpi- control, avirulent and virulent infected pea plants e) 15 dpi- control, avirulent and virulent infected cotyledons (greening of cotyledon) f) 25 dpi – control, avirulent, virulent infected cotyledons.

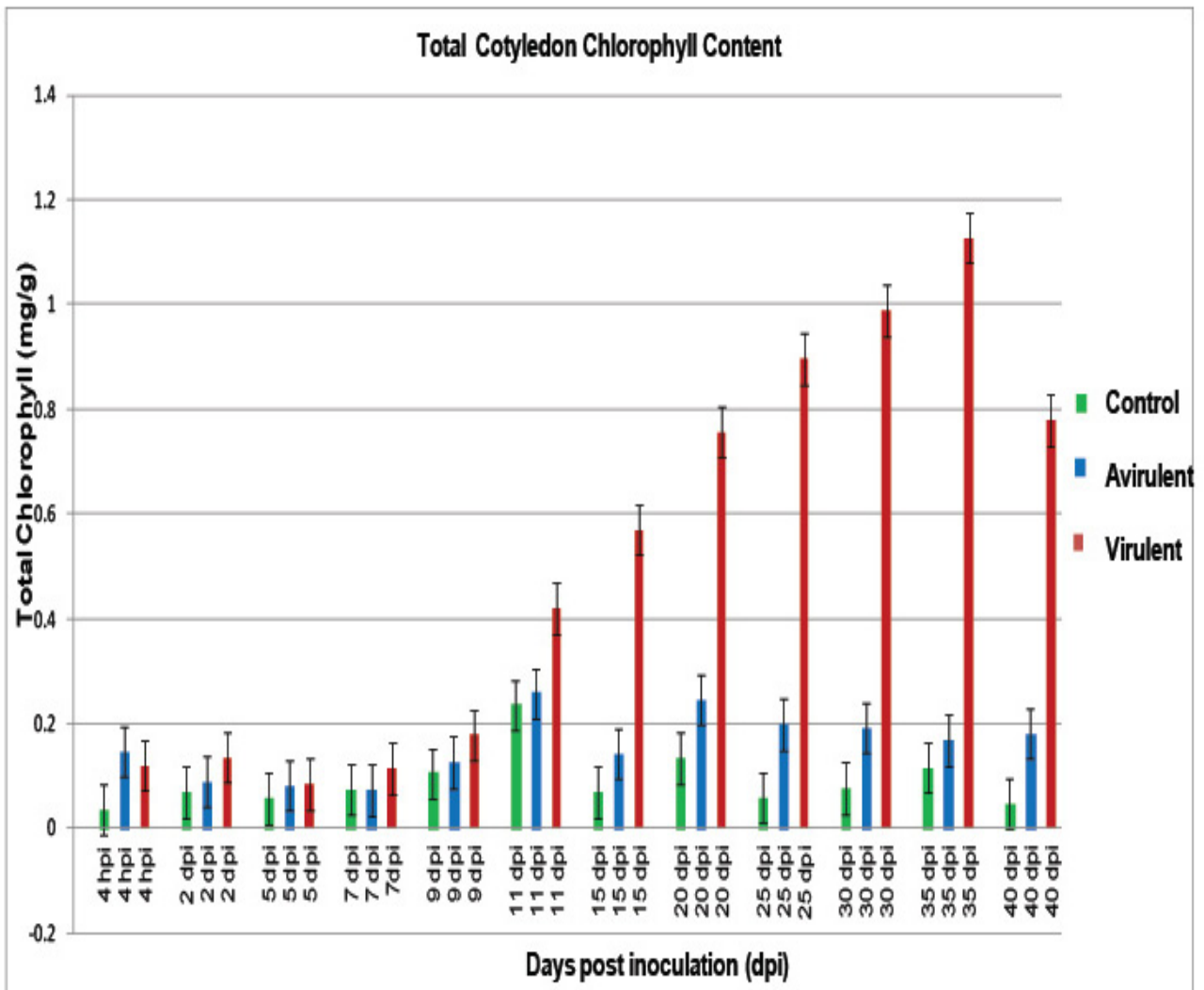


Figure 5.2 **Total chlorophyll content in cotyledon tissues of *P. sativum* infected with *R. fascians*.** The pea seeds were imbibed for 4 h (hpi) with *R. fascians* avirulent strain 589 (Avirulent), virulent strain 602 (Virulent) and without *R. fascians* culture but with Klamt medium as mock inoculation (Control) and grown in sterile agar containers until 40 days post inoculation (dpi). The error bars are +/- one standard deviation of two biological replicates and four technical replicates.

Total Root Chlorophyll Content

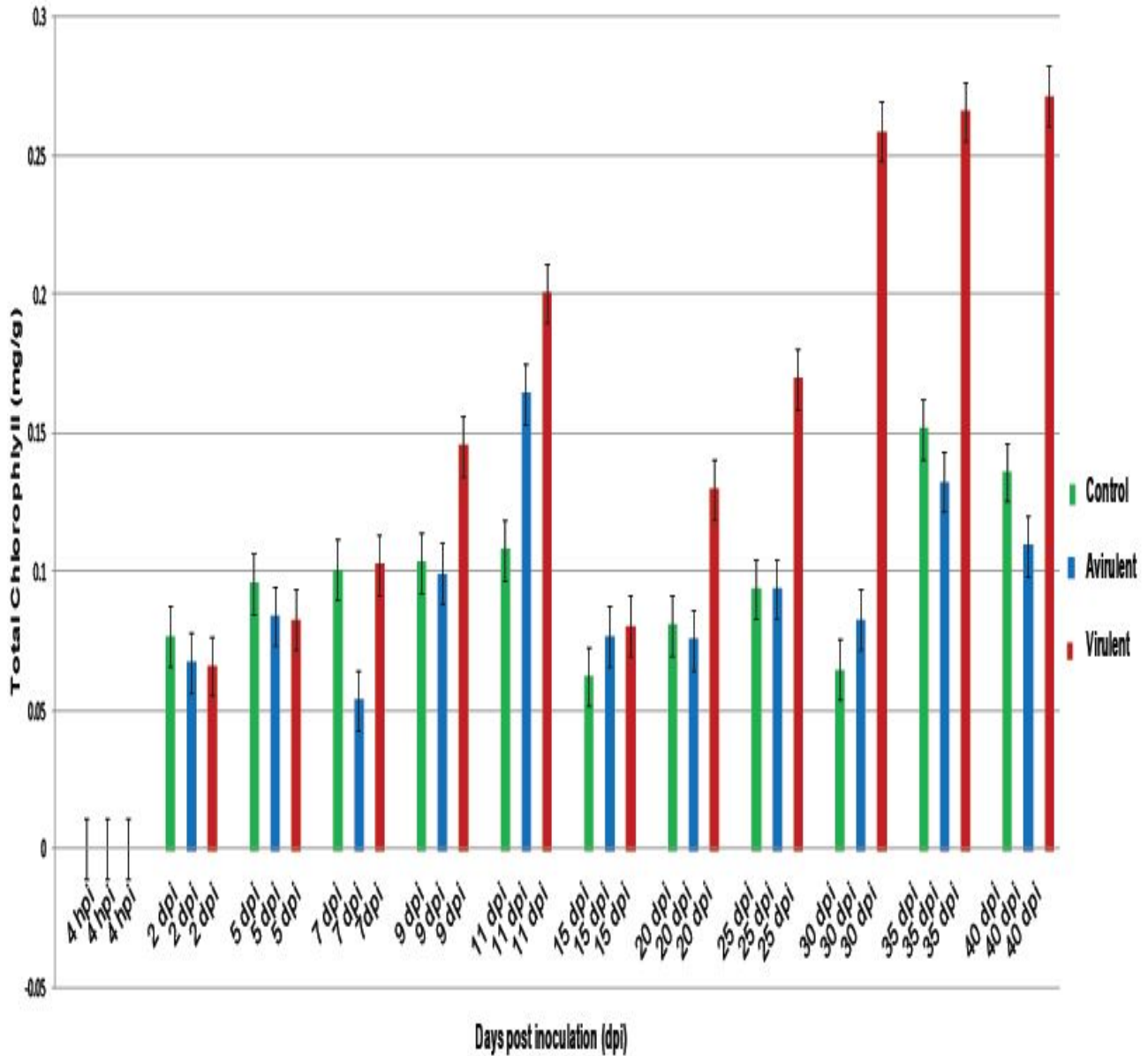


Figure 5.3 **Total chlorophyll content in root tissues of *P. sativum* infected with *R. fascians*.** The pea seeds were imbibed for 4 h (hpi) with *R. fascians* avirulent strain 589 (Avirulent), virulent strain 602 (Virulent) and without *R. fascians* culture but with Klambt medium as mock inoculation (Control) and grown in sterile agar containers until 40 days post inoculation (dpi). The error bars are +/- one standard deviation of two biological replicates and four technical replicates.

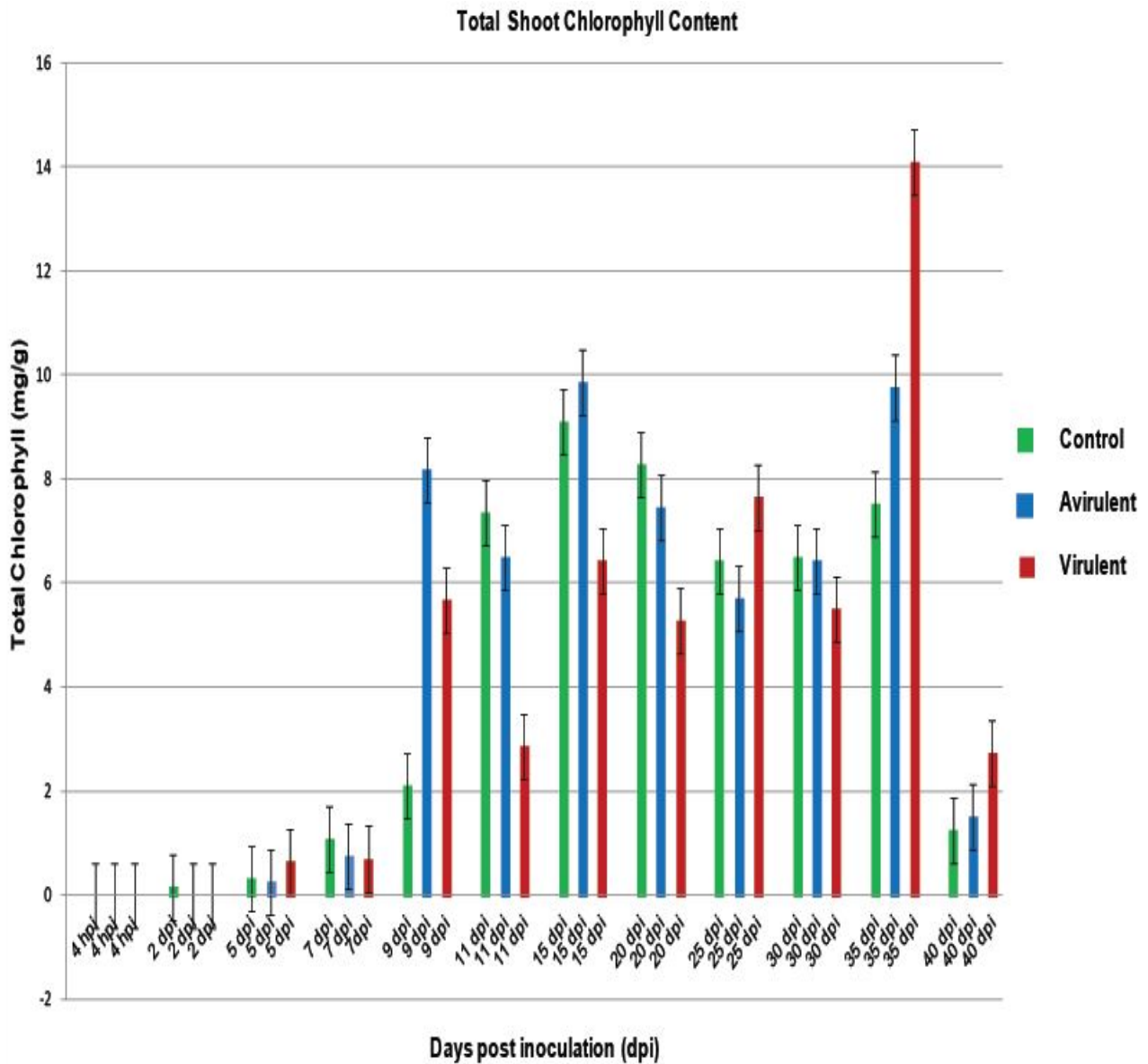


Figure 5.4 **Total chlorophyll content in shoot tissues of *P. sativum* infected with *R. fascians*.** The pea seeds were imbibed for 4 h (hpi) with *R. fascians* avirulent strain 589 (Avirulent), virulent strain 602 (Virulent) and without *R. fascians* culture but with Klambt medium as mock inoculation (Control) and grown in sterile agar containers until 40 days post inoculation (dpi). The error bars are +/- one standard deviation of two biological replicates and four technical replicates.

5.3.2 Identification and isolation of pea transporter genes (*PsSUT* and *PsAAP*)

Sucrose transporter genes (*SUT*) and amino acid permease (*AAP*) genes were identified using a BLAST search of the Genbank database. These genes were studied for their expression mainly in cotyledons infected with virulent strain (602) showed greening and did not shrivel, when compared with con-cot and avir-cot during the growth of pea plants from 15 to 45 dpi.

Dr Jiancheng Song used the pea transcriptome sequence analysis to design the primers (Appendix 4.1.5). The PCR products were sequenced by MACROGEN Inc. Korea.

The phylogenetic analysis was done by using *A. thaliana*, *P. sativum* and other legumes including *G. max*, *M. trunculata*, *V. faba* and *P. vulgaris* for both *SUT* and *AAP* transporter genes along with the isolated *PsSUT* and *PsAAP* gene families by Maximum Parsimony in MEGA4 program with 10,000 bootstrap replicates (Figure 5.5 and 5.6). Based on the phylogenetic tree of *SUT* (Figure 5.5), the isolated *PsSUT1a*, *PsSUT1b* and *PsSUF1* formed a clade with *VfSUT*, *GmSUT1*, *MtSUT1*, *PvSUF1* and *PsSUF1*. *PsSUT1a* and *VfSUT* (bootstrap value 99) branched with other *GmSUT1* with *MtSUT1*. The isolated *PsSUT1b* had high sequence similarity with *PvSUF1* (bootstrap value 94). The isolated *PsSUF1* had sequence identity with the *PsSUF1* (bootstrap value 100). The isolated *PsSUT2* had sequence identity with *MtSUT2* and *AtSUT3* (bootstrap value 100). *PsSUT10* grouped with *GmSUT10* with high bootstrap value of 100. All the *AtSUCs* formed a separate clade except *AtSUC3* and *AtSUC4*. The tree was rooted with *PsAAP1* as an out group.

The *PsAAP* phylogenetic tree analysis, revealed that the fifteen *PsAAP* genes isolated had sequence similarities with legume *AAPs* and *A. thaliana AAPs* (Figure 5.6). *PsAAPs* mainly branched into five main clades. The isolated *PsAAPs* were represented in most of the clades. Mainly *PsAAP2c*, 2a, 2d and 2e formed a clade with subgroups along with *PsAAP2*, *CaAAP2*, *GmAAP2*. The phylogenetic analysis of the isolated *PsAAP3a* had sequences homologous to *PsAAP1* (bootstrap value 99), whereas, the isolated *PsAAP1* had high bootstrap value of 100 with *CaAAP1*. The isolated *PsAAP3a*, *PsAAP3b* formed a clade with *PsAAP1*, *GmAAP3(2)*, *GmAAP3*, *CaAAP3*, *AtAAP3* and *AtAAP5*. Of the 15 *PsAAPs* isolated, seven *PsAAPs* were used for gene expression analysis in this project. The tree was rooted with *PsSUT1* as an outgroup (Figure 5.6).

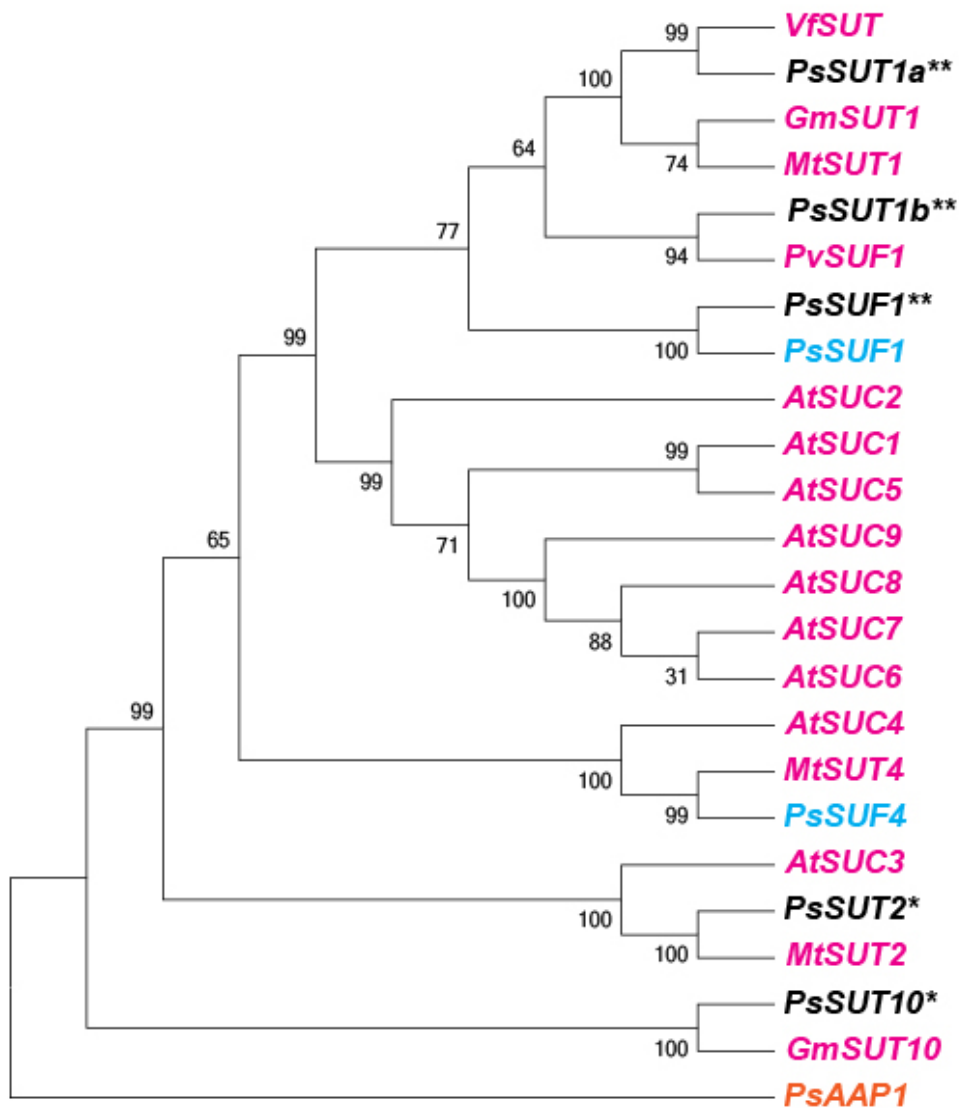


Figure 5.5 **Phylogenetic tree of SUT**. The maximum parsimony phylogenetic tree showing the relationship between *P. sativum* SUT (*PsSUT*) and isolated *PsSUT1a*, *PsSUT1b*, *PsSUF1*, *PsSUT2*, *PsSUT10*, *PsSUT1a* (AF109922.1); *PsSUF1* (DQ221698.2), *PsSUF4*(DQ221697); *Vicia faba* SUT: *VfSUT* (Z93774.1); *Phaseolus vulgaris* SUT: *PvSUF1* (DQ221700); *M. trunculata* SUT: *MtSUT1* (JN255789.1), *MtSUT2* (JN255792), *MtSUT4*(JN255793), *A. thaliana* SUT: *AtSUC2* (NM102118.3), *AtSUC3* (AJ289165), *AtSUC4*(NM100870), *AtSUC9* (NM120699.1); *G. max* SUT: *GmSUT1* (NM001249369.1), *GmSUT10* (XM003533651). The node values are the bootstrap values generated with 10,000 bootstrap replicates. The tree was rooted with *PsAAP1* (AY956395). *The sequences of *P. sativum* SUTs, *PsSUT1a*, *PsSUT1b*, *PsSUF1*, *PsSUT2* and *PsSUT10* isolated in this project. **The *PsSUTs* : *PsSUT1a*, *PsSUT1b* and *PsSUF1* used for gene expression analysis in this project.

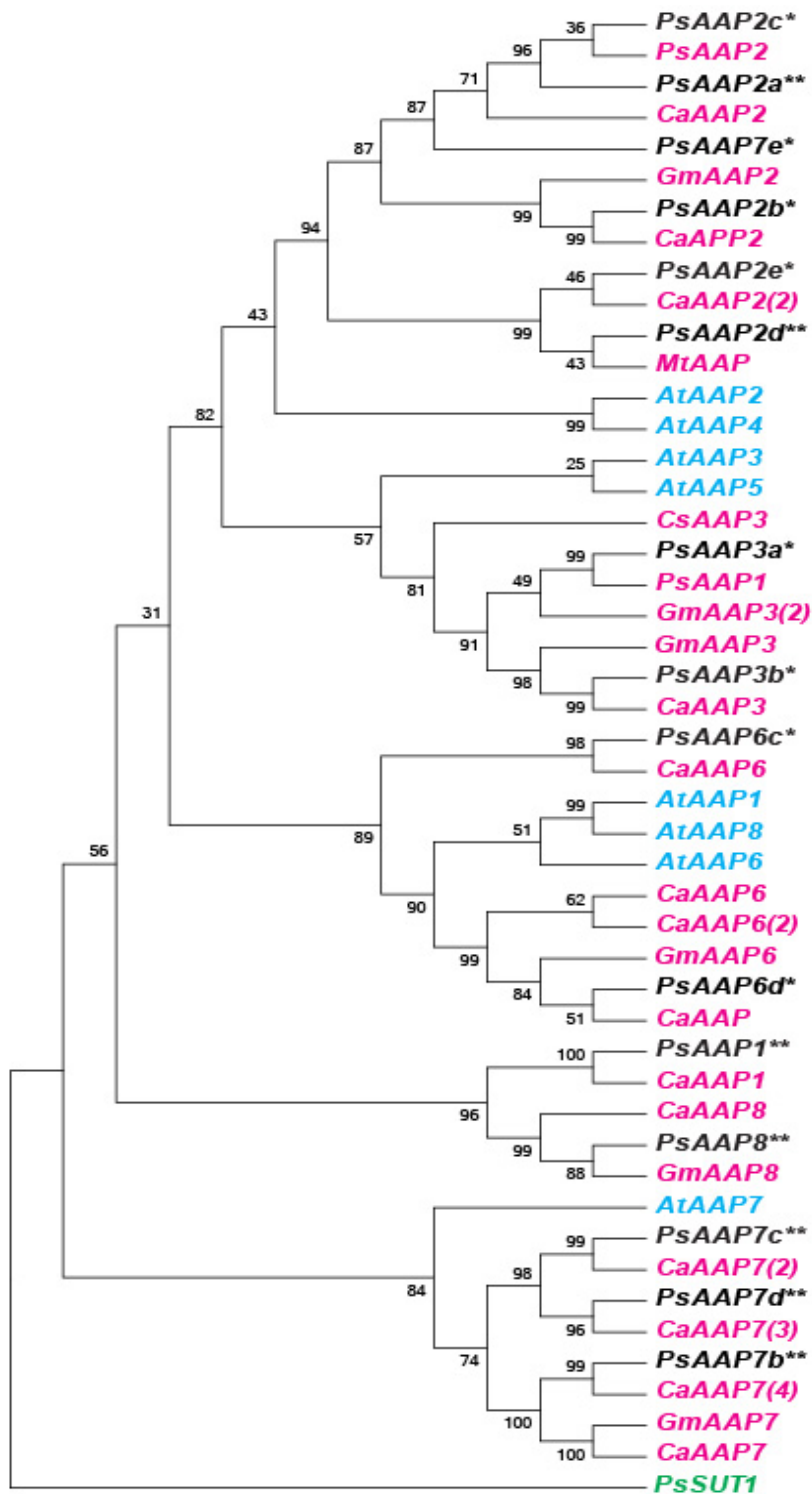


Figure 5.6 **Phylogenetic tree of AAP**. The maximum parsimony phylogenetic tree showing the relationship between *P. sativum* AAP: *PsAAP1* (AY956395), *PsAAP2* (AY956396), all isolated *PsAAP*; *M. tranculata* AAP: *Mt AAP* (XM003630268); *G. max* AAP: *GmAAP2*(XM003523163),*GmAAP3*(XM006596156,XM006578897), *GmAAP7*(XR417829), *GmAAP8* (XM003544625); *C. arietinum* AAP: *CaAAP1*(XM004501077) , *CaAAP2* (XM004502922, XM004503847, XM004502924), *CaAAP3* (XM004498293),*CaAAP6*(XM003550069, XM004496803,XM004498395, NM001255887, XM004501019), *CaAAP7* (XM0044491495, XM004500110,XM004491492,XM004500113), *CaAAP8* (XM004501037); *Citrus sinensis*: *CsAAP3* (XM006472964), *A. thaliana* AAP: *AtAAP1* (X67124.1), *AtAAP2*(NM120958.2), *AtAAP3*(NM106387.2), *AtAAP4* (NM125780.2), *AtAAP5* (NM103536.3),*AtAAP6* (AK229102.1), *AtAAP8* (NM100875.1).The node values are the bootstrap values generated with 10,000 bootstrap replicates. . The *PsSUT1* (AF109922) was used to root the tree. *The sequences of *P. sativum* AAPs isolated in this project. **The *PsAAP*s:*PsAAP2d*, *PsAAP2a*, *PsAAP7c*, *PsAAP7d*, *PsAAP7b*, *PsAAP1* and *PsAAP8* were used for gene expression analysis.

5.3.3 Quantitative expression of pea transporter genes in *P. sativum* infected with *R. fascians* strains

The MIQE standardisation and optimisation of RT-qPCR was the same as described in Section 4.3.4. The primers selected for the gene expression are given in Table 5.1.

Table 5.1 Sequences of the selected RT-qPCR primers used for expression analysis of *P. sativum* transporter genes.

Gene/primer	Species	Forward(F)/reverse (R) primer sequences
<i>PsSUT</i>	<i>P. sativum</i>	<p>PsSUT1a F: 5' TGGGCAGTTATCCGGTGCTTTC</p> <p>PsSUT1a R1: 5' ACACCCATATCATACGCATGACCTTC</p> <p>PsSUF1 F: 5' CAGTGCTTCAGGGGCTGGAC</p> <p>PsSUF1 Ra: 5' CAACACTATCGCCAATACAGCACTG</p> <p>PsSUT1b F: 5' CCGATCGTCGGTTACTACAGTGATC</p> <p>PsSUT1b R1: 5' CCCCgATGAAGGCACGACATG</p>
<i>PsAAP</i>	<i>P. sativum</i>	<p>PsAAP7b F: 5' AGGAGTGTGTCTTTGGCATGGAG</p> <p>PsAAP7b R: 5' ATGGATGCTRATATGATGTAGGCAATTC</p> <p>PsAAP7c F: 5' ATTCATTTGGTTGGAGGATATCAGATATACAG</p> <p>PsAAP7c R: 5' TCCAGTGGTTGAAATCACATAGGTTG</p> <p>PsAAP7d F: 5' ATTCATTTGGTTGGAGGATATCAGATTTATAG</p> <p>PsAAP7d R: 5' TCCAGTTGTGGAAATCACATAAGCTG</p> <p>PsAAP8 F: 5' TGCAATTGGTCTTTGTCTTTCCGTAC</p> <p>PsAAP8 R: 5' TTTCTGATGGAGGTGACCTTAGTGTATC</p>

		PsAAP2a F : 5' AGGTACGGTTTGGACAACGAGT PsAAP2a R: 5' GAGAATGGTGTGAACAGCTTCCATG PsAAP1 F1: 5' GGACTTTCTCTTTCCACCGTTATTCAAG PsAAP1 R1: 5' TGGAGGTGATGATTCAGAGTGTCTTG PsAAP2d F: 5' CATGGGTAGCCTCACAGGAATCAG PsAAP2d R: 5' CAAAGCATGTAAAATGTTGTGGTCACTG
--	--	---

[Note: N = ATGC, M = AC, R = AG, Y = CT, W = AT, K = GT, S = GC, H = ACT, B = CGT, V = CG, D = AGT]

The following gene families were used for the study of relative gene expression in pea cotyledons and shoot tissues:

1. *PsSUT1a*, *PsSUT1b* and *PsSUF1*
2. *PsAAP2d*, *PsAAP2a*, *PsAAP7c*, *PsAAP7d*, *PsAAP7b*, *PsAAP8*, and *PsAAP1*.

Expression is stated as fold-change relative to the relevant tissue (cotyledon and shoot) at 4 hpi or 5 dpi (initial stage) for the three treatments (control, avirulent and virulent).

Cotyledons: The expression patterns of *PsSUT1a*, *PsSUT1b* and *PsSUF1* in con-cot was not similar through the stages tested. *PsSUT1a* expression level was low initially in imbibing seed, and increased at 2 dpi. The highest expression was at 5 dpi, decreased by 9 dpi and was constant from 9 to 35 dpi, whereas *PsSUT1b* expression was highest at 2 dpi, decreased from 5 to 25 dpi and increased slightly from 25 to 35 dpi. *PsSUF1* expression level was highest at 2 dpi, reduced at 9 dpi and was steady from 9 dpi to 35 dpi (Figure 5.7). Generally, con-cot had lower expression compared to avir-cot and vir-cot in the *PsSUTs* and *PsSUF1* genes except at 2 dpi. *PsSUF1* expression level was lower compared to *PsSUT1a* and *PsSUT1b*.

In vir-cot *PsSUT 1a*, *PsSUT1b* and *PsSUF1* genes expression was high at initial stage (4 hpi) immediately after seed imbibition, reduced at 2 dpi, increased at 5 and 9 dpi but reduced later from 25 to 35 dpi (Figure 5.7). The *PsSUT1a*, *1b* and *PsSUF1* expression level was highest at 5 and 9 dpi in vir-cot.

The avir-cot had increased *PsSUTs* and *PsSUF1* genes expression at later stage of growth and highest level of expression was noted at 25 and 35 dpi, which was higher compared to con-cot and vir-cot.

Initial stage of seed imbibition (4 hpi) con-cot had high expression only in *PsAAP7b* compared to other *PsAAP* gene family members isolated. The *PsAAP* gene expression was higher in con-cot compared to avir-cot and vir-cot at 2 dpi for most of the gene family members. *PsAAP* gene family members had slight or no expression in con-cot and avir cot, especially *PsAAP7d* at 4 hpi and 2 dpi and *PsAAP1* from 4 hpi to 15 dpi relative to vir-cot (Figures 5.8 and 5.9).

The seven *PsAAP* gene family members showed elevated expression level at 5 and 9 dpi in vir-cot and mainly at 25 and 35 dpi in avir-cot compared to con-cot (Figure 5.8 and 5.9) which was similar to the pattern of expression of *PsSUT* gene families (Figure 5.7).

The *PsAAP* genes belonging to same gene family members, for example *PsAAP7c* and *PsAAP7d* revealed variations in their expression level whereas, *PsAAP2d*, *PsAAP2a* exhibited similar expression profiles in the three treatments even though the levels of expression were not the same.

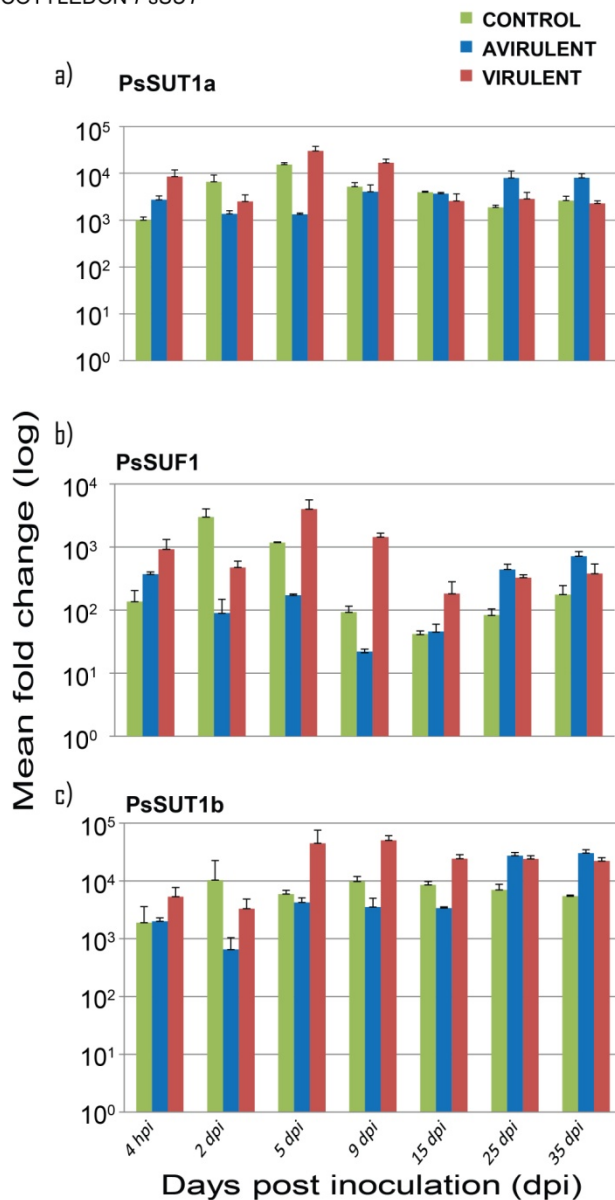


Figure 5.7 **Relative expression of *PsSUT1a*, *1b* and *PsSUF1* in *P. sativum* cotyledon tissues.** Data are means of relative mRNA levels in fold changes (log) detected using three technical replicates for each of two biological replicates. *PsEF*, *U18S*, *PsGAP* and *PsACT* were used as internal controls. Before quantification of the expression level of each target genes, the Ct numbers for each internal control and target were corrected with an internal calibrator and also by using the average correction factor determined for each of the four reference genes. Error bars represent the +/- one SD calculated for the combined technical and biological replicates.

COTYLEDON-*PsAAP*

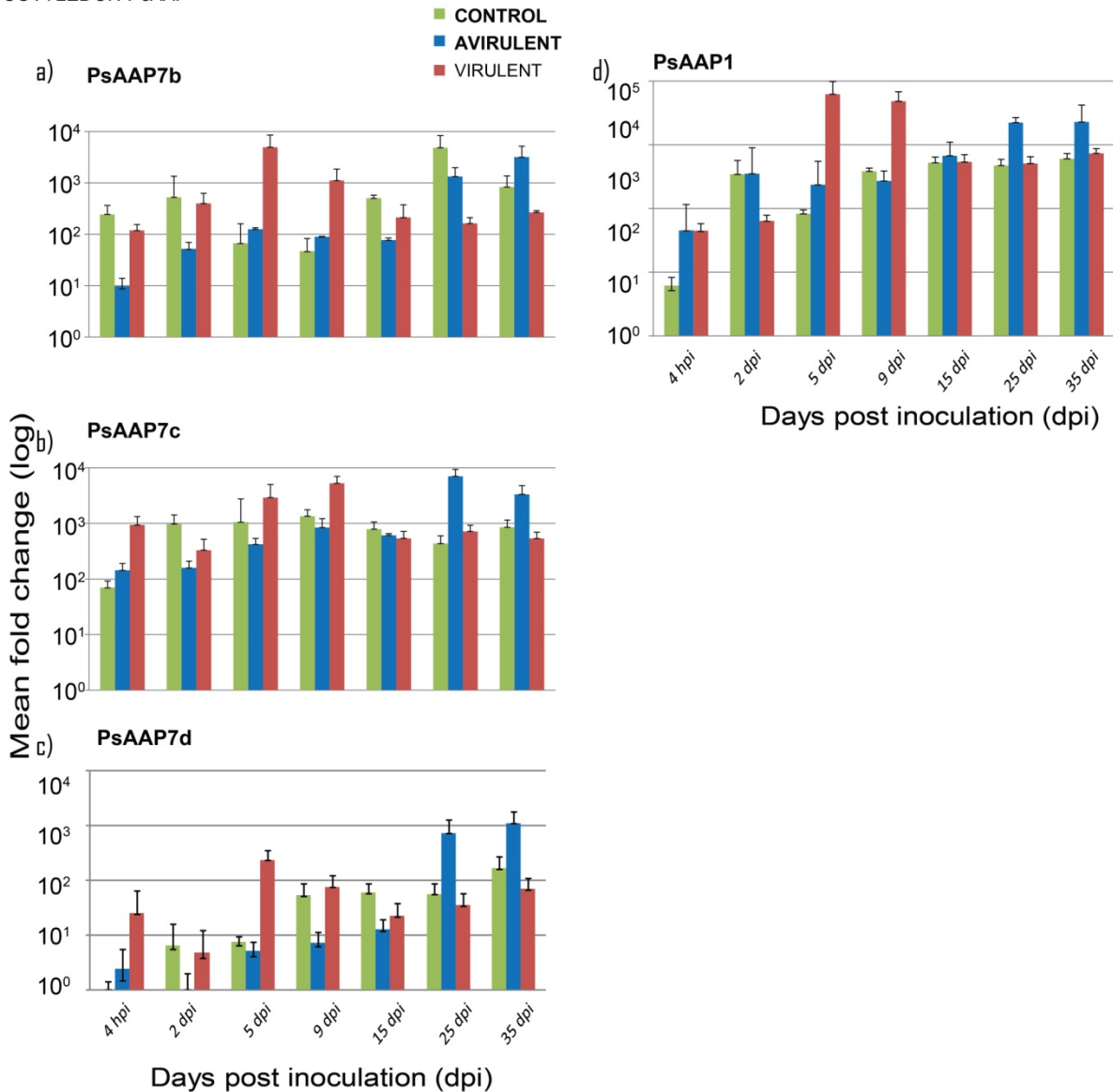


Figure 5.8 Relative expression of *PsAAP7b*, *PsAAP7c*, *PsAAP7d* and *PsAAP1* in *P. sativum* cotyledon tissues. Data are means of relative mRNA levels in fold changes (log) detected using three technical replicates for each of two biological replicates. *PsEF*, *U18S*, *PsGAP* and *PsACT* were used as internal controls. Before quantification of the expression level of each target genes, the Ct numbers for each internal control and target gene were corrected with an internal calibrator and also by using the average correction factor determined for each of the four reference genes. Error bars represent the +/- one SD calculated for the combined technical and biological replicates.

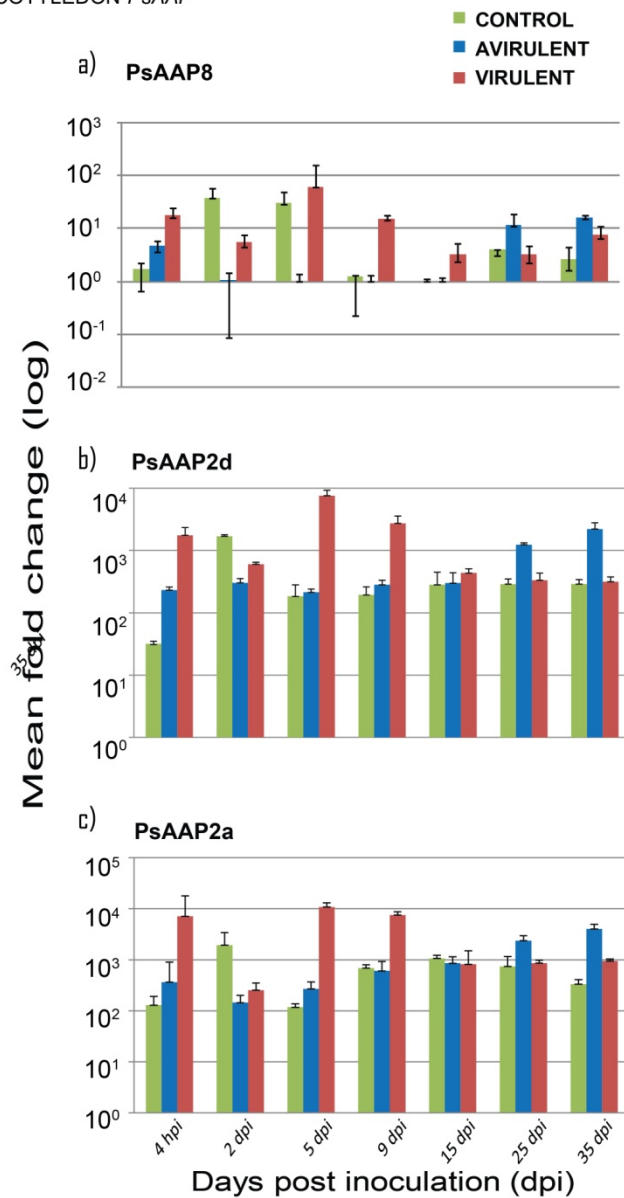


Figure 5.9 **Relative expression of *PsAAP8*, *PsAAP2d* and *PsAAP2a* in *P. sativum* cotyledon tissues.** Data are means of relative mRNA levels in fold changes (log) detected using three technical replicates for each of two biological replicates. *PsEF*, *UI8S*, *PsGAP* and *PsACT* were used as internal controls. Before quantification of the expression level of each target genes, the Ct numbers for each internal control and target gene were corrected with an internal calibrator and also by using the average correction factor determined for each of the four reference genes. Error bars represent the +/- one SD calculated for the combined technical and biological replicates.

Shoot: The transporter genes, *PsSUF1* and *PsAAP2d* were used to study the expression in shoots (Figure 5.10).

PsSUF1 gene expression in con-shoot was relatively low at all growth stages except at initial stage (5 dpi) which was the highest level of expression compared to avir-shoot and vir-shoot. The vir-shoot had high level of *PsSUF1* expression at 15 and 35 dpi. The avir-shoot showed high *PsSUF1* expression at 9 and 25 dpi. *PsSUF1* expression mainly increased with increased growth from 15 to 35 dpi in vir-shoot.

PsAAP2d expression in con-shoot was relatively low compared to avir-shoot and vir-shoot at all points tested. The *PsAAP2d* expression in vir-shoot was less than avir-shoot in all samples except a slight increase or same level from 15 to 35 dpi. Generally, the avir-shoot had high level of *PsAAP2d* expression compared to con-shoot and vir-shoot mainly at 5 and 9 dpi (Figure 5.10).

The *PsSUF1* and *PsAAP2d* expression was comparatively higher in avir-shoot compared to con-shoot and vir-shoot at 9 dpi.

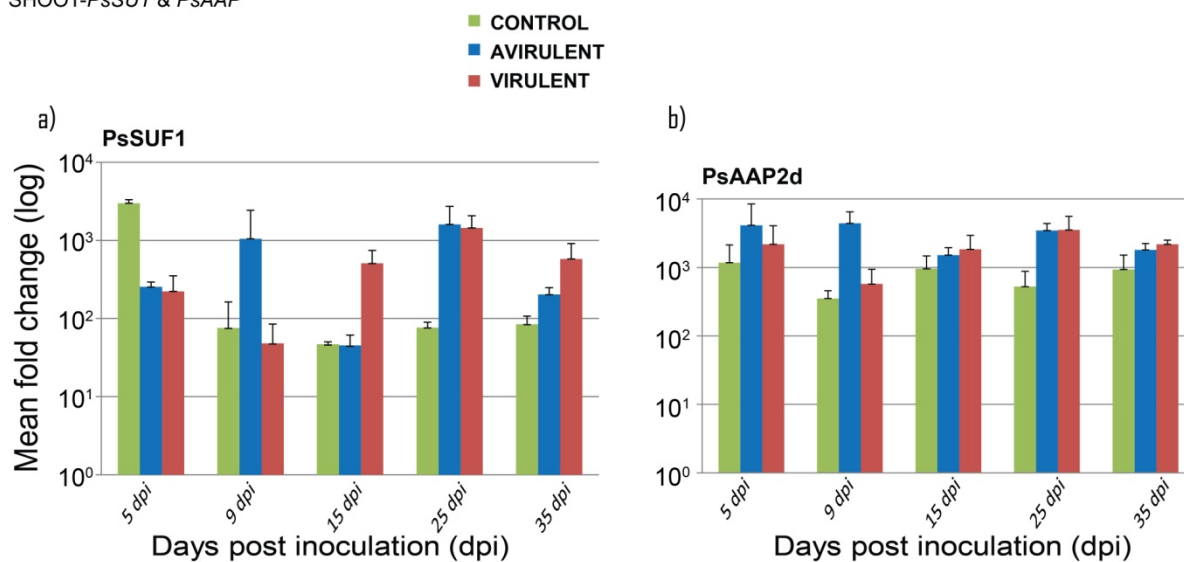


Figure 5.10 **Relative expression of *PsSUF1* and *PsAAP2d* in *P. sativum* shoots tissues.** Data are means of relative mRNA levels in fold changes (log) detected using three technical replicates for each of two biological replicates. *PsEF*, *UI8S*, *PsGAP* and *PsACT* were used as internal controls. Before quantification of the expression level of each target genes, the Ct numbers for each internal control and target gene were corrected with an internal calibrator and also by using the average correction factor determined for each of the four reference genes. Error bars represent the \pm one SD calculated for the combined technical and biological replicates.

5.4 Discussion

The transporter genes (*SUT* and *AAP*) were used in an initial study of the source to sink relationship during infection of pea by *R. fascians*. The distinctive feature of the vir-cot morphology of dark green and intact and robust cotyledons until 45 dpi compared to con-cot and avir-cot led to the investigation of the cotyledons. The persistence of pea cotyledon induced by *Corynebacterium fascians* was noticed by Oduro and Munnecke (1975a) which was explained to be the retention of morphological integrity of cotyledons, and these cotyledons showed traces of lipids, carbohydrates and protein compared to control cotyledons. A similar observation was made by Eason et al. (1995) in *P. sativum* infected with virulent strains of *R. fascians* where the cotyledons were intact and bright green after four weeks of infection.

The increased chlorophyll content of the cotyledon was a distinctive feature of cotyledons infected by *R. fascians* virulent strain 602. (Figure 5.1). The lower levels of chlorophyll content in vir-shoots compared to con-shoot and avir-shoot from 11 to 20 dpi may be due to the loss of chlorophyll during symptom establishment which confirms with the report of Depuydt et al. (2009b) that the chlorophyll content was higher in *Arabidopsis* inoculated with avirulent D188-5 compared to virulent D188 plants through spectrometric analysis at 24 dpi. The elevated levels of chlorophyll in the vir-cot and vir-root from 11 to 40 dpi could be indicative of enhanced cytokinins due to infection by virulent strain 602. The greening process in soybean seedlings was due to chloroplast and photosynthetic development (Harris et al., 1986). The increase in chlorophyll content was observed when cucumber cotyledons were treated with different concentrations of cytokinins by Fletcher and McCullagh (1971) and they suggested that cytokinins played an important role in the chlorophyll formation. It has been suggested that plant tissues infected with *R. fascians* virulent strain D188 never mature and remain as a sink and represent a nutrient-rich niche for *R. fascians* as observed in symptomatic shoot tissues of *Arabidopsis* (Depuydt et al., 2009 a, Depuydt et al., 2009b).

Sucrose uptake transporters (*PsSUTs*) and amino acid permease (*PsAAP*) multi gene families were isolated using pea transcriptome data. Through the phylogenetic analysis *PsSUT1a* grouped with *VfSUT1* with high bootstrap value of 99. The *PsSUT1* and *VfSUT1* shares

96.3% identical amino acids (Weber et al., 1997a) and belonged to the same clade when their sequences were compared (Tegeeder et al., 1999). The isolated *PsSUF1* had high sequence similarity of 100% with the *PsSUF1* in GenBank database. The isolated *PsSUT1b* revealed sequence similarities with *PvSUF1*, *PsSUF1*, *PsSUT1b*, *MtSUT1*, *GmSUT1*, *VfSUT* and *PsSUT1a* and grouped into a clade with subgroups agreeing with Zhou et al. (2007). *PsSUT2* had high sequence similarity with *MtSUT2*, *PsSUT10* and *GmSUT10*.

PsSUT1, *PsSUT1b* and *PsSUF1* expression in cotyledons was mostly high at 2 or 5 dpi, but lower at other growth stages. A northern blot analysis showed that *PsSUT1* is expressed in non-seed tissues, the strongest expression in flowers and weakest expression in sink leaves (Tegeeder et al. 1999). The *PsSUF1* and *PvSUF1* exhibited high seed specificity with *PsSUF1* and *PvSUT1* expression being strongest in cotyledons and seed coats of developing pea and beans (Zhou et al., 2007). The *PsSUF1* expression in con-shoot was high only at 5 dpi (initially) then reduced in later growth stages similar to the *PsSUTs* in cotyledon. Previous studies have been mainly on developing legume seeds involving sugar transporters and amino acid transporters (Tegeeder et al., 2007, Weber et al., 1997a, Weber et al., 1997b, Weber et al., 2005, Zhou et al., 2007), but so far the role of sugar metabolism in germinating cotyledons are not available in literature. The con-cot had low *PsSUTs* and *PsSUF1* expressions except at 2 dpi as the seeds germinated which was expected as the sucrose is transported from source to sink.

PsAAP gene family members phylogenetic analysis revealed that all subgroup gene family members belong to same group/ clade. For example: *PsAAP2a*, *PsAAP2b*, *PsAAP2c*, *PsAAP2d* and *PsAAP2e* of the same gene family had sequence similarities and grouped together in a clade (Figure 4.7). All the isolated *PsAAPs* had representatives in *AtAAP* and legume *AAPs*. The isolated *PsAAP2a*, *PsAAP2b*, *PsAAP2c*, *PsAAP2d*, *PsAAP2e* formed a clade with *AtAAP2*, *AtAAP4* and legumes *MtAAP*, *PsAAP2*, *CaAAP2* and *GmAAP2*. The *AtAAP2* and *AtAAP4* grouped together with high sequence similarity similar to the observation reported by Okumoto et al. (2002). The 7 *PsAAPs* tested for expression was low at all growth stages in control cotyledons and shoots. The *PsAAP1* and *PsAAP2* was isolated by Tegeeder et al. (2000) from pea cotyledon cDNA library. Through northern blotting it was observed that *PsAAP1* expressed in pea cotyledons and strongest expression was noticed in stems and weak in sink leaves, whereas *PsAAP2* was not detected throughout the seeds

(Tegeder et al. 2000). Large amounts of proteins are accumulated in cotyledons during legume seed development and amino acids necessary for the storage are imported into cotyledons from seed apoplasm (Tegeder et al. 2000), but the molecular analysis involved during seed germination is not available so far.

The isolated *PsAAP3a* had high sequence similarity with *PsAAP1* (bootstrap value of 99), whereas the isolated *PsAAP1* had high sequence similarity with *CaAAP1* (bootstrap value 100). The *PsAAP1* expression in con-cot was not prominent at all growth stages compared to vir-cot and avir-cot.

In general, the expression of *PsSUT1*, *PsSUF1* and *PsSUT1b* expressions in vir-cot was high compared to avir-cot and con-cot. The avir-cot had high level of *PsSUTs* and *PsAAPs* expression at 25-35 dpi. *PsSUTs* and *PsSUF1* expression level was higher in the vir-cot, whereas in the vir-shoot it was *vice versa* which does not agree with the data presented by Depuydt et al. (2009b) who reported that the sugar transporter family genes were up-regulated and amino acid transporter family genes were down regulated in the shoots of *Arabidopsis* infected with *R. fascians* virulent strain D188.

The up-regulation of *PsSUTs* and *PsAAP* in the vir-cot compared to con-cot and avir-cot may be due to the establishment of sink strength and correlated to the symptom development. Depuydt et al. (2009b) through microarray and profiling of primary metabolites in *Arabidopsis* infected virulent strain D188 and avirulent strain D188-5 of *R. fascians* revealed higher levels of sugars and amino acids in plants infected by the virulent strain D188 and suggested that *R. fascians* use these as carbon and nitrogen source to maintain its epiphytic and endophytic colonisation. So the high level of *PsSUTs* and *PsAAPs* expression in vir-cot and vir-shoot agrees that upon infection by *R. fascians* source-to-sink transitions occurs and as suggested by Depuydt et al. (2009b) that the status from sugar-producing and exporting changes to sugar-importing and accumulating status due to infection. The up-regulation of transporter genes in vir-cot might also indicate the accumulation of carbohydrates in the cotyledon, which could be a better carbon and nitrogen source for *R. fascians* as suggested by Temmerman et al. (2000) and Depuydt et al. (2009b).

Chapter 6 Final Discussion And Future Work

This study consisted of two broad approaches. One approach was to assess the effect of *R. fascians* infection on *Pisum sativum* using microbiological techniques, including microscopy, to observe the colonisation pattern, epiphytic and endophytic *R. fascians* morphology in association with a natural host, *P. sativum*. The second approach was to study simultaneously the *in planta* expression of key cytokinin biosynthetic (*IPT*), activating (*LOG*), and metabolic (*CKX*) genes of pea and *R. fascians* following inoculation. Additionally, the isolation and *in planta* expression of transporter (*SUT* and *AAP*) genes of control and *R. fascians* infected pea cotyledons and shoots was done to elucidate the process of establishing a nutrient rich niche for *R. fascians* in infected plants.

The virulence in *R. fascians* strain D188 is due to the presence of a conjugative linear plasmid of 200 kb known as pFiD188 that has the genes essential for pathogenesis (Crespi et al. 1992). The U1 region of the pFiD188 plasmid contains three loci involved in virulence: the attenuation (*att*), the fasciation (*fas*) and the hypervirulent (*hyp*) operons (Crespi et al. 1994). The *fas* operon consists of genes involved in cytokinin biosynthesis and is essential for virulence (Crespi et al. 1992). The production of cytokinin by *R. fascians* strain D188 *fas* operon in plasmid pFiD188 is essential for the establishment of symptoms but cytokinin produced chromosomally (tRNA turnover) by *R. fascians* avirulent strains does not affect the host morphologically (Eason et al. 1996, Galis et al. 2005b, Pertry et al. 2009). Screening of 36 wild-type isolates showed the presence of *RfIPT*, *RfLOG* and *RfCKX* genes in 18 isolates previously determined to be virulent (Stange et al. 1996, Eason et al. 1996, Galis et al. 2005b) confirming the integrity of the strains, and, for the first time, showing the presence of *RfLOG* genes in multiple wild type strains of *R. fascians*.

The phenotypic alterations in the pea plants infected with the virulent strain 602 such as stunted growth, multiple shoots, small leaves, thickened primary roots with reduced secondary root growth were observed. These are all regarded as cytokinin induced morphological changes. Other potential cytokinin effects include the delay senescence of the shoots and the greening of the cotyledons. Previous studies have reported similar morphological deformations due to *R. fascians* infection on pea (Eason et al. 1995), *Arabidopsis* (Vereecke et al. 2000, 2003, Manes et al. 2004, Depuydt et al. 2008), and

tobacco (Cornelis et al. 2001) which implies change in the cytokinin balance of the host due to *R. fascians* infection.

The morphology of *R. fascians* itself following inoculation was illustrated using both scanning electron microscopy, to examine the surface colonisation, and light microscopy to examine the epiphytic and endophytic colonisation pattern in pea cotyledons, roots, shoots and leaves. Both strains colonised the surface of cotyledons within 4 h of inoculation (hpi). Colonisation of the surface of roots, shoots and leaves was apparent by five to 45 d post inoculation (dpi). Seed inoculation led to spread of the bacteria from cotyledon to root, shoot and leaves. The number of bacteria increased with growth and time on the infected pea surface. *R. fascians* exhibited both the bacterial and fungal characteristics of an Actinomycete, appearing mainly as rods initially, and later as interconnected rods or hyphal-like structures. The surface colonisation of both virulent and avirulent strains revealed the presence of a mucilage-layer similar to the layer referred to by Cornelis et al. (2001) 'as slime' or by Francis et al. (2012) as 'epiphytic biofilm' on tobacco leaves. Cornelis et al. (2001) suggested that this layer might play a role in modifying the environment around the bacteria during the plant-microbe interaction. Both strains revealed similar surface colonisation patterns but there were variations at different time points and in different organs in the form and spread of the microbes. SEM results were consistent with the observations made by Cornelis et al. (2001) in tobacco leaves and *Arabidopsis* shoots and leaves, but the colonisation on pea shoots and leaves was not clearly illustrated due to the texture of the surface. The pea cotyledon and roots exhibited prominent and dense bacterial colonisation at all time points.

R. fascians virulent strain 602 was observed in the intercellular spaces of the subepidermal layer of the seed coat within 4 h of inoculation, but the penetration of the avirulent strain 589 into the seed coat was apparent only at 2 dpi. In contradiction of Cornelis et al. (2001) suggestion that plasmid pFi188 is required for the penetration of the bacteria into the tobacco leaf, these results showed the presence of both strains inside the intercellular spaces of the subepidermal layer of the seed coat. The presence of *R. fascians* virulent strain 602 in the seed coat within 4 h of inoculation, reveals the need to study the *R. fascians*-plant interaction effect at the early stages of infection. Development of multiple shoots was noticed only at 5 dpi. This indicates that endophytic colonisation preceded symptom manifestation in the host

contradicting the statement by Crespi et al. (1992) and Cornelis et al. (2001). This might be due to variations in the method of inoculation and the organ inoculated. Putan and Miller (2007) in their review have pointed out that *R. fascians* has great ability to survive in soil and the infested soil could be a means of contaminating the host. So, this study gives a clear illustration of the natural scenario occurring in the *R. fascians*-plant interaction. Further, *R. fascians* were observed only as endophytic population in the seed coat but not in cotyledons, roots and shoots. The presence of bacteria inside the internal tissues of spot inoculated *Arabidopsis* stems and sepals were illustrated by Manes et al. (2004). But in this project the bacteria was not visualised as an endophytic population except in the seed coat. This may be due to the sloughing off of the outer layer of the pea roots and of the epidermal layers of shoots in the plants infected with virulent strain 602 but in case of the roots and shoots infected with the avirulent strain 589 the sloughing of the epidermal layer was not observed. The interaction studies of *R. fascians* with *P. sativum* revealed that the colonisation of the plant surface started immediately after infection by both avirulent strain 589 and virulent strain 602. The virulent strain 602 did not immediately cause symptom development and it behaved as a saprophytic epiphyte from the time of inoculation (4 hpi) until 2 dpi as only the single plumule was observed, but by 5 dpi the plumule had developed into multiple shoots clearly indicating that *R. fascians* strain 602 had become pathogenic.

The multi-gene families of *P. sativum* (*IPT*, *LOG*, *CKX*, *RR*) used for expression studies were representatives of their respective phylogenetic groups. In this project, three *PsIPTs*, three *PsLOGs*, five *PsCKXs*, four *PsRRs* multi-gene family members from *P. sativum* and one *IPT*, *LOG* and *CKX* gene from *R. fascians* were isolated. The objective of discriminating between plant (pea) and microbe (*R. fascians*) *IPT*, *LOG* and *CKX* genes was achieved through careful designing of primers. This enabled a study of the differences in the expression profile of the plant genes and *R. fascians* genes between the control and the infected plants.

The expression profile of individual cytokinin biosynthesis (*PsIPT*, *PsLOG*) and metabolic (*PsCKX*) gene family members isolated in this project were tissue and developmentally specific. The multi-gene family members of *PsLOG* were isolated and their expression studied for the first time in this project. Overall, *PsRRs* expression in control cotyledons was high only at 2 dpi and it was low in roots and shoots during all growth stages, indicating

cytokinins levels were low as type-A *RRs* expression is a good indicator of endogenous cytokinin levels.

There was essentially no expression of *R. fascians* cytokinin genes (*RfIPT*, *RfLOG* and *RfCKX*) in control plants and cotyledons, roots and shoots infected with avirulent strain 589 or in the 589 culture cDNA. This confirms that the primers discriminated between pea and *R. fascians* genes. It also confirms the absence of the virulence plasmid in avirulent strain 589 and the absence of cross-contamination of the plants.

The expression pattern of *RfIPT*, *RfLOG* and *RfCKX* showed an up-regulation immediately after inoculation at 4 hpi and could be related to the entry of bacteria into the seed coat at 4 hpi. Depuydt et. al (2008) and Pertry et al. (2009) have indicated that there is a rapid response as shown by the elevated levels of cytokinin mixes within two days of inoculation in *Arabidopsis* shoots infected with *R. fascians* virulent strain D188. The relative expression of pea cytokinin biosynthesis genes, *PsIPTs* and *PsLOGs* in the cotyledons infected with the virulent strain 602 was also high at the time of inoculation indicating high cytokinin synthesis due to the induction of both pea and *R. fascians* cytokinin biosynthesis genes. *PsIPTs* and *PsLOGs* expression reduced with growth which was also reflected in the *RfIPT* and *RfLOG* expression indicating a reduction in cytokinin synthesis at later stages of growth.

In general, the *RfIPT*, *RfLOG* and *RfCKX* expression was high mainly at 15 and 25 dpi in roots and shoots. The pattern of *RfIPT*, *RfLOG* and *RfCKX* expression was similar in vir-roots and vir-shoots at most of the growth stages. Generally, there was gradual increase in expression mostly from 15 to 25 dpi (highest) and a decline with growth in roots and shoots. By this time, as observed in the light microscope, *R. fascians* was prominent, profuse and dense in roots and on the symptomatic multiple shoots infected by virulent strain 602 at 15 and 25 dpi. This confirms that the presence of *R. fascians* virulent plasmid with *fas* locus in virulent strain 602 as well as cytokinin plays an important role in *R. fascians* pathogenesis.

The relative expression of cytokinin *PsIPTs* and *PsLOGs* multi-gene family members revealed variations in response to *R. fascians* avirulent strain 589 compared with the virulent strain 602 infected pea roots and shoots. The expression of *PsIPTs* and *PsLOGs* in vir-root and vir-shoot was reduced initially compared with the mock inoculated control, but was

higher than avir-roots and avir-shoots. The *PsIPTs* and *PsLOGs* expressions mostly peaked at 15 and 25 dpi in roots and shoots infected with the virulent strain and then remained steady with growth. So, there was variation in the *PsIPTs* and *PsLOGs* expression in cotyledons compared to roots and shoots of virulent strain 602 infected plants. The relative expression of *RfIPT* and *RfLOG* was mostly high at 15 dpi in vir-roots and vir-shoots and then remained steady or reduced with growth of plant.

PsIPTs and *PsLOGs* expression in the avir-cot increased mainly at 25 and 35 dpi, but in avir-root and avir-shoot the increase was not observed in *PsIPTs*. The *PsLOGs* expression increased in avir-shoot mainly at 25 dpi. These results support the findings of Eason et al. (1996) and Galis et al. (2005b) related to increase of cytokinin content in the shoots of nonvirulent strain inoculated pea after two weeks.

The decrease of *PsIPTs* and *PsLOGs* expression at later stages of growth (from 25 to 35 dpi) in pea infected by the virulent strain of *R. fascians* was expected as Pertry et al. (2009) showed that, with time iP, tZ, 2MeSiP and 2MeStZ levels decreased in *A. thaliana* tissues infected by virulent strain D188 of *R. fascians* compared to mock-inoculated controls. A similar observation was reported by Depuydt et al. (2008), where the down-regulation of *AtIPTs* was correlated with the reduction of three cytokinin monophosphates (tZMP, cZMP and iPMP) and iP in *Arabidopsis* infected by *R. fascians* at 30 dpi. This reduction of cytokinin biosynthesis by down-regulation of *AtIPT* expression was thought by Depuydt et al. (2008) to be a negative feedback mechanism imposed by increased bacterial cytokinins and they also showed that the increase in endogenous cytokinin in *Arabidopsis* was reflected in the high level of expression of *ARR5*. The cZ and 2MeS-derivatives might originate from tRNA degradation (Murai et al. 1980, Miyawaki et al. 2006) so up-regulation of *PsRRs* might be due to the presence of cytokinins not only from de novo synthesis but also from tRNA turnover.

Compared with both control plants and plants inoculated with *R. fascians* avirulent strain 589, *PsCKX* expression was up-regulated in cotyledons, roots and shoots infected by the virulent strain 602 indicating the activation of the plant homeostatic mechanism. This might be due to high levels of cytokinins in pea tissues infected by the virulent strain. This result is in agreement with Galis et al. (2005a) report of induction of expression in *AtCKX3* promoters

in transgenic plants infected with the virulent strain of *R. fascians* compared to tobacco infected by the avirulent strain. Depuydt et al. (2008) also noted the up-regulation of *AtCKX3* expression in *Arabidopsis* infected by the virulent strain D188 at 7 and 30 dpi and reported a reduction of iP, 7-N and 9-N conjugates, which are CKX enzyme substrates. Depuydt et al. (2009b) also showed up-regulation of two *AtCKXs* due to infection by virulent strain in *Arabidopsis*, highlighting the onset of the cytokinin homeostasis mechanism. The *RfCKX* expression in vir-cots was high immediately after inoculation, prominent at 5 and 9 dpi then reduced. But in case of roots and shoots infected with the virulent strain the *RfCKX* expression was highest at 15 dpi. This indicates that the bacterial and plant cytokinin deactivating gene (*RfCKX* and *PsCKX*) activity was high mainly at 15 dpi coinciding with the time when both *RfIPT*, *RfLOG* and *PsIPT*, *PsLOG* expressions were at their highest.

The up-regulation of the response regulators *PsRR3*, 5, 6 and 9, which are considered to be type-A response regulators in the cotyledons, roots and shoots infected with the virulent strain 602 compared to the control and the avirulent strain 589 infected tissues indicates elevated endogenous cytokinins in pea infected by the virulent strain 602. Depuydt et al. (2009b) through transcriptome analysis, showed up-regulation of *ARR4*, 6, 7, 8 and 16 in *Arabidopsis* shoots infected by virulent strain D188. This supports the suggestion that plants infected with virulent strain of *R. fascians* have elevated cytokinins leading to symptom initiation and development.

The isolated multi-gene family members of *PsSUTs*, *PsSUF* and *PsAAP*, were representatives of their respective phylogenetic groups. The *PsSUTs* expression was higher in germinating control cotyledons but *vice versa* in shoot. This might indicate the transfer of carbohydrates from storage organ (cotyledon) to the other parts of the plant. The expression of the transporter genes decreased with growth, implying that sucrose and amino acids are transported to sinks with maximum transport of nutrients to growing parts of the plant. The expression of *PsSUTs* and *PsSUF1* was high in pea cotyledons infected with virulent strain 602 in most of the growth stages compared to the control cotyledons and cotyledons infected with the avirulent strain 589. Depuydt et al. (2009b) through metabolic profiling of *Arabidopsis* shoots infected with a virulent strain of *R. fascians*, showed up-regulation of sugar transporter genes, accumulation of carbohydrates as source of carbon and suggested that infected tissues were converted into sink tissues facilitating the bacterial growth. The

PsAAPs expression was high in the pea shoots infected with the virulent strain 602 compared to shoots infected with the avirulent strain 589. The amino acids levels were found to be increased during symptom development in *Arabidopsis* shoots by Depuydt et al. (2009b) and they also suggested that it might be used as a nitrogen source by *R. fascians*. The expression of the transporter genes, *PsSUTs* and *PsAAPs*, and the increased chlorophyll content in vir-cot supports the cotyledons becoming sink for *R. fascians* development. Depuydt et al. (2009b) explained increased sink characteristics may be related to symptom establishment which is an energy-demanding process and also provides nutrition to *R. fascians*. As virulent strains of *R. fascians* are biotrophic, the increased expression of the transporter genes (*PsSUTs*, *PsSUFs* and *PsAAPs*) may relate to the use of cotyledons becoming a sink to provide carbohydrates and energy for the survival of the bacteria.

During the infection of pea cotyledons by the virulent strain of *R. fascians*, the plant cytokinin homeostatic mechanism was challenged immediately after inoculation (4 hpi). Accumulation of cytokinins is indicated by the up-regulation of cytokinin biosynthesis genes of pea (*PsIPTs* and *PsLOGs*) and of *R. fascians* (*RfIPT* and *RfLOG*). This triggers the plant to activate its homeostasis mechanisms, such as the up-regulation of its *PsCKXs*. Additionally, *RfCKX* expression is also increased potentially reducing the level of both bacterial and plant cytokinins. However, the up-regulation of *PsRRs* expression in pea tissues indicates that this mechanism was not sufficient to reduce the cytokinin content, so the high level of cytokinins in the host (pea) led to the typical morphological changes of shoot malformations.

In the case of pea cotyledons, roots and shoots infected with the avirulent strain of *R. fascians*, low level of expression of the *PsIPTs* and *PsLOGs* initially, and up-regulation mostly at 25 and 35 dpi, suggests that the cytokinin production increases in the latter stages of growth whereby the plant homeostasis mechanism sets in to keep an optimal level of cytokinin. The expressions pattern of *PsIPTs* and *PsLOGs* in the pea tissues infected with *R. fascians* avirulent strain was similar to the result obtained by Depuydt et al. (2008) through cytokinin profiling in *Arabidopsis* leaves at different time points following infection with strain D188-5 (avirulent).

The expression of *PsCKXs* in the peas infected with the avirulent strain of *R. fascians* were relatively low at most stages of pea growth indicating CKX enzyme activity was low which

is similar to the observation made by Depuydt et al. (2008) where CKX activity in *Arabidopsis* tissue infected with strain D188-5 was below the detection limit. The relatively low expression of all *PsRRs* also supports the suggestion that the active cytokinin level is "normal" in the peas infected with the avirulent strain. This indicates that the plant cytokinin homeostasis mechanism is very effective in the pea infected with *R. fascians* avirulent strain. Additionally, Galis et al. (2005b) suggested that the cytokinins emanating from the avirulent strain might have been converted to inactive 9-glucoside nucleotides and O-glucosides.

This research project focussed only on the cytokinins, but other hormones and compounds such as auxins, putrescine, salicylic acid and the strigolactones also play important roles during *R. fascians* infection of plants. It has been suggested that these hormones are mainly used by plant to prevent the *R. fascians* infection, as well as *R. fascians* manipulating these hormones, mainly auxins, to facilitate their infection and reduce plant immunity.

Future Work

To fully characterise the spatial and temporal expression of the cytokinin multi-gene family members requires isolation of all *PsIPTs*, *PsLOGs* and *PsCKXs*. This would provide a better insight to identify more of the key genes involved during growth and development. Further work is required to study the the key IPT and CKX enzymes at the protein level in transgenic *Arabidopsis* infected with virulent and avirulent strains of *Rhodococcus fascians* by generating transgenic *Arabidopsis* with the identified key *IPT* promoter::*GFP* (green fluorescent protein) reporter gene and *CKX* promoter::*YFP* (yellow fluorescent protein) reporter gene from the pea.

The immediate response of both plant and *R. fascians* cytokinin biosynthesis genes in pea cotyledons infected with *R. fascians* virulent strains needs further experimentation to investigate the signal molecules involved between the plant and microbe for immediate response of the host to the microbe.

Stange et al. (1996) reported that the *fasI* genes on 17 virulent strains of *R. fascians* were on linear plasmids of 200 or 130 kb size, except for a virulent strain 666 where *fasI* was located on a circular plasmid. The characteristics of virulent isolates possessing circular or linear plasmids of varying sizes could be explored further. There was more variation in the type and size of plasmids containing the virulence, as isolates 605 and 606 with 130 kb linear plasmid was found to be less virulent.

Profiling the endogenous cytokinins in pea cotyledons, roots and shoots infected with avirulent and virulent strain of *R. fascians* at different time points may enhance our knowledge of the relationship between the expression of cytokinin biosynthesis, metabolism and response regulator genes in both pea and *R. fascians*. Additionally, the source of Methylthio-trans zeatin (MeStZ) needs to be ascertained.

The *R. fascians* interaction with pea needs further in depth study of the endophytic colonisation of the bacteria in the infected host through use of oligonucleotides probes or fluorescent dyes to locate the bacteria.

The effect of *R. fascians* in cotyledons needs further exploration in terms of the role of other genes including invertase, senescence associated (*SAG*) genes and *SWEET* genes. Recently, ' *SWEET*' sugar transporter, a plasma protein, was identified which is located in the phloem parenchyma that exports sucrose to *SUT1* sugar loader. *SWEET* has also been identified as a pathogen resistance loci, which was induced in rice by blight pathogen, *Xanthomonas oryzae* infection (Schroder et al. 2013). The study of other metabolic genes in the cotyledons would further elucidate the effect of *R. fascians* on host metabolism.

Recent, Stes et al. (2012) have shown a role for plant-derived auxin in the *R. fascians Arabidopsis* interaction whereby *R. fascians* produces putrescine and IAA to assist in symptom development and reduce plant immunity. The future challenges would be to investigate the precise nature and function of plant defenses due to infection by *R. fascians* and to study the role of bacterial and plant auxin in the infection processes.

REFERENCES

- Abe I, Tanaka H, Abe T, Noguchi H. 2007.** Enzymatic formation of unnatural cytokinin analogs by adenylate isopentenyltransferase from mulberry. *Biochemical and Biophysical Research Communications*, **355**: 795-800.
- Akiyoshi DE, Klee H, Amasino RM, Nester EW, Gordon MP. 1984.** T-DNA of *Agrobacterium tumefaciens* encodes an enzyme of cytokinin biosynthesis. *Proceedings of the National Academy of Sciences*, **81**: 5994-5998.
- Akiyoshi DE, Regier DA, Gordon MP. 1987.** Cytokinin production by *Agrobacterium* and *Pseudomonas* spp. *Journal of Bacteriology*, **169**: 4242-4248.
- Anderson JP, Gleason CA, Foley RC, Thrall PH, Burdon JB, Singh KB. 2010.** Plants versus pathogens: an evolutionary arms race. *Functional Plant Biology*, **37**: 499-512.
- Anonymous. 2000.** Analysis of the genome sequence of the flowering plant *Arabidopsis thaliana*. *Nature*, **408**: 796-815.
- Anonymous. 2006.** *Rhodococcus fascians*. *Crop Protection Compendium*. Wallingford, UK.: CAB International.
- Anton BP, Saleh L, Benner JS, Raleigh EA, Kasif S, Roberts RJ. 2008.** RimO, a MiaB-like enzyme, methylthiolates the universally conserved Asp88 residue of ribosomal protein S12 in *Escherichia coli*. *Proceedings of the National Academy of Sciences, U S A*, **105**: 1826-31.
- Aoki N, Hirose T, Scofield GN, Whitfeld PR, Furbank RT. 2003.** The sucrose transporter gene family in rice. *Plant Cell Physiology*, **44**: 223-32.
- Argyros RD, Mathews DE, Chiang Y-H, Palmer CM, Thibault DM, Etheridge N, Argyros DA, Mason MG, Kieber JJ, Schaller GE. 2008.** Type B response regulators of *Arabidopsis* play key roles in cytokinin signaling and plant development. *The Plant Cell* **20**: 2102-2116.
- Armstrong DJ, Firtel RA. 1989.** Cytokinin oxidase activity in the cellular slime mold, *Dictyostelium discoideum*. *Developmental Biology*, **136**: 491-9.
- Armstrong DJ, Scarbrough E, Skoog F. 1976.** Cytokinins in *Corynebacterium fascians* cultures: isolation and identification of 6-(4-Hydroxy-3-methyl-cis-2-butenylamino)-2-methylthiopurine. *Plant Physiology*, **58**: 749-52.
- Asakura Y, Hagino T, Ohta Y, Aoki K, Yonekura-Sakakibara K, Deji A, Yamaya T, Sugiyama T, Sakakibara H. 2003.** Molecular characterization of His-Asp phosphorelay signaling factors in maize leaves: Implications of the signal divergence by cytokinin-inducible response regulators in the cytosol and the nuclei. *Plant Molecular Biology*, **52**: 331-341.
- Ashikari M, Sakakibara H, Lin S, Yamamoto T, Takashi T, Nishimura A, Angeles E, Qian Q, Kitano H, Matsuoka M. 2005.** Cytokinin oxidase regulates rice grain production. *Science*, **309**: 741 - 745.
- Åstot C, Dolezal K, Nordström A, Wang Q, Kunkel T, Moritz T, Chua N-H, Sandberg G. 2000.** An alternative cytokinin biosynthesis pathway. *Proceedings of the National Academy of Sciences*, **97**: 14778-14783.
- Ayre BG. 2011.** Membrane-transport systems for sucrose in relation to whole-plant carbon partitioning. *Molecular Plant*.
- Baker KF. 1950.** Bacterial fasciation disease of ornamental plants in California. *Plant Disease Reporter*, **34**: 121-126.
- Bar T, Okon Y. 1993.** Tryptophan conversion to indole-3-acetic acid via indole-3-acetamide in *Azospirillum brasilense* Sp7. *Canadian Journal of Microbiology*, **39**: 81-86.
- Barash I, Manulis-Sasson S. 2007.** Virulence mechanisms and host specificity of gall-forming *Pantoea agglomerans*. *Trends in Microbiology*, **15**: 538-545.
- Barry GF, Rogers SG, Fraley RT, Brand L. 1984.** Identification of a cloned cytokinin biosynthetic gene. *Proceedings of the National Academy of Sciences*, **81**: 4776-4780.
- Bassil NV, Mok D, Mok MC. 1993.** Partial purification of a cis-trans-isomerase of zeatin from immature seed of *Phaseolus vulgaris* L. *Plant Physiology*, **102**: 867-872.

- Beveridge TJ, Davies JA. 1983.** Cellular responses of *Bacillus subtilis* and *Escherichia coli* to the Gram stain. *Journal of Bacteriology*, **156**: 846-858.
- Bilyeu K, Cole J, Laskey J, Riekhof W, Esparza T, Kramer M, Morris R. 2001.** Molecular and biochemical characterization of a cytokinin oxidase from maize. *Plant Physiology*, **125**: 378 - 386.
- Blackwell JR, Horgan R. 1994.** Cytokinin biosynthesis by extracts of *Zea mays*. *Phytochemistry*, **35**: 339-342.
- Bradbury JF. 1986.** *Guide to the Plant Pathogenic Bacteria Rhodococcus Zopf*. Kew, UK: CAB International Mycological Institute.
- Brandstatter I, Kieber JJ. 1998.** Two genes with similarity to bacterial response regulators are rapidly and specifically induced by cytokinin in *Arabidopsis*. *The Plant Cell* **10**: 1009-1019.
- Brown NA. 1927.** Sweet pea fasciation, a form of crown gall. *Phytopathology*, **17**.
- Brugiere N, Bohn J, Humbert S, Rizzo N, Habben J. 2008.** A member of the maize isopentenyl transferase gene family, *Zea mays* isopentenyl transferase 2 (*ZmIPT2*), encodes a cytokinin biosynthetic enzyme expressed during kernel development. *Plant Mol Biol*, **67**: 215 - 229.
- Brugière N, Humbert S, Rizzo N, Bohn J, Habben J. 2008.** A member of the maize isopentenyl transferase gene family, *Zea mays* isopentenyl transferase 2 (*ZmIPT2*), encodes a cytokinin biosynthetic enzyme expressed during kernel development. *Plant Molecular Biology*, **67**: 215-229.
- Brugiere N, Shuping J, Hanke S, Zinselmeier C, Roessler J, Niu X, Jones R, Habben J. 2003.** Cytokinin oxidase gene expression in maize is localized to the vasculature, and is induced by cytokinins, abscisic acid, and abiotic stress. *Plant Physiology*, **132**: 1228 - 1240.
- Bukhalid RA, Chung SY, Loria R. 1998.** *nec1*, a gene conferring a necrogenic phenotype, is conserved in plant-pathogenic *Streptomyces* spp. and linked to a transposase pseudogene. *Molecular Plant Microbe Interactions*, **11**: 960-7.
- Burkle L, Cedzich A, Dopke C, Stransky H, Okumoto S, Gillissen B, Kuhn C, Frommer WB. 2003.** Transport of cytokinins mediated by purine transporters of the PUP family expressed in phloem, hydathodes, and pollen of *Arabidopsis*. *The Plant Journal*, **34**: 13-26.
- Burr TJ, Katz BH, Abawi GS, and Crosier, D.C. . 1991.** Comparison of tumorigenic strains of *Erwinia herbicola* isolated from table beet with *E. h. gypsophila*. *Plant Disease*, **75**: 855-858.
- Bustin SA, Benes V, Garson JA, Hellems J, Huggett J, Kubista M, Mueller R, Nolan T, Pfaffl MW, Shipley GL, Vandesompele J, Wittwer CT. 2009.** The MIQE guidelines: minimum information for publication of quantitative real-time PCR experiments. *Clin Chem*, **55**: 611-22.
- Carleton HM, Druvy RAB. 1957.** In: Carleton HM, ed. *Histological Technique: for normal pathological tissues and the identification of parasites*. 3 ed. New York: London Oxford University Press.
- Chalupowicz L, Barash I, Schwartz M, Aloni R, Manulis S. 2006.** Comparative anatomy of gall development on *Gypsophila paniculata* induced by bacteria with different mechanisms of pathogenicity. *Planta*, **224**: 429-437.
- Chang L, Ramireddy E, Schmölling T. 2013.** Lateral root formation and growth of *Arabidopsis* is redundantly regulated by cytokinin metabolism and signalling genes. *Journal of Experimental Botany*, **64**: 5021-5032.
- Chatfield SP, Stirnberg P, Forde BG, Leyser O. 2000.** The hormonal regulation of axillary bud growth in *Arabidopsis*. *The Plant Journal*, **24**: 159-69.
- Chen CM, Kristopeit SM. 1981a.** Metabolism of cytokinin : dephosphorylation of cytokinin ribonucleotide by 5¹-nucleotidases from wheat germ cytosol. *Plant Physiology*, **67**: 494-498.
- Chen CM, Kristopeit SM. 1981b.** Metabolism of cytokinin: deribosylation of cytokinin ribonucleoside by adenosine nucleosidase from wheat germ cells. *Plant Physiology*, **68**: 1020-3.

- Cherayil JDa, Lipsett MN. 1977.** Zeatin ribonucleosides in the transfer ribonucleic acid of *Rhizobium leguminosarum*, *Agrobacterium tumefaciens*, *Corynebacterium fascians*, and *Erwinia amylovora*. *Journal of Bacteriology*, **131**: 741-744.
- Chilton MD, Saiki RK, Yadav N, Gordon MP, Quetier F. 1980.** T-DNA from *Agrobacterium* Ti plasmid is in the nuclear DNA fraction of crown gall tumor cells. *Proceedings of the National Academy of Sciences, U S A*, **77**: 4060-4.
- Choi J, Choi D, Lee S, Ryu CM, Hwang I. 2011.** Cytokinins and plant immunity: old foes or new friends? *Trends in Plant Science*, **16**: 388-94.
- Chomczynski P, Sacchi N. 1987.** Single-step method of RNA isolation by acid guanidinium thiocyanate-phenol-chloroform extraction. *Analytical Biochemistry*, **162**: 156-159.
- Clark E, Manulis S, Ophir Y, Barash Ia, Gafni Y. 1993.** Cloning and characterization of *iaaM* and *iaaH* from *Erwinia herbicola* pathovar *gypsophila*. *Phytopathology*, **83**: 234-240.
- Connolly DM, Winkler ME. 1991.** Structure of *Escherichia coli* K-12 *miaA* and characterization of the mutator phenotype caused by *miaA* insertion mutations. *Journal of Bacteriology*, **173**: 1711-21.
- Cooksey DAa, Keim R. 1983.** Association of *Corynebacterium fascians* with fasciation disease of *Impatiens* and *Hebe* in California. *Plant disease*, **67**: 1389.
- Corbesier L, Prinsen E, Jacquard A, Lejeune P, Van Onckelen H, Perilleux C, Bernier G. 2003.** Cytokinin levels in leaves, leaf exudate and shoot apical meristem of *Arabidopsis thaliana* during floral transition. *Journal of Experimental Botany*, **54**: 2511-7.
- Cornelis K, Ritsema T, Nijse J, Holsters M, Goethals K, Jaziri M. 2001.** The plant pathogen *Rhodococcus fascians* colonizes the exterior and interior of the aerial parts of plants. *Molecular Plant-Microbe Interactions*, **14**: 599-608.
- Crespi M, Messens E, Caplan AB, Van Montagu M, Desomer J. 1992.** Fasciation induction by the phytopathogen *Rhodococcus fascians* depends upon a linear plasmid encoding a cytokinin synthase gene. *EMBO Journal*, **11**: 795-804.
- Crespi M, Vereecke D, Temmerman W, Van Montagu Ma, Desomer J. 1994.** The *fas* operon of *Rhodococcus fascians* encodes new genes required for efficient fasciation of host plants. *Journal of Bacteriology*, **176**: 2492-2501.
- D'Agostino IB, Deruere J, Kieber JJ. 2000.** Characterization of the response of the *Arabidopsis* response regulator gene family to cytokinin. *Plant Physiology*, **124**: 1706-17.
- Davies PJ. 1995.** *Plant hormones: physiology, biochemistry and molecular biology*. Dordrecht, The Netherlands: Kluwer Academic Publishers.
- Depuydt S, De Veylder L, Holsters M, Vereecke D. 2009 a.** Eternal youth, the fate of developing *Arabidopsis* leaves upon *Rhodococcus fascians* infection. *Plant Physiology*, **149**: 1387-1398.
- Depuydt S, Doležal K, Van Lijsebettens M, Moritz T, Holsters Ma, Vereecke D. 2008.** Modulation of the hormone setting by *Rhodococcus fascians* results in ectopic KNOX activation in *Arabidopsis*. *Plant Physiology*, **146**: 1267-1281.
- Depuydt S, Trenkamp S, Fernie AR, Elftieh S, Renou JP, Vuylsteke M, Holsters M, Vereecke D. 2009b.** An integrated genomics approach to define niche establishment by *Rhodococcus fascians*. *Plant Physiology*, **149**: 1366-1386.
- Derveaux S, Vandesompele J, Hellemans J. 2010.** How to do successful gene expression analysis using real-time PCR. *Methods*, **50**: 227-230.
- Devos S, Laukens K, Deckers P, Van Der Straeten D, Beeckman T, Inzé D, Van Onckelen H, Witters E, Prinsen E. 2006.** A hormone and proteome approach to picturing the initial metabolic events during *Plasmodiophora brassicae* infection on *Arabidopsis*. *Molecular Plant-Microbe Interactions*, **19**: 1431-1443.
- Devos S, Vissenberg K, Verbelen JP, Prinsen E. 2005.** Infection of Chinese cabbage by *Plasmodiophora brassicae* leads to a stimulation of plant growth: impacts on cell wall metabolism and hormone balance. *New Phytologist*, **166**: 241-50.

- Devos Sa, Prinsen E. 2006.** Plant hormones: a key in clubroot development *Proceedings 33rd PGRSA Annual Meeting*.
- Doidy J, Grace E, Kühn C, Simon-Plas F, Casieri L, Wipf D. 2012.** Sugar transporters in plants and in their interactions with fungi. *Trends in Plant Science*, **17**: 413-422.
- Dowson WJ. 1957.** *Plant diseases due to bacteria*. England: Cambridge University Press.
- Eason JR. 1993.** *The role of plasmids and cytokinins in pathogenicity of Rhodococcus fascians.*, PhD, University of Otago, Dunedin, New Zealand.
- Eason JR, Jameson EP, Bannister P. 1995.** Virulence assessment of *Rhodococcus fascians* strains on pea cultivars. *Plant Pathology*, **44**: 141-147.
- Eason JR, Morris RO, Jameson EP. 1996.** The relationship between virulence and cytokinin production by *Rhodococcus fascians* (Tilford 1936) Goodfellow 1984. *Plant Pathology*, **45**: 323-331.
- Escobar MA, Dandekar AM. 2003.** *Agrobacterium tumefaciens* as an agent of disease. *Trends in Plant Science*, **8**: 380-6.
- Evans T, Song J, Jameson EP. 2012.** Micro-scale chlorophyll analysis and developmental expression of a cytokinin oxidase/dehydrogenase gene during leaf development and senescence. *Plant Growth Regulation*, **66**: 95-99.
- Eviatar-Ribak T, Shalit-Kaneh A, Chappell-Maor L, Amsellem Z, Eshed Y, Lifschitz E. 2013.** A cytokinin-activating enzyme promotes tuber formation in tomato. *Current Biology*, **23**: 1057-1064.
- Faiss M, Zalubilova J, Strnad M, Schmulling T. 1997.** Conditional transgenic expression of the *ipt* gene indicates a function for cytokinins in paracrine signaling in whole tobacco plants. *The Plant Journal*, **12**: 401-15.
- Faivre-Amiot A. 1967.** Quelques observations sur la présence de *Corynebacterium fascians* (Tilford) Dowson dans les cultures maraichères et florales en France. *Phytiatr Phytopharm.*, **16**: 165-176.
- Finnerty WR. 1992.** The biology and genetics of the genus *Rhodococcus*. *Annual Review of Microbiology*, **46**: 193-218.
- Fischer W-N, André B, Rentsch D, Krolkiewicz S, Tegeder M, Breikreuz K, Frommer WB. 1998.** Amino acid transport in plants. *Trends in Plant Science*, **3**: 188-195.
- Fletcher RA, McCullagh D. 1971.** Cytokinin-induced chlorophyll formation in cucumber cotyledons. *Planta*, **101**: 88-90.
- Forizs L, Lestrade S, Mol A, Dierick J-F, Gerbaux C, Diallo B, El Jaziri M, Baucher M, Vandeputte O. 2009.** Metabolic shift in the phytopathogen *Rhodococcus fascians* in response to cell-free extract of infected tobacco plant tissues. *Current Microbiology*, **58**: 483-487.
- Francis I. 2009.** *Secrets of pFID188, the linear virulence plasmid of Rhodococcus fascians strain D188*, PhD, University of Gent, Gent.
- Francis I, De Keyser A, De Backer P, Simon-Mateo C, Kalkus J, Pertry I, Ardiles-Diaz W, De Rycke R, Vandeputte OM, El Jaziri M, Holsters M, Vereecke D. 2012.** pFID188, the linear virulence plasmid of *Rhodococcus fascians* D188. *Molecular Plant-Microbe Interactions*, **25**: 637-47.
- Francis I, Gevers D, Karimi M, Holsters M, Vereecke D. 2007.** Linear Plasmids and Phytopathogenicity. In: Meinhardt F, Klassen R, eds. *Microbial Linear Plasmids*: Springer Berlin Heidelberg.
- Frébort I, Kowalska M, Hluska T, Frébortová J, Galuszka P. 2011.** Evolution of cytokinin biosynthesis and degradation. *Journal of Experimental Botany*.
- Fusseder A, Ziegler P, Peters W, Beck E. 1989.** Turnover of O-glucosides of dihydrozeatin and dihydrozeatin-9-riboside during the cell growth cycle of photoautotrophic cell suspension cultures of *Chenopodium rubrum*. *Botanica Acta*, **102**: 335-340.

- Gafni Y, Clark E, Barash I, Ophir Y, Zutra D, Manulis S. 1991.** Identification of a plasmid DNA probe for detection of strains of *Erwinia herbicola* pathogenic on *Gypsophila paniculata*. *Phytopathology*, **81**: 54-57.
- Galis I, Bilyeu K, Godinho M, Jameson P. 2005a.** Expression of three *Arabidopsis* cytokinin oxidase/dehydrogenase promoter::GUS chimeric constructs in tobacco: response to developmental and biotic factors. *Plant Growth Regulation*, **45**: 173 - 182.
- Galis I, Bilyeu K, Wood G, Jameson PE. 2005b.** *Rhodococcus fascians*: Shoot proliferation without elevated cytokinins? *Plant Growth Regulation*, **46**: 109-115.
- Galuszka P, Frebort I, Sebela M, Sauer P, Jacobsen S, Pec P. 2001.** Cytokinin oxidase or dehydrogenase? Mechanism of cytokinin degradation in cereals. *European Journal of Biochemistry*, **268**: 450-61.
- Galuszka P, Frebortova J, Werner T, Yamada M, Strnad M, Schmulling T, Frebort I. 2004.** Cytokinin oxidase/dehydrogenase genes in barley and wheat: cloning and heterologous expression. *European Journal of Biochemistry*, **271**: 3990-4002.
- Galuszka P, Popelková H, Werner T, Frébortová J, Pospíšilová H, Mik V, Köllmer I, Schmülling T, Frébort I. 2007.** Biochemical characterization of cytokinin oxidases/dehydrogenases from *Arabidopsis thaliana* expressed in *Nicotiana tabacum* L. *Journal of Plant Growth Regulation*, **26**: 255-267.
- Gardan L, Bollet.C, Abu Ghorrah M, Grimont F, and, Grimont PAD. 1992.** DNA relatedness among the pathovar strains of *Pseudomonas syringae* subsp. *savastanoi* Janse (1982) and proposal of *Pseudomonas savastanoi* sp. nov. *International Journal of Systemic Bacteriology*, **42**: 606-612.
- Gillissen B, Burkle L, Andre B, Kuhn C, Rentsch D, Brandl B, Frommer WB. 2000.** A new family of high-affinity transporters for adenine, cytosine, and purine derivatives in *Arabidopsis*. *Plant Cell*, **12**: 291-300.
- Goethals K, Vereecke D, Jaziri M, Van Montagu M, Holsters M. 2001a.** Leafy gall formation by *Rhodococcus fascians*. *Annual Review of Phytopathology*, **39**: 27-52.
- Goethals K, Vereecke D, Jaziri M, Van Montagu M, Holsters M. 2001b.** Leafy gall formation by *Rhodococcus fascians*.
- Golovko A, Sitbon F, Tillberg E, Nicander B. 2002.** Identification of a tRNA isopentenyltransferase gene from *Arabidopsis thaliana*. *Plant Molecular Biology*, **49**: 161-9.
- Goodfellow M. 1984.** Reclassification of *Corynebacterium fascians* (Tilford) Dawson in the genus *Rhodococcus* as *Rhodococcus fascians* comb. nov. *Systematics Applied Microbiology*, **5**: 225-229.
- Gray J, Wang J, Gelvin SB. 1992.** Mutation of the *miaA* gene of *Agrobacterium tumefaciens* results in reduced vir gene expression. *Journal of Bacteriology*, **174**: 1086-98.
- Gürtler V, Mayall, B. C. and Seviour, R. . 2004.** Can whole genome analysis refine the taxonomy of the genus *Rhodococcus*? . *FEMS Microbiological Reviews*, **28**: 377-403.
- Gutierrez L, Mauriat M, Pelloux J, Bellini C, Van Wuytswinkel O. 2008.** Towards a systematic validation of references in real-time RT-PCR. *The Plant Cell* **20**: 1734-1735.
- Hacker J, Bender L, Ott M, Wingender J, Lund B, Marre R, Goebel W. 1990.** Deletions of chromosomal regions coding for fimbriae and hemolysins occur in vitro and in vivo in various extraintestinal *Escherichia coli* isolates. *Microbial Pathogenesis*, **8**: 213-25.
- Harris M, Mackender RO, Smith DL. 1986.** Photosynthesis of cotyledons of soybean seedlings. *New Phytologist*, **104**: 319-329.
- Hecht S, Eisenreich W, Adam P, Amslinger S, Kis K, Bacher A, Arigoni D, Rohdich F. 2001.** Studies on the nonmevalonate pathway to terpenes: the role of the GcpE (IspG) protein. *Proceedings of the National Academy of Sciences*, **98**: 14837-14842.

- Held M, Pepper A, Bozdarov J, Smith M, Emery RJN, Guinel F. 2008.** The pea nodulation mutant r50 (sym16) displays altered activity and expression profiles for cytokinin dehydrogenase. *Journal of Plant Growth Regulation*, **27**: 170-180.
- Helgeson JP, Leonard NJ. 1966.** Cytokinins: identification of compounds isolated from *Corynebacterium fascians*. *Proceedings of the National Academy of Sciences, U S A*, **56**: 60-3.
- Heyl A, Riefler M, Romanov GA, Schmülling T. 2012.** Properties, functions and evolution of cytokinin receptors. *European Journal of Cell Biology*, **91**: 246-256.
- Higuchi M, Pischke MS, Mahonen AP, Miyawaki K, Hashimoto Y, Seki M, Kobayashi M, Shinozaki K, Kato T, Tabata S, Helariutta Y, Sussman MR, Kakimoto T. 2004.** *In planta* functions of the *Arabidopsis* cytokinin receptor family. *Proceedings of the National Academy of Sciences, U S A*, **101**: 8821-6.
- Hinnebusch J, Tilly K. 1993.** Linear plasmids and chromosomes in bacteria. *Molecular Microbiology*, **10**: 917-22.
- Hirose N, Takei K, Kuroha T, Kamada-Nobusada T, Hayashi H, Sakakibara H. 2008.** Regulation of cytokinin biosynthesis, compartmentalization and translocation. *Journal of Experimental Botany*, **59**: 75-83.
- Holt JG, N.R. Krieg, P.H.A. Sneath, J.T. Staley and S.T. Williams. 1994.** *Bergey's Manual of Determinative Bacteriology, 9th Edition*: 518-537.
- Hoof HA, Huttinga H, Knaap A, Maas Geesteranus HP, Mosch WHM, Raay-Wieringa DGJ. 1979.** Tumours of *Begonia* and some other ornamentals, induced by *Corynebacterium fascians*. *Netherlands Journal of Plant Pathology*, **85**: 87-98.
- Houba-Herlin N, Pethe C, d'Alayer J, Laloue M. 1999.** Cytokinin oxidase from *Zea mays*: purification, cDNA cloning and expression in moss protoplasts. *The Plant Journal*, **17**: 615-26.
- Hutchison CE, Kieber JJ. 2002.** Cytokinin Signaling in *Arabidopsis*. *The Plant Cell* **14**: S47-S59.
- Hwang I, Sheen J. 2001.** Two-component circuitry in *Arabidopsis* cytokinin signal transduction. *Nature*, **413**: 383-9.
- Hwang I, Sheen J, Muller B. 2012.** Cytokinin signaling networks. *Annual Review of Plant Biology*, **63**: 353-80.
- Iacobellis NS, Sisto A, Surico G, Evidente A, DiMaio E. 1994.** Pathogenicity of *Pseudomonas syringae* subsp. *savastanoi* mutants defective in phytohormone production. *Journal of Phytopathology*, **140**: 238-248.
- Imamura A, Hanaki N, Umeda H, Nakamura A, Suzuki T, Ueguchi C, Mizuno T. 1998.** Response regulators implicated in His-to-Asp phosphotransfer signaling in *Arabidopsis*. *Proceedings of the National Academy of Sciences*, **95**: 2691-2696.
- Inoue T, Higuchi M, Hashimoto Y, Seki M, Kobayashi M, Kato T, Tabata S, Shinozaki K, Kakimoto T. 2001.** Identification of CRE1 as a cytokinin receptor from *Arabidopsis*. *Nature*, **409**: 1060-3.
- Jacobs SE, Habish HA, Dadd AH. 1965.** Studies on induced mutants of *Corynebacterium fascians* and on their pathogenicity in comparison with that of 'natural' strains. *Annals of Applied Biology*, **56**: 161-170.
- Jain M, Tyagi A, Khurana J. 2006.** Molecular characterization and differential expression of cytokinin-responsive type-A response regulators in rice (*Oryza sativa*). *BMC Plant Biology*, **6**: 1-11.
- Jameson PE. 2000.** Cytokinins and auxins in plant-pathogen interactions – An overview. *Plant Growth Regulation*, **32**: 369-380.
- Jameson PE, Morris ROa, Eason JR. 1991.** Cytokinin production by *Corynebacterium fascians*: immunoaffinity purification and detection by RIA and ELISA. *Annual meeting of the New Zealand Society of Plant Physiologist*. Dunedin.
- Johansen DA. 1940.** *Plant Microtechnique*. New York: McGraw-Hill Book Company.
- Jones GE, Catton FW, Bateson M. 1977.** Root Galls on raspberry. *Plant Pathology*, **26**: 96-97.

- Joshi MV, Loria R. 2007.** *Streptomyces turgidiscabies* possesses a functional cytokinin biosynthetic pathway and produces leafy galls. *Molecular Plant-Microbe Interactions*, **20**: 751-758.
- Kado CI, Heskett MG. 1970.** Selective media for isolation of *Agrobacterium*, *Corynebacterium*, *Erwinia*, *Pseudomonas* and *Xanthomonas*. *Phytopathology*, **60**: 969-976.
- Kakimoto T. 2001.** Identification of plant cytokinin biosynthetic enzymes as dimethylallyl diphosphate: ATP/ADP isopentenyltransferases. *Plant and Cell Physiology*, **42**: 677-685.
- Kakimoto T. 2003.** Perception and signal transduction of cytokinins. *Annual Review of Plant Biology*, **54**: 605-627.
- Kamada-Nobusada T, Sakakibara H. 2009.** Molecular basis for cytokinin biosynthesis. *Phytochemistry*, **70**: 444 - 449.
- Kamínek M, Pačes V, Corse J, Challice JS. 1979.** Effect of stereospecific hydroxylation of N⁶-(Δ^2 -Isopentenyl)adenosine on cytokinin activity. *Planta*, **145**: 239-243.
- Kasahara H, Takei K, Ueda N, Hishiyama S, Yamaya T, Kamiya Y, Yamaguchi S, Sakakibara H. 2004.** Distinct isoprenoid origins of *cis*- and *trans*-zeatin biosyntheses in *Arabidopsis*. *Journal of Biological Chemistry*, **279**: 14049-54.
- Kemp DR. 1978.** Indole-3 ylacetic acid meatobolism in *Corynebacterium fascians*. In: Loutit MWMJAR, ed. *Microbial Ecology*. Berlin: Springer.
- Kers JA, Cameron KD, Joshi MV, Bukhalid RA, Morello JE, Wach MJ, Gibson DM, Loria R. 2005.** A large, mobile pathogenicity island confers plant pathogenicity on *Streptomyces* species. *Molecular Microbiology*, **55**: 1025-33.
- Kiba T, Aoki K, Sakakibara H, Mizuno T. 2004.** Arabidopsis response regulator, ARR22, ectopic expression of which results in phenotypes similar to the wol cytokinin-receptor mutant. *Plant and Cell Physiology*, **45**: 1063-1077.
- Kieber JJ, Schaller GE. 2010.** The perception of cytokinin: A story 50 years in the making. *Plant Physiology*, **154**: 487-492.
- Kitin P, Iliev I, Scaltsoyiannes A, Nellas C, Rubos A, Funada R. 2005.** A comparative histological study between normal and fasciated shoots of *Prunus avium* generated *in vitro*. *Plant Cell, Tissue and Organ Culture*, **82**: 141-150.
- Klämbt D, Thies Ga, Skoog F. 1966.** Isolation of cytokinins from *Corynebacterium fascians*. *Proceedings of the National Academy of Sciences of the United States of America*, **56**: 52-59.
- Klee H, Montoya A, Horodyski F, Lichtenstein C, Garfinkel D, Fuller S, Flores C, Peschon J, Nester E, Gordon M. 1984.** Nucleotide sequence of the *tms* genes of the pTiA6NC octopine Ti plasmid: two gene products involved in plant tumorigenesis. *Proceedings of the National Academy of Sciences*, **81**: 1728-1732.
- Krall L, Raschke M, Zenk MH, Baron C. 2002.** The Tzs protein from *Agrobacterium tumefaciens* C58 produces zeatin riboside 5'-phosphate from 4-hydroxy-3-methyl-2-(E)-butenyl diphosphate and AMP. *FEBS Letters*, **527**: 315-8.
- Kudo T, Kiba T, Sakakibara H. 2010.** Metabolism and long-distance translocation of cytokinins. *Journal of Integrative Plant Biology*, **52**: 53-60.
- Kühn C, Grof CPL. 2010.** Sucrose transporters of higher plants. *Current Opinion in Plant Biology*, **13**: 287-297.
- Kuiper D. 1993.** Sink strength: Established and regulated by plant growth regulators. *Plant, Cell and Environment*, **16**: 1025-1026.
- Kurakawa T, Ueda N, Maekawa M, Kobayashi K, Kojima M, Nagato Y, Sakakibara H, Kyojuka J. 2007.** Direct control of shoot meristem activity by a cytokinin-activating enzyme. *Nature*, **445**: 652 - 655.
- Kuroha T, Tokunaga H, Kojima M, Ueda N, Ishida T, Nagawa S, Fukuda H, Sugimoto K, Sakakibara H. 2009.** Functional analyses of *LONELY GUY* cytokinin-activating enzymes reveal the importance of the direct activation pathway in *Arabidopsis*. *Plant Cell*, **21**: 3152-69.

- Lacey MS. 1936.** Studies in bacteriosis. XXII. 1. Isolation of a bacterium associated with "fasciatio" of sweet peas, "cauliflower" strawberry plants and "leafy gall" of various plants. *Annals of Applied Biology*, **23**: 302-310.
- Lacey MS. 1955.** The cytology and relationships of *Corynebacterium fascians*. *Transactions of the British Mycological Society*, **38**: 49-IN2.
- Larkin M, De Mot R, Kulakov L, Nagy I. 1998.** Applied aspects of *Rhodococcus* genetics. *Antonie van Leeuwenhoek*, **74**: 133-153.
- Lawson E, Gantotti B, Starr M. 1982.** A 78-megadalton plasmid occurs in avirulent strains as well as virulent strains of *Corynebacterium fascians*. *Current Microbiology*, **7**: 327-332.
- Le DT, Nishiyama R, Watanabe Y, Vankova R, Tanaka M, Seki M, Ham LH, Yamaguchi-Shinozaki K, Shinozaki K, Tran L-SP. 2012.** Identification and expression analysis of cytokinin metabolic genes in soybean under normal and drought conditions in relation to cytokinin levels. *PLoS ONE*, **7**: e42411.
- Lee CW, Efetova M, Engelmann JC, Kramell R, Wasternack C, Ludwig-Muller J, Hedrich R, Deeken R. 2009.** *Agrobacterium tumefaciens* promotes tumor induction by modulating pathogen defense in *Arabidopsis thaliana*. *Plant Cell*, **21**: 2948-62.
- Letham DS. 1963.** Zeatin, a factor inducing cell division isolated from *Zea mays*. *Life Science*, **8**: 569-73.
- Li-Qing C, Bi-Huei H, Sylvie L, Hitomi T, Mara LH, Xiao-Qing Q, Woei-Jiun G, Jung-Gun K, William U, Bhavna C, Diane C, Ginny A, Frank FW, Shauna CS, Mary Beth M, Wolf BF. 2010.** Sugar transporters for intercellular exchange and nutrition of pathogens. *Nature*, **468**: 527-532.
- Lichter A, Barash I, Valinsky L, Manulis S. 1995.** The genes involved in cytokinin biosynthesis in *Erwinia herbicola* pv. *gypsophila*: characterization and role in gall formation. *Journal of Bacteriology*, **177**: 4457-65.
- Liu Z, Lv Y, Zhang M, Liu Y, Kong L, Zou M, Lu G, Cao J, Yu X. 2013.** Identification, expression, and comparative genomic analysis of the *IPT* and *CKX* gene families in Chinese cabbage (*Brassica rapa* ssp. *pekinensis*). *BMC Genomics*, **14**: 1-20.
- Loria R, Kers J, Joshi M. 2006.** Evolution of plant pathogenicity in *Streptomyces*. *Annual Review of Phytopathology*. Palo Alto: Annual Reviews.
- Ma Q-H. 2008.** Genetic engineering of cytokinins and their application to agriculture. *Critical Reviews in Biotechnology*, **28**: 213-232.
- Macdonald EM, Powell GK, Regier DA, Glass NL, Roberto F, Kosuge T, Morris RO. 1986.** Secretion of zeatin, ribosylzeatin, and ribosyl-1"-methylzeatin by *Pseudomonas savastanoi*: plasmid-coded cytokinin biosynthesis. *Plant Physiology*, **82**: 742-7.
- Maes T, Vereecke D, Ritsema T, Cornelis K, Thu HNT, Van Montagu M, Holsters M, Goethals K. 2001.** The att locus of *Rhodococcus fascians* strain D188 is essential for full virulence on tobacco through the production of an autoregulatory compound. *Molecular Microbiology*, **42**: 13-28.
- Mähönen AP, Higuchi M, Törmäkangas K, Miyawaki K, Pischke MS, Sussman MR, Helariutta Y, Kakimoto T. 2006.** Cytokinins Regulate a Bidirectional Phosphorelay Network in *Arabidopsis*. *Current Biology*, **16**: 1116-1122.
- Manes C-L, Beeckman T, Ritsema T, Van Montagu M, Goethals K, Holsters M. 2004.** Phenotypic alterations in *Arabidopsis thaliana* plants caused by *Rhodococcus fascians* infection. *Journal of Plant Research*, **117**: 139-145.
- Manes CLDO, Van Montagu M, Prinsen E, Goethals K, Holsters M. 2001.** *De novo* cortical cell division triggered by the phytopathogen *Rhodococcus fascians* in tobacco. *Molecular Plant-Microbe Interactions*, **14**: 189-195.
- Manulis S, Haviv-Chesner A, Brandl MT, Lindow SE, Barash I. 1998.** Differential involvement of indole-3-acetic acid biosynthetic pathways in pathogenicity and epiphytic fitness of *Erwinia herbicola* pv. *gypsophila*. *Molecular Plant-Microbe Interactions*, **11**: 634-42.

- Martin RG, Rosner JL. 2001.** The AraC transcriptional activators. *Current Opinion in Microbiology*, **4**: 132-7.
- Mason MG, Mathews DE, Argyros DA, Maxwell BB, Kieber JJ, Alonso JM, Ecker JR, Schaller GE. 2005.** Multiple type-B response regulators mediate cytokinin signal transduction in *Arabidopsis*. *The Plant Cell* **17**: 3007-3018.
- Mathews LJ, Morris ROa, Blevins DG. 1992.** Genetic mechanisms for *Rhizobium* cytokinin biosynthesis, and their relationship to nodule development. *Plant Pathology*, **99** (supplement): 37.
- Mazzola M, White FF. 1994.** A mutation in the indole-3-acetic acid biosynthesis pathway of *Pseudomonas syringae* pv. *syringae* affects growth in *Phaseolus vulgaris* and syringomycin production. *Journal of Bacteriology*, **176**: 1374-82.
- McCullen CA, Binns AN. 2006.** *Agrobacterium tumefaciens* and plant cell interactions and activities required for interkingdom macromolecular transfer. *Annual Review of Cell and Developmental Biology*, **22**: 101-27.
- Miller CO. 1961.** A kinetin-like compound in maize. *Proceedings of the National Academy of Sciences*, **47**: 170-174.
- Miller CO, Skoog F, Okumura FS, Von Saltza MH, Strong FM. 1955 a.** Structure and synthesis of kinetin1. *Journal of the American Chemical Society*, **77**: 2662-2663.
- Miller CO, Skoog F, Strong FMa, Von Saltza MH. 1955 b.** Kinetin, a cell division factor from deoxyribonucleic acid. *Journal of American Chemical Society*, **78**: 2662-2663.
- Miller HJ, Janse JD, Kamerman W, Muller PJ. 1980.** Recent observations on leafy gall in *Liliaceae* and some other families. *Netherlands Journal of Plant Pathology*, **86**: 55-68.
- Miyawaki K, Kakimoto T, Matsumoto-Kitano M. 2004.** Expression of cytokinin biosynthetic isopentenyltransferase genes in *Arabidopsis*: tissue specificity and regulation by auxin, cytokinin and nitrate. *The Plant Journal*, **37**: 128 - 138.
- Miyawaki K, Tarkowski P, Matsumoto-Kitano M, Kato T, Sato S, Tarkowska D, Tabata S, Sandberg G, Kakimoto T. 2006.** Roles of *Arabidopsis* ATP/ADP isopentenyltransferases and tRNA isopentenyltransferases in cytokinin biosynthesis. *Proceedings of the National Academy of Sciences*, **103**: 16598-16603.
- Mok D, Mok M. 2001.** Cytokinin metabolism and action. *Annual Review of Plant Physiology and Plant Molecular Biology*, **89**: 89 - 118.
- Moore WC. 1943.** Report on fungus, bacterial and other diseases of crops in England and Wales for the years 1943-1946. London: Ministry of Agriculture and Fisheries Bulletin
- Moriguchi K, Maeda Y, Satou M, Hardayani NS, Kataoka M, Tanaka N, Yoshida K. 2001.** The complete nucleotide sequence of a plant root-inducing (Ri) plasmid indicates its chimeric structure and evolutionary relationship between tumor-inducing (Ti) and symbiotic (Sym) plasmids in Rhizobiaceae. *Journal of Molecular Biology*, **307**: 771-84.
- Morris R, Blevins D, Dietrich J, Durley R, Gelvin S, Gray J, Hommes N, Kaminek M, Mathews L, Meilan R, Reinbott T, Sayavedra-Soto L. 1993.** Cytokinins in plant-pathogenic bacteria and developing cereal grains. *Australian Journal of Plant Physiology*, **20**: 621 - 637.
- Morris RO. 1986.** Genes specifying auxin and cytokinin biosynthesis in phytopathogens. *Annual Review of Plant Physiology and Plant Molecular Biology*, **37**: 509-538.
- Morris RO. 1987.** Molecular aspects of hormone synthesis and action genes specifying auxin and cytokinin biosynthesis in prokaryotes. In: Davies PJ, ed. *Plant Hormones*. Dordrecht: Kluwer Academic Publishers.
- Morris RO, Bilyeu KD, Laskey JG, Cheikh NN. 1999.** Isolation of a gene encoding a glycosylated cytokinin oxidase from maize. *Biochemical and Biophysical Research Communications*, **255**: 328-333.
- Muller B, Sheen J. 2007.** *Arabidopsis* cytokinin signaling pathway. *Science Signaling*, **2007**: cm5.

- Murai N. 1994.** Cytokinin biosynthesis in tRNA and cytokinin incorporation into plant RNA. In: Mok DWSMaMC, ed. *Cytokinins: Chemistry, Activity and Function*. Boca Raton, FL.: CRC Press.
- Murai N, Skoog F, Doyle ME, Hanson RS. 1980.** Relationships between cytokinin production, presence of plasmids, and fasciation caused by strains of *Corynebacterium fascians*. *Proceedings of the National Academy of Sciences*, **77**: 619-623.
- Nam HG. 1997.** The molecular genetic analysis of leaf senescence. *Current Opinion in Biotechnology*, **8**: 200-207.
- Nishida H, Ohnishi Y, Beppu T, Horinouchi S. 2007.** Evolution of gamma-butyrolactone synthases and receptors in *Streptomyces*. *Environmental Microbiology*, **9**: 1986-94.
- Nishimura C, Ohashi Y, Sato S, Kato T, Tabata S, Ueguchi C. 2004.** Histidine kinase homologs that act as cytokinin receptors possess overlapping functions in the regulation of shoot and root growth in *Arabidopsis*. *Plant Cell*, **16**: 1365-77.
- Noodén LD, Guamét JJ, John I. 1997.** Senescence mechanisms. *Physiologia Plantarum*, **101**: 746-753.
- Oduro KA, and, Munnecke DE. 1975a.** Persistence of Pea Cotyledons Induced by *Corynebacterium fascians*. *Phytopathology*, **65**: 1114-1116.
- Oduro KAa, Munnecke DE. 1975b.** Persistence of pea cotyledons induced by *Corynebacterium fascians*. *Phytopathology*, **65**: 1114-1116.
- Oka A. 2003.** New insights into cytokinins. *Journal of Plant Research*, **116**: 217-220.
- Okumoto S, Schmidt R, Tegeder M, Fischer WN, Rentsch D, Frommer WB, Koch W. 2002.** High affinity amino acid transporters specifically expressed in xylem parenchyma and developing seeds of *Arabidopsis*. *Journal of Biological Chemistry*, **277**: 45338-46.
- Op den Camp RHM, De Mita S, Lillo A, Cao Q, Limpens E, Bisseling T, Geurts R. 2011.** A phylogenetic strategy based on a legume-specific whole genome duplication yields symbiotic cytokinin type-a response regulators. *Plant Physiology*, **157**: 2013-2022.
- Pačes V, Werstiuk E, Hall Ross H. 1971.** Conversion of N⁶-(Δ^2 -Isopentenyl)adenosine to adenosine by an enzyme activity in tobacco tissue. *Plant Physiology*, **48**: 775-778.
- Pape H. 1938.** Eine noch wenig beachtete Krankheit der Zierpflanzen. *Blumen und Pflanzen Bau ver. Gartenwelt.*, **42**: 384-386.
- Patten CL, Glick BR. 1996.** Bacterial biosynthesis of indole-3-acetic acid. *Canadian Journal of Microbiology*, **42**: 207-20.
- Pennycock SR, Young JMa, Fletcher MJ. 1989.** Plant diseases recorded in New Zealand. Auckland, NZ: Plant Diseases Division, DSIR.
- Pertry I. 2009.** *How the fas locus contributes to Rhodococcus fascians cytokinin production : an in-depth molecular and biochemical analysis*, PhD, Ghent University, Gent.
- Pertry I, Václavíková K, Depuydt S, Galuszka P, Spíchal L, Temmerman W, Stes E, Schmölling T, Kakimoto T, Van Montagu MCE, Strnad M, Holsters M, Tarkowski P, Vereecke D. 2009.** Identification of *Rhodococcus fascians* cytokinins and their modus operandi to reshape the plant. *Proceedings of the National Academy of Sciences of the United States of America*, **106**: 929-934.
- Pertry I, Václavíková K, Gemrotová M, Spíchal L, Galuszka P, Depuydt S, Temmerman W, Stes E, De Keyser A, Riefler M, Biondi S, Novák O, Schmölling T, Strnad M, Tarkowski P, Holsters M, Vereecke D. 2010.** *Rhodococcus fascians* impacts plant development through the dynamic fas-mediated production of a cytokinin mix. *Molecular Plant-Microbe Interactions*, **23**: 1164-1174.
- Pfaffl MW. 2001.** A new mathematical model for relative quantification in real-time RT-PCR. *Nucleic Acids Research*, **29**: 1-13.
- Picardeau M, Vincent V. 1997.** Characterization of large linear plasmids in Mycobacteria. *Journal of Bacteriology*, **179**: 2753-6.

- Powell GK, Morris RO. 1986.** Nucleotide sequence and expression of a *Pseudomonas savastanoi* cytokinin biosynthetic gene: homology with *Agrobacterium tumefaciens* *tmr* and *tzs* loci. *Nucleic Acids Research*, **14**: 2555-65.
- Prinsen E, Kamínek M, van Onckelen HA. 1997.** Cytokinin biosynthesis: A black box? *Plant Growth Regulation*, **23**: 3-15.
- Punwani JA, Hutchison CE, Schaller GE, Kieber JJ. 2010.** The subcellular distribution of the *Arabidopsis* histidine phosphotransfer proteins is independent of cytokinin signaling. *The Plant Journal*, **62**: 473-82.
- Putnam ML, Miller ML. 2007.** *Rhodococcus fascians* in herbaceous perennials. *Plant Disease*, **91**: 1064-1076.
- Quoirin M, Bona C, Souza Efd, Schwartsburd PB. 2004.** Induction of leafy galls in *Acacia mearnsii* De Wild seedlings infected by *Rhodococcus fascians*. *Brazilian Archives of Biology and Technology*, **47**: 339-346.
- Rainey FA, Burghardt J, Kroppenstedt RM, Klatt S, Stackebrandt E. 1995.** Phylogenetic analysis of the genera *Rhodococcus* and *Nocardia* and evidence for the evolutionary origin of the genus *Nocardia* from within the radiation of *Rhodococcus* species. *Microbiology*, **141**: 523-528.
- Rathbone M, Hall R. 1972.** Concerning the presence of the cytokinin, N 6-(Δ^2 -isopentenyl) adenine, in cultures of *Corynebacterium fascians*. *Planta*, **108**: 93-102.
- Riefler M, Novak O, Strnad M, Schmülling T. 2006.** *Arabidopsis* cytokinin receptor mutants reveal functions in shoot growth, leaf senescence, seed size, germination, root development, and cytokinin metabolism. *The Plant Cell* **18**: 40-54.
- Riesmeier JW, Hirner B, Frommer WB. 1993.** Potato sucrose transporter expression in minor veins indicates a role in phloem loading. *The Plant Cell* **5**: 1591-8.
- Riesmeier JW, Willmitzer L, Frommer WB. 1992.** Isolation and characterization of a sucrose carrier cDNA from spinach by functional expression in yeast. *EMBO Journal*, **11**: 4705-13.
- Robert-Seilaniantz A, Navarro L, Bari R, Jones JD. 2007.** Pathological hormone imbalances. *Current Opinion in Plant Biology*, **10**: 372-9.
- Rohdich F, Hecht S, Gartner K, Adam P, Krieger C, Amslinger S, Arigoni D, Bacher A, Eisenreich W. 2002.** Studies on the nonmevalonate terpene biosynthetic pathway: metabolic role of IspH (LytB) protein. *Proceedings of the National Academy of Sciences, U S A*, **99**: 1158-63.
- Rohmer M, Knani M, Simonin P, Sutter B, Sahm H. 1993.** Isoprenoid biosynthesis in bacteria: a novel pathway for the early steps leading to isopentenyl diphosphate. *Biochemical Journal*, **295**: 517-524.
- Roitsch T, Ehneß R. 2000.** Regulation of source/sink relations by cytokinins. *Plant Growth Regulation*, **32**: 359-367.
- Romanov GA, Lomin SN, Schmulling T. 2006.** Biochemical characteristics and ligand-binding properties of *Arabidopsis* cytokinin receptor AHK3 compared to CRE1/AHK4 as revealed by a direct binding assay. *Journal of Experimental Botany*, **57**: 4051-8.
- Roussaux J. 1965.** Etude préliminaire des modifications induites chez le pois express Alaska par le *Corynebacterium fascians* (Tilford) Dawson. *Review of General Botany*, **72**: 21-53.
- Roussaux J. 1975.** Stimulation and inhibition reaction in plants infected by *Corynebacterium fascians* (Tilford) Dawson. *Marcellia*, **38**: 305-310.
- Sakai H, Aoyama T, Bono H, Oka A. 1998.** Two-component response regulators from *Arabidopsis thaliana* contain a putative DNA-binding motif. *Plant and Cell Physiology*, **39**: 1232-1239.
- Sakai H, Aoyama T, Oka A. 2000.** *Arabidopsis* *ARR1* and *ARR2* response regulators operate as transcriptional activators. *The Plant Journal*, **24**: 703-11.
- Sakai H, Honma T, Aoyama T, Sato S, Kato T, Tabata S, Oka A. 2001.** *ARR1*, a transcription factor for genes immediately responsive to cytokinins. *Science*, **294**: 1519-21.
- Sakakibara H. 2005.** Cytokinin biosynthesis and regulation. *Vitamins and Hormones*, **72**: 271-87.

- Sakakibara H. 2006.** Cytokinins: activity, biosynthesis, and translocation. *Annual Review of Plant Biology*, **57**: 431-49.
- Sakakibara H, Kasahara H, Ueda N, Kojima M, Takei K, Hishiyama S, Asami T, Okada K, Kamiya Y, Yamaya T, Yamaguchi S. 2005.** *Agrobacterium tumefaciens* increases cytokinin production in plastids by modifying the biosynthetic pathway in the host plant. *Proceedings of the National Academy of Sciences of the United States of America*, **102**: 9972-9977.
- Sakamoto T, Sakakibara H, Kojima M, Yamamoto Y, Nagasaki H, Inukai Y, Sato Y, Matsuoka M. 2006.** Ectopic expression of KNOTTED1-like homeobox protein induces expression of cytokinin biosynthesis genes in rice. *Plant Physiology*, **142**: 54-62.
- Sakano Y, Okada Y, Matsunaga A, Suwama T, Kaneko T, Ito K, Noguchi H, Abe I. 2004.** Molecular cloning, expression, and characterization of adenylate isopentenyltransferase from hop (*Humulus lupulus* L.). *Phytochemistry*, **65**: 2439-2446.
- Scarborough E, Armstrong DJ, Skoog F, Frihart CR, Leonard NJ. 1973.** Isolation of cis-zeatin from *Corynebacterium fascians* cultures. *Proceedings of the National Academy of Sciences, U S A*, **70**: 3825-9.
- Schaller GE, Doi K, Hwang I, Kieber JJ, Khurana JP, Kurata N, Mizuno T, Pareek A, Shiu S-H, Wu P, Yip WK. 2007.** Nomenclature for Two-Component Signaling Elements of Rice. *Plant Physiology*, **143**: 555-557.
- Schmülling T, Werner T, Riefler M, Krupková E, Bartrina y Manns I. 2003.** Structure and function of cytokinin oxidase/dehydrogenase genes of maize, rice, *Arabidopsis* and other species. *Journal of Plant Research*, **116**: 241-252.
- Schmulling T, Werner T, Riefler M, Krupkova E, Manns I. 2003.** Structure and function of cytokinin oxidase/dehydrogenase genes of maize, rice, *Arabidopsis* and other species. *J Plant Res*, **116**: 241 - 252.
- Shantz EM, Steward FC. 1955.** The Identification of compound A from coconut milk as 1,3-diphenylurea. *Journal of the American Chemical Society*, **77**: 6351-6353.
- Simon-Mateo C, Depuydt S, CL DEOM, Cnudde F, Holsters M, Goethals K, Vereecke D. 2006.** The phytopathogen *Rhodococcus fascians* breaks apical dominance and activates axillary meristems by inducing plant genes involved in hormone metabolism. *Molecular Plant Pathology*, **7**: 103-12.
- Singh S, Letham DS, Jameson PE, Zhang R, Parker CW, Bandenoch-Jones J, Nooden LD. 1988.** Cytokinin biochemistry in relation to leaf senescence: IV. Cytokinin metabolism in soybean explants. *Plant Physiology*, **88**: 788-94.
- Sisto A, Cipriani MG, Morea M. 2004.** Knot formation caused by *Pseudomonas syringae* subsp. *savastanoi* on olive plants is *hrp*-dependent. *Phytopathology*, **94**: 484-9.
- Skoog F, Miller CO. 1957.** Chemical regulation of growth and organ formation in plant tissues cultured *in vitro*. *Symposium of Society of Experimental Biology*, **11**: 118-30.
- Song J, Jiang L, Jameson EP. 2012.** Co-ordinate regulation of cytokinin gene family members during flag leaf and reproductive development in wheat. *BMC Plant Biology*, **12**: 78.
- Spichal L, Rakova NY, Riefler M, Mizuno T, Romanov GA, Strnad M, Schmulling T. 2004.** Two cytokinin receptors of *Arabidopsis thaliana*, CRE1/AHK4 and AHK3, differ in their ligand specificity in a bacterial assay. *Plant Cell Physiology*, **45**: 1299-305.
- Stange J, R. R., Jeffares D, Young C, Scott DB, Eason JR, Jameson PE. 1996.** PCR amplification of the *fas-1* gene for the detection of virulent strains of *Rhodococcus fascians*. *Plant Pathology*, **45**: 407-417.
- Stes E, Francis I, Pertry I, Dolzblasz A, Depuydt S, Vereecke D. 2013.** The leafy gall syndrome induced by *Rhodococcus fascians*. *FEMS Microbiology Letters*, **342**: 187-195.
- Stes E, Holsters M, Vereecke D. 2010.** Phytopathogenic strategies of *Rhodococcus fascians*. In: Alvarez HM, ed. *Biology of Rhodococcus*: Springer Berlin Heidelberg.

- Stes E, Vandeputte OM, El Jaziri M, Holsters M, Vereecke D. 2011.** A successful bacterial coup d'état: How *Rhodococcus fascians* redirects plant development.
- Strnad M. 1997.** The aromatic cytokinins. *Physiologia Plantarum*, **101**: 674-688.
- Sugawara H, Ueda N, Kojima M, Makita N, Yamaya T, Sakakibara H. 2008.** Structural insight into the reaction mechanism and evolution of cytokinin biosynthesis. *Proceedings of the National Academy of Science, U S A*, **105**: 2734-9.
- Sun J, Niu QW, Tarkowski P, Zheng B, Tarkowska D, Sandberg G, Chua NH, Zuo J. 2003.** The *Arabidopsis* *AtIPT8/PGA22* gene encodes an isopentenyl transferase that is involved in de novo cytokinin biosynthesis. *Plant Physiology*, **131**: 167-76.
- Surico G, Iacobellis NS, Sisto A. 1985.** Studies on the role of indole-3-acetic acid and cytokinins in the formation of knots on olive and oleander plants by *Pseudomonas syringae* pv. *savastanoi*. *Physiological Plant Pathology*, **26**: 309-320.
- Suzuki T, Miwa K, Ishikawa K, Yamada H, Aiba H, Mizuno T. 2001.** The *Arabidopsis* sensor Histidine kinase, AHK4, can respond to cytokinins. *Plant and Cell Physiology*, **42**: 107-113.
- Takei K, Dekishima Y, Eguchi T, Yamaya T, Sakakibara H. 2003.** A new method for enzymatic preparation of isopentenyladenine-type and trans-zeatin-type cytokinins with radioisotope-labeling. *Journal of Plant Research*, **116**: 259-63.
- Takei K, Sakakibara H, Sugiyama T. 2001a.** Identification of genes encoding adenylate isopentenyltransferase, a cytokinin biosynthesis enzyme, in *Arabidopsis thaliana*. *Journal of Biological Chemistry*, **276**: 26405 - 26410.
- Takei K, Sakakibara H, Taniguchi M, Sugiyama T. 2001b.** Nitrogen-dependent accumulation of cytokinins in root and their translocation to leaf: implication of cytokinin species that induces gene expression of maize response regulator. *Plant and Cell Physiology*, **42**: 85-93.
- Takei K, Ueda N, Aoki K, Kuromori T, Hirayama T, Shinzaki K, Yamaya T, Sakakibara H. 2004a.** *AtIPT3* is a key determinant of nitrate-dependent cytokinin biosynthesis in *Arabidopsis*. *Plant Cell Physiology*, **45**: 1053 - 1062.
- Takei K, Yamaya T, Sakakibara H. 2004b.** *Arabidopsis* *CYP735A1* and *CYP735A2* encode cytokinin hydroxylases that catalyze the biosynthesis of *trans*-Zeatin. *Journal of Biological Chemistry*, **279**: 41866-72.
- Tamura K, Dudley J, Nei Ma, Kumar S. 2007.** MEGA4: Molecular Evolutionary Genetics Analysis (MEGA) software version 4.0. *Molecular Biology and Evolution* **24**: 1596-1599.
- Tanaka M, Takei K, Kojima M, Sakakibara H, Mori H. 2006.** Auxin controls local cytokinin biosynthesis in the nodal stem in apical dominance. *The Plant Journal*, **45**: 1028-36.
- Taniguchi M, Sasaki N, Tsuge T, Aoyama T, Oka A. 2007.** ARR1 directly activates cytokinin response genes that encode proteins with diverse regulatory functions. *Plant Cell Physiology*, **48**: 263-77.
- Taya Y, Tanaka Y, Nishimura S. 1978.** 5'-AMP is a direct precursor of cytokinin in *Dictyostelium discoideum*. *Nature*, **271**: 545-7.
- Tegeder M, Offler CE, Frommer WB, Patrick JW. 2000.** Amino acid transporters are localized to transfer cells of developing pea seeds. *Plant Physiology*, **122**: 319-326.
- Tegeder M, Tan Q, Grennan AK, Patrick JW. 2007.** Amino acid transporter expression and localisation studies in pea (*Pisum sativum*). *Functional Plant Biology*, **34**: 1019-1028.
- Tegeder M, Wang XD, Frommer WB, Offler CE, Patrick JW. 1999.** Sucrose transport into developing seeds of *Pisum sativum* L. *The Plant Journal*, **18**: 151-61.
- Tegeder M, Ward JM. 2012.** Molecular Evolution of Plant AAP and LHT Amino Acid Transporters. *Frontiers in Plant Science*, **3**: 21.
- Temmerman W, Vereecke D, Dreesen R, Van Montagu M, Holsters M, Goethals K. 2000.** Leafy gall formation is controlled by *fasR*, an AraC-type regulatory gene in *Rhodococcus fascians*. *Journal of Bacteriology*, **182**: 5832-5840.

- Thimann KV, Sachs T. 1966.** The role of cytokinins in the "fasciation" disease caused by *Corynebacterium fascians*. *American Journal of Botany*, **53**: 731-739.
- Thompson JD, Gibson TJ, Plewniak F, Jeanmougin F, Higgins DG. 1997.** The CLUSTAL_X windows interface: flexible strategies for multiple sequence alignment aided by quality analysis tools. *Nucleic Acids Research*, **25**: 4876-82.
- Tilford PE. 1936.** Fasciation of sweet peas caused by *Phytopomonas fascians* *Journal of Agricultural Research*, **53**: 383-394.
- To JP, Deruere J, Maxwell BB, Morris VF, Hutchison CE, Ferreira FJ, Schaller GE, Kieber JJ. 2007.** Cytokinin regulates type-A *Arabidopsis* Response Regulator activity and protein stability via two-component phosphorelay. *Plant Cell*, **19**: 3901-14.
- To JPC, Haberer G, Ferreira FJ, Deruère J, Mason MG, Schaller GE, Alonso JM, Ecker JR, Kieber JJ. 2004.** Type-A *Arabidopsis* response regulators are partially redundant negative regulators of cytokinin signaling. *The Plant Cell* **16**: 658-671.
- Tokunaga H, Kojima M, Kuroha T, Ishida T, Sugimoto K, Kiba T, Sakakibara H. 2012.** *Arabidopsis* lonely guy (*LOG*) multiple mutants reveal a central role of the *LOG*-dependent pathway in cytokinin activation. *The Plant Journal*, **69**: 355-65.
- Tomich M, Planet PJ, Figurski DH. 2007.** The *tad* locus: postcards from the widespread colonization island. *Nature Reviews Microbiology*, **5**: 363-75.
- Ueguchi C, Sato S, Kato T, Tabata S. 2001.** The AHK4 gene involved in the cytokinin-signaling pathway as a direct receptor molecule in *Arabidopsis thaliana*. *Plant Cell Physiology*, **42**: 751-5.
- Vandeputte O, Oden S, Mol A, Vereecke D, Goethals K, El Jaziri M, Prinsen E. 2005.** Biosynthesis of auxin by the gram-positive phytopathogen *Rhodococcus fascians* is controlled by compounds specific to infected plant tissues. *Applied Environmental Microbiology*, **71**: 1169-77.
- Vandesompele J, De Preter K, Pattyn F, Poppe B, Van Roy N, De Paepe A, Speleman F. 2002.** Accurate normalization of real-time quantitative RT-PCR data by geometric averaging of multiple internal control genes. *Genome Biology*, **3**: research0034.1 - research0034.11.
- Vantomme R, Elia S, Swings J, and, DeLey J. 1982.** *Corynebacterium fascians* (Tilford 1936) Dowson 1942, the causal agent of leafy gall on lily crops in Belgium. *Parasitica*, **38**: 183-192.
- Vaseva-Gemisheva I, Lee D, Karanov E. 2005.** Response of *Pisum Sativum* Cytokinin Oxidase/Dehydrogenase Expression and Specific Activity to Drought Stress and Herbicide Treatments. *Plant Growth Regulation*, **46**: 199-208.
- Vasil'eva GG, Glian'ko AK, Mironova NV, Putilina TE, Luzova GB. 2007.** Active oxygen species in pea seedlings during the interactions with symbiotic and pathogenic microorganisms. *Prikl Biokhim Mikrobiol*, **43**: 240-5.
- Vedam V, Kannenberg E, Datta A, Brown D, Haynes-Gann JG, Sherrier DJ, Carlson RW. 2006.** The pea nodule environment restores the ability of a *Rhizobium leguminosarum* lipopolysaccharide acpXL mutant to add 27-hydroxyoctacosanoic acid to its lipid A. *Journal of Bacteriology*, **188**: 2126-33.
- Vereecke D, BursSENS S, Simón-Mateo C, Inzé D, Van Montagu M, Goethals K, Jaziri M. 2000.** The *Rhodococcus fascians*-plant interaction: morphological traits and biotechnological applications. *Planta*, **210**: 241-251.
- Vereecke D, Cornelis K, Temmerman W, Jaziri M, Van Montagu M, Holsters M, Goethals K. 2002.** Chromosomal locus that affects pathogenicity of *Rhodococcus fascians*. *Journal of Bacteriology*, **184**: 1112-1120.
- Vereecke D, Temmerman W, Jaziri M, Holsters, M. and , Goethals K. 2003.** Towards an understanding of the *Rhodococcus fascians*- plant interaction. In: Stacey GaK, N., ed. *Molecular Plant Microbe Interactions*. St.Paul, MN: American Phytopathological Society.
- Walters DR, McRoberts N. 2006.** Plants and biotrophs: a pivotal role for cytokinins? *Trends in Plant Science*, **11**: 581-586.

- Wang Y, Luo JP, Wei ZJ, Zhang JC. 2009.** Molecular cloning and expression analysis of a cytokinin oxidase (*DhCKX*) gene in *Dendrobium huoshanense*. *Molecular Biological Reports*, **36**: 1331-8.
- Weber H, Borisjuk L, Heim U, Sauer N, Wobus U. 1997a.** A role for sugar transporters during seed development: molecular characterization of a hexose and a sucrose carrier in fava bean seeds. *The Plant Cell* **9**: 895-908.
- Weber H, Borisjuk L, Wobus U. 1997b.** Sugar import and metabolism during seed development. *Trends in Plant Science*, **2**: 169-174.
- Weber H, Borisjuk L, Wobus U. 2005.** Molecular physiology of legume seed development. *Annual Review of Plant Biology*, **56**: 253-279.
- Weinthal DM, Barash I, Panijel M, Valinsky L, Gaba V, Manulis-Sasson S. 2007.** Distribution and replication of the pathogenicity plasmid pPATH in diverse populations of the gall-forming bacterium *Pantoea agglomerans*. *Applied Environmental Microbiology*, **73**: 7552-61.
- Wellburn AR. 1994.** The spectral determination of chlorophylls a and b, as well as total carotenoids, using various solvents with spectrophotometers of different resolution. *Journal of Plant Physiology*, **144**: 307-313.
- Werner T, Kollmer I, Bartrina I, Holst K, Schmulling T. 2006.** New insights into the biology of cytokinin degradation. *Plant Biology* **8**: 371-81.
- Werner T, Motyka V, Laucou V, Smets R, Van Onckelen H, Schmölling T. 2003.** Cytokinin-deficient transgenic arabidopsis plants show multiple developmental alterations indicating opposite functions of cytokinins in the regulation of shoot and root meristem activity. *The Plant Cell* **15**: 2532-2550.
- Werner T, Motyka V, Strnad M, Schmölling T. 2001.** Regulation of plant growth by cytokinin. *Proceedings of the National Academy of Sciences*, **98**: 10487-10492.
- Werner T, Schmölling T. 2009.** Cytokinin action in plant development. *Current Opinion in Plant Biology*, **12**: 527-538.
- Whitty CD, Hall RH. 1974.** A cytokinin oxidase in *Zea mays*. *Canadian Journal of Biochemistry*, **52**: 789-99.
- Williams PH. 1934.** Leafy gall of the *Chrysanthemum*. *Review of Applied Mycology*: 638.
- Wilson EE. 1935.** The olive knot disease: its inception, development and control. *Hilgardia*, **9**: 233-264.
- Wulfetange K, Lomin SN, Romanov GA, Stolz A, Heyl A, Schmulling T. 2011.** The cytokinin receptors of *Arabidopsis* are located mainly to the endoplasmic reticulum. *Plant Physiology*, **156**: 1808-18.
- Xie W, Zhou C, Huang RH. 2007.** Structure of tRNA dimethylallyltransferase: RNA modification through a channel. *Journal of Molecular Biology*, **367**: 872-81.
- Yamada H, Suzuki T, Terada K, Takei K, Ishikawa K, Miwa K, Yamashino T, Mizuno T. 2001.** The *Arabidopsis* AHK4 histidine kinase is a cytokinin-binding receptor that transduces cytokinin signals across the membrane. *Plant and Cell Physiology*, **42**: 1017-1023.
- Yanai O, Shani E, Dolezal K, Tarkowski P, Sablowski R, Sandberg G, Samach A, Ori N. 2005.** *Arabidopsis* KNOX1 proteins activate cytokinin biosynthesis. *Current Biology*, **15**: 1566-71.
- Yonekura-Sakakibara K, Kojima M, Yamaya T, Sakakibara H. 2004.** Molecular characterization of cytokinin-responsive histidine kinases in maize. Differential ligand preferences and response to cis-zeatin. *Plant Physiology*, **134**: 1654-1661.
- Young JM, Saddler GS, Takikawa Y, De Boer SH, Vauterin L, Gardan L, Gvozdyak RI, and , Stead DE. 1996.** Names of plant pathogenic bacteria 1864–1995. . *Review of Plant Pathology*, **75**: 721-763.
- Zhou C, Huang RH. 2008.** Crystallographic snapshots of eukaryotic dimethylallyltransferase acting on tRNA: insight into tRNA recognition and reaction mechanism. *Proceedings of the National Academy of Sciences. U S A*, **105**: 16142-7.

- Zhou Y, Qu H, Dibley KE, Offler CE, Patrick JW. 2007.** A suite of sucrose transporters expressed in coats of developing legume seeds includes novel pH-independent facilitators. *The Plant Journal*, **49**: 750-64.
- Zhu J, Oger PM, Schrammeijer B, Hooykaas PJ, Farrand SK, Winans SC. 2000.** The bases of crown gall tumorigenesis. *Journal of Bacteriology*, **182**: 3885-95.
- Zhu L, Zhang Y, Teh JS, Zhang J, Connell N, Rubin H, Inouye M. 2006.** Characterization of mRNA interferases from *Mycobacterium tuberculosis*. *Journal of Biological Chemistry*, **281**: 18638-43.
- Zubko E, Adams CJ, Macháèková I, Malbeck J, Scollan C, Meyer P. 2002.** Activation tagging identifies a gene from *Petunia hybrida* responsible for the production of active cytokinins in plants. *The Plant Journal*, **29**: 797-808.
- Zutra D, Cohen J, Gera Aa, Loebenstein G. 1994.** Association of *Rhodococcus (Corynebacterium) fascians* with the stunting-fasciation syndrome of carnation in Israel. *ISHS Acta Horticulturae*, **377**: 319-323.

Appendices

A. Chapter 2

2.1 Kado and Heskett '523' Medium

(Kado and Heskett, 1970)

Chemicals	gL ⁻¹
Casein hydrolysate	8
Yeast Extract	4
K ₂ HPO ₄	2
MgSO ₄ .7H ₂ O	0.3
Sucrose	10
(NH ₄) ₂ SO ₄	2

Modify pH to 7.0 with NaOH

Add 1.5% agar to solidify

2.2 Klambt Medium

(Klämbt et al., 1966)

Basic nutrient Media (Solution A)

Chemicals	gL ⁻¹
Sucrose	20.0
L-Asparagine	2.5
NH ₄ NO ₂	1.0
KH ₂ PO ₄	1.0
Thiamine HCl	0.001

Micro-nutrient media (Solution B)

Chemicals	gL ⁻¹
H ₃ BO ₃	0.62
KI	0.083
Na ₂ MoO ₄ .2H ₂ O	0.025
CoCl ₂ .6H ₂ O	0.0025

MgSO ₄ .2H ₂ O	37.0
MnSO ₄ .4H ₂ O	2.23
ZnSO ₄ .7H ₂ O	0.86
CuSO ₄ .5H ₂ O	0.0025

Solution C

Na₂Fe-EDTA 3.5gL⁻¹

Mix 1 litre solution A, 1 ml solution B and 1 ml solution C.

Adjust to pH 7.0 with KOH.

2.3 Hoglands Mineral Salts Solution

(Lawson et al. 1982)

Solution A

Chemical	mlL ⁻¹
1M KH ₂ PO ₄	1
1M KNO ₃	5
1M Ca(NO ₃) ₂	5
1M MgSO ₄ .4H ₂ O	2

Solution B

Chemical	gL ⁻¹
H ₃ BO ₃	2.86
MnCl.4H ₂ O	1.8
ZnSO ₄ .7H ₂ O	0.22
CuSO ₄ .5H ₂ O	0.008

Solution C

FeNa-EDTA 0.5%

Mix 1 L solution A, 1 ml solution B and 1 ml solution C.

2.4 25x TAE

121g Tris base

28.5ml glacial acetic acid

9.3g EDTA

Made up to 1L with nanopure water

2.7 TE Buffer

10 ml 1 M Tris (pH 8)

2 ml 0.5 M EDTA (pH 8)

Made up to 1 L with nanopure water

2.7.1 1 M Tris Stock

121 g Tris base

Made up to 1 L with nanopure water, Adjust pH to 8.0 with HCL

2.7.2 0.5 M EDTA stock

146 g EDTA

Made up to 1 L with nanopure water, Adjust pH to 8.0 with HCL

2.8 6 x Agarose gel loading dye

60mM EDTA

10mM Tris-HCl (pH 7.6)

0.03% Xylene cyanol FF

0.03% Bromophenol blue

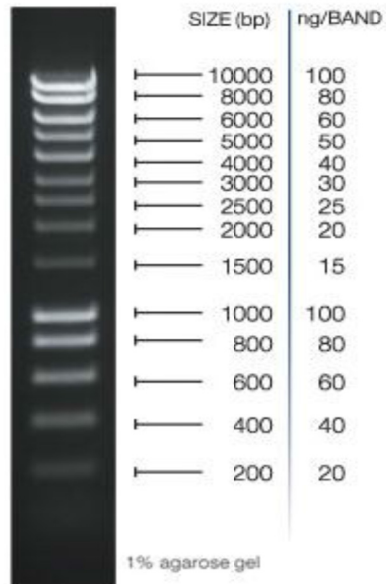
60% glycerol

2.9 DEPC water

DEPC is added to Nanopure water (0.1% (v/v)) and vigorously shaken to mix, then incubated on a shaker for 12 hours, then autoclaved for 45min.

2.10 Bioline HyperLadder™

An agarose gel run with 5 µl of HyperLadder™ 1.2 µl of HyperLadder™ 1 was sufficient for visualisation.



B. Chapter 3

3.1.1 Brush inoculation of 3 d seedling of *P. sativum* without or with *R. fascians* avirulent 589 strain or virulent 602 strain in SEM.

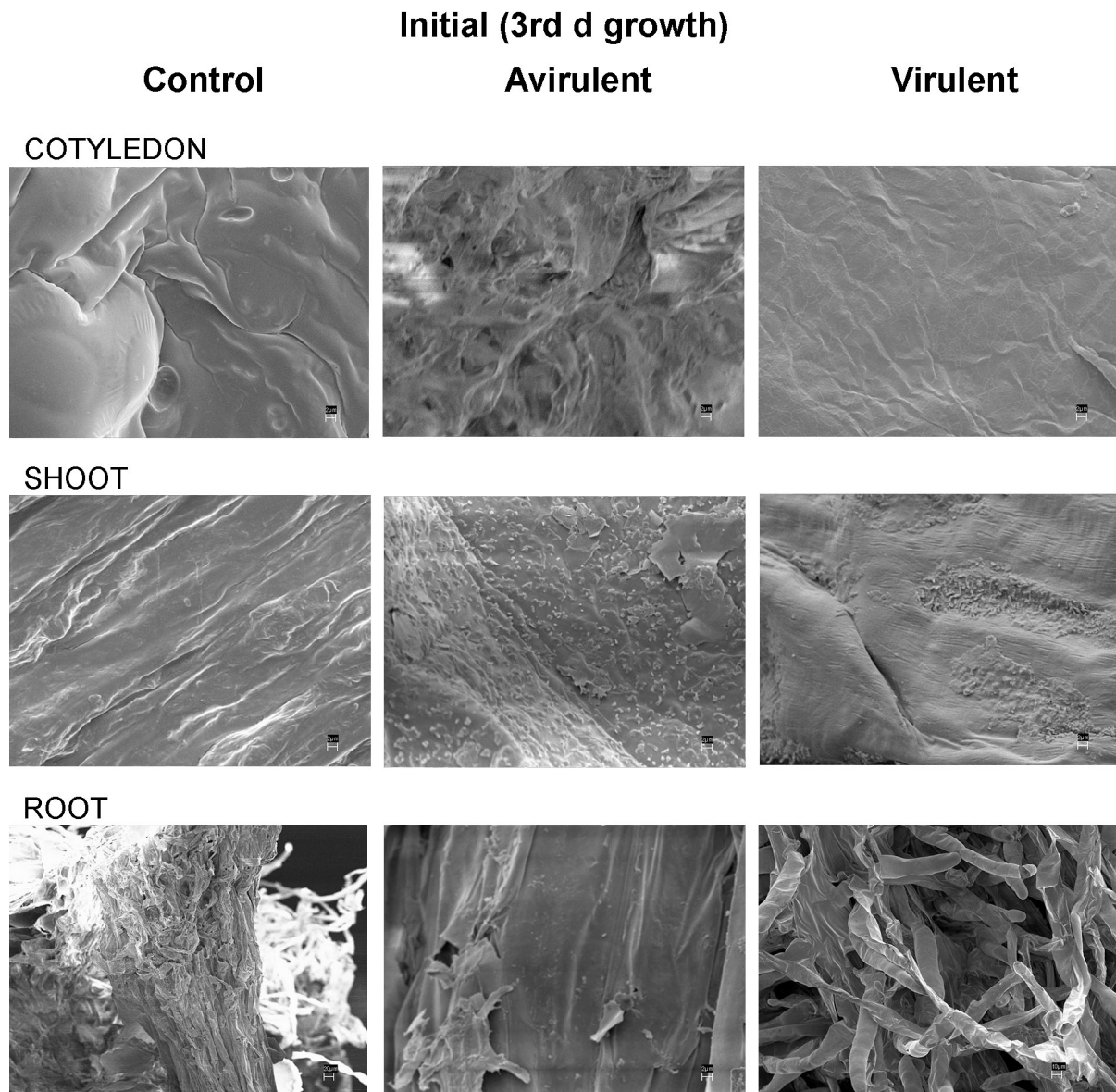


Figure 3.1 **Surface colonisation of *R. fascians* on *P. sativum*.** Scanning electron micrographs of the surface of pea tissues at initial day of brushing the shoot with Klambt's medium (Control), *R. fascians* avirulent 589 strain (Avirulent) and virulent 602 strain (Virulent) at 3 d of growth. Control with uninfected cotyledon, shoot and root without the presence of *R. fascians* at initial day of inoculation, Avirulent 589 strain infected cotyledon and root with no bacteria on the surface but rod-shaped bacteria visualised on shoot at initial day. Virulent 602 strain infected cotyledon and root without the bacteria but seen as patches on shoot.

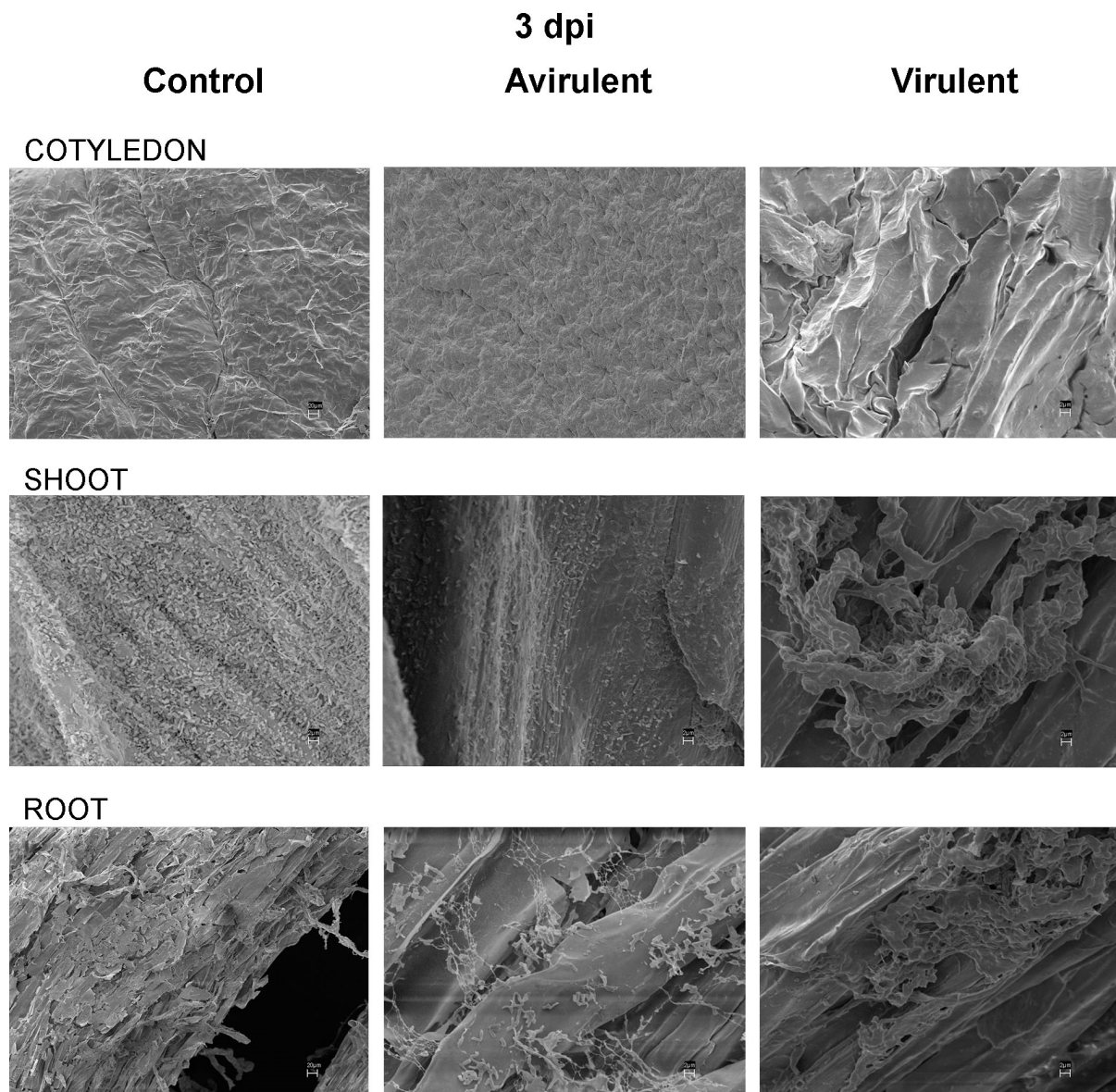


Figure 3.2 **Surface colonisation of *R. fascians* on *P. sativum*.** Scanning electron micrographs of surface of pea tissues at 3 d after brushing the shoot with Klambt's medium (Control), *R. fascians* avirulent 589 strain (Avirulent) and virulent 602 strain (Virulent). Control with uninfected cotyledon, shoot and root without the presence of *R. fascians*. Avirulent 589 strain infected cotyledon with no bacteria on the surface but rod-shaped bacteria visualised on the shoot surface and rods and interconnected rods with mesh-like material on the root surface. Virulent 602 strain infected cotyledon without the bacterial colonies but on shoot surface, a dense mass of colonisation and on root surface, a mucilage-like mass.

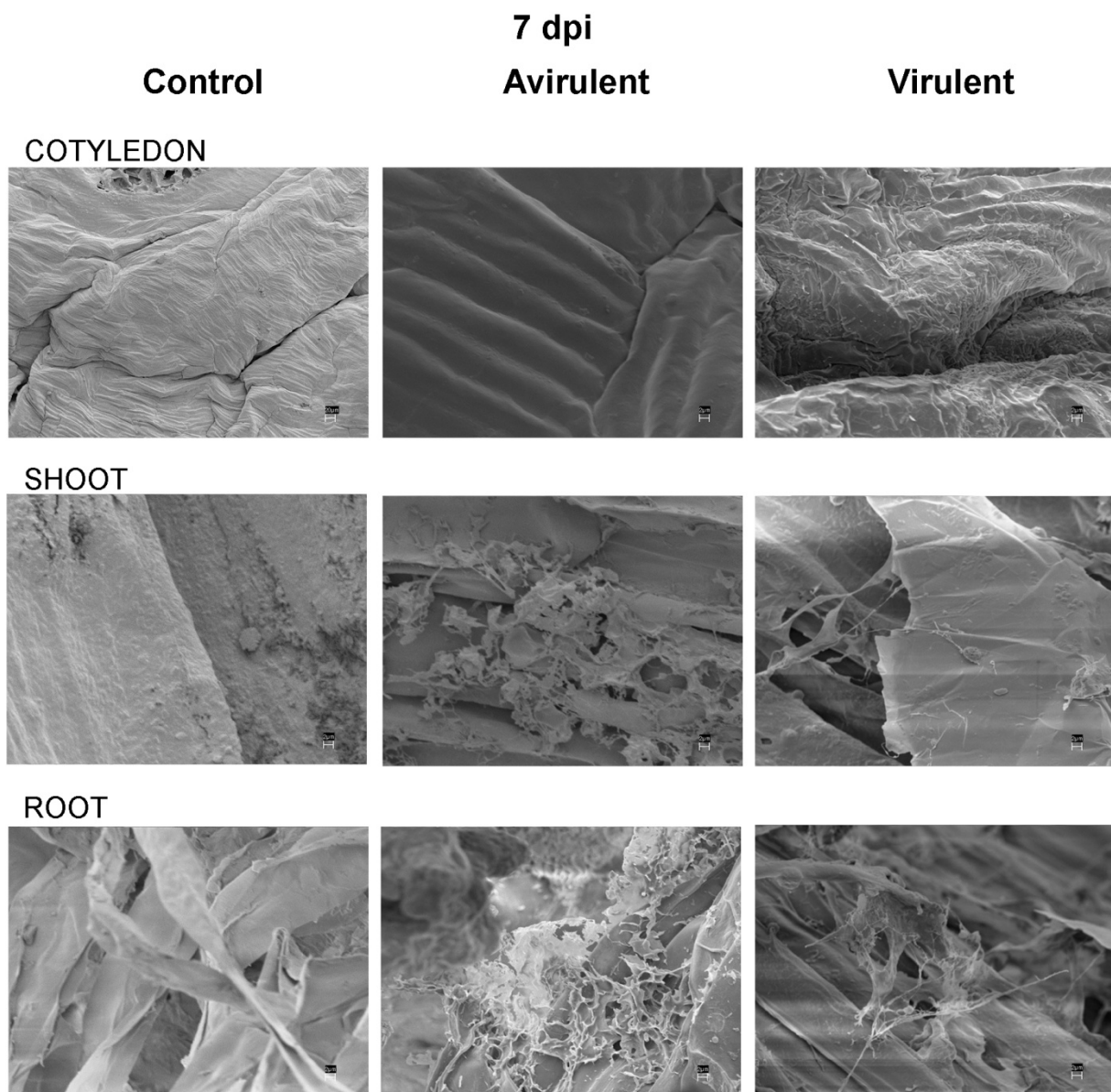


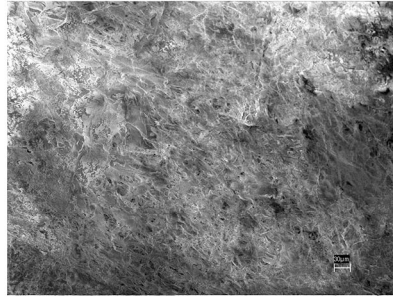
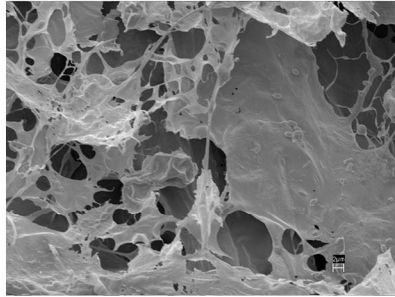
Figure 3.3 **Surface colonisation of *R. fascians* on *P. sativum*.** Scanning electron micrographs of the surface of pea tissues at 7 d after brushing the shoot with Klambt's medium (Control), *R. fascians* avirulent 589 strain (Avirulent) and virulent 602 strain (Virulent). Control with uninfected cotyledon, shoot and root without the presence of *R. fascians*. Avirulent 589 strain infected cotyledon with no bacteria on surface but on shoot surface, mass of interconnected rods and hyphae, and mesh-like material on root surface. Virulent 602 strain infected cotyledon with no bacterial presence but on shoot and root surface hyphae-like structures.

13 dpi

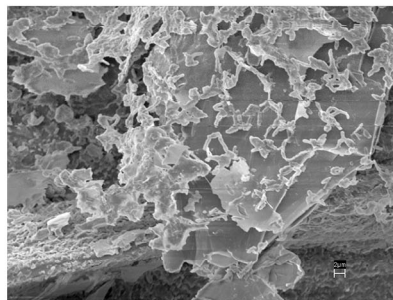
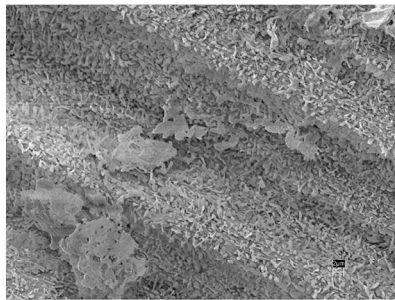
Avirulent

Virulent

COTYLEDON



SHOOT



ROOT

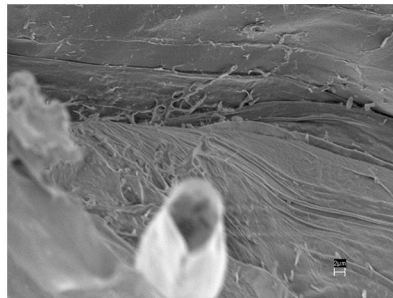
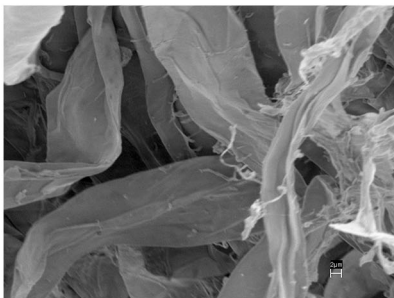


Figure 3.4 **Surface colonisation of *R. fascians* on *P. sativum*.** Scanning electron micrographs of surface of pea tissues at 13 d after brushing the shoot with Klambt's medium (Control), *R. fascians* avirulent 589 strain (Avirulent) and virulent 602 strain (Virulent). Avirulent 589 strain infected cotyledon with hyphae-like bacteria on the surface, small patches of bacterial colonisation on shoot surface and a few hyphae on root surface. Virulent 602 strain infected cotyledon with dense hyphal-like colonisation, on shoot surface a mass of mesh-like colonisation and on the root surface, fine hyphal-like bacteria.

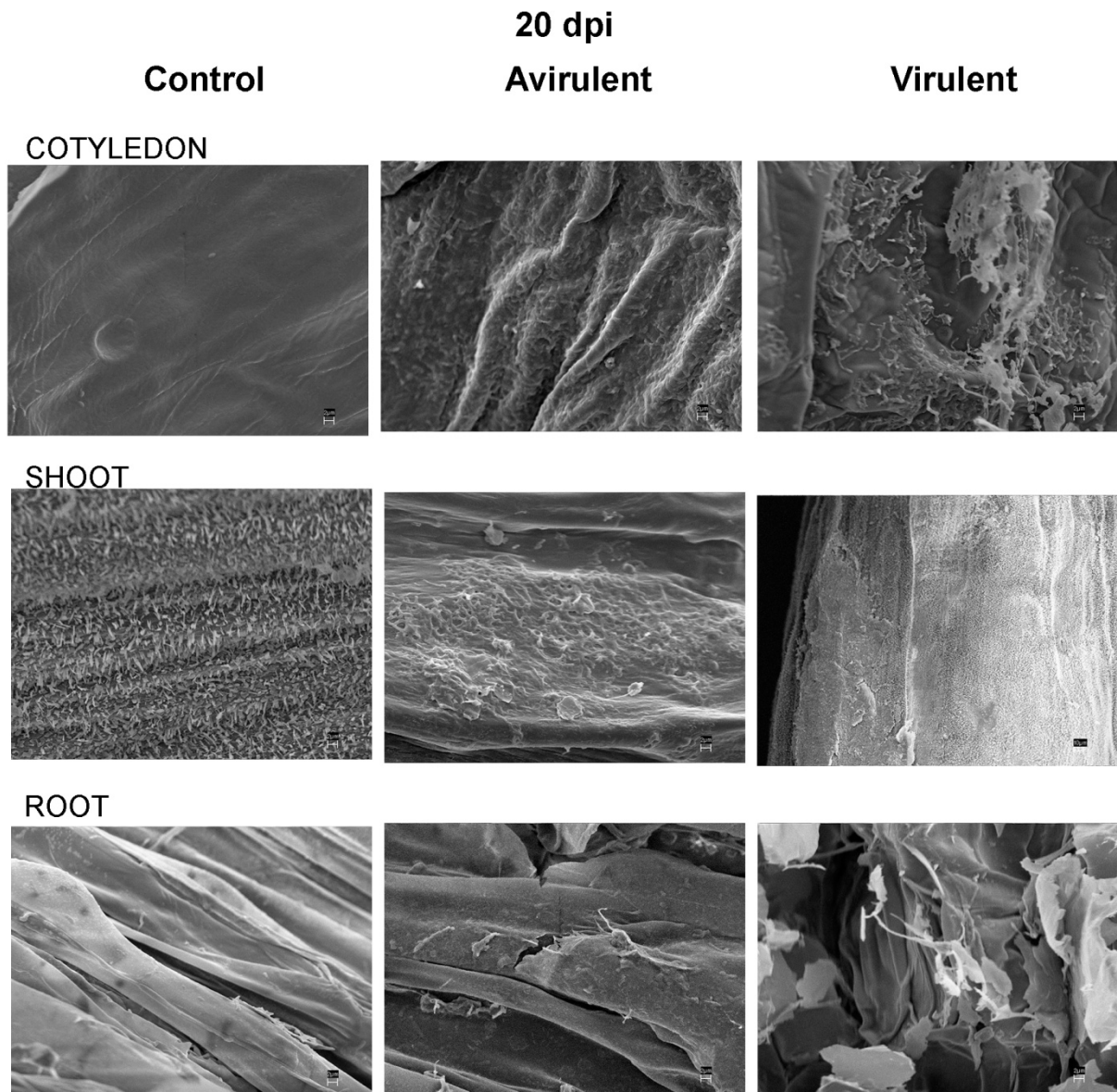


Figure 3.5 **Surface colonisation of *R. fascians* on *P. sativum*.** Scanning electron micrographs of surface of pea tissues at 20 d after brushing the shoot with Klambt's medium (Control), *R. fascians* avirulent 589 strain (Avirulent) and virulent 602 strain (Virulent). Control with uninfected cotyledon, shoot and root without the presence of *R. fascians*. Avirulent 589 strain infected cotyledon with rods embedded on the surface, matrix-like colonies on shoot and no bacterial colonies on root surface. Virulent 602 strain infected cotyledon with patches of interconnected rods, on shoot and root surface colonisation not apparent.

C. Chapter 4

4.1 Primers designed from pea transcriptome analysis for the genes of interest by Dr Jiancheng Song

4.1.1 *PsIPT* PRIMERS

PsI604 F1: 5' GCATGATTGAAGCGGGTCAAGTTAAC

PsI604 R1: 5' TTGAACTTGTTTACTTGCAAGGTTACAG

PsI604 F2: 5' GGGTCAAGTTAACGAAGTTCGTGAC

PsI604 R2: 5' CATCAAGACGGTGCATGTTCCCTC

PsI605F1: 5' GGGTTGATGTTGCACTTCCTGTC

PsI605R1: 5' ATCGGCTGAATTTGCTTCTGCAG

PsI605F2: 5' TCTTCGCTTCAATCGCGTGTTG

PsI605R2: 5' TGTCGTTGTCGATTTGCAAGAGTG

PsI421F1: 5' GCTGAAACGAGTCGACGACATGT

PsI421R1: 5' CCTTCACTGCTTCCTGGTATGCAC

PsI421F2: 5' GAAACGAGTCGACGACATGTTTGAC

PsI421R2: 5' AGCTGACACGTGTTATCCTTAATCG

4.1.2 *PsCKX* PRIMERS

#	Name	Sequence
1	PsC910 F1	5' GGGATGATAGACTCAGTAGTGGTAC
2	PsC910 F2	5' CACCAAAGGGACCACCTACTGA
3	PsC910 R1	5' TCTCTGAACAAATCTATTCCATTTATCTCCA
4	PsC910 R2	5' CAGGTGCAAGAATAGCCATTGGATC
5	PsC910 RF	5' GCTATTTAAAGCCCAACCACACCTG
6	PsC910 RR	5' ATATGAATGCATACACCTTAGTAATTGGTTG
7	Ps942 F1	5' TGTTTTACCTGGTGGCATTCTGAG
8	Ps942 F2	5' TTGGATGCTGAGACTGGAGTAC
9	Ps942 R1	5' GAATTGCATCTTCATGGCATTGAATTG

10	Ps942 R2	5' CGCTGGCCTGTTGCTAAGATTC
11	Ps942 RFa	5' AAGAAACAATGGCGGCAGTGAAG
12	Ps942 RFb	5' AGGGCACGGACACTCGATAAAC
13	Ps942 RR	5' GTTTAAGCTCTAATCTCACTGCAAATAATTATTC
14	PsC209 F1	5' AAATGTATCATTGTTGAGTTCTTGAATAGAGT
15	PsC209 F2	5' TTGAATAGAGTTAGAAGTGGAGAGTTGAAG
16	PsC209 R1	5' TCATCTGGTATTGTTGCTGACATC
17	PsC209 R2	5' CTTTCCAATTATCAAATCTACTTGAGTGCA
18	PsC209 RF	5' TCCCACAAACACTACACAAAACCAC
19	PsC209 RR	5' AATGATTCTGTCAACCTAACATATCTAAGGT
20	PsC399 F1	5'ATCACTAAAACAACATGAAATGCAGGTAC
21	PsC399 F2	5' GTACATGTTGGGAACCTTCCTCCATAC
22	PsC399 R1	5' TGAGGACCATGCTTAAACGCTTGT
23	PsC399 R2	5' CCCTGTTCTATAACAATCTGAAGCTG
24	PsC399 F3	5' AGAGACCAAGAGAGATTAATATCTCAAGATAATG
25	PsC399 R3	5' GTTGATGTATTTAGCTAATTCTAGGCAGAAG
26	PsC399 RF	5' TCATACGCATTCTCATAGGAATAGTTGA
27	PsC627 F1	5' TTTACAGTGTACTTGGAGGCTTAGGA
28	PsC627 R1	5' AGTTCTTCCATCTGATTTGAACTTGCT
29	PsC627 F2	5'AGTTGAGAAACACTTGTCCCCTTG
30	PsC627 R2	5' GATAGGACCATTGCTTGTTCCTTTGAC
31	PsC627 RF	5' TGGCTTTAACCTTCTTCACCCTTTAAC
32	PsC930 F1	5' GGTCCCATACTCATTACCCTGTCA
33	PsC930 F2	5' ACCAGGTGGAACCGTAAAACATCT
34	PsC930 R1	5' GGCATGGGTGCAGAAATCTAAGATC
35	PsC930 R2	5' GTAATGAGCAAGATATTGCTTCACATTTAGT
36	PsC930 RFa	5' GGTGAAATGGATTAGGGTGCTCTATTC
37	PsC930 RFb	5' GAGATCAAGAAAATTTGATATCACTTAAGGACA
38	PsC131 F1	5' YATCTCNNTTGGATAAAEWTTCTCAAAYTCTC
39	PsC131 F2	5' ATGGGGTKGTGKTGAAYATGACT
40	PsC131 R1	5' GTAACAACATCCAATTCAWGAACATTGG
41	PsC131 R2	5' TTCTCKYAGARCAAGTCACWAKG

4.1.3 *PsLOG* PRIMERS

***PsLOG1/3* (ref:LC1283-2)**

PsLOG1F: 5' TSARCTTGGAAMGAATTGGTKTCAAG

PsLOG1R: 5' AAWGCATCWGARTGYTTAGCCATYTCAG

***PsLOG6* (ref:LC4749rc)**

PsLOG6F1: 5' ATAAACCKGTGGGGTTRTTGAACGTG

PsLOG6F2: 5' ACTACAACTCGYTGCTGGCATTCA

PsLOG6R: 5' TGACTTTGCWGTGTTAACYAACTGTTG

***PsLOG7* degenerate (ref: PsLOG7-9078)**

PsLOG7F: 5' AAGARACCAAWTCCARRTTCAAGAGGA

PsLOG7R1: 5' YCCACCATCATGAACHGACYTGAG

PsLOG7R2: 5' RGATACDGCTCTCACTTCMCCRATAG

***PsLOG8/9* (ref: CL1655-1rc)**

PsLOG8F1: 5' GAAGTAAGAATTGTTTCTGATATGCATGAG

PsLOG8F2: 5' GCGGCAATGGCTCAAGAAGCTG

PsLOG8R1: 5' GCAAAAAGTTATAGTAACCATCAACATTCAGTAG

PsLOG8R2: 5' TTCCGAGCACCAGGCTTAATGAAG

4.1.4 *PsRR* PRIMERS

***PsRR5* (ref: Ug10019rc)**

PsRR5 F1: 5' RAARCCRGTC AARTTGTCAGATGTAAG

PsRR5 F2: 5' GAAAGATTTYRTCATGAGAGGTGAAGTG

PsRR5 R: 5' ATTTCTTRGAKGATAATGKTGATGGTGAGAGTGGTGAG

***PsRR6* (ref: Ug16070rc)**

PsRR6F1: 5' GTGGTTATGTCSTCTGAGAAAYATCTTG

PsRR6F2: 5' GAAYATCTTGACCCGAATYGATAGTTG

PsRR6R: 5' RGWCGATAGAGATGRAATGSAATCATCTG

PsRR3 (Ug10200rc)

PsRR3F: 5' TCCCGGGTTTGAAGGTGGATCTAG

PsRR3R1: 5' TGCACCTTCCTCCAAACATCTGTC

PsRR3R2: 5' TTYACGTCAGATAATTTCACTGGCTTCAC

PsRR9 (ref: Ug28469)

PsRR9F: 5' CAGRAATGACAGGYTATGATCTGCTG

PsRR9R1: 5' YTCAGCTTGTTTACATCTGAYTGTTGAAC

PsRR9R2: 5' WWCATTCTTAACTTTTGWYTTCAACAAATGTG

[Note: N = ATGC, M = AC, R = AG, Y = CT, W = AT, K = GT, S = GC, H = ACT, B = CGT, V = CG, D = AGT]

4.1.5 Transporter gene primers

PsAAP PRIMERS

PsAAP498F: 5' AGGAGTGTTGTCTTTGGCATGGAG

PsAAP498R: 5' ATGGATGCTRTAATGATGTAGGCAATTC

PsAAP600F: 5' CW TTCAGAACTGCTTATGTTGCATCAAC

PsAAP600R: 5' YYAATGGATCCAACMAGAGTGAACAATC

PsAAP9261F: 5' ATTCATTTGGTTGGAGGATATCAGATATACAG

PsAAP9261R: 5' TCCAGTGGTTGAAATCACATAGGTTG

PsAAP9262F: 5' ATTCATTTGGTTGGAGGATATCAGATTTATAG

PsAAP9262R: 5' TCCAGTTGTGGAAATCACATAAGCTG

PsAAP446F: 5' TGCAATTGGTCTTTGTCTTTCCGTAC

PsAAP446R: 5' TTTCTGATGGAGGTGACCTTAGTGTATC

PsAAP303F: 5' AGGACAAGTTATTGGAGTGGATGTCAC

PsAAP303R: 5' CACACATTGCATAGAAGAATGTGGTGATTG

PsAAP367F: 5' CGGGCTCGTTGTTGGAGTGGATGTCAC

PsAAP367R: 5' CGCATAATGAATAAAAGAATGTGGTGATTG
PsAAP051F: 5' CCGGTTTCGGTTTCTATAATCCTTTCTG
PsAAP051R: 5' RWTGACCTCCAAACCAATCTAAAGAGGTTG
PsAAP224F: 5' CGGAAGTGTTTGGACTGCAAGTTC
PsAAP224R: 5' TACTCCACCAAGAATGGAGCGAAC
PsAAP675 F : 5'AGGTACGGTTTGGACAACGAGT
PsAAP675 R: 5' GAGAATGGTGTGAACAGCTTCCATG
PsAAP328F: 5' AGAAGTTGTAAGATCTGTCTTAGGAGGAAG
PsAAP328R: 5' GCTGCAACTATTGAGAGCCATGAAAG
PsAAP931F : 5'AAGCTTTGTGCATTGGCTCAGTAC
PsAAP931R: 5' GCAGCAATAATAGAGAGCCATGAAAGTTC
PsAAP532F : 5' GGATACACGGTAGCTTCTGCCATAAG
PsAAP532R: 5' GCCTAGACCAATCGTCGAATATGTAAAG
PsAAP180F1: 5' GGACTTTCTCTTCCACCGTTATTCAAG
PsAAP180R1: 5' TGGAGGTGATGATTTTCAGAGTGTCTTG
PsAAP180F2: 5' ACTATCAATTATTTTAGGCTACTTTGGAGGAC
PsAAP180R2: 5' CTCAATGTTTGAAGCCCAATCCAAC
PsAAP840F: 5' TGTAGGATTTCAAGCAATCCATACATGATC
PsAAP840R: 5' TGTTGATGACACATTTCCACTGCTTC
PsAAP4401F: 5' CATGGGTAGCCTCACAGGAATCAG
PsAAP4401R: 5' CAAAGCATGTAAAATGTTGTGGTCACTG
PsAAP4403F: 5' CGCTGGATTTGGTGTCTCGAAAG
PsAAP4403R: 5' CATAAATATGTTTTGATTGTAGACTGGCAAAC
PsAAP4405F: 5' GCTATGCTGCATTTGGAGACACATC
PsAAP4405R: 5' CCAAATTAATCGAAATAGATTTAGATGGTAAGGATG

PoSUT PRIMERS

PoSUT366F: 5' TGGGCAGTTATCCGGTGCTTTC
PoSUT366R1: 5' ACACCCATATCATACGCATGACCTTC

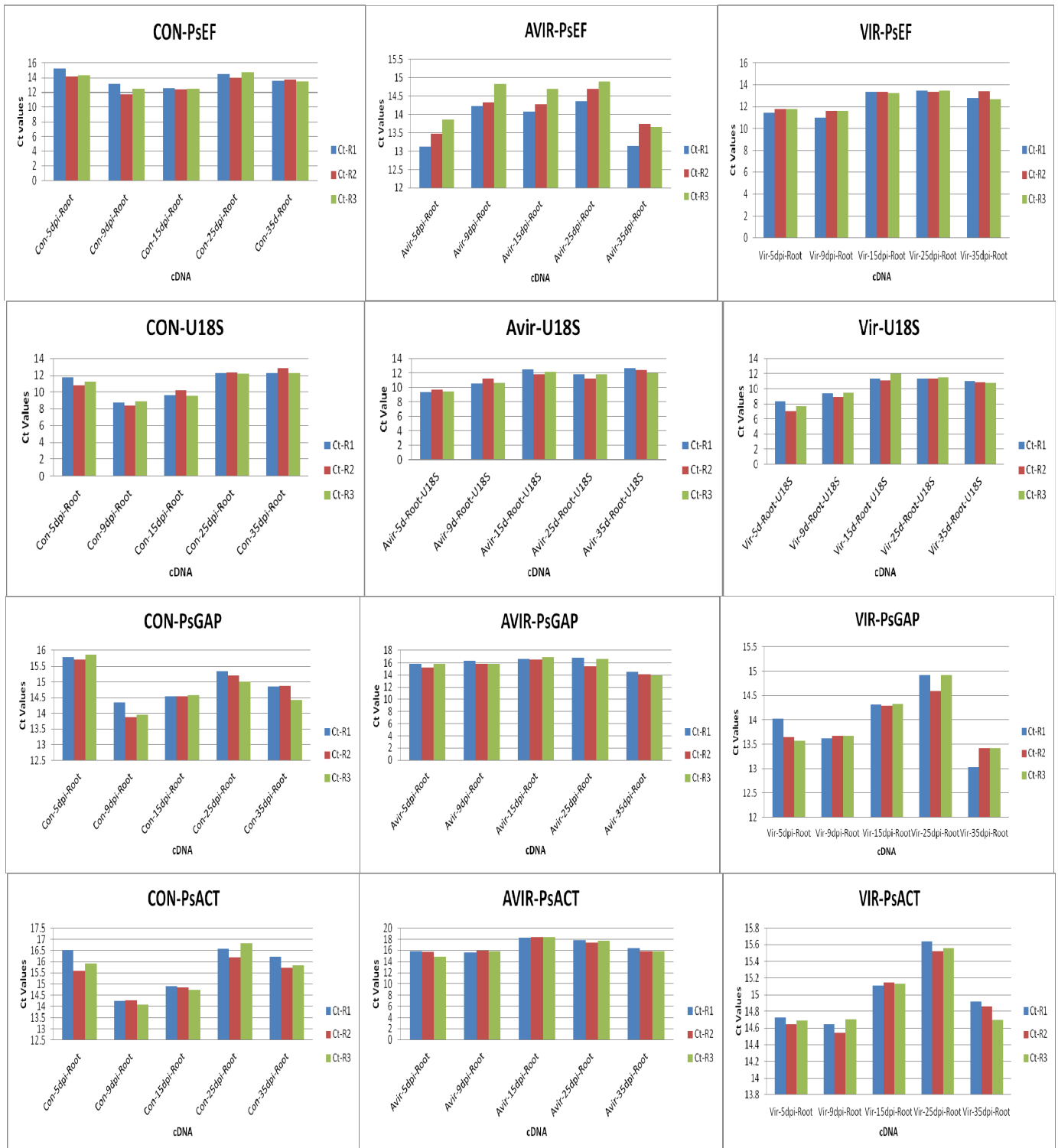
PsSUT366R2: 5' GCCAAGATATCAACACCCAGTGAC
PsSUT948F: 5' CAGTGCTTCAGGGGCTGGAC
PsSUT948Ra: 5' CAACACTATCGCCAATACAGCACTG
PsSUT948Rb: 5' GTAAAATAATAATTGCTAATACACCACTGATGAC
PsSUT666F: 5' CCGATCGTCGGTTACTACAGTGATC
PsSUT666R1: 5' CCCCATGAAGGCACGACATG
PsSUT666R2: 5' CTTCTATGGTCGTCAGCAGCGAG
PsSUT164F: 5' GGAAGTGGACCATGGGATCAG
PsSUT164R1a: 5' CATATGATACCTCATAACACGGATTCGAG
PsSUT164R1b: 5' GAACATGATACCTCATACTGGGTTTCTAG
PsSUT164R2a: 5' GGTTGAAATCTTGAGGAGAGGAAACTC
PsSUT164R2b: 5' CCACAGCTAAAGTGAGGTTGGATG
PsSUT674F: 5' AATGTGTAAGTGGATGGGTGCAAG
PsSUT674R1: 5' AAKGGAACACTRTAGGTAATCGCAAG
PsSUT674R2: 5' ACCWCCTGAATCAGCAGTYAAYTCTG
PsSUT102F: 5' AGGGATCATTTACCAAAGGCGAAG
PsSUT102R1: 5' GTWAAGARRACTTGAGCAATGATAAAKGTG
PsSUT102R2: 5' CCACAMYCTATTCATTTCTTCAATTGGAAC
PsSUT428F: 5' CATTACCAAGGCAGCTCAGCATG
PsSUT428R: 5' GARCTCCSARAGATAAACCTTGTCCAG

[Note: N = ATGC, M = AC, R = AG, Y = CT, W = AT, K = GT, S = GC, H = ACT,
B = CGT, V = CG, D = AGT]

4.2 Graphs for the expressions of all four reference genes in shoot and root tissues of pea.

4.2.1 Root and Shoot –Four Reference genes expression in qRT-PCR in control, avirulent and virulent treatments (Figure 4.1)

A. Root tissue



B. Shoot tissue

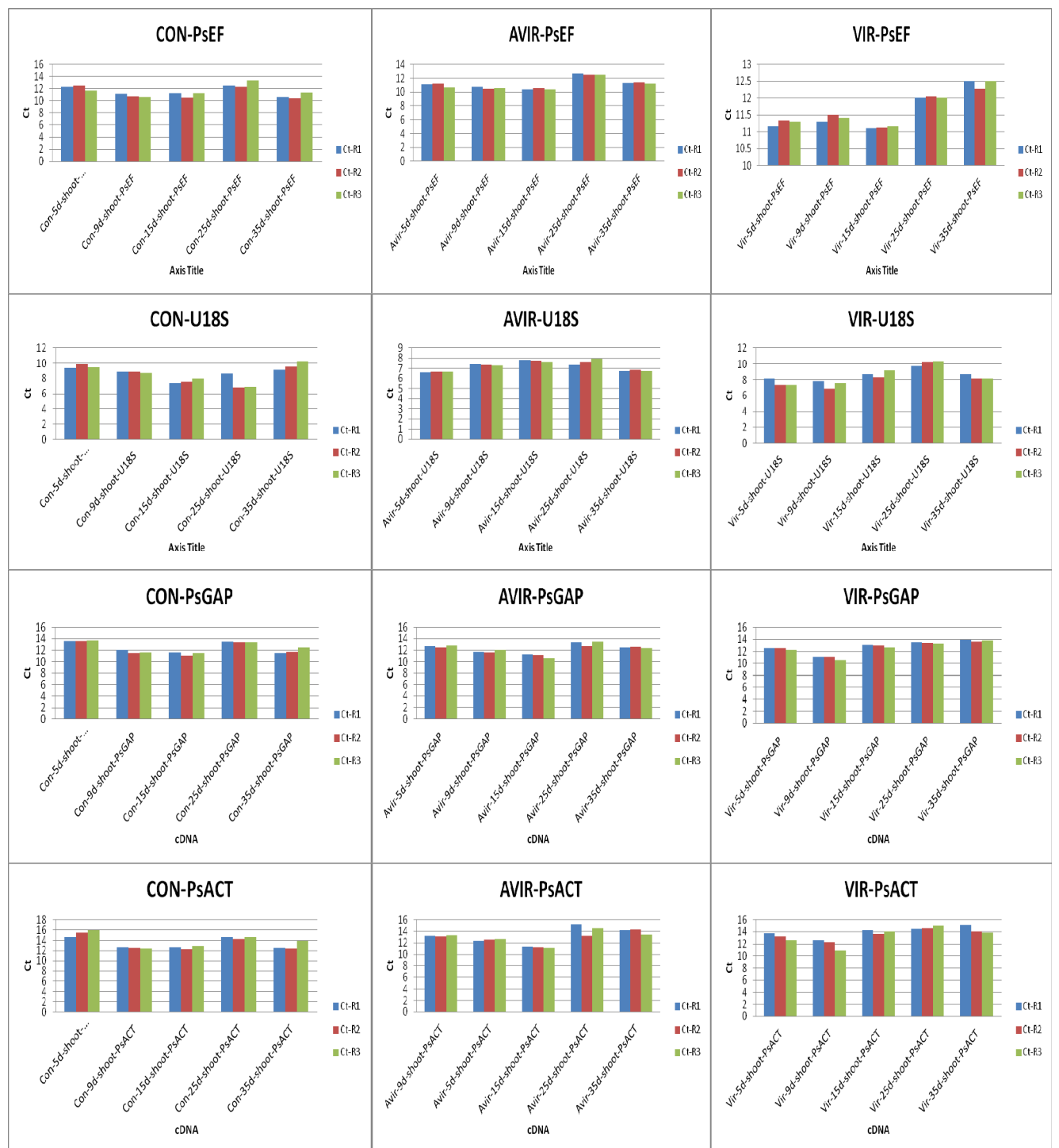


Figure 4.1 The expression (Ct values) of four reference genes *PsEF*, *U18S*, *PsGAP* and *PsACT* in pea tissue from the three treatments (control (CON), inoculated with avirulent (AVIR) and virulent (VIR) strains of *R. fascians*) at different stages of growth period. A. Root tissue B. Shoot tissue.